09:38:12 OCA PAD AMENDMENT - PROJECT HEADER INFORMATION 04/28/97

Active

Project #: E-25-W56 Cost share #: E-25-374 Rev #: 12
Center # : 10/24-6-R8119-0A0 Center shr #: 10/22-1-F8119-0A0 OCA file #:
Work type : RES
Contract#: RK72740 Mod #: 9 Document : PO
Prime #: NAS1-20102, TASK ASSIGNMENT #5 Contract entity: GTRC

Subprojects ? : N CFDA: NA
Main project #: PE #: NA

Project unit: MECH ENGR Unit code: 02.010.126
Project director(s):
CUNEFARE K A MECH ENGR (404)894-3200

Sponsor/division names: LOCKHEED AERONAUT SYS CO-GA /
Sponsor/division codes: 261 / 007

Award period: 940321 to 971101 (performance) 971101 (reports)

Sponsor amount	New this change	Total to date
Contract value	63,302.00	293,752.00
Funded	63,302.00	293,752.00
Cost sharing amount		13,624.00

Does subcontracting plan apply ?: N

Title: OPTIMIZATION IN STRUCTURAL ACOUSTICS USING FEM/BEM

PROJECT ADMINISTRATION DATA

OCA contact: Robert D. Simpkins 894-4820

Sponsor technical contact

DR. S.P. ENGELSTAD
(404)494-9178

LOCKHEED AERONAUTICAL SYSTEMS CO.
86 SOUTH COBB DRIVE
MARIETTA, GA 30063

Sponsor issuing office

LAURIE DYSERT, MAIL ZONE 0510
(404)494-8359

LOCKHEED AERONAUTICAL SYSTEMS CO.
MATERIAL CONTRACTS AND SUPPORT SERV.
DEPT. 52-34
86 SOUTH COBB DRIVE
MARIETTA, GA 30063-0510

Security class (U,C,S,TS) : U ONR resident rep. is ACO (Y/N): N
Defense priority rating : supplemental sheet
Equipment title vests with: Sponsor X GIT
NASA CLAUSES 18-52.245-70 AND 18-45.505-14 APPLY.
Administrative comments -
MODIFICATION NO. 9 ADDS $63,302 AND EXTENDS PERIOD OF PERFORMANCE TO 11/1/97.

4
35

Closeout Notice Date 05-JAN-1998

Project Number E-25-W56 Doch Id 45573

Center Number 10/24-6-R8119-0A0

Project Director CUNEFARE, KENNETH

Project Unit MECH ENGR

Sponsor LOCKHEED AERONAUT SYS CO-GA/

Division Id 5262

Contract Number RK72740 Contract Entity GTRC

Prime Contract Number NAS1-20102, TASK ASSIGNMENT #5

Title OPTIMIZATION IN STRUCTURAL ACOUSTICS USING FEM/BEM

Effective Completion Date 01-NOV-1997 (Performance) 01-NOV-1997 (Reports)

Closeout Action:	Y/N	Date Submitted
Final Invoice or Copy of Final Invoice	Y	
Final Report of Inventions and/or Subcontracts	Y	
Government Property Inventory and Related Certificate	Y	
Classified Material Certificate	N	
Release and Assignment	N	
Other	N	

Comments

Distribution Required:

Project Director/Principal Investigator	Y
Research Administrative Network	Y
Accounting	Y
Research Security Department	N
Reports Coordinator	Y
Research Property Team	Y
Supply Services Department/Procurement	Y
Georgia Tech Research Corporation	Y
Project File	Y

NOTE: Final Patent Questionnaire sent to PDPI

LG94ER0131

OPTIMIZATION IN STRUCTURAL ACOUSTICS USING FEM/BEM

S.P. Engelstad
Acoustics
Lockheed Aeronautical Systems Company
Marietta, Georgia 30063-0685
and
K.A. Cunefare
Department of Mechanical Engineering
Georgia Institute of Technology
Atlanta, Georgia 30332-0405

August 1994

Interim Report Prepared for
NASA Langley Research Center
Contract NAS1-20102 Task 5

OPTIMIZATION IN STRUCTURAL ACOUSTICS USING FEM/BEM

S.P. Engelstad and K.A. Cunefare

SUMMARY

A research program has been initiated to develop a computational scheme using Finite Element and Boundary Element Methods (FEM/BEM) to minimize noise transmission into an aircraft fuselage interior by optimizing selected structural parameters. This report describes the results of the first year of this program, and describes plans for the follow-on work. This year's results included successful coupling of the selected FEM, BEM, and optimization software to demonstrate the algorithm. Initial results were obtained for a uniform unstiffened cylinder. A stiffened cylinder optimization analysis was in progress at the time this report was written. The results were quite promising in terms of the global noise reduction achieved, and problem areas were identified for streamlining the computations for next year's work.

1. INTRODUCTION

This document briefly outlines the progress and accomplishments of the joint Lockheed/Georgia Tech research program directed toward optimizing the acoustic environment inside aircraft structures. The objective of the research is to develop design tools such that the structure of an aircraft fuselage may be tailored in such a way as to minimize the interior noise levels.

This research seeks to exploit the current state of the art in structural dynamic modeling codes, acoustic radiation modeling codes, and optimization to tailor the structural details of cylindrical aircraft structures for minimum interior noise levels. To date, the research has focused on two cylindrical shell models: one bare isotropic model and one stiffened model. In order to perform the intended optimization on these models, an extensive program development and integration effort was necessary. This development effort involved the use of a UNIX shell script to integrate an optimization code (CONMIN), a structural analysis code (MSC/NASTRAN), and an acoustic analysis code (COMET/ACOUSTICS, developed by Automated Analysis Corporation (AAC)). In the following sections, we briefly review the theoretical basis for our optimization approach, the computational structure of the integrated optimization algorithm, and a discussion of results to date.

This effort is funded by the Structural Acoustics Branch of NASA Langley Research Center under Task Order Contract NAS1-20102, Task 5. J. H. Robinson is the NASA technical monitor.

2. OPTIMIZATION FORMULATION

The method of feasible directions is used to minimize a particular objective function. The objective function for this phase of the work was the sum of the squares of the pressure amplitudes at data recovery nodes in the internal volume of the cylinder. Upper and lower bounds are imposed on the permissible values in the design variables. The optimization problem is therefore posed as

$$\text{Minimize:} \quad F(\mathbf{b}) = \sum_{i=1}^{NDRN} | p_i(\mathbf{b}) |^2 = \sum_{i=1}^{NDRN} p_i(\mathbf{b})\, p_i^*(\mathbf{b}) \tag{1}$$

$$\text{Subject to:} \quad g_j(\mathbf{b}) \leq 0 \quad j = 1, NIC \tag{2}$$

In Eqs. (1) and (2), p_i represents the pressure at the *i*th point within the volume, **b** represents the vector of design variables, *NDRN* is the number of data recovery nodes in the acoustic model, g_j represents an inequality constraint on the *j*th design variable, and *NIC* represents the number of inequality constraints. For the problem posed here, *NIC=NDES*, where *NDES* is the number of design variables.

The method of feasible directions employs an iterative solution technique, where the design variables at an iteration *q* are determined as

$$\mathbf{b}^q = \mathbf{b}^{q-1} + \alpha^* S^q \tag{3}$$

The vector *S* represents a search direction within the design space **b**, and α^* is the distance to move in direction *S*. The search direction *S* is determined from

$$\nabla F(\mathbf{b}) \bullet S + \kappa = 0 \tag{4}$$

with

$$S \bullet S = 1 \tag{5}$$

The optimum value of α^* is then determined by an interpolation technique along *S*.

The determination of *S* requires the gradient of the objective with respect to the design variables. The gradient of our objective function with respect to a design variables b_j is

$$\frac{\partial F}{\partial b_j} = 2 \sum_{i=1}^{NDRN} Re\left(p_i \frac{\partial p_i}{\partial b_j}\right) \tag{6}$$

As a consequence of the coupled structural acoustic problem, the derivative in Eq. (6) is chain-ruled as

$$\frac{\partial p_i}{\partial b_j} = \frac{\partial p_i}{\partial v}\frac{\partial v}{\partial b_j} \tag{7}$$

where v represents the surface normal velocity at the boundary between the cylinder wall and the interior acoustic volume. Each of the derivatives in Eq. (7) is generated using separate computational codes: $\partial p/\partial v$ by COMET/ACOUSTICS, $\partial v/\partial b$ by NASTRAN.

2.1 Computational Structure

The overall optimization structure is generated by integrating a number of stand-alone codes, with data exchange and process control coordinated by a UNIX shell script. The principle programs integrated were CONMIN, NASTRAN and COMET/ACOUSTICS. Two other programs, VBCGEN and MERGE, were used for data manipulation or translation between codes. Additional translation code, provided by AAC, was integrated into the CONMIN code. In the following, the integration of the optimizer, CONMIN, with NASTRAN and COMET/ACOUSTICS is discussed.

The CONMIN code, superficially flowcharted in Figure 1, implements the method of feasible directions. Based on the decision in Step 3, CONMIN calls for either gradient evaluations or objective function evaluations. The mechanisms for responding to these CONMIN calls are depicted in Figures 2 and 3. For evaluating the objective function, Figure 2, steps 2, 3, and 4 are external to the CONMIN code. For evaluating the gradient of the objective function, Figure 3, steps 2, 3, 4 and 5 are external to the CONMIN code.

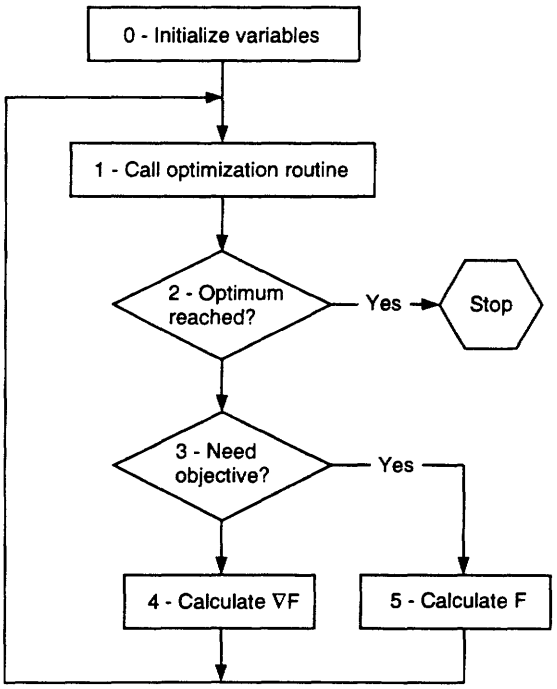

Figure 1. CONMIN Flowchart for Objective Function and Gradient Evaluation

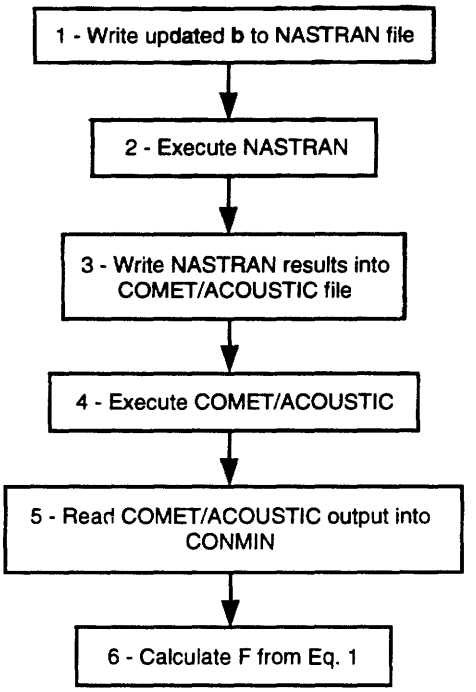

Figure 2. Program Calling Sequence for Objective Function Evaluation

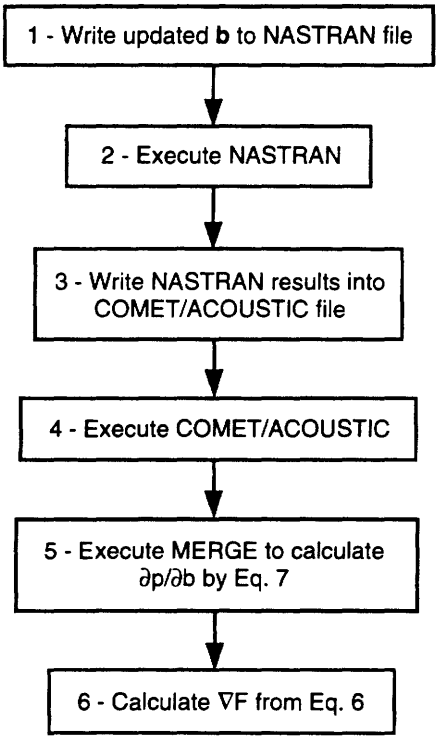

Figure 3. Program Calling Sequence for Gradient Evaluation

A UNIX shell script was developed to integrate the execution of the various codes required for the optimization. Figure 4 depicts the general flow of the shell script. Figure 4 does not do the script justice, as the script is over 800 lines long, and provides substantial flexibility to the user, as well as extensive error trapping, diagnostics and execution history tracking. Appendix A is the usage guide for the script, and indicates some of the capabilities implemented in the script. The shell script, CONMIN, VBCGEN, COMET/ACOUSTICS and MERGE run on NASA Langley's DEC ALPHA. NASTRAN runs on NASA Langley's DEC 5000.

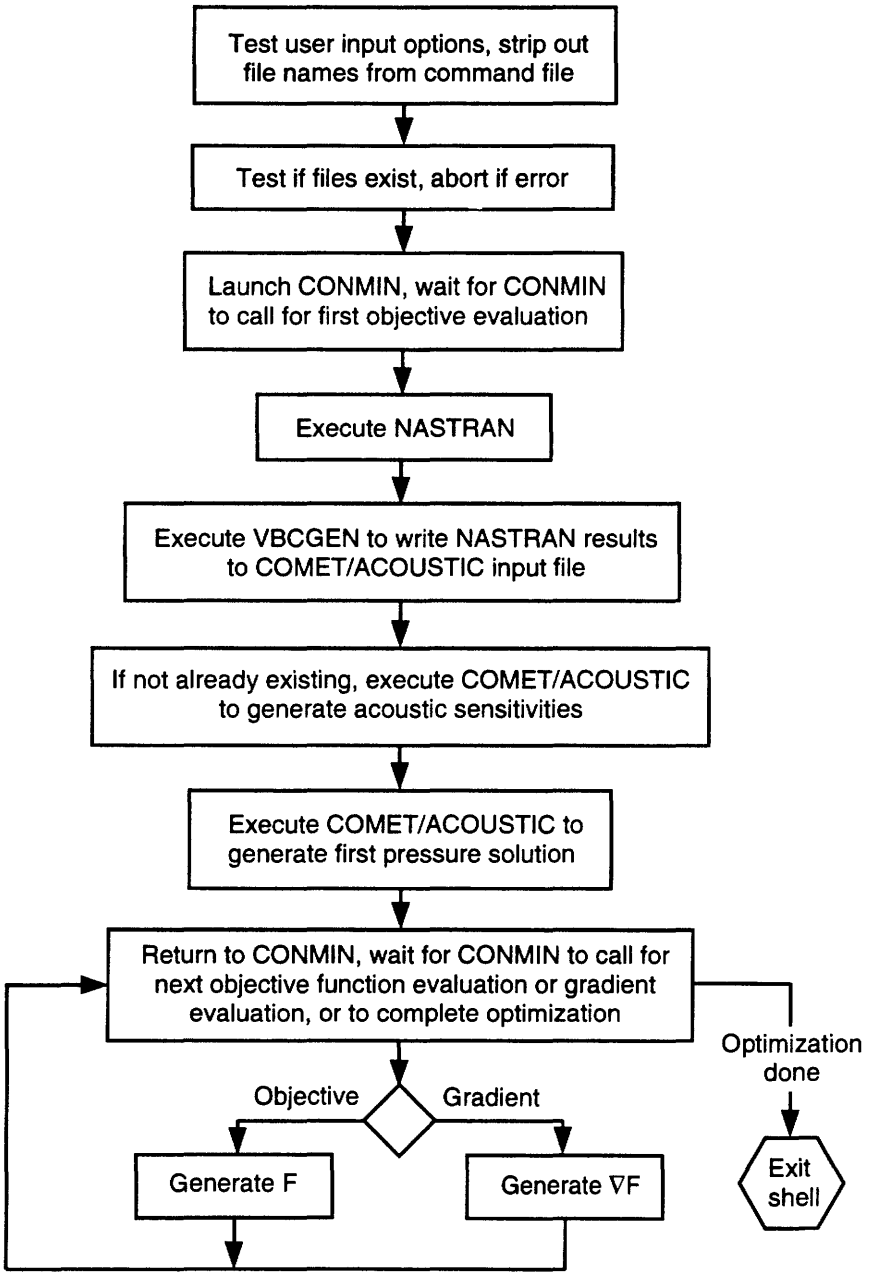

Figure 4. Conceptual Flow Chart of Shell Script

3. MODELS AND RESULTS

3.1 Uniform Cylinder

In this study an unstiffened uniform thickness cylinder, clamped at both ends is investigated to represent a fuselage structure. The excitation is a single tone exterior monopole source on one side of the fuselage, chosen to represent a propellor source. The cylinder geometry and excitation were modeled after that of the NASA Composite test cylinder in Reference 1 and also the numerical model of Reference 2. Optimization was performed with the objective to minimize the global acoustic levels by tailoring the thickness distribution of the shell elements. The optimization for this year's work was performed at a single frequency, the excitation frequency.

3.1.1 Model Description. The aluminum cylinder has length L=3.66 m, a radius of 0.838 m, and a thickness of 1.7 mm. Selecting to study only symmetric modal response, only one quarter of the cylinder was modeled. Figure 5 illustrates the structural finite element model. A cylindrical coordinate system (r,θ,x) is used with the origin in the center of the clamped end, and with the x-axis running along the length of the cylinder.

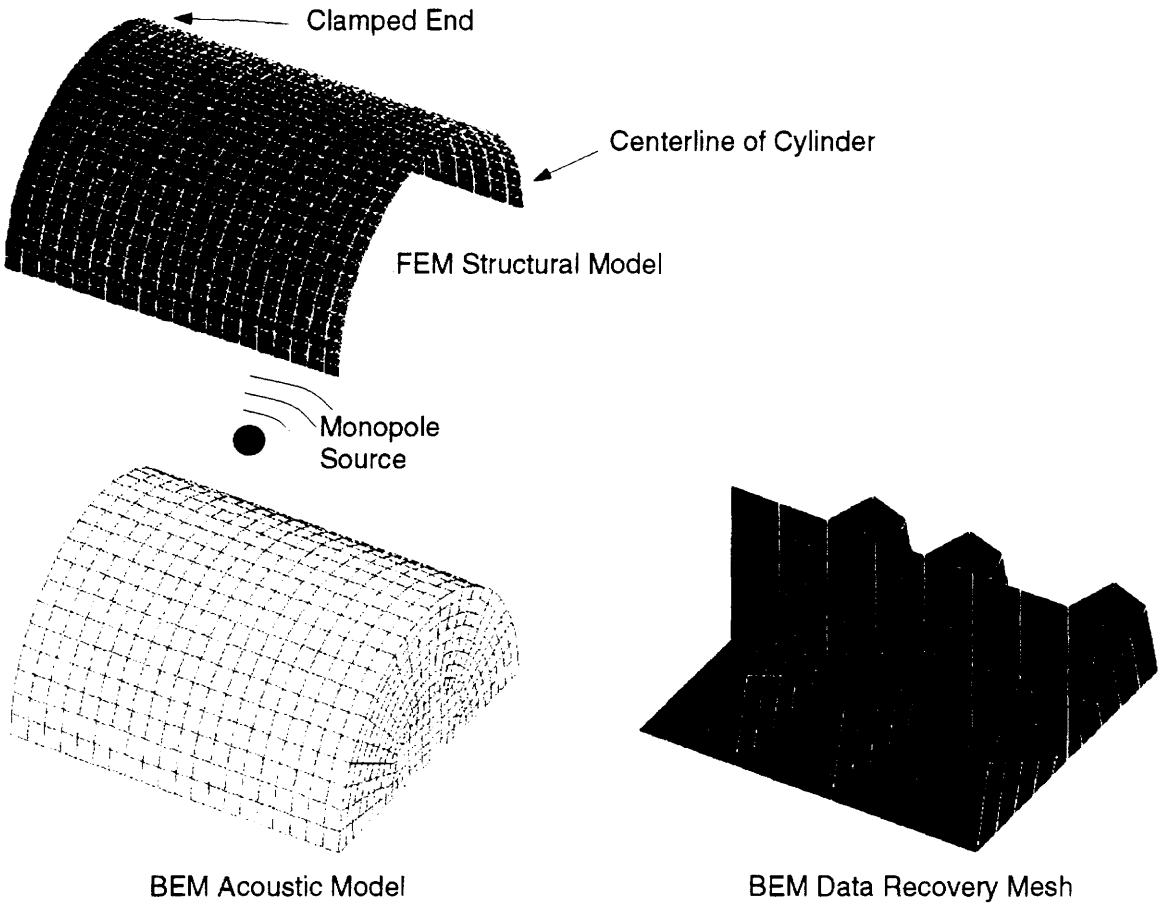

Figure 5. Finite Element and Boundary Element Models

The primary exterior acoustic field is a single monopole source located at 0.168 m from the shell and at x/L=0.5 and θ=0 (similar to Reference 2). Since a one-way coupled structural acoustic formulation is utilized here, the exterior acoustic problem had to be solved separately. This problem is composed of radiation of the monopole onto the rigid cylinder (blocked pressure), and was solved using COMET/ACOUSTICS to produce the complex acoustic pressures on the surface of the shell. A FORTRAN code was written to integrate these pressures to produce equivalent complex nodal forces to use in the NASTRAN structural model.

Figure 5 also illustrates the BEM boundary mesh and data recovery interior mesh. The boundary mesh density was set to handle the wavelengths appropriate for an analysis frequency of 250 Hz or less. The data recovery mesh was modeled after that in Reference 2, however the mesh density was dramatically reduced to keep the CPU time in computing sensitivity derivatives reasonable. A total of 188 data recovery nodes were used in this mesh.

A modal solution is used to compute the structural velocity response in NASTRAN, using modal contributions out to 300 Hz. Modal (viscous) damping at 1% of critical is applied to the cylinder. Figure 6 shows the vibration natural modes of this unstiffened cylinder, the vibration natural modes of the stiffened cylinder (to be discussed in the next section), and the acoustic natural modes of the cylindrical cavity. For the cavity only the zero radial modes are plotted in Figure 6. Due to the symmetry defined in the problem, only odd axial mode numbers of the structure occur, and only even axial modes of the cavity are excited. The frequency selected for the monopole excitation and the optimization corresponds to that of the (2,1) mode of the cylinder at 154.2 Hz. A contour of this mode shape is shown in Figure 7. This mode was selected as one that responds well to the excitation, and efficiently forces the cavity. In Figure 6, it is seen that the (2,1) structural mode at 154.2 Hz forces the off resonance response of the (2,0) and (2,2) acoustic modes at 197.2 and 218.0 Hz, respectively.

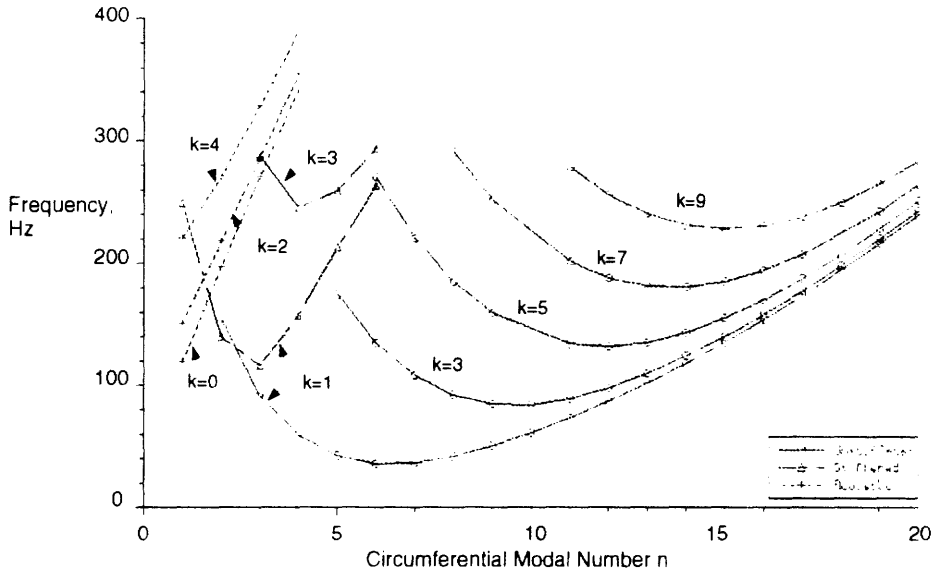

Figure 6. Cylinder and Cavity Natural Modes (k = axial mode no.)

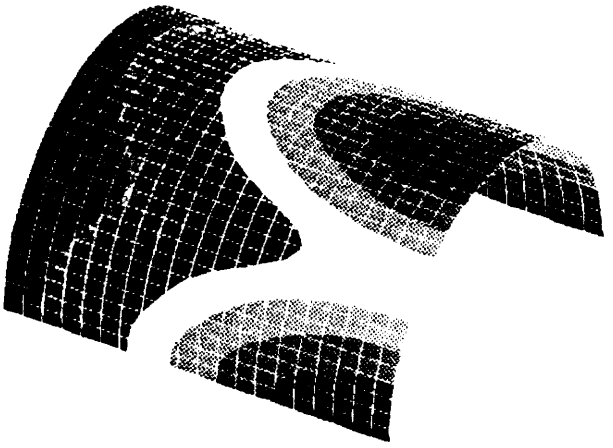

Figure 7. Contour of (2,1) Cylinder Natural Mode (154.2 Hz)

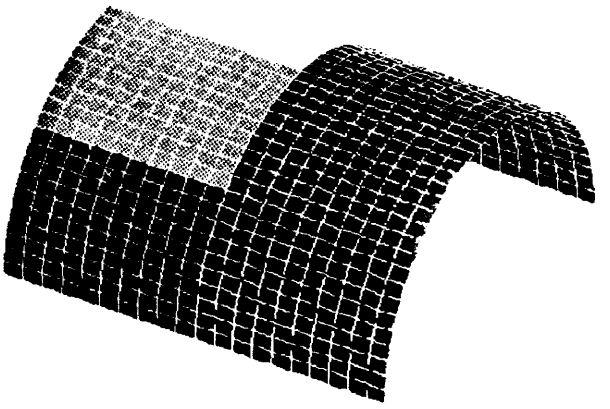

Figure 8. Initial Thickness Design Variable Groups

3.1.2 Optimization Results. Initially a coarse grouping of design variables was selected so that eight groups of elements had the same thickness design variable. These thickness design groups are illustrated in Figure 8. The interior noise level contours for the initial uniform thickness cylinder are shown in Figure 9. The actual peak interior level was 149.2 dB (note that this is very high due to the arbitrary selection of the magnitude of the external monopole source).

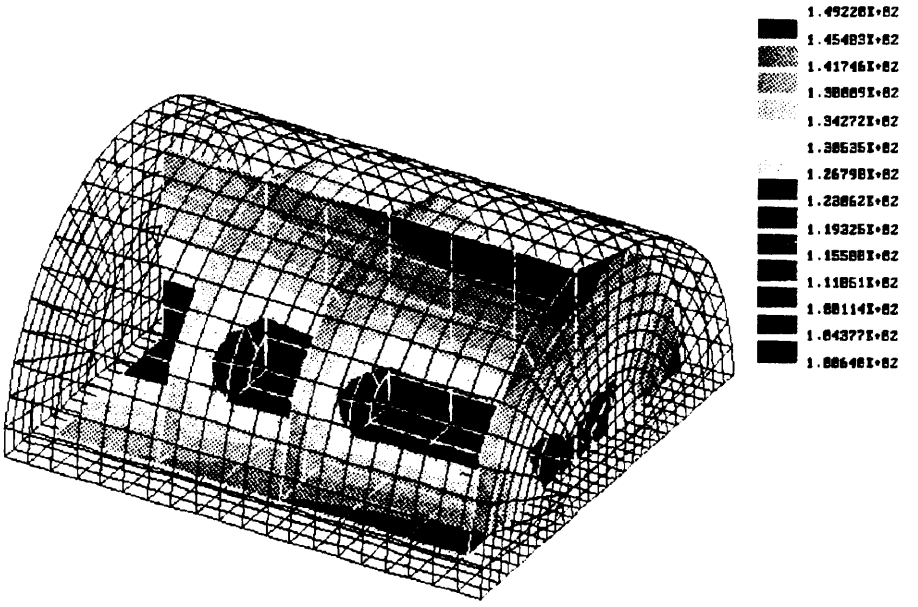

Figure 9. Interior Acoustic Levels for Uniform Thickness Cylinder (dB)

The optimal thickness distribution and resulting acoustic contours are illustrated in Figures 10 and 11, respectively. It is interesting to note that the optimized thickness distribution and acoustic contours show the effect of the nonsymmetric loading on one side of the shell. The peak acoustic level has been reduced to 121.7 dB, a reduction of 27.5 dB. The structural resonances adjacent to the 154.2 Hz excitation/optimization frequency are now 151.0 and 157.5 Hz, so the structure is now being excited off resonance. Figure 12 shows a contour of the resonance at 151.0 Hz. Note that the mode is very complex with very short wavelength motion, both in the axial and circumferential directions. This mode does not couple well with the global acoustic response of the cavity. The other nearby structural modes are very similar to this mode, and the (2,1) mode disappeared altogether. Note also that this mode is actually too complex in the circumferentiral direction for the grid density of the FEM model to capture accurately.

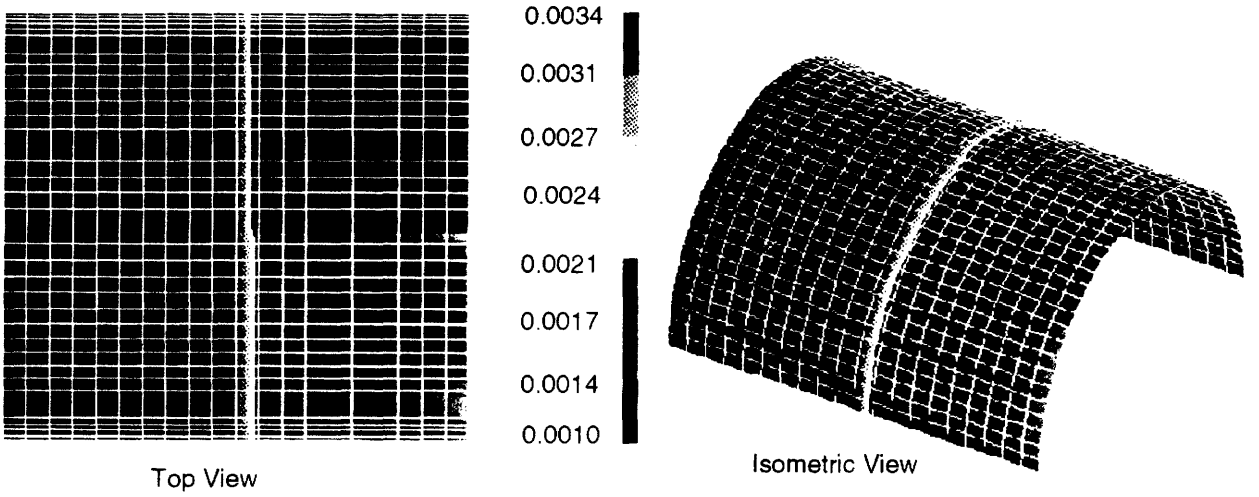

Figure 10. Contours of Optimal Thickness Distribution (mm)

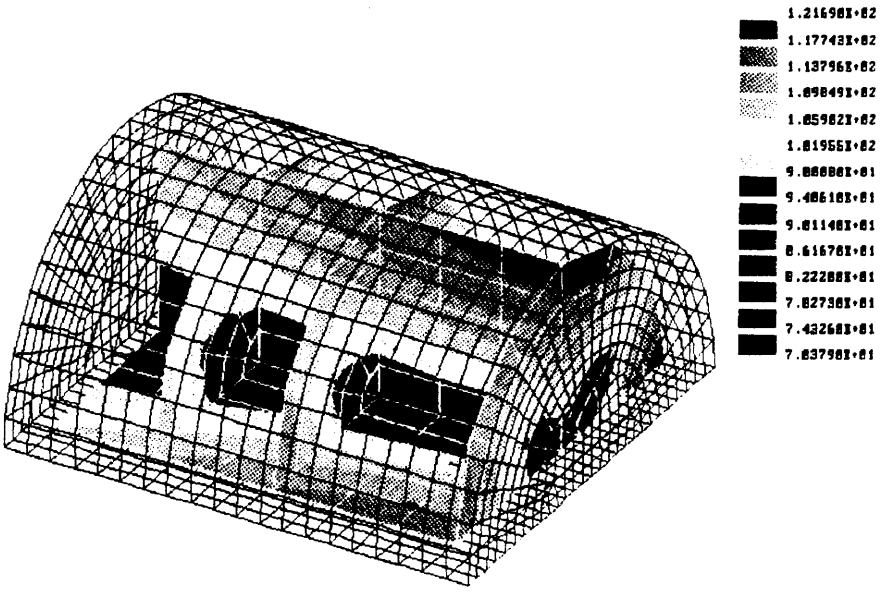

Figure 11. Optimized Acoustic Levels (dB)

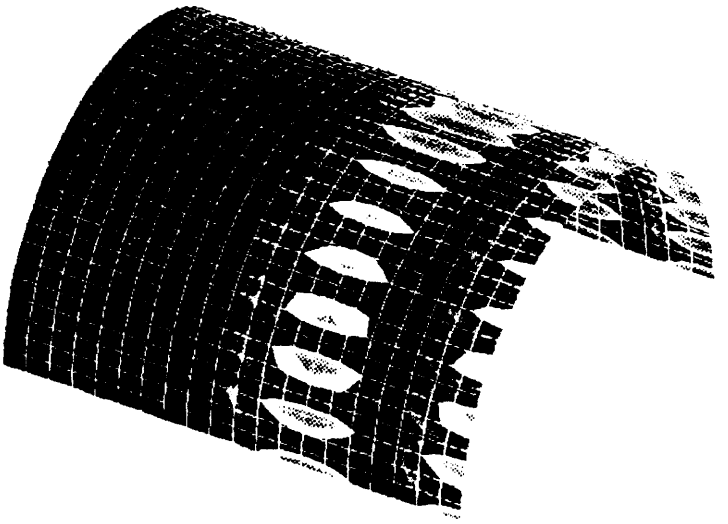

Figure 12. Contours of Resonance at 151.0 Hz

Next two other thickness design variable groups were tested, to study the effects of circumferential and longitudinal variation of the thickness. These are illustrated in Figure 13. For brevity, the results will not be illustrated here.

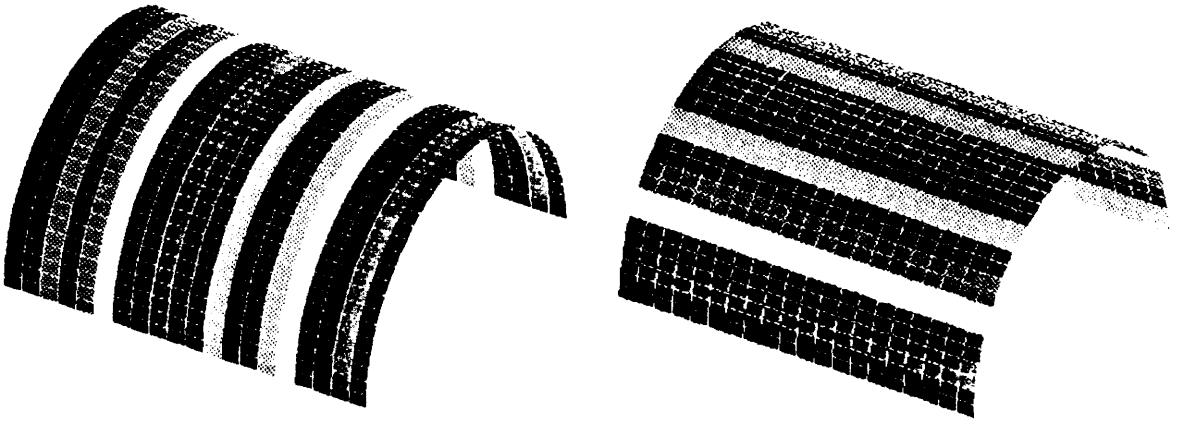

Figure 13. Design Variable Grouping Studies

3.1.3 Algorithm Performance. For each of the uniform cylinder models, the starting design vector was a uniform thickness distribution which yielded a structural resonance near the frequency of interest. For the model with design variables grouped in 20 circumferential strips, a starting design vector with all variables set to their upper bounds was also considered. Table 1 summarizes the results of the optimization in terms of the objective function. Clearly, the routine is capable of producing designs that yield significant reductions in interior noise levels at a single frequency. At this time, we have no assessment as to how the designs perform at other than the design frequency.

Table 1. Starting values, ending values and dB reduction in the objective function for each model and starting design vector

Model	Starting F	Ending F	dB reduction
Uniform, 8 variables	1.0	0.00126	29.0
Uniform, 20 variables, circumferential	1.0	0.00173	27.6
Uniform, 20 variables all at upper bound, circumferential	1.0	0.00513	22.9

In addition to the results presented above, we are interested in the computational efficiency of the algorithm. Measures of computational efficiency are the average, maximum and minimum execution times for each of the codes that constitute the algorithm. Tables 2 and 3 summarize the performance for each of the models considered here. The times are elapsed clock times, not cpu time, so the influence of varying user loads on the NASA Langley ALPHA and DEC 5000 are included. The time for CONMIN is the time in each iteration that CONMIN is actually processing. With the current algorithm and control script, CONMIN is always executing, but it spends the vast majority of the time waiting for the external codes to complete their tasks.

Table 2 - Uniform cylinder with 8 design variable groupings. Average, maximum and minimum execution times, minutes.

Program	Average	Max	Min
CONMIN (per iteration)	0.9	1.4	0.1
NASTRAN	36.6	131.5	8.8
COMET/ACOUSTIC	3.4	5.7	1.5
VBCGEN	0.3	0.6	0.1
MERGE	100.8	166.4	39.0

Table 3 - Uniform cylinder with 20 design variable groupings, circumferentially oriented. Average, maximum and minimum execution times, minutes.

Program	Average	Max	Min
CONMIN (per iteration)	1.5	2.0	0.2
NASTRAN	25.0	40.0	8.0
COMET/ACOUSTIC	4.0	12.5	1.5
VBCGEN	0.5	1.3	0.1
MERGE	270	1020	90

Total execution time for the algorithm depends on how many function and gradient evaluations are performed. Due to a number of factors, the algorithm tends to not run without interruptions. Interruptions require user intervention to restart the control script. The model with 8 design variables took approximately three days to converge to a solution, including numerous interruptions. The model with 20 circumferential design variable groupings took eight days, with interruptions, for the first converged solution. With the design variables set at the upper bound, this model took 89 hours to converge, including one 14 hour interruption. The significant differences in these overall execution times are caused by the difference in the total number of function and gradient evaluations required.

The production runs to date have identified a number of issues that will require addressing. The generation of the initial acoustic sensitivity data, $\partial p/\partial v$, by COMET/ACOUSTICS requires an unacceptable amount of time. For the 188 data recover nodes in the models used, COMET/ACOUSTICS required 39 hours to generate sensitivities. Once generated, however, they were used in all subsequent analyses. The MERGE program, which performs the chain-rule calculation, is also a significant bottleneck.

3.2 Stiffened Cylinder

In this study, frame and stringer stiffeners were added to the cylinder. The optimization was performed with the same objective to minimize global acoustic levels, however the design variables were selected to be the heights of the frame stiffeners.

3.2.1 Model Description. This model has exactly the same degrees of freedom as in the unstiffened problem since the frame and stringer stiffeners are modeled using offset beam elements. Figure 14 shows the FEM model with stiffeners, including the cross section dimensions.

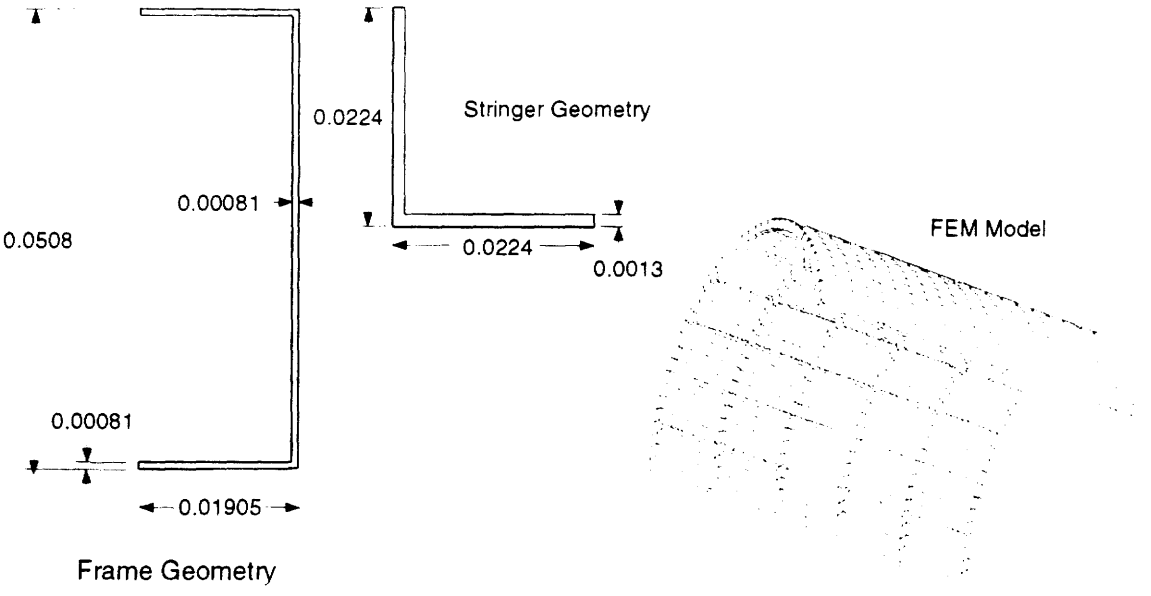

Figure 14. FEM Model with Stiffeners

3.2.2. Optimization Results. Eighteen groups of beam elements were chosen with independent frame stiffener design variables and are shown in Figure 15. The equations relating the area and inertias of these beams to the cross section dimensions were incorporated in the NASTRAN file using DEQATN and DVPREL2 input cards. These nonlinear relationships allowed the element properties to be related to the height dimension of the stiffeners. The same structural resonance (2,1) mode was studied, which for this problem is at a frequency of 139.5 Hz. At this frequency, the coupling with the cavity was less efficient than the unstiffened model, with a peak acoustic level of 101.7 dB. An optimal design for this stiffened cylinder was not achieved by the time this document was written, as the analysis was still in progress.

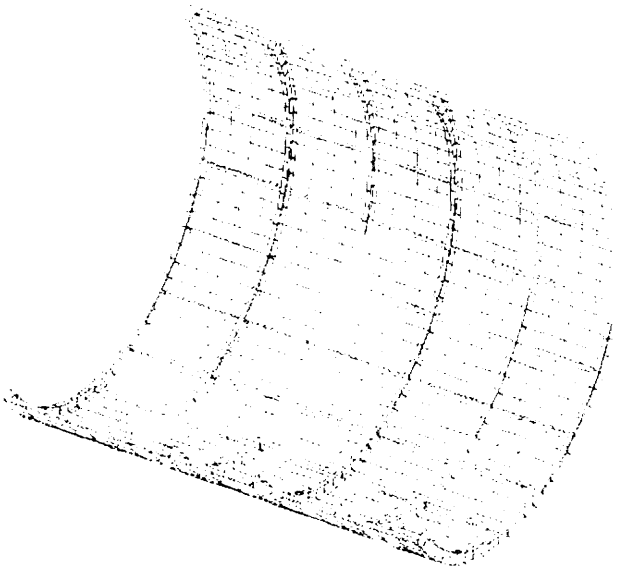

Figure 15. Frame Stiffener Design Variable Groupings

4. PLANS FOR FUTURE WORK

While this year's efforts involved optimization at a single frequency, the goal for next year's work will be to improve the optimization algorithm so that multi-frequency optimal design can be performed. Thus the ability to optimize multiple peaks across a frequency range will be investigated. Utilizing the uniform and stiffened cylinder study problems, the CONMIN optimization code will be modified so that resonance frequency tracking will be performed as opposed to simple resonance avoidance. This will allow the optimization procedure to follow resonance peaks, thereby tailoring the structural natural modes so that they become inefficient acoustic radiators.

New and more complicated optimization objective functions will be studied. Composite objective functions which minimize noise transmission with side conditions on weight as well as those that minimize weight with a side condition on noise transmission will be evaluated. As the first year's work only optimized the sum of squared acoustic pressure in the cavity interior, the

performance of other acoustic quantities will be investigated in the objective function, such as acoustic power, intensity or energy density.

Studies which improve the computational efficiency of the design algorithm will be investigated. Advantages/disadvantages of the fully coupled indirect BEM solution versus the one-way coupled solution will be evaluated as pertain to sensitivity computation and other CPU bottlenecks. Refinements in design variable groupings will be made to reduce the CPU expenditure for NASTRAN sensitivities. A complimentary optimization algorithm will be developed that implements the same functionality as the current CONMIN based optimizer, but which uses the nonlinear SIMPLEX algorithm. This optimization algorithm will be used to efficiently search the boundaries of the design space for the optimum solution on the boundary.

The resonance tracking capability will require improvement to the COMET/ACOUSTICS code in order to increase efficiency. As the current CPU bottleneck in the algorithm is the computation of acoustic sensitivities in the COMET/ACOUSTICS code and the resultant chain rule computations in the MERGE program, a close scrutiny of these calculations will be made to reduce the CPU time. COMET/ACOUSTICS will be modified to incorporate frequency interpolation on both acoustic pressure and sensitivity. Since sensitivity calculations are only made in the one-way coupled solutions, sensitivity calculations will be developed for the fully coupled indirect solution, to investigate the potential for CPU savings.

To improve the generality of the overall optimization algorithm, the data translators VBCGEN and MERGE will be upgraded to handle general coordinate systems. NASTRAN DMAP code will be developed to implement resonance tracking in NASTRAN, as well.

5. CONCLUDING REMARKS

Much has been accomplished this year towards achieving our overall objectives. With the valuable assistance from AAC in supplying translator codes, a computational algorithm has been assembled for single frequency optimization using NASTRAN (FEM), COMET/ACOUSTICS (BEM), and CONMIN (optimizer). Preliminary optimization results were obtained on the unstiffened shell, and optimization runs were in progress for the stiffened shell at the time this report was written.

Next year's efforts will involve multi-frequency optimization with frequency tracking (to remain on-resonance with the structural natural modes) within a frequency band. Different objective function formulations, as well as improvements to the computational efficiency of the design algorithm will be investigated.

6. REFERENCES

1. Jackson, A.C., Balena, F.J., LaBarge, W.L., Pei, G., Pitman, W.A., and Wittlin, G., "Transport Composite Fuselage Technology - Impact Dynamics and Acoustic Transmission," NASA CR - 4035, 1986.

2. Grosveld, F.W., Coats, T.J., Lester, H.C., and Silcox, R.J., "A Numerical Study of Active Structural Acoustic Control in a Stiffened, Double Wall Cylinder," Proceedings of NOISE-CON 94, National Conference on Noise Control Engineering, Ft. Lauderdale, Fl., May 1-4, 1994, pp. 404-408.

Appendix A. Usage guide to NASA shell script

Usage: $Cmd -c CFile -n NFile -a AFile [options]

required:

-c CFILE Fully qualified filename of the CONMIN input file

-n NFILE Filename of the NASTRAN input file, without .dat extension

-a AFILE Filename of the COMET/ACOUSTIC input file, without .dat extension

options:

-u username user name on remote host. Use if your username on the remote host is different from that on the local host

-p programname name of the code to launch as optimization code. CONMIN is the default.

-m memorysize size of the COMET executeable, in form XXM, where XX is a number (4, 8, 16, 32). 4M is the default.

-r hostname machine name for remote host. Use if NASTRAN is to run on other than risque. risque is the default

-s Flag to indicate that a COMET sensitivity file already exists, with name AFILE.srslt

-M Flag to indicate that initial MERGE results already exist, with root names NFILE

-N Flag to indicate that Nastran results already exists, with root names NFILE

-P Flag to indicate that COMET pressure results already exist, with root name AFILE

-R Flag to indicate that COMET restart file already exists, with root name AFILE

$Cmd refers to the current name of the shell script. The most current version is /usr2/users/cunefare/bin/ns3. If you put the directory /usr2/users/cunefare/bin on your search path, you need only issue "ns3" as the command. You may also copy the script to your own /bin directory (which should be on your search path). If you do not do either of these, you must provide the full directory specification to execute the script.

As of 7/27/94, there is a known bug that will kill CONMIN if you log off before the optimization is completed. We are investigating this, but have no effective solution or work-around at present, other than not logging off.

The CONMIN input file name must be the complete name of the file containing the basic CONMIN parameter definitions. CONMIN writes user specified debug and progress statements to the file "log.dat". These are statements generated in the user portion of CONMIN. CONMIN also writes user requested optimization data to the file CONMIN.out. These are statements generated by the optimization portion of the code (see the CONMIN quick reference guide for various print options).

The NASTRAN input file name must be the root file name, without a ".dat" extension. Note that

the input file to NASTRAN will always have the ".dat" extension. This is in accordance with the manner in which a user would call NASTRAN, independent of the script. The script builds the names of the output files (.sens, .f06, etc.) from the root name, appending the suffixes as necessary. The script will extract the sensitivity output file name specified on the "ASSIGN OUTPUT4=filename..." line of the NASTRAN input file.

The COMET/ACOUSTIC input file name must be the root file name, without a ".dat" extension. Note that the actual input file to COMET must always have the ".dat" extension. The script builds the names of the output files from the root name, appending the suffixes as necessary. Note that the COMET input file includes a line for the jobname. **The jobname must match the COMET input filename**. Output from COMET is stored in comet.out. Merge_sense.exe writes its standard output and error to merge_sense.exe.out, while vbcgen writes its error output to vbcgen.err.

The -s, -M, -N, -P and -R options provide the user a restart capability for the script, and the capability to perform the initial acoustic sensitivity analysis independent of the shell script. These options apply to files that are generated for the same set of velocity boundary conditions and design variables.

-s tells the script that a COMET/ACOUSTIC sensitivity file already exists, and that its name is AFILE.srslt. The script assumes that the current AFILE.dat has been modified such that it is asking for a pressure solution, and to generate a COMET/ACOUSTIC restart file.

-P tells the script that an initial pressure solution has already been generated, and an associated COMET/ACOUSTIC restart file, for the current velocities and design variables. The script assumes the pressures are in the file AFILE.rslt, and the restart file is AFILE.rest. The script assumes that the AFILE.dat file is configured to generate pressure solutions from the restart file.

-R tells the script that a COMET/ACOUSTIC restart file exits, but not pressures. The script assumes restart file name is AFILE.rest. The script assumes that the AFILE.dat file is configured to generate pressure solutions from the restart file.

NOTE: If the user specifies the -P option, the -s option must also be specified.

-M tells the script that a MERGE output file already exists, for the current velocities and design variables. The script assumes the file's name is AFILE.sens.

-N tells the script that NASTRAN has already been executed for the current design variables. The script assumes the output files are named NFILE.ext, where .ext refers to the extensions of the various files generated by NASTRAN.

The script will test for the existence of the files that are implied by the s, M, N, P and R options. If these files do not exist, the script will abort with an error message.

E-25-W56
#'s 7, 8, 9, 10, 11

LOCKHEED AERONAUT SY CO-GA
GEORGIA INSTITUTE OF TECHNOLOGY
ANALYSIS OF PERSONAL SERVICES
CONTRACT TERM 03-21-94 - 10-31-96
CONTRACT #RF 72760
PRIME #NAS1-20102, TASK ASSIGNMENT #6

EMPLOYEE	TITLE	MONTH	ANNUAL SALARY		TIME	AMOUNT	ESTIMATED
JULY 1, 1995 - OCTOBER 31, 1995							
BIESEL, VAN B.	RES ENGR I	JUL	3,621.66	MONTHLY	50.00%	1,810.84	43.33
		AUG	3,621.66	MONTHLY	50.00%		0.00
		SEP	3,621.66	MONTHLY	50.00%		0.00
		OCT	3,621.66	MONTHLY	50.00%		0.00
		NOV	3,621.66	MONTHLY	50.00%		0.00
		DEC	3,621.66	MONTHLY	50.00%		0.00
		JAN	3,621.66	MONTHLY	50.00%		0.00
		FEB	3,621.66	MONTHLY	50.00%		0.00
		MAR	3,621.66	MONTHLY	50.00%		0.00
		APR	3,621.66	MONTHLY	50.00%		0.00
		MAY	3,621.66	MONTHLY	50.00%		0.00
		JUN	3,621.66	MONTHLY	50.00%		0.00
	TOTAL					1,810.84	43.33
CRANE, SCOTT P.	GRAD ASST	JUL	1,250.00	MONTHLY	33.00%	1,250.00	57.20
		AUG	1,250.00	MONTHLY	33.00%		0.00
		SEP	1,250.00	MONTHLY	33.00%		0.00
		OCT	1,250.00	MONTHLY	33.00%		0.00
		NOV	1,250.00	MONTHLY	33.00%		0.00
		DEC	1,250.00	MONTHLY	33.00%		0.00
		JAN	1,250.00	MONTHLY	33.00%		0.00
		FEB	1,250.00	MONTHLY	33.00%		0.00
		MAR	1,250.00	MONTHLY	33.00%		0.00
		APR	1,250.00	MONTHLY	33.00%		0.00
		MAY	1,250.00	MONTHLY	33.00%		0.00
		JUN	1,250.00	MONTHLY	33.00%		0.00
	TOTAL					1,250.00	57.20
CUNEFARE, KENNETH	ASST PROF	JUL	6,066.04	MONTHLY	18.80%	4,586.16	24.64
		AUG	6,066.04	MONTHLY	18.80%		0.00
		SEP	6,066.04	MONTHLY	18.80%		0.00
		OCT	6,066.04	MONTHLY	18.80%		0.00
		NOV	6,066.04	MONTHLY	18.80%		0.00
		DEC	6,066.04	MONTHLY	18.80%		0.00
		JAN	6,066.04	MONTHLY	18.80%		0.00
		FEB	6,066.04	MONTHLY	18.80%		0.00
		MAR	6,066.04	MONTHLY	18.80%		0.00
		APR	6,066.04	MONTHLY	18.80%		0.00
		MAY	6,066.04	MONTHLY	18.80%		0.00
		JUN	6,066.04	MONTHLY	18.80%		0.00
	TOTAL					4,586.16	24.64
8/4/95E25W56B.XLS							
	GRAND TOTAL FOR 1994-95					7,647.00	125.17

LOCKHEED AERONAUTICAL SYSTEMS CO-GA
GEORGIA INSTITUTE OF TECHNOLOGY
ANALYSIS OF PERSONAL SERVICES
CONTRACT TERM ... - 10-31-95
CONTRACT ...
PRIME #NAS1-20102 ... ASSIGNMENT #6

EMPLOYEE	TITLE	MONTH	ANNUAL SALARY		TIME	AMOUNT	ESTIMATED
JULY 1, 1993 - JUNE 30, 1994							
BIESEL, VAN B.	RES ENGR I	JUL	3,395.31	MONTHLY	50.00%		0.00
		AUG	3,395.31	MONTHLY	50.00%		0.00
		SEP	3,395.31	MONTHLY	50.00%		0.00
		OCT	3,395.31	MONTHLY	50.00%		0.00
		NOV	3,395.31	MONTHLY	50.00%		0.00
		DEC	3,395.31	MONTHLY	50.00%		0.00
		JAN	3,395.31	MONTHLY	50.00%		0.00
		FEB	3,395.31	MONTHLY	50.00%		0.00
		MAR	3,395.31	MONTHLY	50.00%		0.00
		APR	3,395.31	MONTHLY	50.00%		0.00
		MAY	3,395.31	MONTHLY	50.00%		0.00
		JUN	3,395.31	MONTHLY	50.00%		0.00
							0.00
CRANE, SCOTT P.	... ASST	JUL	1,375.00	MONTHLY	33.00%		0.00
		AUG	1,375.00	MONTHLY	33.00%		0.00
		SEP	1,375.00	MONTHLY	33.00%		0.00
		OCT	1,375.00	MONTHLY	33.00%		0.00
		NOV	1,375.00	MONTHLY	33.00%		0.00
		DEC	1,375.00	MONTHLY	33.00%		0.00
		JAN	1,375.00	MONTHLY	33.00%		0.00
		FEB	1,375.00	MONTHLY	33.00%		0.00
		MAR	1,375.00	MONTHLY	33.00%		0.00
		APR	1,375.00	MONTHLY	33.00%		0.00
		MAY	1,375.00	MONTHLY	33.00%		0.00
		JUN	1,375.00	MONTHLY	33.00%		0.00
	TOTAL					0.00	0.00
CUNEFARE, KENNETH	ASST PROF	JUL	6,066.04	MONTHLY	18.80%		0.00
		AUG	6,066.04	MONTHLY	18.80%		0.00
		SEP	6,066.04	MONTHLY	18.80%		0.00
		OCT	6,066.04	MONTHLY	18.80%		0.00
		NOV	6,066.04	MONTHLY	18.80%		0.00
		DEC	6,066.04	MONTHLY	18.80%		0.00
		JAN	6,066.04	MONTHLY	18.80%		0.00
		FEB	6,066.04	MONTHLY	18.80%		0.00
		MAR	6,066.04	MONTHLY	18.80%		0.00
		APR	6,066.04	MONTHLY	18.80%	2,143.08	11.56
		MAY	6,066.04	MONTHLY	18.80%	2,143.08	11.56
		JUN	6,066.04	MONTHLY	18.80%		0.00
	TOTAL					4,286.16	23.11
8/4/95E25W56B.XLS							
	GRAND TOTAL FOR 1994-95					4,286.16	23.11

E-25-W56 #12

GEORGIA INSTITUTE OF TECHNOLOGY
OFFICE OF GRANTS AND CONTRACTS ACCOUNTING

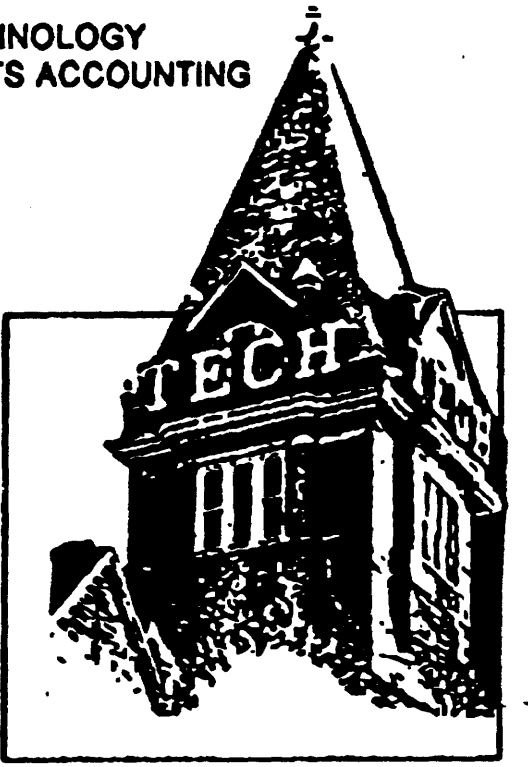

190 BOBBY DODD WAY
ATLANTA, GEORGIA 30332-0259

DATE: 9-13 95

NUMBER OF PAGES 7
(INCLUDING THIS PAGE)

TO: Wanda Simon

FROM: Jill Redmond 4-6757

SUBJECT: E-25-W56 Deliverable

MESSAGE: Sept Deliverable

(IF THIS MESSAGE IS ILLEGIBLE OR IF THERE IS A TRANSMISSION PROBLEM, PLEASE CALL (404) 894-4624).

GEORGIA TECH RESEARCH CORPORATION

PLEASE REMIT TO:
GEORGIA TECH RESEARCH CORPORATION
P.O. BOX 100117
ATLANTA, GEORGIA 30384

INVOICE NO. E-25-W56 - 0906
246R81190A0

PAYABLE UPON RECEIPT OF INVOICE
PAYER'S ACCOUNT NUMBER:
RK72740

LASC-GEORGIA
ATTN: ACCOUNTS PAYABLE
S/81-49, ZONE 0285
86 SOUTH COBB DRIVE
MARIETTA GA 30063-0285

GTRC ACCOUNTING
No. _____
Date _____
D D _____
_____

INVOICE DATE	DESCRIPTION	CUMULATIVE AMOUNT	CURRENT AMOUNT
8/01/95	OPTIMIZATION IN STRUCTURAL ACOUSTICS USING FEM/BEM PRIME: NAS1-20102 TASK 5		
TO	PERSONAL SERVICES	50,405.04	7,647.0
	FRINGE BENEFITS	9,054.59	1,586.4
	MATERIALS AND SUPPLIES	3,263.81	51.0
	OTHER INDIRECT		
8/31/95	EQUIPMENT	3,365.00	
	TRAVEL	2,964.10	
	CAPITAL OUTLAY		
	SUBCONTRACTS NON-MTDC		
	SUBCONTRACTS MTDC		
	INDIRECT	26,560.80	3,992.3
		95,613.34	13,276.7

I certify that all expenditures reported (or payment requested) are for appropriate purposes and in accordance with the provisions of the application and award documents

David V. Welch, Director Grants & Cont. Accts.

IF YOU HAVE QUESTIONS CONCERNING THIS INVOICE,
CONTACT: JILL REDMOND PHONE: (404)894-6757

PLEASE PAY THIS TOTAL AMOUNT > $ 13,276.7

RETURN THIS COPY WITH PAYMENT

LOCKHEED AERONAUT SY CO-GA
GEORGIA INSTITUTE OF TECHNOLOGY
ANALYSIS OF PERSONAL SERVICES
CONTRACT TERM 03-21-94 - 10-31-95
CONTRACT #RF72740
PRIME #NAS1-20102, TASK ASSIGNMENT #5

EMPLOYEE	TITLE	MONTH	MONTHLY SALARY		TIME	PROJECT AMOUNT	**ESTIMATED HOURS
JULY 1, 1994 - JUNE 30, 1995							
BIESEL, VAN B.	RES ENGR I	JUL	3,395.31	MONTHLY	50.00%		0.00
		AUG	3,395.31	MONTHLY	50.00%		0.00
		SEP	3,395.31	MONTHLY	50.00%		0.00
		OCT	3,395.31	MONTHLY	50.00%		0.00
		NOV	3,395.31	MONTHLY	50.00%		0.00
		DEC	3,395.31	MONTHLY	50.00%	1,009.47	25.87
		JAN	3,395.31	MONTHLY	50.00%	1,708.33	43.77
		FEB	3,395.31	MONTHLY	50.00%	1,708.33	43.77
		MAR	3,395.31	MONTHLY	50.00%	1,708.33	43.77
		APR	3,395.31	MONTHLY	50.00%	1,708.33	43.77
		MAY	3,395.31	MONTHLY	50.00%	1,708.33	43.77
		JUN	3,395.31	MONTHLY	50.00%	1,708.33	43.77
	TOTAL					11,259.45	288.51
CRANE, SCOTT P.	GRAD ASST	JUL	1,375.00	MONTHLY	33.00%	1,333.33	55.68
		AUG	1,375.00	MONTHLY	33.00%	1,333.33	55.68
		SEP	1,375.00	MONTHLY	33.00%	1,333.33	55.68
		OCT	1,375.00	MONTHLY	33.00%	1,250.00	52.20
		NOV	1,375.00	MONTHLY	33.00%	1,250.00	52.20
		DEC	1,375.00	MONTHLY	33.00%	1,250.00	52.20
		JAN	1,375.00	MONTHLY	33.00%	183.34	7.66
		FEB	1,375.00	MONTHLY	33.00%	183.34	7.66
		MAR	1,375.00	MONTHLY	33.00%	183.34	7.66
		APR	1,375.00	MONTHLY	33.00%	183.34	7.66
		MAY	1,375.00	MONTHLY	33.00%	183.34	7.66
		JUN	1,375.00	MONTHLY	33.00%	183.34	7.66
	TOTAL					8,850.03	369.58
CUNEFARE, KENNETH	ASST PROF	JUL	6,066.04	MONTHLY	18.80%	2,857.44	15.41
		AUG	6,066.04	MONTHLY	18.80%	2,857.44	15.41
		SEP	6,066.04	MONTHLY	18.80%	2,857.44	15.41
		OCT	6,066.04	MONTHLY	18.80%		0.00
		NOV	6,066.04	MONTHLY	18.80%		0.00
		DEC	6,066.04	MONTHLY	18.80%		0.00
		JAN	6,066.04	MONTHLY	18.80%		0.00
		FEB	6,066.04	MONTHLY	18.80%		0.00
		MAR	6,066.04	MONTHLY	18.80%		0.00
		APR	6,066.04	MONTHLY	18.80%		0.00
		MAY	6,066.04	MONTHLY	18.80%		0.00
		JUN	6,066.04	MONTHLY	18.80%		0.00
	TOTAL					8,572.32	46.23
	GRAND TOTAL FOR 1994-95					28,681.80	704.31

LOCKHEED AERONAUT SY CO-GA
GEORGIA INSTITUTE OF TECHNOLOGY
ANALYSIS OF PERSONAL SERVICES
CONTRACT TERM 03-21-94 - 10-31-95
CONTRACT #RF72740
PRIME #NAS1-20102, TASK ASSIGNMENT #6

EMPLOYEE	TITLE	MONTH	MONTHLY SALARY		TIME	PROJECT AMOUNT	**ESTIMATED HOURS
JULY 1, 1993 - JUNE 30, 1994							
BIESEL, VAN B.	RES ENGR I	JUL	3,395.31	MONTHLY	50.00%		0.00
		AUG	3,395.31	MONTHLY	50.00%		0.00
		SEP	3,395.31	MONTHLY	50.00%		0.00
		OCT	3,395.31	MONTHLY	50.00%		0.00
		NOV	3,395.31	MONTHLY	50.00%		0.00
		DEC	3,395.31	MONTHLY	50.00%		0.00
		JAN	3,395.31	MONTHLY	50.00%		0.00
		FEB	3,395.31	MONTHLY	50.00%		0.00
		MAR	3,395.31	MONTHLY	50.00%		0.00
		APR	3,395.31	MONTHLY	50.00%		0.00
		MAY	3,395.31	MONTHLY	50.00%		0.00
		JUN	3,395.31	MONTHLY	50.00%		0.00
	TOTAL					0.00	0.00
CRANE, SCOTT P.	GRAD ASST	JUL	1,375.00	MONTHLY	33.00%		0.00
		AUG	1,375.00	MONTHLY	33.00%		0.00
		SEP	1,375.00	MONTHLY	33.00%		0.00
		OCT	1,375.00	MONTHLY	33.00%		0.00
		NOV	1,375.00	MONTHLY	33.00%		0.00
		DEC	1,375.00	MONTHLY	33.00%		0.00
		JAN	1,375.00	MONTHLY	33.00%		0.00
		FEB	1,375.00	MONTHLY	33.00%		0.00
		MAR	1,375.00	MONTHLY	33.00%		0.00
		APR	1,375.00	MONTHLY	33.00%		0.00
		MAY	1,375.00	MONTHLY	33.00%		0.00
		JUN	1,375.00	MONTHLY	33.00%		0.00
	TOTAL					0.00	0.00
CUNEFARE, KENNETH	ASST PROF	JUL	6,066.04	MONTHLY	18.80%		0.00
		AUG	6,066.04	MONTHLY	18.80%		0.00
		SEP	6,066.04	MONTHLY	18.80%		0.00
		OCT	6,066.04	MONTHLY	18.80%		0.00
		NOV	6,066.04	MONTHLY	18.80%		0.00
		DEC	6,066.04	MONTHLY	18.80%		0.00
		JAN	6,066.04	MONTHLY	18.80%		0.00
		FEB	6,066.04	MONTHLY	18.80%		0.00
		MAR	6,066.04	MONTHLY	18.80%		0.00
		APR	6,066.04	MONTHLY	18.80%	2,143.08	11.56
		MAY	6,066.04	MONTHLY	18.80%	2,143.08	11.56
		JUN	6,066.04	MONTHLY	18.80%		0.00
	TOTAL					4,286.16	23.11
	GRAND TOTAL FOR 1993-94					4,286.16	23.11

LOCKHEED AERONAUT SY CO-GA
GEORGIA INSTITUTE OF TECHNOLOGY
ANALYSIS OF PERSONAL SERVICES
CONTRACT TERM 03-21-94 - 10-31-96
CONTRACT #RF72740
PRIME #NAS1-20102, TASK ASSIGNMENT #5

EMPLOYEE	TITLE	MONTH	MONTHLY SALARY		TIME	PROJECT AMOUNT	**ESTIMATED HOURS
JULY 1, 1995 - OCTOBER 31, 1995							
BIESEL, VAN B.	RES ENGR I	JUL	3,621.68	MONTHLY	50.00%	1,810.84	43.33
		AUG	3,621.68	MONTHLY	50.00%	1,810.84	43.33
		SEP	3,621.68	MONTHLY	50.00%		0.00
		OCT	3,621.68	MONTHLY	50.00%		0.00
		NOV	3,621.68	MONTHLY	50.00%		0.00
		DEC	3,621.68	MONTHLY	50.00%		0.00
		JAN	3,621.68	MONTHLY	50.00%		0.00
		FEB	3,621.68	MONTHLY	50.00%		0.00
		MAR	3,621.68	MONTHLY	50.00%		0.00
		APR	3,621.68	MONTHLY	50.00%		0.00
		MAY	3,621.68	MONTHLY	50.00%		0.00
		JUN	3,621.68	MONTHLY	50.00%		0.00
	TOTAL					3,621.68	86.67
CRANE, SCOTT P.	GRAD ASST	JUL	1,250.00	MONTHLY	33.00%	1,250.00	57.20
		AUG	1,250.00	MONTHLY	33.00%	1,250.00	57.20
		SEP	1,250.00	MONTHLY	33.00%		0.00
		OCT	1,250.00	MONTHLY	33.00%		0.00
		NOV	1,250.00	MONTHLY	33.00%		0.00
		DEC	1,250.00	MONTHLY	33.00%		0.00
		JAN	1,250.00	MONTHLY	33.00%		0.00
		FEB	1,250.00	MONTHLY	33.00%		0.00
		MAR	1,250.00	MONTHLY	33.00%		0.00
		APR	1,250.00	MONTHLY	33.00%		0.00
		MAY	1,250.00	MONTHLY	33.00%		0.00
		JUN	1,250.00	MONTHLY	33.00%		0.00
	TOTAL					2,500.00	114.40
CUNEFARE, KENNETH	ASST PROF	JUL	6,066.04	MONTHLY	18.80%	4,586.16	24.64
		AUG	6,066.04	MONTHLY	18.80%	4,586.16	24.64
		SEP	6,066.04	MONTHLY	18.80%		0.00
		OCT	6,066.04	MONTHLY	18.80%		0.00
		NOV	6,066.04	MONTHLY	18.80%		0.00
		DEC	6,066.04	MONTHLY	18.80%		0.00
		JAN	6,066.04	MONTHLY	18.80%		0.00
		FEB	6,066.04	MONTHLY	18.80%		0.00
		MAR	6,066.04	MONTHLY	18.80%		0.00
		APR	6,066.04	MONTHLY	18.80%		0.00
		MAY	6,066.04	MONTHLY	18.80%		0.00
		JUN	6,066.04	MONTHLY	18.80%		0.00
	TOTAL					9,172.32	49.27
	GRAND TOTAL FOR 1995-96					15,294.00	250.34

LOCKHEED AERONAUT SY CO-GA
GEORGIA INSTITUTE OF TECHNOLOGY
ANALYSIS OF PERSONAL SERVICES
CONTRACT TERM 03-21-94 - 10-31-96
CONTRACT #RF72740
PRIME #NAS1-20102, TASK ASSIGNMENT #5

EMPLOYEE	TITLE	MONTH	MONTHLY SALARY	TIME	PROJECT AMOUNT	**ESTIMATED HOURS

** NOTE: Georgia Tech does not track personal service charges for professional staff by the hour. We use the Planned-Confirmation System as required by the Federal goverment's guidlines in Circular A-21. The figures here are estimates based upon the annual salary, the number of work hours in a year, the percentage of budgeted effort as required by the contract, and the actual charges each month for this project.

GEORGIA TECH RESEARCH CORPORATION E-25-W56 #13

PLEASE REMIT TO:
GEORGIA TECH RESEARCH CORPORATION
P.O. BOX 100117
ATLANTA, GEORGIA 30384

INVOICE NO. E-25-W56 - 1005
246R81190A0

PAYABLE UPON RECEIPT OF INVOICE
PAYER'S ACCOUNT NUMBER:
RK72740

LASC-GEORGIA
ATTN: ACCOUNTS PAYABLE
S/81-49, ZONE 0285
86 SOUTH COBB DRIVE
MARIETTA GA 30063-0285

GTRC ACCOUNTING
No.
Date
D D

INVOICE DATE	DESCRIPTION	CUMULATIVE AMOUNT	CURRENT AMOUNT
9/01/95	OPTIMIZATION IN STRUCTURAL ACOUSTICS USING FEM/BEM PRIME: NAS1-20102 TASK 5		
TO	PERSONAL SERVICES	58,052.04	7,647.0
	FRINGE BENEFITS	10,641.05	1,586.4
	MATERIALS AND SUPPLIES	3,263.81	
	OTHER INDIRECT		
9/30/95	EQUIPMENT	3,365.00	
	TRAVEL	2,964.10	
	CAPITAL OUTLAY		
	SUBCONTRACTS NON-MTDC		
	SUBCONTRACTS MTDC		
	INDIRECT	30,531.19	3,970.3
		108,817.19	13,203.8

IF YOU HAVE QUESTIONS CONCERNING THIS INVOICE,
CONTACT: [illegible] PHONE: [illegible]

PLEASE PAY THIS TOTAL AMOUNT > $ 13,203.8

RETAIN THIS COPY FOR YOUR RECORDS

LOCKHEED AERONAUT SY CO-GA
GEORGIA INSTITUTE OF TECHNOLOGY
ANALYSIS OF PERSONAL SERVICES
CONTRACT TERM 03-21-94 - 10-31-95
CONTRACT #RF72740
PRIME #NAS1-20102, TASK ASSIGNMENT #5

EMPLOYEE	TITLE	MONTH	MONTHLY SALARY		TIME	PROJECT AMOUNT	**ESTIMATED HOURS
JULY 1, 1994 - JUNE 30, 1995							
BIESEL, VAN B.	RES ENGR I	JUL	3,395.31	MONTHLY	50.00%		0.00
		AUG	3,395.31	MONTHLY	50.00%		0.00
		SEP	3,395.31	MONTHLY	50.00%		0.00
		OCT	3,395.31	MONTHLY	50.00%		0.00
		NOV	3,395.31	MONTHLY	50.00%		0.00
		DEC	3,395.31	MONTHLY	50.00%	1,009.47	25.87
		JAN	3,395.31	MONTHLY	50.00%	1,708.33	43.77
		FEB	3,395.31	MONTHLY	50.00%	1,708.33	43.77
		MAR	3,395.31	MONTHLY	50.00%	1,708.33	43.77
		APR	3,395.31	MONTHLY	50.00%	1,708.33	43.77
		MAY	3,395.31	MONTHLY	50.00%	1,708.33	43.77
		JUN	3,395.31	MONTHLY	50.00%	1,708.33	43.77
	TOTAL					11,259.45	288.51
CRANE, SCOTT P.	GRAD ASST	JUL	1,375.00	MONTHLY	33.00%	1,333.33	55.68
		AUG	1,375.00	MONTHLY	33.00%	1,333.33	55.68
		SEP	1,375.00	MONTHLY	33.00%	1,333.33	55.68
		OCT	1,375.00	MONTHLY	33.00%	1,250.00	52.20
		NOV	1,375.00	MONTHLY	33.00%	1,250.00	52.20
		DEC	1,375.00	MONTHLY	33.00%	1,250.00	52.20
		JAN	1,375.00	MONTHLY	33.00%	183.34	7.66
		FEB	1,375.00	MONTHLY	33.00%	183.34	7.66
		MAR	1,375.00	MONTHLY	33.00%	183.34	7.66
		APR	1,375.00	MONTHLY	33.00%	183.34	7.66
		MAY	1,375.00	MONTHLY	33.00%	183.34	7.66
		JUN	1,375.00	MONTHLY	33.00%	183.34	7.66
	TOTAL					8,850.03	369.58
CUNEFARE, KENNETH	ASST PROF	JUL	6,066.04	MONTHLY	18.80%	2,857.44	15.41
		AUG	6,066.04	MONTHLY	18.80%	2,857.44	15.41
		SEP	6,066.04	MONTHLY	18.80%	2,857.44	15.41
		OCT	6,066.04	MONTHLY	18.80%		0.00
		NOV	6,066.04	MONTHLY	18.80%		0.00
		DEC	6,066.04	MONTHLY	18.80%		0.00
		JAN	6,066.04	MONTHLY	18.80%		0.00
		FEB	6,066.04	MONTHLY	18.80%		0.00
		MAR	6,066.04	MONTHLY	18.80%		0.00
		APR	6,066.04	MONTHLY	18.80%		0.00
		MAY	6,066.04	MONTHLY	18.80%		0.00
		JUN	6,066.04	MONTHLY	18.80%		0.00
	TOTAL					8,572.32	46.23
	GRAND TOTAL FOR 1994-95					28,681.80	704.31

LOCKHEED AERONAUT SY CO-GA
GEORGIA INSTITUTE OF TECHNOLOGY
ANALYSIS OF PERSONAL SERVICES
CONTRACT TERM 03-21-94 - 10-31-96
CONTRACT #RF72740
PRIME #NAS1-20102, TASK ASSIGNMENT #6

EMPLOYEE	TITLE	MONTH	MONTHLY SALARY	TIME		PROJECT AMOUNT	**ESTIMATED HOURS
JULY 1, 1993 - JUNE 30, 1994							
BIESEL, VAN B.	RES ENGR I	JUL	3,395.31	MONTHLY	50.00%		0.00
		AUG	3,395.31	MONTHLY	50.00%		0.00
		SEP	3,395.31	MONTHLY	50.00%		0.00
		OCT	3,395.31	MONTHLY	50.00%		0.00
		NOV	3,395.31	MONTHLY	50.00%		0.00
		DEC	3,395.31	MONTHLY	50.00%		0.00
		JAN	3,395.31	MONTHLY	50.00%		0.00
		FEB	3,395.31	MONTHLY	50.00%		0.00
		MAR	3,395.31	MONTHLY	50.00%		0.00
		APR	3,395.31	MONTHLY	50.00%		0.00
		MAY	3,395.31	MONTHLY	50.00%		0.00
		JUN	3,395.31	MONTHLY	50.00%		0.00
	TOTAL					0.00	0.00
CRANE, SCOTT P.	GRAD ASST	JUL	1,375.00	MONTHLY	33.00%		0.00
		AUG	1,375.00	MONTHLY	33.00%		0.00
		SEP	1,375.00	MONTHLY	33.00%		0.00
		OCT	1,375.00	MONTHLY	33.00%		0.00
		NOV	1,375.00	MONTHLY	33.00%		0.00
		DEC	1,375.00	MONTHLY	33.00%		0.00
		JAN	1,375.00	MONTHLY	33.00%		0.00
		FEB	1,375.00	MONTHLY	33.00%		0.00
		MAR	1,375.00	MONTHLY	33.00%		0.00
		APR	1,375.00	MONTHLY	33.00%		0.00
		MAY	1,375.00	MONTHLY	33.00%		0.00
		JUN	1,375.00	MONTHLY	33.00%		0.00
	TOTAL					0.00	0.00
CUNEFARE, KENNETH	ASST PROF	JUL	6,066.04	MONTHLY	18.80%		0.00
		AUG	6,066.04	MONTHLY	18.80%		0.00
		SEP	6,066.04	MONTHLY	18.80%		0.00
		OCT	6,066.04	MONTHLY	18.80%		0.00
		NOV	6,066.04	MONTHLY	18.80%		0.00
		DEC	6,066.04	MONTHLY	18.80%		0.00
		JAN	6,066.04	MONTHLY	18.80%		0.00
		FEB	6,066.04	MONTHLY	18.80%		0.00
		MAR	6,066.04	MONTHLY	18.80%		0.00
		APR	6,066.04	MONTHLY	18.80%	2,143.08	11.56
		MAY	6,066.04	MONTHLY	18.80%	2,143.08	11.56
		JUN	6,066.04	MONTHLY	18.80%		0.00
	TOTAL					4,286.16	23.11
	GRAND TOTAL FOR 1993-94					4,286.16	23.11

LOCKHEED AERONAUT SY CO-GA
GEORGIA INSTITUTE OF TECHNOLOGY
ANALYSIS OF PERSONAL SERVICES
CONTRACT TERM 03-21-94 - 10-31-96
CONTRACT #RF72740
PRIME #NAS1-20102, TASK ASSIGNMENT #6

EMPLOYEE	TITLE	MONTH	MONTHLY SALARY		TIME	PROJECT AMOUNT	**ESTIMATED HOURS
JULY 1, 1995 - OCTOBER 31, 1995							
BIESEL, VAN B.	RES ENGR I	JUL	3,621.66	MONTHLY	50.00%	1,810.84	43.33
		AUG	3,621.66	MONTHLY	50.00%	1,810.84	43.33
		SEP	3,621.66	MONTHLY	50.00%	1,810.84	43.33
		OCT	3,621.66	MONTHLY	50.00%		0.00
		NOV	3,621.66	MONTHLY	50.00%		0.00
		DEC	3,621.66	MONTHLY	50.00%		0.00
		JAN	3,621.66	MONTHLY	50.00%		0.00
		FEB	3,621.66	MONTHLY	50.00%		0.00
		MAR	3,621.66	MONTHLY	50.00%		0.00
		APR	3,621.66	MONTHLY	50.00%		0.00
		MAY	3,621.66	MONTHLY	50.00%		0.00
		JUN	3,621.66	MONTHLY	50.00%		0.00
	TOTAL					5,432.52	130.00
CRANE, SCOTT P.	GRAD ASST	JUL	1,250.00	MONTHLY	33.00%	1,250.00	57.20
		AUG	1,250.00	MONTHLY	33.00%	1,250.00	57.20
		SEP	1,250.00	MONTHLY	33.00%	1,250.00	57.20
		OCT	1,250.00	MONTHLY	33.00%		0.00
		NOV	1,250.00	MONTHLY	33.00%		0.00
		DEC	1,250.00	MONTHLY	33.00%		0.00
		JAN	1,250.00	MONTHLY	33.00%		0.00
		FEB	1,250.00	MONTHLY	33.00%		0.00
		MAR	1,250.00	MONTHLY	33.00%		0.00
		APR	1,250.00	MONTHLY	33.00%		0.00
		MAY	1,250.00	MONTHLY	33.00%		0.00
		JUN	1,250.00	MONTHLY	33.00%		0.00
	TOTAL					3,750.00	171.60
CUNEFARE, KENNETH	ASST PROF	JUL	6,066.04	MONTHLY	18.80%	4,586.16	24.64
		AUG	6,066.04	MONTHLY	18.80%	4,586.16	24.64
		SEP	6,066.04	MONTHLY	18.80%	4,586.16	24.64
		OCT	6,066.04	MONTHLY	18.80%		0.00
		NOV	6,066.04	MONTHLY	18.80%		0.00
		DEC	6,066.04	MONTHLY	18.80%		0.00
		JAN	6,066.04	MONTHLY	18.80%		0.00
		FEB	6,066.04	MONTHLY	18.80%		0.00
		MAR	6,066.04	MONTHLY	18.80%		0.00
		APR	6,066.04	MONTHLY	18.80%		0.00
		MAY	6,066.04	MONTHLY	18.80%		0.00
		JUN	6,066.04	MONTHLY	18.80%		0.00
	TOTAL					13,758.48	73.91
	GRAND TOTAL FOR 1995-96					22,941.00	375.51

LOCKHEED AERONAUT SY CO-GA
GEORGIA INSTITUTE OF TECHNOLOGY
ANALYSIS OF PERSONAL SERVICES
CONTRACT TERM 03-21-94 - 10-31-95
CONTRACT #RF72740
PRIME #NAS1-20102, TASK ASSIGNMENT #5

EMPLOYEE	TITLE	MONTH	MONTHLY SALARY	TIME	PROJECT AMOUNT	**ESTIMATED HOURS

** NOTE: Georgia Tech does not track personal service charges for professional staff by the hour. We use the Planned-Confirmation System as required by the Federal goverment's guidlines in Circular A-21. The figures here are estimates based upon the annual salary, the number of work hours in a year, the percentage of budgeted effort as required by the contract, and the actual charges each month for this project.

GEORGIA INSTITUTE OF TECHNOLOGY
OFFICE OF GRANTS AND CONTRACTS ACCOUNTING

190 BOBBY DODD WAY
ATLANTA, GEORGIA 30332-0259

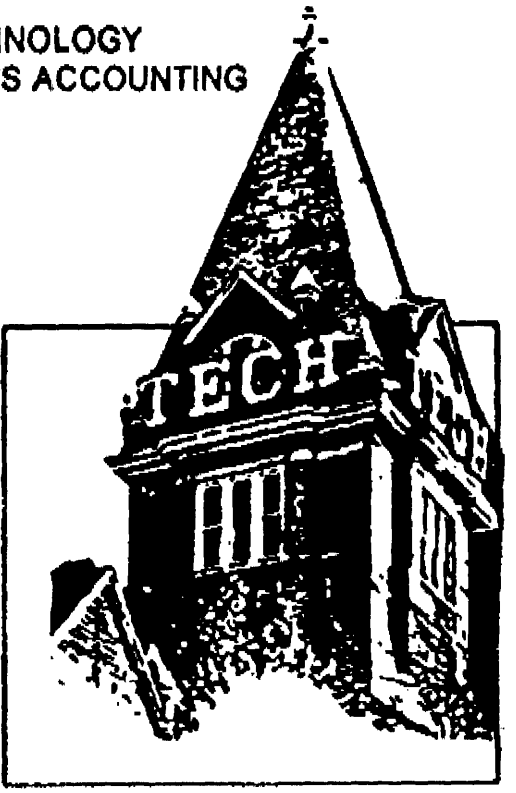

DATE: 11-2-95

NUMBER OF PAGES 7
(INCLUDING THIS PAGE)

TO: Wanda Simon

FROM: Jill Redmond 4-6757

SUBJECT: E-25-W56 Deliverable

MESSAGE: or Deliverable

(IF THIS MESSAGE IS ILLEGIBLE OR IF THERE IS A TRANSMISSION PROBLEM, PLEASE CALL (404) 894-4624).

E-25-W56
#14

LOCKHEED AERONAUTICAL SYSTEMS
GEORGIA INSTITUTE OF TECHNOLOGY
ANALYSIS OF PERSONAL SERVICES
CONTRACT TERM 03-21-94 - 10-31-96
CONTRACT #RF72748
PRIME #NAS1-19192, TASK ASSIGNMENT #6

EMPLOYEE	TITLE	MONTH	MONTHLY SALARY	TIME		PROJECT AMOUNT	**ESTIMATED HOURS
JULY 1, 1994 - JUNE 30, 1995							
BIESEL, VAN B.	RES ENGR I	JUL	3,395.31	MONTHLY	50.00%		0.00
		AUG	3,395.31	MONTHLY	50.00%		0.00
		SEP	3,395.31	MONTHLY	50.00%		0.00
		OCT	3,395.31	MONTHLY	50.00%		0.00
		NOV	3,395.31	MONTHLY	50.00%		0.00
		DEC	3,395.31	MONTHLY	50.00%	1,009.47	25.87
		JAN	3,395.31	MONTHLY	50.00%	1,708.33	43.77
		FEB	3,395.31	MONTHLY	50.00%	1,708.33	43.77
		MAR	3,395.31	MONTHLY	50.00%	1,708.33	43.77
		APR	3,395.31	MONTHLY	50.00%	1,708.33	43.77
		MAY	3,395.31	MONTHLY	50.00%	1,708.33	43.77
		JUN	3,395.31	MONTHLY	50.00%	1,708.33	43.77
	TOTAL					13,354.45	342.21
CRANE, SCOTT P.	GRAD ASST	JUL	1,375.00	MONTHLY	53.00%	1,333.33	35.66
		AUG	1,375.00	MONTHLY	53.00%	1,333.33	35.66
		SEP	1,375.00	MONTHLY	53.00%	1,333.33	35.66
		OCT	1,375.00	MONTHLY	53.00%	1,291.00	34.50
		NOV	1,375.00	MONTHLY	53.00%	1,250.00	33.39
		DEC	1,375.00	MONTHLY	53.00%	1,250.00	33.39
		JAN	1,375.00	MONTHLY	53.00%	183.34	7.66
		FEB	1,375.00	MONTHLY	53.00%	183.34	7.66
		MAR	1,375.00	MONTHLY	53.00%	183.34	7.66
		APR	1,375.00	MONTHLY	53.00%	183.34	7.66
		MAY	1,375.00	MONTHLY	53.00%	183.34	7.66
		JUN	1,375.00	MONTHLY	53.00%	183.34	7.66
	TOTAL					8,850.03	369.58
CUNEFARE, KENNETH	ASST PROF	JUL	6,066.04	MONTHLY	18.60%	2,857.44	15.41
		AUG	6,066.04	MONTHLY	18.60%	2,857.44	15.41
		SEP	6,066.04	MONTHLY	18.60%	2,857.44	15.41
		OCT	6,066.04	MONTHLY	18.60%		0.00
		NOV	6,066.04	MONTHLY	18.60%		0.00
		DEC	6,066.04	MONTHLY	18.60%		0.00
		JAN	6,066.04	MONTHLY	18.60%		0.00
		FEB	6,066.04	MONTHLY	18.60%		0.00
		MAR	6,066.04	MONTHLY	18.60%		0.00
		APR	6,066.04	MONTHLY	18.60%		0.00
		MAY	6,066.04	MONTHLY	18.60%		0.00
		JUN	6,066.04	MONTHLY	18.60%		0.00
	TOTAL					8,572.32	46.23
	GRAND TOTAL FOR 1994-96					28,881.80	704.31

LOCKHEED AERONAUTICAL SYSTEMS CO-GA
GEORGIA INSTITUTE OF TECHNOLOGY
ANALYSIS OF PERSONAL SERVICES
CONTRACT TERM 03-21-94 - 10-31-94
CONTRACT #RF72748
PRIME #NAS1-20102, TASK ASSIGNMENT #6

EMPLOYEE	TITLE	MONTH	MONTHLY SALARY		TIME	PROJECT AMOUNT	**ESTIMATED HOURS
JULY 1, 1993 - JUNE 30, 1994							
BIESEL, VAN B.	RES ENGR I	JUL	3,395.31	MONTHLY	50.00%		0.00
		AUG	3,395.31	MONTHLY	50.00%		0.00
		SEP	3,395.31	MONTHLY	50.00%		0.00
		OCT	3,395.31	MONTHLY	50.00%		0.00
		NOV	3,395.31	MONTHLY	50.00%		0.00
		DEC	3,395.31	MONTHLY	50.00%		0.00
		JAN	3,395.31	MONTHLY	50.00%		0.00
		FEB	3,395.31	MONTHLY	50.00%		0.00
		MAR	3,395.31	MONTHLY	50.00%		0.00
		APR	3,395.31	MONTHLY	50.00%		0.00
		MAY	3,395.31	MONTHLY	50.00%		0.00
		JUN	3,395.31	MONTHLY	50.00%		0.00
	TOTAL					0.00	0.00
CRANE, SCOTT P.	GRAD ASST	JUL	1,375.00	MONTHLY	33.00%		0.00
		AUG	1,375.00	MONTHLY	33.00%		0.00
		SEP	1,375.00	MONTHLY	33.00%		0.00
		OCT	1,375.00	MONTHLY	33.00%		0.00
		NOV	1,375.00	MONTHLY	33.00%		0.00
		DEC	1,375.00	MONTHLY	33.00%		0.00
		JAN	1,375.00	MONTHLY	33.00%		0.00
		FEB	1,375.00	MONTHLY	33.00%		0.00
		MAR	1,375.00	MONTHLY	33.00%		0.00
		APR	1,375.00	MONTHLY	33.00%		0.00
		MAY	1,375.00	MONTHLY	33.00%		0.00
		JUN	1,375.00	MONTHLY	33.00%		0.00
	TOTAL					0.00	0.00
CUNEFARE, KENNETH	ASST PROF	JUL	6,066.04	MONTHLY	18.50%		0.00
		AUG	6,066.04	MONTHLY	18.50%		0.00
		SEP	6,066.04	MONTHLY	18.50%		0.00
		OCT	6,066.04	MONTHLY	18.50%		0.00
		NOV	6,066.04	MONTHLY	18.50%		0.00
		DEC	6,066.04	MONTHLY	18.50%		0.00
		JAN	6,066.04	MONTHLY	18.50%		0.00
		FEB	6,066.04	MONTHLY	18.50%		0.00
		MAR	6,066.04	MONTHLY	18.50%		0.00
		APR	6,066.04	MONTHLY	18.50%	2,143.08	11.56
		MAY	6,066.04	MONTHLY	18.50%	2,143.08	11.56
		JUN	6,066.04	MONTHLY	18.50%		0.00
	TOTAL					4,286.16	23.11
	GRAND TOTAL FOR 1993-94					4,286.16	23.11

LOCKHEED AERONAUTICAL SYSTEMS CO-GA
GEORGIA INSTITUTE OF TECHNOLOGY
ANALYSIS OF PERSONAL SERVICES
CONTRACT TERM 03-21-94 - 10-31-96
CONTRACT #RF72748
PRIME #NAS1-20102, TASK ASSIGNMENT #6

EMPLOYEE	TITLE	MONTH	MONTHLY SALARY		TIME	PROJECT AMOUNT	**ESTIMATED HOURS
JULY 1, 1995 - OCTOBER 31, 1996							
BIESEL, VAN S.	RES ENGR I	JUL	3,621.66	MONTHLY	50.00%	1,810.84	43.33
		AUG	3,621.66	MONTHLY	50.00%	1,810.84	43.33
		SEP	3,621.66	MONTHLY	50.00%	1,810.84	43.33
		OCT	3,621.66	MONTHLY	50.00%	3,621.66	86.67
		NOV	3,621.66	MONTHLY	50.00%		0.00
		DEC	3,621.66	MONTHLY	50.00%		0.00
		JAN	3,621.66	MONTHLY	50.00%		0.00
		FEB	3,621.66	MONTHLY	50.00%		0.00
		MAR	3,621.66	MONTHLY	50.00%		0.00
		APR	3,621.66	MONTHLY	50.00%		0.00
		MAY	3,621.66	MONTHLY	50.00%		0.00
		JUN	3,621.66	MONTHLY	50.00%		0.00
	TOTAL					9,054.18	216.67
CRANE, SCOTT P.	GRAD ASST	JUL	1,250.00	MONTHLY	33.00%	1,250.00	57.20
		AUG	1,250.00	MONTHLY	33.00%	1,250.00	57.20
		SEP	1,250.00	MONTHLY	33.00%	1,250.00	57.20
		OCT	1,250.00	MONTHLY	33.00%		0.00
		NOV	1,250.00	MONTHLY	33.00%		0.00
		DEC	1,250.00	MONTHLY	33.00%		0.00
		JAN	1,250.00	MONTHLY	33.00%		0.00
		FEB	1,250.00	MONTHLY	33.00%		0.00
		MAR	1,250.00	MONTHLY	33.00%		0.00
		APR	1,250.00	MONTHLY	33.00%		0.00
		MAY	1,250.00	MONTHLY	33.00%		0.00
		JUN	1,250.00	MONTHLY	33.00%		0.00
	TOTAL					3,750.00	171.60
CUNEFARE, KENNETH	ASST PROF	JUL	6,066.04	MONTHLY	18.80%	4,586.16	24.64
		AUG	6,066.04	MONTHLY	18.80%	4,586.16	24.64
		SEP	6,066.04	MONTHLY	18.80%	4,586.16	24.64
		OCT	6,066.04	MONTHLY	18.80%	1,639.83	8.81
		NOV	6,066.04	MONTHLY	18.80%		0.00
		DEC	6,066.04	MONTHLY	18.80%		0.00
		JAN	6,066.04	MONTHLY	18.80%		0.00
		FEB	6,066.04	MONTHLY	18.80%		0.00
		MAR	6,066.04	MONTHLY	18.80%		0.00
		APR	6,066.04	MONTHLY	18.80%		0.00
		MAY	6,066.04	MONTHLY	18.80%		0.00
		JUN	6,066.04	MONTHLY	18.80%		0.00
	TOTAL					15,398.31	82.72
	GRAND TOTAL FOR 1995-96					28,202.49	470.99

LOCKHEED AERONAUTICS CO-GA
GEORGIA INSTITUTE OF TECHNOLOGY
ANALYSIS OF PERSONAL SERVICES
CONTRACT TERM 03-21-94 - 10-31-95
CONTRACT #RF*2740
PRIME #NAS1-20102, TASK ASSIGNMENT #6

EMPLOYEE	TITLE	MONTH	MONTHLY SALARY	TIME	PROJECT AMOUNT	**ESTIMATED HOURS

** NOTE. Georgia Tech does not track personal service charges for professional staff by the hour. We use the Planned-Confirmation System as required by the Federal government's guidelines in Circular A-21. The figures here are estimates based upon the annual salary, the number of work hours in a year, the percentage of budgeted effort as required by the contract, and the actual charges each month for this project.

LOCKHEED AERONAUTICAL SYSTEMS CO-GA
GEORGIA INSTITUTE OF TECHNOLOGY
ANALYSIS OF PERSONAL SERVICES
CONTRACT TERM 03-21-94 - 11-30-96
CONTRACT #RF72746
PRIME #NAS1-20102, TASK ASSIGNMENT #6

E-25-W56
#15

EMPLOYEE	TITLE	MONTH	MONTHLY SALARY	TIME		PROJECT AMOUNT	**ESTIMATED HOURS
JULY 1, 1994 - JUNE 30, 1996							
BIESEL, VAN B	RES ENGR I	JUL	3,396.31	MONTHLY	50.00%		0.00
		AUG	3,396.31	MONTHLY	50.00%		0.00
		SEP	3,396.31	MONTHLY	50.00%		0.00
		OCT	3,396.31	MONTHLY	50.00%		0.00
		NOV	3,396.31	MONTHLY	50.00%		0.00
		DEC	3,396.31	MONTHLY	50.00%	1,009.47	25.87
		JAN	3,396.31	MONTHLY	50.00%	1,708.33	43.77
		FEB	3,396.31	MONTHLY	50.00%	1,708.33	43.77
		MAR	3,396.31	MONTHLY	50.00%	1,708.33	43.77
		APR	3,396.31	MONTHLY	50.00%	1,708.33	43.77
		MAY	3,396.31	MONTHLY	50.00%	1,708.33	43.77
		JUN	3,396.31	MONTHLY	50.00%	1,708.33	43.77
	TOTAL					11,259.45	288.51
CRANE, SCOTT P.	GRAD ASST	JUL	1,375.00	MONTHLY	33.00%	1,333.33	55.68
		AUG	1,375.00	MONTHLY	33.00%	1,333.33	55.68
		SEP	1,375.00	MONTHLY	33.00%	1,333.33	55.68
		OCT	1,375.00	MONTHLY	33.00%	1,250.00	52.20
		NOV	1,375.00	MONTHLY	33.00%	1,250.00	52.20
		DEC	1,375.00	MONTHLY	33.00%	1,250.00	52.20
		JAN	1,375.00	MONTHLY	33.00%	183.34	7.66
		FEB	1,375.00	MONTHLY	33.00%	183.34	7.66
		MAR	1,375.00	MONTHLY	33.00%	183.34	7.66
		APR	1,375.00	MONTHLY	33.00%	183.34	7.66
		MAY	1,375.00	MONTHLY	33.00%	183.34	7.66
		JUN	1,375.00	MONTHLY	33.00%	183.34	7.66
	TOTAL					8,850.03	369.58
CUNEFARE, KENNETH	ASST PROF	JUL	6,066.04	MONTHLY	18.80%	2,857.44	15.41
		AUG	6,066.04	MONTHLY	18.80%	2,857.44	15.41
		SEP	6,066.04	MONTHLY	18.80%	2,857.44	15.41
		OCT	6,066.04	MONTHLY	18.80%		0.00
		NOV	6,066.04	MONTHLY	18.80%		0.00
		DEC	6,066.04	MONTHLY	18.80%		0.00
		JAN	6,066.04	MONTHLY	18.80%		0.00
		FEB	6,066.04	MONTHLY	18.80%		0.00
		MAR	6,066.04	MONTHLY	18.80%		0.00
		APR	6,066.04	MONTHLY	18.80%		0.00
		MAY	6,066.04	MONTHLY	18.80%		0.00
		JUN	6,066.04	MONTHLY	18.80%		0.00
	TOTAL					8,572.32	46.23
	GRAND TOTAL FOR 1994-96					28,681.80	704.31

LOCKHEED AERONAUTSY CO-GA
GEORGIA INSTITUTE OF TECHNOLOGY
ANALYSIS OF PERSONAL SERVICES
CONTRACT TERM 03-21-94 - 11-30-96
CONTRACT #RF72740
PRIME #NAS1-20102, TASK ASSIGNMENT #6

EMPLOYEE	TITLE	MONTH	MONTHLY SALARY		TIME	PROJECT AMOUNT	**ESTIMATED HOURS
JULY 1, 1995 - JUNE 30, 1996							
BIESEL, VAN B.	RES ENGR I	JUL	3,621.66	MONTHLY	50.00%	1,810.84	43.33
		AUG	3,621.66	MONTHLY	50.00%	1,810.84	43.33
		SEP	3,621.66	MONTHLY	50.00%	1,810.84	43.33
		OCT	3,621.66	MONTHLY	50.00%	3,621.66	86.67
		NOV	3,621.66	MONTHLY	50.00%	1,810.84	43.33
		DEC	3,621.66	MONTHLY	50.00%		0.00
		JAN	3,621.66	MONTHLY	50.00%		0.00
		FEB	3,621.66	MONTHLY	50.00%		0.00
		MAR	3,621.66	MONTHLY	50.00%		0.00
		APR	3,621.66	MONTHLY	50.00%		0.00
		MAY	3,621.66	MONTHLY	50.00%		0.00
		JUN	3,621.66	MONTHLY	50.00%		0.00
	TOTAL					10,865.02	260.00
CRANE, SCOTT P.	GRAD ASST	JUL	1,250.00	MONTHLY	33.00%	1,250.00	57.20
		AUG	1,250.00	MONTHLY	33.00%	1,250.00	57.20
		SEP	1,250.00	MONTHLY	33.00%	1,250.00	57.20
		OCT	1,250.00	MONTHLY	33.00%		0.00
		NOV	1,250.00	MONTHLY	33.00%		0.00
		DEC	1,250.00	MONTHLY	33.00%		0.00
		JAN	1,250.00	MONTHLY	33.00%		0.00
		FEB	1,250.00	MONTHLY	33.00%		0.00
		MAR	1,250.00	MONTHLY	33.00%		0.00
		APR	1,250.00	MONTHLY	33.00%		0.00
		MAY	1,250.00	MONTHLY	33.00%		0.00
		JUN	1,250.00	MONTHLY	33.00%		0.00
	TOTAL					3,750.00	171.60
CUNEFARE, KENNETH	ASST PROF	JUL	6,066.04	MONTHLY	18.80%	4,586.16	24.64
		AUG	6,066.04	MONTHLY	18.80%	4,586.16	24.64
		SEP	6,066.04	MONTHLY	18.80%	4,586.16	24.64
		OCT	6,066.04	MONTHLY	18.80%	1,639.83	8.81
		NOV	6,066.04	MONTHLY	18.80%	1,639.83	8.81
		DEC	6,066.04	MONTHLY	18.80%		0.00
		JAN	6,066.04	MONTHLY	18.80%		0.00
		FEB	6,066.04	MONTHLY	18.80%		0.00
		MAR	6,066.04	MONTHLY	18.80%		0.00
		APR	6,066.04	MONTHLY	18.80%		0.00
		MAY	6,066.04	MONTHLY	18.80%		0.00
		JUN	6,066.04	MONTHLY	18.80%		0.00
	TOTAL					17,038.14	91.53
	GRAND TOTAL FOR 1995-96					31,653.16	523.13

LOCKHEED AERONAUT SY CO-GA

GE[illegible] OF TECHNOLOGY

ANALYSIS OF PERSONAL SERVICES

CONTRACT TERM 03-21-84 - 11-30-95

CONTRACT #RF72740

PRIME #NAS1-20102, TASK ASSIGNMENT #5

EMPLOYEE	TITLE	MONTH	MONTHLY SALARY	TIME	PROJECT AMOUNT	**ESTIMATED HOURS

** NOTE: Georgia Tech does not track personal service charges for professional staff by the hour. We use the Planned Confirmation System as required by the Federal goverment's guidlines in Circular A-21. The figures here are estimates based upon the annual salary, the number of work hours in a year, the percentage of budgeted effort as required by the contract, and the actual charges each month for this project.

LOCKHEED AERONAUTICAL SYSTEMS CO-GA

GEORGIA INSTITUTE OF TECHNOLOGY

ANALYSIS OF PERSONAL SERVICES

CONTRACT TERM 03-21-94 - 11-30-96

CONTRACT #RF72748

PRIME #NAS1-20102, TASK ASSIGNMENT #8

EMPLOYEE	TITLE	MONTH	MONTHLY SALARY	TIME		PROJECT AMOUNT	**ESTIMATED HOURS
JULY 1, 1993 - JUNE 30, 1994							
BIESEL, VAN B	RES ENGR I	JUL	3,395.31	MONTHLY	50.00%		0.00
		AUG	3,395.31	MONTHLY	50.00%		0.00
		SEP	3,395.31	MONTHLY	50.00%		0.00
		OCT	3,395.31	MONTHLY	50.00%		0.00
		NOV	3,395.31	MONTHLY	50.00%		0.00
		DEC	3,395.31	MONTHLY	50.00%		0.00
		JAN	3,395.31	MONTHLY	50.00%		0.00
		FEB	3,395.31	MONTHLY	50.00%		0.00
		MAR	3,395.31	MONTHLY	50.00%		0.00
		APR	3,395.31	MONTHLY	50.00%		0.00
		MAY	3,395.31	MONTHLY	50.00%		0.00
		JUN	3,395.31	MONTHLY	50.00%		0.00
	TOTAL					0.00	0.00
CRANE, SCOTT P	GRAD ASST	JUL	1,375.00	MONTHLY	33.00%		0.00
		AUG	1,375.00	MONTHLY	33.00%		0.00
		SEP	1,375.00	MONTHLY	33.00%		0.00
		OCT	1,375.00	MONTHLY	33.00%		0.00
		NOV	1,375.00	MONTHLY	33.00%		0.00
		DEC	1,375.00	MONTHLY	33.00%		0.00
		JAN	1,375.00	MONTHLY	33.00%		0.00
		FEB	1,375.00	MONTHLY	33.00%		0.00
		MAR	1,375.00	MONTHLY	33.00%		0.00
		APR	1,375.00	MONTHLY	33.00%		0.00
		MAY	1,375.00	MONTHLY	33.00%		0.00
		JUN	1,375.00	MONTHLY	33.00%		0.00
	TOTAL					0.00	0.00
CUNEFARE, KENNETH	ASST PROF	JUL	6,066.04	MONTHLY	18.80%		0.00
		AUG	6,066.04	MONTHLY	18.80%		0.00
		SEP	6,066.04	MONTHLY	18.80%		0.00
		OCT	6,066.04	MONTHLY	18.80%		0.00
		NOV	6,066.04	MONTHLY	18.80%		0.00
		DEC	6,066.04	MONTHLY	18.80%		0.00
		JAN	6,066.04	MONTHLY	18.80%		0.00
		FEB	6,066.04	MONTHLY	18.80%		0.00
		MAR	6,066.04	MONTHLY	18.80%		0.00
		APR	6,066.04	MONTHLY	18.80%	2,143.08	11.56
		MAY	6,066.04	MONTHLY	18.80%	2,143.08	11.56
		JUN	6,066.04	MONTHLY	18.80%		0.00
	TOTAL					4,286.16	23.11
	GRAND TOTAL FOR 1993-94					4,286.16	23.11

SENT BY:GRANTS & CONTRACTS

E-25 W56
#16

[illegible]
[illegible] TECHNOLOGY
ANALYSIS OF PERSONAL SERVICES
CONTRACT TERM 03-31-94 12-31-96
CONTRACT #RF7274U
PRIME #NAS1-20102, TASK ASSIGNMENT #6

EMPLOYEE	TITLE	MONTH	MONTHLY SALARY	TIME		PROJECT AMOUNT	**ESTIMATED HOURS
JULY 1, 1994 - JUNE 30, 1996							
BIESEL, VAN B	RES ENGR I	[illegible]	3,395.31	MONTHLY	50.00%		0.00
		[illegible]	3,395.31	MONTHLY	50.00%		0.00
		[illegible]	3,395.31	MONTHLY	50.00%		0.00
		[illegible]	3,395.31	MONTHLY	50.00%		0.00
		[illegible]	3,395.31	MONTHLY	50.00%		0.00
		[illegible]	3,395.31	MONTHLY	[illegible]	[illegible]	[illegible]
		[illegible]	3,395.31	MONTHLY	[illegible]	[illegible]	[illegible]
		FEB	3,395.31	MONTHLY	50.00%	[illegible]	43.77
		MAR	3,395.31	MONTHLY	50.00%	[illegible]	43.77
		[illegible]	3,395.31	MONTHLY	[illegible]	228.33	[illegible]
		[illegible]	3,395.31	MONTHLY	[illegible]	[illegible]	[illegible]
		[illegible]	3,395.31	MONTHLY	50.00%	[illegible]	[illegible]
	TOTAL					[illegible] 45	265.31
[illegible]	[illegible]	[illegible]	375.00	MONTHLY	[illegible]	[illegible]	
		[illegible]	[illegible] 00	MONTHLY	[illegible]	[illegible]	
		[illegible]	[illegible] 00	MONTHLY	[illegible]	[illegible]	
		[illegible]	375.00	MONTHLY	[illegible]	[illegible]	[illegible]
		[illegible]	375.00	MONTHLY	[illegible]	[illegible]	[illegible]
		[illegible]	375.00	MONTHLY	[illegible]	[illegible]	[illegible]
		[illegible]	375.00	MONTHLY	[illegible]	[illegible]	[illegible]
		[illegible]	375.00	MONTHLY	[illegible]	[illegible]	[illegible]
		[illegible]	375.00	MONTHLY	[illegible]	[illegible]	[illegible]
		[illegible]	375.00	MONTHLY	[illegible]	[illegible]	[illegible]
	TOTAL					[illegible] 03	[illegible]
GUNEPARE, KENNETH	ASSOCIATE	[illegible]	6,066.04	MONTHLY	[illegible]	1,857.44	[illegible]
		[illegible]	6,066.04	MONTHLY	[illegible]	1,857.44	[illegible]
		[illegible]	6,066.04	MONTHLY	[illegible]	1,857.44	[illegible]
		[illegible]	6,066.04	MONTHLY	[illegible]	[illegible]	[illegible]
		[illegible]	6,066.04	MONTHLY	18.60%	[illegible]	[illegible]
		[illegible]	6,066.04	MONTHLY	18.60%	[illegible]	0.00
		[illegible]	6,066.04	MONTHLY	[illegible]	[illegible]	[illegible]
		[illegible]	6,066.04	MONTHLY	[illegible]	[illegible]	[illegible]
		[illegible]	6,066.04	MONTHLY	[illegible]	[illegible]	[illegible]
		[illegible]	6,066.04	MONTHLY	[illegible]	[illegible]	[illegible]
		[illegible]	6,066.04	MONTHLY	[illegible]	[illegible]	[illegible]
	TOTAL					[illegible]	[illegible]
	[illegible]					[illegible] 50	[illegible]

2/1/96E25W56 XLS

LOCKHEED AERONAUTICS CO-GA
GEORGIA INSTITUTE OF TECHNOLOGY
ANALYSIS OF PERSONAL SERVICES
CONTRACT TERM 03-21-94 - 12-31-96
CONTRACT #RF72740
PRIME #NAS1-20102, TASK ASSIGNMENT #6

EMPLOYEE	TITLE	MONTH	MONTHLY SALARY	TIME		PROJECT AMOUNT	**ESTIMATED HOURS
JULY 1, 1993 - JUNE 30, 1994							
BIESEL, VAN B	RES ENGR I	JUL	3,395.31	MONTHLY	50.00%		0.00
		AUG	3,395.31	MONTHLY	50.00%		0.00
		SEP	3,395.31	MONTHLY	50.00%		0.00
		OCT	3,395.31	MONTHLY	50.00%		0.00
		NOV	3,395.31	MONTHLY	50.00%		0.00
		DEC	3,395.31	MONTHLY	50.00%		0.00
		JAN	3,395.31	MONTHLY	50.00%		0.00
		FEB	3,395.31	MONTHLY	50.00%		0.00
		MAR	3,395.31	MONTHLY	50.00%		0.00
		APR	3,395.31	MONTHLY	50.00%		0.00
		MAY	3,395.31	MONTHLY	50.00%		0.00
		JUN	3,395.31	MONTHLY	50.00%		0.00
	TOTAL					0.00	0.00
CRANE, SCOTT P	GRAD ASST	JUL	1,375.00	MONTHLY	33.00%		0.00
		AUG	1,375.00	MONTHLY	33.00%		0.00
		SEP	1,375.00	MONTHLY	33.00%		0.00
		OCT	1,375.00	MONTHLY	33.00%		0.00
		NOV	1,375.00	MONTHLY	33.00%		0.00
		DEC	1,375.00	MONTHLY	33.00%		0.00
		JAN	1,375.00	MONTHLY	33.00%		0.00
		FEB	1,375.00	MONTHLY	33.00%		0.00
		MAR	1,375.00	MONTHLY	33.00%		0.00
		APR	1,375.00	MONTHLY	33.00%		0.00
		MAY	1,375.00	MONTHLY	33.00%		0.00
		JUN	1,375.00	MONTHLY	33.00%		0.00
	TOTAL					0.00	0.00
CUNEFARE, KENNETH	ASST PROF	JUL	6,066.04	MONTHLY	18.80%		0.00
		AUG	6,066.04	MONTHLY	18.80%		0.00
		SEP	6,066.04	MONTHLY	18.80%		0.00
		OCT	6,066.04	MONTHLY	18.80%		0.00
		NOV	6,066.04	MONTHLY	18.80%		0.00
		DEC	6,066.04	MONTHLY	18.80%		0.00
		JAN	6,066.04	MONTHLY	18.80%		0.00
		FEB	6,066.04	MONTHLY	18.80%		0.00
		MAR	6,066.04	MONTHLY	18.80%		0.00
		APR	6,066.04	MONTHLY	18.80%	2,143.08	11.56
		MAY	6,066.04	MONTHLY	18.80%	2,143.08	11.56
		JUN	6,066.04	MONTHLY	18.80%		0.00
	TOTAL					4,286.16	23.11
	GRAND TOTAL FOR 1993-94					4,286.16	[illegible]

LOCKHEED AERONAUTICAL SYSTEMS CO-GA
GEORGIA INSTITUTE OF TECHNOLOGY
ANALYSIS OF PERSONAL SERVICES
CONTRACT TERM 03-21-94 - 12-31-96
CONTRACT #RF72740
PRIME #NAS1-20102, TASK ASSIGNMENT #6

EMPLOYEE	TITLE	MONTH	MONTHLY SALARY	TIME		PROJECT AMOUNT	ESTIMATED HOURS
JULY 1, 1995 - JUNE 30, 1996							
BIESEL, VAN B	RES ENGR I	JUL	3,621.66	MONTHLY	50.00%	1,810.84	43.33
		AUG	3,621.66	MONTHLY	50.00%	1,810.84	43.33
		SEP	3,621.66	MONTHLY	50.00%	1,810.84	43.33
		OCT	3,621.66	MONTHLY	50.00%	3,621.66	86.67
		NOV	3,621.66	MONTHLY	50.00%	1,810.84	43.33
		DEC	3,621.66	MONTHLY	50.00%		0.00
		JAN	3,621.66	MONTHLY	50.00%		0.00
		FEB	3,621.66	MONTHLY	50.00%		0.00
		MAR	3,621.66	MONTHLY	50.00%		0.00
		APR	3,621.66	MONTHLY	50.00%		0.00
		MAY	3,621.66	MONTHLY	50.00%		0.00
		JUN	3,621.66	MONTHLY	50.00%		0.00
	TOTAL					10,865.02	260.00
CRANE, SCOTT P	GRAD ASST	JUL	1,250.00	MONTHLY	33.00%	1,250.00	57.20
		AUG	1,250.00	MONTHLY	33.00%	1,250.00	57.20
		SEP	1,250.00	MONTHLY	33.00%	1,250.00	57.20
		OCT	1,250.00	MONTHLY	33.00%		0.00
		NOV	1,250.00	MONTHLY	33.00%		0.00
		DEC	1,250.00	MONTHLY	33.00%		0.00
		JAN	1,250.00	MONTHLY	33.00%		0.00
		FEB	1,250.00	MONTHLY	33.00%		0.00
		MAR	1,250.00	MONTHLY	33.00%		0.00
		APR	1,250.00	MONTHLY	33.00%		0.00
		MAY	1,250.00	MONTHLY	33.00%		0.00
		JUN	1,250.00	MONTHLY	33.00%		0.00
	TOTAL					3,750.00	171.60
DUNEGARD, KENNETH	ASST PROF	JUL	6,066.04	MONTHLY	18.80%	4,566.16	24.64
		AUG	6,066.04	MONTHLY	18.80%	4,566.16	24.64
		SEP	6,066.04	MONTHLY	18.80%	4,566.16	24.64
		OCT	6,066.04	MONTHLY	18.80%	1,539.83	8.31
		NOV	6,066.04	MONTHLY	18.80%	1,539.83	8.31
		DEC	6,066.04	MONTHLY	18.80%	1,539.83	8.31
		JAN	6,066.04	MONTHLY	18.80%		0.00
		FEB	6,066.04	MONTHLY	18.80%		0.00
		MAR	6,066.04	MONTHLY	18.80%		0.00
		APR	6,066.04	MONTHLY	18.80%		0.00
		MAY	6,066.04	MONTHLY	18.80%		0.00
		JUN	6,066.04	MONTHLY	18.80%		0.00
	TOTAL					16,677.97	100.34
	GRAND TOTAL FOR 1995-96					33,292.99	531.94

LOCKHEED ALRONAUTICS SYSTEMS
GEORGIA INSTITUTE OF TECHNOLOGY
ANALYSIS OF PERSONAL SERVICES
CONTRACT TERM 03-21-94 - 12-31-95
CONTRACT #RF7/740
PRIME #NAS1-20102, TASK ASSIGNMENT #6

EMPLOYEE	TITLE	MONTH	MONTHLY SALARY	TIME	PROJECT AMOUNT	**ESTIMATED HOURS

** NOTE

Georgia Tech does not track personal service charges for professional staff by the hour. We use the Planned-Confirmation System as required by the Federal government's guidelines in Circular A-21. The figures here are estimates based upon the annual salary divided by number of work hours in a year. The percentage of time spent on the project as required by the contract, and the actual charges each month for this project.

E-25-W56
#17

[illegible]
[illegible] INSTITUTE OF TECHNOLOGY
ANALYSIS OF PERSONAL SERVICES
CONTRACT TERM [illegible]
CONTRACT #[illegible]
PRIME #NAS1-20102, TASK ASSIGNMENT #6

EMPLOYEE	TITLE	MONTH	MONTHLY SALARY	TIME	PROJECT AMOUNT	ESTIMATED HOURS
JULY 1, 1995 - JUNE 30, 1996						
RIESEL VAN R	[illegible]	JUL	3,621.66	[illegible]	[illegible]	[illegible]
		AUG	3,621.66	MON	[illegible]	[illegible]
		SEP	3,621.66	MONTHLY	[illegible]	43.33
		OCT	3,621.66	MONTHLY	[illegible]	86.67
		NOV	3,621.66	MONTHLY	[illegible]	43.33
		DEC	3,621.66	MONTHLY	50.00%	0.00
		JAN	3,621.66	MONTHLY	50.00%	0.00
		FEB	3,621.66	MONTH	50.00%	0.00
		MAR	3,621.66	MONTHLY	0.00%	0.00
		APR	3,621.66	MONTHLY	0.00%	0.00
		MAY	3,621.66	MONTHLY	0.00%	0.00
		[illegible]	[illegible]	[illegible]	[illegible]	0.00
	TOTAL				[illegible]	260.00
[illegible]	[illegible]	JUL	1,250.00	MONTHLY	33.00%	[illegible]
		AUG	1,250.00	MONTHLY	33.00%	[illegible]
		SEP	1,250.00	MONTHLY	33.00%	[illegible]
		OCT	1,250.00	MONTHLY	33.00%	0.00
		NOV	1,250.00	MONTHLY	33.00%	0.00
		DEC	1,250.00	MONTHLY	33.00%	0.00
		JAN	1,250.00	MONTHLY	33.00%	0.00
		FEB	1,250.00	MONTHLY	33.00%	0.00
		MAR	1,250.00	MONTHLY	0.00%	0.00
		APR	1,250.00	MONTHLY	33.00%	0.00
		MAY	1,250.00	MONTHLY	33.00%	0.00
		[illegible]	[illegible]	[illegible]	[illegible]	0.00
	TOTAL				[illegible]	[illegible]
[illegible]	[illegible]	JUL	6,066.04	MONTHLY	8.80%	[illegible]
		AUG	6,066.04	MONTHLY	[illegible]	[illegible]
		SEP	6,066.04	MONTHLY	8.8%	[illegible]
		OCT	6,066.04	MONTHLY	8.80%	[illegible]
		NOV	6,066.04	MONTHLY	8.80%	8.91
		DEC	6,066.04	MONTHLY	15.80%	8.13
		JAN	6,066.04	MONTHLY	15.80%	[illegible]
		FEB	6,066.04	MONTHLY	[illegible]	[illegible]
		MAR	6,066.04	MONTHLY	[illegible]	[illegible]
		APR	6,066.04	MONTHLY	8.80%	0.00
		MAY	6,066.04	MONTHLY	15.80%	0.00
		[illegible]	[illegible]	[illegible]	[illegible]	[illegible]
	TOTAL				[illegible]	[illegible]
	GRAND TOTAL FOR 1996 86				33,165.92	531.26

LOCKHEED AERONAUTICAL CO-OP
GEORGIA INSTITUTE OF TECHNOLOGY
ANALYSIS OF PERSONAL SERVICES
CONTRACT TERM 03-21-84 - 12-31-96
CONTRACT #RF72740
PRIME #NAS1-20102, TASK ASSIGNMENT #8

EMPLOYEE	TITLE	MONTH	MONTHLY SALARY	TIME		PROJECT AMOUNT	**ESTIMATED HOURS
JULY 1, 1993 - JUNE 30, 1994							
BIESEL, VAN B.	RES ENGR I	JUL	3,395.31	MONTHLY	50.00%		0.00
		AUG	3,395.31	MONTHLY	50.00%		0.00
		SEP	3,395.31	MONTHLY	50.00%		0.00
		OCT	3,395.31	MONTHLY	50.00%		0.00
		NOV	3,395.31	MONTHLY	50.00%		0.00
		DEC	3,395.31	MONTHLY	50.00%		0.00
		JAN	3,395.31	MONTHLY	50.00%		0.00
		FEB	3,395.31	MONTHLY	50.00%		0.00
		MAR	3,395.31	MONTHLY	50.00%		0.00
		APR	3,395.31	MONTHLY	50.00%		0.00
		MAY	3,395.31	MONTHLY	50.00%		0.00
		JUN	3,395.31	MONTHLY	50.00%		0.00
	TOTAL					0.00	0.00
CRANE, SCOTT P	GRAD ASST	JUL	1,375.00	MONTHLY	33.00%		0.00
		AUG	1,375.00	MONTHLY	33.00%		0.00
		SEP	1,375.00	MONTHLY	33.00%		0.00
		OCT	1,375.00	MONTHLY	33.00%		0.00
		NOV	1,375.00	MONTHLY	33.00%		0.00
		DEC	1,375.00	MONTHLY	33.00%		0.00
		JAN	1,375.00	MONTHLY	33.00%		0.00
		FEB	1,375.00	MONTHLY	33.00%		0.00
		MAR	1,375.00	MONTHLY	33.00%		0.00
		APR	1,375.00	MONTHLY	33.00%		0.00
		MAY	1,375.00	MONTHLY	33.00%		0.00
		JUN	1,375.00	MONTHLY	33.00%		0.00
	TOTAL					0.00	0.00
JUNEFARE, KENNETH	ASST PROF	JUL	6,066.04	MONTHLY	18.80%		0.00
		AUG	6,066.04	MONTHLY	18.80%		0.00
		SEP	6,066.04	MONTHLY	18.80%		0.00
		OCT	6,066.04	MONTHLY	18.80%		0.00
		NOV	6,066.04	MONTHLY	18.80%		0.00
		DEC	6,066.04	MONTHLY	18.80%		0.00
		JAN	6,066.04	MONTHLY	18.80%		0.00
		FEB	6,066.04	MONTHLY	18.80%		0.00
		MAR	6,066.04	MONTHLY	18.80%		0.00
		APR	6,066.04	MONTHLY	18.80%	2,143.08	11.56
		MAY	6,066.04	MONTHLY	18.80%	2,143.08	11.56
		JUN	6,066.04	MONTHLY	18.80%		0.00
	TOTAL					4,286.16	23.11
	GRAND TOTAL FOR 1993-94					4,286.16	23.11

LOCKHEED AERONAUTICAL CO.
GEORGIA INSTITUTE OF TECHNOLOGY
ANALYSIS OF PERSONAL SERVICES
CONTRACT TERM 03-21-94 - 12-31-96
CONTRACT #RF72740
PRIME #NAS1-20102, TASK ASSIGNMENT #5

EMPLOYEE	TITLE	MONTH	MONTHLY SALARY	TIME		PROJECT AMOUNT	**ESTIMATED HOURS
JULY 1, 1994 - JUNE 30, 1996							
BIESEL, VAN B.	RES ENGR I	JUL	3,395.31	MONTHLY	50.00%		0.00
		AUG	3,395.31	MONTHLY	50.00%		0.00
		SEP	3,395.31	MONTHLY	50.00%		0.00
		OCT	3,395.31	MONTHLY	50.00%		0.00
		NOV	3,395.31	MONTHLY	50.00%		0.00
		DEC	3,395.31	MONTHLY	50.00%	1,069.47	25.87
		JAN	3,395.31	MONTHLY	50.00%	1,708.33	43.77
		FEB	3,395.31	MONTHLY	50.00%	1,708.33	43.77
		MAR	3,395.31	MONTHLY	50.00%	1,708.33	43.77
		APR	3,395.31	MONTHLY	50.00%	1,708.33	43.77
		MAY	3,395.31	MONTHLY	50.00%	1,708.33	43.77
		JUN	3,395.31	MONTHLY	50.00%	1,708.33	43.77
	TOTAL					11,259.45	288.51
CRANE, SCOTT P.	GRAD ASST	JUL	1,375.00	MONTHLY	33.00%	1,333.33	55.68
		AUG	1,375.00	MONTHLY	33.00%	1,333.33	55.68
		SEP	1,375.00	MONTHLY	33.00%	1,333.33	55.68
		OCT	1,375.00	MONTHLY	33.00%	1,250.00	52.20
		NOV	1,375.00	MONTHLY	33.00%	1,250.00	52.20
		DEC	1,375.00	MONTHLY	33.00%	1,250.00	52.20
		JAN	1,375.00	MONTHLY	33.00%	183.34	7.66
		FEB	1,375.00	MONTHLY	33.00%	183.34	7.66
		MAR	1,375.00	MONTHLY	33.00%	183.34	7.66
		APR	1,375.00	MONTHLY	33.00%	183.34	7.66
		MAY	1,375.00	MONTHLY	33.00%	183.34	7.66
		JUN	1,375.00	MONTHLY	33.00%	183.34	7.66
	TOTAL					8,650.03	368.58
DUNEFARE, KENNETH	ASST PROF	JUL	6,066.04	MONTHLY	18.80%	2,857.44	15.41
		AUG	6,066.04	MONTHLY	18.80%	2,857.44	15.41
		SEP	6,066.04	MONTHLY	18.80%	2,857.44	15.41
		OCT	6,066.04	MONTHLY	18.80%		0.00
		NOV	6,066.04	MONTHLY	18.80%		0.00
		DEC	6,066.04	MONTHLY	18.80%		0.00
		JAN	6,066.04	MONTHLY	18.80%		0.00
		FEB	6,066.04	MONTHLY	18.80%		0.00
		MAR	6,066.04	MONTHLY	18.80%		0.00
		APR	6,066.04	MONTHLY	18.80%		0.00
		MAY	6,066.04	MONTHLY	18.80%		0.00
		JUN	6,066.04	MONTHLY	18.80%		0.00
	TOTAL					8,572.32	46.23
	GRAND TOTAL FOR 1994-96					28,681.80	704.31

LOCKHEED AERONAUTICAL SYSTEMS CO-GA
GEORGIA INSTITUTE OF TECHNOLOGY
ANALYSIS OF PERSONAL SERVICES
CONTRACT TERM 03-21-94 - 12-31-98
CONTRACT #RF72740
PRIME #NAS1-20102, TASK ASSIGNMENT #6

EMPLOYEE	TITLE	MONTH	MONTHLY SALARY	TIME	PROJECT AMOUNT	**ESTIMATED HOURS

** NOTE: Georgia Tech does not track personal service charges for professional staff by the hour. We use the Planned Confirmation System as required by the Federal government's guidelines in OMB A-21. The figures here are estimates based upon the annual salary, the number of work hours in a year, the percentage of time assigned as required by the contract, and the actual charges each month for this project.

GEORGIA TECH RESEARCH CORPORATION

PLEASE REMIT TO:

GEORGIA TECH RESEARCH CORPORATION
P. O. BOX 100117
ATLANTA, GEORGIA 30384

INVOICE NO. E-25-W56 - 020796
246R81190A0

PAYABLE UPON RECEIPT OF INVOICE

PAYER'S ACCOUNT NUMBER:
RK72740

LASC-GEORGIA
ATTN: ACCOUNTS PAYABLE
S/81-49, ZONE 0285
86 SOUTH COBB DRIVE
MARIETTA GA 30063-0285

GTRC ACCOUNTING
NO.
Date
O D

INVOICE DATE	DESCRIPTION	CUMULATIVE AMOUNT	CURRENT AMOUNT
01/01/96	OPTIMIZATION IN STRUCTURAL ACOUSTICS USING FEM/BEM PRIME: NAS1-20102 TASK 5		
TO	PERSONAL SERVICES	69,916.79	1,512.16
	FRINGE BENEFITS	13,583.51	313.16
	MATERIALS AND SUPPLIES	3,396.90	0.00
01/31/96	EQUIPMENT	3,365.00	0.00
	TRAVEL	3,190.80	0.00
	CAPITAL OUTLAY		
	SUBCONTRACTS NON-MTDC		
	SUBCONTRACTS MTDC		
	INDIRECT CHARGES	37,054.00	811.80
		130,506.00	2,699.72

IF YOU HAVE QUESTIONS CONCERNING THIS INVOICE
CONTACT: J. Redmond PHONE: 404 894 6752

PLEASE REMIT THIS TOTAL AMOUNT > $ 2,699.72

RETAIN THIS COPY FOR YOUR RECORDS

E-25-W56
23

Georgia Institute of Technology

Home of the 1996 Olympic Village

OFFICE OF GRANTS AND CONTRACTS ACCOUNTING/
RISK MANAGEMENT
190 BOBBY DODD WAY
ATLANTA, GEORGIA 30332-0258
PHONE (404) 894-4524 FAX (404) 894-5519

DATE 8 [illegible] 96 NO. OF PAGES 7
(INCLUDING THIS PAGE)

TO Wanda Simon

FROM Jill Redmond

SUBJECT July Aug Oct Nov Dec

1 copy need

MESSAGE

(If this message is illegible or if you have a transmission problem, please contact our office at (404) 894-4524)

GEORGIA TECH RESEARCH CORPORATION

PLEASE REMIT TO:
GEORGIA TECH RESEARCH CORPORATION
P.O. BOX 100013
ATLANTA GEORGIA 30384

INVOICE NO. E-[illegible]-08021
246R81190A0

PAYABLE UPON RECEIPT OF INVOICE
PAYER'S ACCOUNT NUMBER:
RK72740

LASC-GEORGIA
ATTN: ACCOUNTS PAYABLE
S/81-49, ZONE 0285
86 SOUTH COBB DRIVE
MARIETTA GA 30063-0285

GTRC ACCOUNTING
NO:
DATE:
C/O:

INVOICE DATE	DESCRIPTION	CUMULATIVE AMOUNT	CURRENT AMOUNT
/01/96	OPTIMIZATION IN STRUCTURAL ACOUSTICS USING FEM/BEM PRIME: NAS1-20102 TASK 5		
TO	PERSONAL SERVICES	98,583.89	9,239.49
	FRINGE BENEFITS	19,887.35	2,154.38
	MATERIALS AND SUPPLIES	3,971.21	48.54
	OTHER INDIRECT		
/31/96	EQUIPMENT	3,365.00	
	TRAVEL	3,729.62	
	CAPITAL OUTLAY		
	SUBCONTRACTS NON-MTDC		
	SUBCONTRACTS MTDC		
	INDIRECT	53,312.66	5,662.01
		182,849.73	17,100.42

IF YOU HAVE QUESTIONS CONCERNING THIS INVOICE
CONTACT: JILL REDMOND PHONE: (404)894-6757

PLEASE PAY THIS TOTAL AMOUNT > $ 17,100.42

GTRC FILE COPY

LOCKHEED AERONAUT IY CO-GA
GEORGIA INSTITUTE OF TECHNOLOGY
ANALYSIS OF PERSONAL SERVICES
CONTRACT TERM 03-21-94 - 01-31-97
CONTRACT #RF72740
PRIME #NAS1-20102, TASK ASSIGNMENT #5

EMPLOYEE	TITLE	MONTH	MONTHLY SALARY		TIME	PROJECT AMOUNT	**ESTIMATED HOURS
JULY 1, 1994 - JUNE 30, 1995							
BIESEL, VAN B.	RES ENGR I	JUL	3,395.31	MONTHLY	50.00%		0.00
		AUG	3,395.31	MONTHLY	50.00%		0.00
		SEP	3,395.31	MONTHLY	50.00%		0.00
		OCT	3,395.31	MONTHLY	50.00%		0.00
		NOV	3,395.31	MONTHLY	50.00%		0.00
		DEC	3,395.31	MONTHLY	50.00%	1,009.47	25.87
		JAN	3,395.31	MONTHLY	50.00%	1,708.33	43.77
		FEB	3,395.31	MONTHLY	50.00%	1,708.33	43.77
		MAR	3,395.31	MONTHLY	50.00%	1,708.33	43.77
		APR	3,396.31	MONTHLY	50.00%	1,708.33	43.77
		MAY	3,395.31	MONTHLY	50.00%	1,708.33	43.77
		JUN	3,395.31	MONTHLY	50.00%	1,708.33	43.77
	TOTAL					11,259.45	288.51
CRANE, SCOTT P.	GRAD ASST	JUL	1,375.00	MONTHLY	33.00%	1,333.33	55.68
		AUG	1,375.00	MONTHLY	33.00%	1,333.33	55.68
		SEP	1,375.00	MONTHLY	33.00%	1,333.33	55.68
		OCT	1,375.00	MONTHLY	33.00%	1,250.00	52.20
		NOV	1,375.00	MONTHLY	33.00%	1,250.00	52.20
		DEC	1,375.00	MONTHLY	33.00%	1,250.00	52.20
		JAN	1,375.00	MONTHLY	33.00%	183.34	7.66
		FEB	1,375.00	MONTHLY	33.00%	183.34	7.66
		MAR	1,375.00	MONTHLY	33.00%	183.34	7.66
		APR	1,375.00	MONTHLY	33.00%	183.34	7.66
		MAY	1,375.00	MONTHLY	33.00%	183.34	7.66
		JUN	1,375.00	MONTHLY	33.00%	183.34	7.66
	TOTAL					8,850.03	369.58
CUNEFARE, KENNETH	ASST PROF	JUL	6,066.04	MONTHLY	18.80%	2,857.44	15.41
		AUG	6,066.04	MONTHLY	18.80%	2,857.44	15.41
		SEP	6,066.04	MONTHLY	18.80%	2,857.44	15.41
		OCT	6,066.04	MONTHLY	18.80%		0.00
		NOV	6,066.04	MONTHLY	18.80%		0.00
		DEC	6,066.04	MONTHLY	18.80%		0.00
		JAN	6,066.04	MONTHLY	18.80%		0.00
		FEB	6,066.04	MONTHLY	18.80%		0.00
		MAR	6,066.04	MONTHLY	18.80%		0.00
		APR	6,066.04	MONTHLY	18.80%		0.00
		MAY	6,066.04	MONTHLY	18.80%		0.00
		JUN	6,066.04	MONTHLY	18.80%		0.00
	TOTAL					8,572.32	46.23
	GRAND TOTAL FOR 1994-95					28,681.80	704.31

LOCKHEED AERONAUTICAL SYSTEMS CO-GA
GEORGIA INSTITUTE OF TECHNOLOGY
ANALYSIS OF PERSONAL SERVICES
CONTRACT TERM 03-21-94 - 01-31-97
CONTRACT #RF72740
PRIME #NAS1-20102, TASK ASSIGNMENT #5

EMPLOYEE	TITLE	MONTH	MONTHLY SALARY		TIME	PROJECT AMOUNT	**ESTIMATED HOURS
JULY 1, 1993 - JUNE 30, 1994							
BIESEL, VAN B	RES ENGR I	JUL	3,395.31	MONTHLY	50.00%		0.00
		AUG	3,395.31	MONTHLY	50.00%		0.00
		SEP	3,395.31	MONTHLY	50.00%		0.00
		OCT	3,395.31	MONTHLY	50.00%		0.00
		NOV	3,395.31	MONTHLY	50.00%		0.00
		DEC	3,395.31	MONTHLY	50.00%		0.00
		JAN	3,395.31	MONTHLY	50.00%		0.00
		FEB	3,395.31	MONTHLY	50.00%		0.00
		MAR	3,395.31	MONTHLY	50.00%		0.00
		APR	3,395.31	MONTHLY	50.00%		0.00
		MAY	3,395.31	MONTHLY	50.00%		0.00
		JUN	3,395.31	MONTHLY	50.00%		0.00
	TOTAL					0.00	0.00
CRANE, SCOTT P.	GRAD ASST	JUL	1,375.00	MONTHLY	33.00%		0.00
		AUG	1,375.00	MONTHLY	33.00%		0.00
		SEP	1,375.00	MONTHLY	33.00%		0.00
		OCT	1,375.00	MONTHLY	33.00%		0.00
		NOV	1,375.00	MONTHLY	33.00%		0.00
		DEC	1,375.00	MONTHLY	33.00%		0.00
		JAN	1,375.00	MONTHLY	33.00%		0.00
		FEB	1,375.00	MONTHLY	33.00%		0.00
		MAR	1,375.00	MONTHLY	33.00%		0.00
		APR	1,375.00	MONTHLY	33.00%		0.00
		MAY	1,375.00	MONTHLY	33.00%		0.00
		JUN	1,375.00	MONTHLY	33.00%		0.00
	TOTAL					0.00	0.00
JUNEFARE, KENNETH	ASST PROF	JUL	6,066.04	MONTHLY	18.80%		0.00
		AUG	6,066.04	MONTHLY	18.80%		0.00
		SEP	6,066.04	MONTHLY	18.80%		0.00
		OCT	6,066.04	MONTHLY	18.80%		0.00
		NOV	6,066.04	MONTHLY	18.80%		0.00
		DEC	6,066.04	MONTHLY	18.80%		0.00
		JAN	6,066.04	MONTHLY	18.80%		0.00
		FEB	6,066.04	MONTHLY	18.80%		0.00
		MAR	6,066.04	MONTHLY	18.80%		0.00
		APR	6,066.04	MONTHLY	18.80%	2,143.08	11.56
		MAY	6,066.04	MONTHLY	18.80%	2,143.08	11.56
		JUN	6,066.04	MONTHLY	18.80%		0.00
	TOTAL					4,286.16	23.11
	GRAND TOTAL FOR 1993-94					4,286.16	23.11

LOCKHEED AERONAUTICAL SYSTEMS CO-GA
GEORGIA INSTITUTE OF TECHNOLOGY
ANALYSIS OF PERSONAL SERVICES
CONTRACT TERM 03-21-94 - 01-31-97
CONTRACT #RF72740
PRIME #NAS1-20102, TASK ASSIGNMENT #5

EMPLOYEE	TITLE	MONTH	MONTHLY SALARY		TIME	PROJECT AMOUNT	**ESTIMATED HOURS
JULY 1, 1996 - JUNE 30, 1996							
BIESEL, VAN B	RES ENGR I	JUL	3,621.66	MONTHLY	50.00%	1,810.84	43.33
		AUG	3,621.66	MONTHLY	50.00%	1,810.84	43.33
		SEP	3,621.66	MONTHLY	50.00%	1,810.84	43.33
		OCT	3,621.66	MONTHLY	50.00%	3,621.66	86.67
		NOV	3,621.66	MONTHLY	50.00%	1,810.84	43.33
		DEC	3,621.66	MONTHLY	50.00%		0.00
		JAN	3,621.66	MONTHLY	50.00%		0.00
		FEB	3,621.66	MONTHLY	50.00%	3,621.68	86.67
		MAR	3,621.66	MONTHLY	50.00%	1,810.84	43.33
		APR	3,621.66	MONTHLY	50.00%	1,810.84	43.33
		MAY	3,621.66	MONTHLY	50.00%	1,810.84	43.33
		JUN	3,621.66	MONTHLY	50.00%	1,810.92	43.34
	TOTAL					21,730.14	520.00
DATER, BRIAN	GRAD ASST	JUL	0.00	MONTHLY	50.00%	0.00	0.00
		AUG	0.00	MONTHLY	50.00%	0.00	0.00
		SEP	0.00	MONTHLY	50.00%	0.00	0.00
		OCT	0.00	MONTHLY	50.00%	0.00	0.00
		NOV	0.00	MONTHLY	50.00%	0.00	0.00
		DEC	0.00	MONTHLY	50.00%	0.00	0.00
		JAN	1,350.00	MONTHLY	33.00%	450.00	19.07
		FEB	1,350.00	MONTHLY	33.00%	450.00	19.07
		MAR	1,350.00	MONTHLY	33.00%	450.00	19.07
		APR	1,350.00	MONTHLY	33.00%	450.00	19.07
		MAY	1,350.00	MONTHLY	33.00%	450.00	19.07
		JUN	1,350.00	MONTHLY	33.00%	450.00	19.07
	TOTAL					2,700.00	114.40
CRANE, SCOTT P.	GRAD ASST	JUL	1,250.00	MONTHLY	33.00%	1,250.00	57.20
		AUG	1,250.00	MONTHLY	33.00%	1,250.00	57.20
		SEP	1,250.00	MONTHLY	33.00%	1,250.00	57.20
		OCT	1,250.00	MONTHLY	33.00%		0.00
		NOV	1,250.00	MONTHLY	33.00%		0.00
		DEC	1,250.00	MONTHLY	33.00%		0.00
		JAN	1,250.00	MONTHLY	33.00%		0.00
		FEB	1,250.00	MONTHLY	33.00%		0.00
		MAR	1,250.00	MONTHLY	33.00%		0.00
		APR	1,250.00	MONTHLY	33.00%		0.00
		MAY	1,250.00	MONTHLY	33.00%		0.00
		JUN	1,250.00	MONTHLY	33.00%		0.00
	TOTAL					3,750.00	171.60

LOCKHEED AERONAUTICS CO-GA
GEORGIA INSTITUTE OF TECHNOLOGY
ANALYSIS OF PERSONAL SERVICES
CONTRACT TERM 03-21-94 - 01-31-97
CONTRACT #RF72740
PRIME #NAS1-20102, TASK ASSIGNMENT #5

EMPLOYEE	TITLE	MONTH	MONTHLY SALARY		TIME	PROJECT AMOUNT	**ESTIMATED HOURS
CUNEFARE, KENNETH	ASST PROF	JUL	6,066.04	MONTHLY	18.80%	4,586.16	24.64
		AUG	6,066.04	MONTHLY	18.80%	4,586.16	24.64
		SEP	6,066.04	MONTHLY	18.80%	4,586.16	24.64
		OCT	6,066.04	MONTHLY	18.80%	1,639.83	8.81
		NOV	6,066.04	MONTHLY	18.80%	1,639.83	8.81
		DEC	6,066.04	MONTHLY	18.80%	1,639.83	8.81
		JAN	6,066.04	MONTHLY	18.80%	1,512.77	8.13
		FEB	6,066.04	MONTHLY	18.80%	1,766.99	9.49
		MAR	6,066.04	MONTHLY	18.80%	1,639.83	8.81
		APR	6,066.04	MONTHLY	18.80%	819.92	4.40
		MAY	6,066.04	MONTHLY	18.80%	819.92	4.40
		JUN	6,066.04	MONTHLY	18.80%	819.92	4.40
	TOTAL					26,057.22	139.98
	GRAND TOTAL FOR 1995-96					54,237.36	831.58

JULY 1, 1996 - JANUARY 31, 1997

[illegible]ESEL, VAN B	RES ENGR I	JUL	3,839.00	MONTHLY	50.00%	1,919.50	43.33
		AUG	3,839.00	MONTHLY	50.00%	0.00	0.00
		SEP	3,839.00	MONTHLY	50.00%	0.00	0.00
		OCT	3,839.00	MONTHLY	50.00%	0.00	0.00
		NOV	3,839.00	MONTHLY	50.00%	0.00	0.00
		DEC	3,839.00	MONTHLY	50.00%	0.00	0.00
		JAN	3,839.00	MONTHLY	50.00%	0.00	0.00
		FEB	3,839.00	MONTHLY	50.00%	0.00	0.00
		MAR	3,839.00	MONTHLY	50.00%	0.00	0.00
		APR	3,839.00	MONTHLY	50.00%	0.00	0.00
		MAY	3,839.00	MONTHLY	50.00%	0.00	0.00
		JUN	3,839.00	MONTHLY	50.00%	0.00	0.00
	TOTAL					1,919.50	43.33
[illegible]ATER, BRIAN	GRAD ASST	JUL	1,166.66	MONTHLY	100.00%	1,166.66	0.00
		AUG	1,166.66	MONTHLY	100.00%	0.00	0.00
		SEP	1,166.66	MONTHLY	100.00%	0.00	0.00
		OCT	1,166.66	MONTHLY	100.00%	0.00	0.00
		NOV	1,166.66	MONTHLY	100.00%	0.00	0.00
		DEC	1,166.66	MONTHLY	100.00%	0.00	0.00
		JAN	1,166.66	MONTHLY	100.00%	0.00	0.00
		FEB	1,166.66	MONTHLY	100.00%	0.00	0.00
		MAR	1,166.66	MONTHLY	100.00%	0.00	0.00
		APR	1,166.66	MONTHLY	100.00%	0.00	0.00
		MAY	1,166.66	MONTHLY	100.00%	0.00	0.00
		JUN	1,166.66	MONTHLY	100.00%	0.00	0.00
	TOTAL					1,166.66	0.00

LOCKHEED AERONAUTICAL CO-GA
GEORGIA INSTITUTE OF TECHNOLOGY
ANALYSIS OF PERSONAL SERVICES
CONTRACT TERM 03-21-94 - 01-31-97
CONTRACT #RF72740
PRIME #NAS1-20102, TASK ASSIGNMENT #5

EMPLOYEE	TITLE	MONTH	MONTHLY SALARY		TIME	PROJECT AMOUNT	**ESTIMATED HOURS
CUNEFARE, KENNETH	ASST PROF	JUL	6,559.33	MONTHLY	93.00%	6,149.33	151.12
		AUG	6,559.33	MONTHLY	93.00%	0.00	0.00
		SEP	6,559.33	MONTHLY	93.00%	0.00	0.00
		OCT	6,559.33	MONTHLY	0.00%	0.00	0.00
		NOV	6,559.33	MONTHLY	0.00%	0.00	0.00
		DEC	6,559.33	MONTHLY	0.00%	0.00	0.00
		JAN	6,559.33	MONTHLY	0.00%	0.00	0.00
		FEB	6,559.33	MONTHLY	0.00%	0.00	0.00
		MAR	6,559.33	MONTHLY	0.00%	0.00	0.00
		APR	6,559.33	MONTHLY	0.00%	0.00	0.00
		MAY	6,559.33	MONTHLY	0.00%	0.00	0.00
		JUN	6,559.33	MONTHLY	0.00%	0.00	0.00
	TOTAL					6,149.33	151.12
	GRAND TOTAL FOR 1995-96					9,235.49	194.46

* NOTE

Georgia Tech uses actual hourly personal service charges for professional staff by the hour. We use the Planned Confirmation System as required by the Federal government's guidlines in Circular A-21. The figures here are estimates based upon the annual salary, the number of work hours in a year, the percentage of budgeted effort as required by the contract, and the actual charges each month for this project.

E 25.W56

through Sept #25

LOCKHEED AERONAUT SY CO-GA
GEORGIA INSTITUTE OF TECHNOLOGY
ANALYSIS OF PERSONAL SERVICES
CONTRACT TERM 03-21-94 - 01-31-97
CONTRACT #RF72740
PRIME #NAS1-20102, TASK ASSIGNMENT #5

EMPLOYEE	TITLE	MONTH	MONTHLY SALARY		TIME	PROJECT AMOUNT	**ESTIMATED HOURS
JULY 1, 1996 - JANUARY 31, 1997							
BIESEL, VAN B.	RES ENGR I	JUL	3,839.00	MONTHLY	50.00%	1,919.50	43.33
		AUG	3,839.00	MONTHLY	50.00%	1,919.50	43.33
		SEP	3,839.00	MONTHLY	50.00%	1,919.50	43.33
		OCT	3,839.00	MONTHLY	50.00%	0.00	0.00
		NOV	3,839.00	MONTHLY	50.00%	0.00	0.00
		DEC	3,839.00	MONTHLY	50.00%	0.00	0.00
		JAN	3,839.00	MONTHLY	50.00%	0.00	0.00
		FEB	3,839.00	MONTHLY	50.00%	0.00	0.00
		MAR	3,839.00	MONTHLY	50.00%	0.00	0.00
		APR	3,839.00	MONTHLY	50.00%	0.00	0.00
		MAY	3,839.00	MONTHLY	50.00%	0.00	0.00
		JUN	3,839.00	MONTHLY	50.00%	0.00	0.00
	TOTAL					5,758.50	130.00
DATER, BRIAN	GRAD ASST	JUL	1,166.66	MONTHLY	100.00%	1,166.66	173.33
		AUG	1,166.66	MONTHLY	100.00%	1,166.66	173.33
		SEP	1,166.66	MONTHLY	100.00%	1,166.66	173.33
		OCT	1,166.66	MONTHLY	100.00%	0.00	0.00
		NOV	1,166.66	MONTHLY	100.00%	0.00	0.00
		DEC	1,166.66	MONTHLY	100.00%	0.00	0.00
		JAN	1,166.66	MONTHLY	100.00%	0.00	0.00
		FEB	1,166.66	MONTHLY	100.00%	0.00	0.00
		MAR	1,166.66	MONTHLY	100.00%	0.00	0.00
		APR	1,166.66	MONTHLY	100.00%	0.00	0.00
		MAY	1,166.66	MONTHLY	100.00%	0.00	0.00
		JUN	1,166.66	MONTHLY	100.00%	0.00	0.00
	TOTAL					3,499.98	520.00
CUNEFARE, KENNETH	ASST PROF	JUL	6,559.33	MONTHLY	93.00%	6,149.33	151.12
		AUG	6,559.33	MONTHLY	93.00%	6,149.33	151.12
		SEP	6,559.33	MONTHLY	93.00%	6,149.33	151.12
		OCT	6,559.33	MONTHLY	0.00%	0.00	0.00
		NOV	6,559.33	MONTHLY	0.00%	0.00	0.00
		DEC	6,559.33	MONTHLY	0.00%	0.00	0.00
		JAN	6,559.33	MONTHLY	0.00%	0.00	0.00

LOCKHEED AERONAUT SY CO-GA
GEORGIA INSTITUTE OF TECHNOLOGY
ANALYSIS OF PERSONAL SERVICES
CONTRACT TERM 03-21-94 - 01-31-97
CONTRACT #RF72740
PRIME #NAS1-20102, TASK ASSIGNMENT #5

EMPLOYEE	TITLE	MONTH	MONTHLY SALARY		TIME	PROJECT AMOUNT	**ESTIMATED HOURS
		FEB	6,559.33	MONTHLY	0.00%	0.00	0.00
		MAR	6,559.33	MONTHLY	0.00%	0.00	0.00
		APR	6,559.33	MONTHLY	0.00%	0.00	0.00
		MAY	6,559.33	MONTHLY	0.00%	0.00	0.00
		JUN	6,559.33	MONTHLY	0.00%	0.00	0.00
	TOTAL					18,447.99	453.37
	GRAND TOTAL FOR 1996-97					27,706.47	1,103.37

** NOTE: Georgia Tech does not track personal service charges for professional staff by the hour. We use the Planned-Confirmation System as required by the Federal goverment's guidlines in Circular A-21. The figures here are estimates based upon the annual salary, the number of work hours in a year, the percentage of budgeted effort as required by the contract, and the actual charges each month for this project.

GEORGIA TECH RESEARCH CORPORATION

PLEASE REMIT TO:
GEORGIA TECH RESEARCH CORPORATION
P.O. BOX 100117
ATLANTA, GEORGIA 30384

INVOICE NO. E-25-W56 9-24-97
246R8TT90A0

PAYABLE UPON RECEIPT OF INVOICE

SPONSOR ACCOUNT #

LASC-GEORGIA
ATTN: ACCOUNTS PAYABLE
S/81-49, ZONE 0285
86 SOUTH COBB DRIVE
MARIETTA, GA 30063-0285

GTRC ACCOUNTING
CHECK NUMBER
DATE
D D
AMOUNT

INVOICE DATE	DESCRIPTION	CUMULATIVE AMOUNT	CURRENT AMOUNT
1-1-97	TITLE OF PROJECT		
TO			
	PERSONAL SERVICES	149,783.06	26,348.96
8-31-97			
	FRINGE BENFITS	31,160.24	6,195.38
	MATERIALS AND SUPPLIES	5,543.57	649.56
	EQUIPMENT	3,365.00	
	TRAVEL	4,811.82	427.86
	CAPITAL OUTLAY		
	SUBCONTRACTS NON MTDC		
	SUBCONTRACTS MTDC		
	INDIRECT	85,474.57	16,567.00
		280,138.26	50,188.76
	IF YOU HAVE ANY QUESTIONS CONCERNING THIS INVOICE CONTACT JIM WOODRUFF (404) 894-8757.		
	PLEASE PAY THIS TOTAL AMOUNT $		50,188.76

RETAIN THIS COPY FOR YOUR RECORDS

I certify that all expenditures reported (or payment requested) are for appropriate purposes and in accordance with the provisions of the application and award documents.

Charles T. Duffy, Interim Director
Grants & Contracts Accounting

EMPLOYEE	TITLE	MONTH	MONTHLY SALARY		TIME	PROJECT AMOUNT	**ESTIMATED HOURS
JULY 1, 1997 - JANUARY 31, 1998							
BIESEL, VAN B.	RES ENGR I	JUL	3,839.00	MONTHLY	50.00%	1,015.41	22.92
		AUG	3,839.00	MONTHLY	50.00%	1,015.41	22.92
		SEP	3,839.00	MONTHLY	50.00%	0.00	0.00
		OCT	3,839.00	MONTHLY	50.00%	0.00	0.00
		NOV	3,839.00	MONTHLY	50.00%	0.00	0.00
		DEC	3,839.00	MONTHLY	50.00%	0.00	0.00
		JAN	3,839.00	MONTHLY	50.00%	0.00	0.00
		FEB	3,839.00	MONTHLY	50.00%	0.00	0.00
		MAR	3,839.00	MONTHLY	50.00%	0.00	0.00
		APR	3,839.00	MONTHLY	50.00%	0.00	0.00
		MAY	3,839.00	MONTHLY	50.00%	0.00	0.00
		JUN	3,839.00	MONTHLY	50.00%	0.00	0.00
	TOTAL					2,030.82	45.85
DATER, BRIAN	GRAD ASST	JUL	1,166.66	MONTHLY	100.00%	0.00	0.00
		AUG	1,166.66	MONTHLY	100.00%	0.00	0.00
		SEP	1,166.66	MONTHLY	100.00%	0.00	0.00
		OCT	1,166.66	MONTHLY	100.00%	0.00	0.00
		NOV	1,166.66	MONTHLY	100.00%	0.00	0.00
		DEC	1,166.66	MONTHLY	100.00%	0.00	0.00
		JAN	1,166.66	MONTHLY	100.00%	0.00	0.00
		FEB	1,166.66	MONTHLY	100.00%	0.00	0.00
		MAR	1,166.66	MONTHLY	100.00%	0.00	0.00
		APR	1,166.66	MONTHLY	100.00%	0.00	0.00
		MAY	1,166.66	MONTHLY	100.00%	0.00	0.00
		JUN	1,166.66	MONTHLY	100.00%	0.00	0.00
	TOTAL					0.00	0.00
CUNEFARE, KENNETH	ASST PROF	JUL	6,559.33	MONTHLY	93.00%	4,903.33	120.50
		AUG	6,559.33	MONTHLY	93.00%	4,903.33	120.50
		SEP	6,559.33	MONTHLY	93.00%	0.00	0.00
		OCT	6,559.33	MONTHLY	0.00%	0.00	0.00
		NOV	6,559.33	MONTHLY	0.00%	0.00	0.00
		DEC	6,559.33	MONTHLY	0.00%	0.00	0.00
		JAN	6,559.33	MONTHLY	0.00%	0.00	0.00
		FEB	6,559.33	MONTHLY	0.00%	0.00	0.00
		MAR	6,559.33	MONTHLY	0.00%	0.00	0.00
		APR	6,559.33	MONTHLY	0.00%	0.00	0.00
		MAY	6,559.33	MONTHLY	0.00%	0.00	0.00
		JUN	6,559.33	MONTHLY	0.00%	0.00	0.00
	TOTAL					9,806.66	241.01
	GRAND TOTAL FOR 1997-98					**11,837.48**	**286.85**
	Life of Contract Total					**149,783.06**	**4,196.79**

** NOTE: Georgia Tech does not track personal service charges for professional staff by the hour. We use the Planned-Confirmation System as required by the Federal goverment's guidlines in Circular A-21. The figures here are estimates based upon the annual salary, the number of work hours in a year, the percentage of budgeted effort as required by the contract, and the actual charges each month for this project.

EMPLOYEE	TITLE	MONTH	MONTHLY SALARY		TIME	PROJECT AMOUNT	ESTIMATED HOURS
JULY 1, 1996 - JANUARY 31, 1997							
BIESEL, VAN B.	RES ENGR I	JUL	3,839.00	MONTHLY	50.00%	1,919.50	43.33
		AUG	3,839.00	MONTHLY	50.00%	1,919.50	43.33
		SEP	3,839.00	MONTHLY	50.00%	1,919.50	43.33
		OCT	3,839.00	MONTHLY	50.00%	959.75	21.67
		NOV	3,839.00	MONTHLY	50.00%	959.75	21.67
		DEC	3,839.00	MONTHLY	50.00%	959.75	21.67
		JAN	3,839.00	MONTHLY	50.00%	959.75	21.67
		FEB	3,839.00	MONTHLY	50.00%	959.75	21.67
		MAR	3,839.00	MONTHLY	50.00%	959.75	21.67
		APR	3,839.00	MONTHLY	50.00%	959.75	21.67
		MAY	3,839.00	MONTHLY	50.00%	959.75	21.67
		JUN	3,839.00	MONTHLY	50.00%	959.75	21.67
	TOTAL					14,396.25	325.00
DATER, BRIAN	GRAD ASST	JUL	1,166.66	MONTHLY	100.00%	1,166.66	173.33
		AUG	1,166.66	MONTHLY	100.00%	1,166.66	173.33
		SEP	1,166.66	MONTHLY	100.00%	1,166.66	173.33
		OCT	1,166.66	MONTHLY	100.00%	1,166.66	173.33
		NOV	1,166.66	MONTHLY	100.00%	1,166.66	173.33
		DEC	1,166.66	MONTHLY	100.00%	1,166.66	173.33
		JAN	1,166.66	MONTHLY	100.00%	1,166.66	173.33
		FEB	1,166.66	MONTHLY	100.00%	1,166.66	173.33
		MAR	1,166.66	MONTHLY	100.00%	1,166.66	173.33
		APR	1,166.66	MONTHLY	100.00%	0.00	0.00
		MAY	1,166.66	MONTHLY	100.00%	0.00	0.00
		JUN	1,166.66	MONTHLY	100.00%	0.00	0.00
	TOTAL					10,499.94	1,560.00
CUNEFARE, KENNETH	ASST PROF	JUL	6,559.33	MONTHLY	93.00%	6,149.33	151.12
		AUG	6,559.33	MONTHLY	93.00%	6,149.33	151.12
		SEP	6,559.33	MONTHLY	93.00%	6,149.33	151.12
		OCT	6,559.33	MONTHLY	0.00%	0.00	0.00
		NOV	6,559.33	MONTHLY	0.00%	0.00	0.00
		DEC	6,559.33	MONTHLY	0.00%	0.00	0.00
		JAN	6,559.33	MONTHLY	0.00%	0.00	0.00
		FEB	6,559.33	MONTHLY	0.00%	0.00	0.00
		MAR	6,559.33	MONTHLY	0.00%	0.00	0.00
		APR	6,559.33	MONTHLY	0.00%	1,751.00	0.00
		MAY	6,559.33	MONTHLY	0.00%	1,751.00	0.00
		JUN	6,559.33	MONTHLY	0.00%	1,751.00	0.00
	TOTAL					23,700.99	453.37
	GRAND TOTAL FOR 1996 97					48,597.18	2,338.37

EMPLOYEE	TITLE	MONTH	SALARY		TIME	PROJECT AMOUNT	ESTIMATED HOURS
JULY 1, 1996 - JUNE 30, 1996							
BIESEL, VAN B.	RES ENGR I	JUL	3,621.66	MONTHLY	50.00%	1,810.84	43.33
		AUG	3,621.66	MONTHLY	50.00%	1,810.84	43.33
		SEP	3,621.66	MONTHLY	50.00%	1,810.84	43.33
		OCT	3,621.66	MONTHLY	50.00%	3,621.66	86.67
		NOV	3,621.66	MONTHLY	50.00%	1,810.84	43.33
		DEC	3,621.66	MONTHLY	50.00%	0.00	0.00
		JAN	3,621.66	MONTHLY	50.00%	0.00	0.00
		FEB	3,621.66	MONTHLY	50.00%	3,621.68	86.67
		MAR	3,621.66	MONTHLY	50.00%	1,810.84	43.33
		APR	3,621.66	MONTHLY	50.00%	1,810.84	43.33
		MAY	3,621.66	MONTHLY	50.00%	1,810.84	43.33
		JUN	3,621.66	MONTHLY	50.00%	1,810.92	43.34
	TOTAL					21,730.14	520.00
DATER, BRIAN	GRAD ASST	JUL	0.00	MONTHLY	50.00%	0.00	0.00
		AUG	0.00	MONTHLY	50.00%	0.00	0.00
		SEP	0.00	MONTHLY	50.00%	0.00	0.00
		OCT	0.00	MONTHLY	50.00%	0.00	0.00
		NOV	0.00	MONTHLY	50.00%	0.00	0.00
		DEC	0.00	MONTHLY	50.00%	0.00	0.00
		JAN	1,350.00	MONTHLY	33.00%	450.00	19.07
		FEB	1,350.00	MONTHLY	33.00%	450.00	19.07
		MAR	1,350.00	MONTHLY	33.00%	450.00	19.07
		APR	1,350.00	MONTHLY	33.00%	450.00	19.07
		MAY	1,350.00	MONTHLY	33.00%	450.00	19.07
		JUN	1,350.00	MONTHLY	33.00%	450.00	19.07
	TOTAL					2,700.00	114.40
CRANE, SCOTT P.	GRAD ASST	JUL	1,250.00	MONTHLY	33.00%	1,250.00	57.20
		AUG	1,250.00	MONTHLY	33.00%	1,250.00	57.20
		SEP	1,250.00	MONTHLY	33.00%	1,250.00	57.20
		OCT	1,250.00	MONTHLY	33.00%	0.00	0.00
		NOV	1,250.00	MONTHLY	33.00%	0.00	0.00
		DEC	1,250.00	MONTHLY	33.00%	0.00	0.00
		JAN	1,250.00	MONTHLY	33.00%	0.00	0.00
		FEB	1,250.00	MONTHLY	33.00%	0.00	0.00
		MAR	1,250.00	MONTHLY	33.00%	0.00	0.00
		APR	1,250.00	MONTHLY	33.00%	0.00	0.00
		MAY	1,250.00	MONTHLY	33.00%	0.00	0.00
		JUN	1,250.00	MONTHLY	33.00%	0.00	0.00
	TOTAL					3,750.00	171.60
CUNEFARE, KENNETH	ASST PROF	JUL	6,066.04	MONTHLY	18.80%	4,586.16	24.64
		AUG	6,066.04	MONTHLY	18.80%	4,586.16	24.64
		SEP	6,066.04	MONTHLY	18.80%	4,586.16	24.64
		OCT	6,066.04	MONTHLY	18.80%	1,639.83	8.81
		NOV	6,066.04	MONTHLY	18.80%	1,639.83	8.81
		DEC	6,066.04	MONTHLY	18.80%	1,639.83	8.81
		JAN	6,066.04	MONTHLY	18.80%	1,512.77	8.13
		FEB	6,066.04	MONTHLY	18.80%	1,766.89	9.49
		MAR	6,066.04	MONTHLY	18.80%	1,639.83	8.81
		APR	6,066.04	MONTHLY	18.80%	819.92	4.40
		MAY	6,066.04	MONTHLY	18.80%	819.92	4.40
		JUN	6,066.04	MONTHLY	18.80%	819.92	4.40
	TOTAL					26,057.22	139.98
	GRAND TOTAL FOR 1996-96					54,237.36	831.58

EMPLOYEE	TITLE	MONTH	MONTHLY SALARY		TIME	PROJECT AMOUNT	ESTIMATED HOURS
JULY 1, 1993 - JUNE 30, 1994							
BIESEL, VAN B.	RES ENGR I	JUL	3,395.31	MONTHLY	50.00%		0.00
		AUG	3,395.31	MONTHLY	50.00%		0.00
		SEP	3,395.31	MONTHLY	50.00%		0.00
		OCT	3,395.31	MONTHLY	50.00%		0.00
		NOV	3,395.31	MONTHLY	50.00%		0.00
		DEC	3,395.31	MONTHLY	50.00%		0.00
		JAN	3,395.31	MONTHLY	50.00%		0.00
		FEB	3,395.31	MONTHLY	50.00%		0.00
		MAR	3,395.31	MONTHLY	50.00%		0.00
		APR	3,395.31	MONTHLY	50.00%		0.00
		MAY	3,395.31	MONTHLY	50.00%		0.00
		JUN	3,395.31	MONTHLY	50.00%		0.00
	TOTAL					0.00	0.00
CRANE, SCOTT P.	GRAD ASST	JUL	1,375.00	MONTHLY	33.00%		0.00
		AUG	1,375.00	MONTHLY	33.00%		0.00
		SEP	1,375.00	MONTHLY	33.00%		0.00
		OCT	1,375.00	MONTHLY	33.00%		0.00
		NOV	1,375.00	MONTHLY	33.00%		0.00
		DEC	1,375.00	MONTHLY	33.00%		0.00
		JAN	1,375.00	MONTHLY	33.00%		0.00
		FEB	1,375.00	MONTHLY	33.00%		0.00
		MAR	1,375.00	MONTHLY	33.00%		0.00
		APR	1,375.00	MONTHLY	33.00%		0.00
		MAY	1,375.00	MONTHLY	33.00%		0.00
		JUN	1,375.00	MONTHLY	33.00%		0.00
	TOTAL					0.00	0.00
CUNEFARE, KENNETH	ASST PROF	JUL	6,066.04	MONTHLY	18.80%		0.00
		AUG	6,066.04	MONTHLY	18.80%		0.00
		SEP	6,066.04	MONTHLY	18.80%		0.00
		OCT	6,066.04	MONTHLY	18.80%		0.00
		NOV	6,066.04	MONTHLY	18.80%		0.00
		DEC	6,066.04	MONTHLY	18.80%		0.00
		JAN	6,066.04	MONTHLY	18.80%		0.00
		FEB	6,066.04	MONTHLY	18.80%		0.00
		MAR	6,066.04	MONTHLY	18.80%		0.00
		APR	6,066.04	MONTHLY	18.80%	2,143.08	11.56
		MAY	6,066.04	MONTHLY	18.80%	2,143.08	11.56
		JUN	6,066.04	MONTHLY	18.80%	2,143.08	11.56
	TOTAL					6,429.24	34.67
	GRAND TOTAL FOR 1993-94					6,429.24	34.67

LOCKHEED AERONAUT SY CO-GA
GEORGIA INSTITUTE OF TECHNOLOGY
ANALYSIS OF PERSONAL SERVICES
CONTRACT TERM 03-21-94 - 11-01-97
CONTRACT #RF72740, PROJECT # E-25-W56, DELIVERABLE # 30 - 35
PRIME #NAS1-20102, TASK ASSIGNMENT #5

EMPLOYEE	TITLE	MONTH	MONTHLY SALARY		TIME	PROJECT AMOUNT	**ESTIMATED HOURS
JULY 1, 1994 - JUNE 30, 1995							
BIESEL, VAN B.	RES ENGR I	JUL	3,395.31	MONTHLY	50.00%		0.00
		AUG	3,395.31	MONTHLY	50.00%		0.00
		SEP	3,395.31	MONTHLY	50.00%		0.00
		OCT	3,395.31	MONTHLY	50.00%		0.00
		NOV	3,395.31	MONTHLY	50.00%		0.00
		DEC	3,395.31	MONTHLY	50.00%	1,009.47	25.87
		JAN	3,395.31	MONTHLY	50.00%	1,708.33	43.77
		FEB	3,395.31	MONTHLY	50.00%	1,708.33	43.77
		MAR	3,395.31	MONTHLY	50.00%	1,708.33	43.77
		APR	3,395.31	MONTHLY	50.00%	1,708.33	43.77
		MAY	3,395.31	MONTHLY	50.00%	1,708.33	43.77
		JUN	3,395.31	MONTHLY	50.00%	1,708.33	43.77
	TOTAL					11,259.45	288.51
CRANE, SCOTT P.	GRAD ASST	JUL	1,375.00	MONTHLY	33.00%	1,333.33	55.68
		AUG	1,375.00	MONTHLY	33.00%	1,333.33	55.68
		SEP	1,375.00	MONTHLY	33.00%	1,333.33	55.68
		OCT	1,375.00	MONTHLY	33.00%	1,250.00	52.20
		NOV	1,375.00	MONTHLY	33.00%	1,250.00	52.20
		DEC	1,375.00	MONTHLY	33.00%	1,250.00	52.20
		JAN	1,375.00	MONTHLY	33.00%	183.34	7.66
		FEB	1,375.00	MONTHLY	33.00%	183.34	7.66
		MAR	1,375.00	MONTHLY	33.00%	183.34	7.66
		APR	1,375.00	MONTHLY	33.00%	183.34	7.66
		MAY	1,375.00	MONTHLY	33.00%	183.34	7.66
		JUN	1,375.00	MONTHLY	33.00%	183.34	7.66
	TOTAL					8,860.03	369.58
CUNEFARE, KENNETH	ASST PROF	JUL	6,066.04	MONTHLY	18.80%	2,857.44	15.41
		AUG	6,066.04	MONTHLY	18.80%	2,857.44	15.41
		SEP	6,066.04	MONTHLY	18.80%	2,857.44	15.41
		OCT	6,066.04	MONTHLY	18.80%		0.00
		NOV	6,066.04	MONTHLY	18.80%		0.00
		DEC	6,066.04	MONTHLY	18.80%		0.00
		JAN	6,066.04	MONTHLY	18.80%		0.00
		FEB	6,066.04	MONTHLY	18.80%		0.00
		MAR	6,066.04	MONTHLY	18.80%		0.00
		APR	6,066.04	MONTHLY	18.80%		0.00
		MAY	6,066.04	MONTHLY	18.80%		0.00
		JUN	6,066.04	MONTHLY	18.80%		0.00
	TOTAL					8,572.32	46.23
	GRAND TOTAL FOR 1994-95					28,691.80	704.31

Georgia Institute of Technology
The George W. Woodruff School of Mechanical Engineering

17 October, 1997

Dr. Steve Engelstad
Lockheed Martin Aeronautical Systems Co.
Dept. 7347
Zone 0685
Marietta, GA 30063

Dear Steve,

The attached document is our final report for the project 'Optimization in structural acoustics using FEM/BEM.' I understand that Lockheed will be responsible for any subsequent revisions to this document that may be required by NASA.

I have enjoyed our collaboration on this research project. I hope that we will be able to do so again on future projects.

If you wish to discuss this report with me, I may be reached at (404) 894-4726.

Sincerely,

Kenneth A. Cunefare
Associate Professor

Atlanta, Georgia 30332-0405 U.S.A.
Administration Office 404•894•3200
Finance Office 404•894•7400
Graduate Program 404•894•3204
Undergraduate Office 404•894•3203
Fax 404•894•8336 or
web site: http://www.me.gatech.edu/

Georgia Institute of Technology
The George W. Woodruff School of Mechanical Engineering

17 October, 1997

Dr. Steve Engelstad
Lockheed Martin Aeronautical Systems Co.
Dept. 7347
Zone 0685
Marietta, GA 30063

Dear Steve,

The attached document is our final report for the project 'Optimization in structural acoustics using FEM/BEM.' I understand that Lockheed will be responsible for any subsequent revisions to this document that may be required by NASA.

I have enjoyed our collaboration on this research project. I hope that we will be able to do so again on future projects.

If you wish to discuss this report with me, I may be reached at (404) 894-4726.

Sincerely,

Kenneth A. Cunefare
Associate Professor

Atlanta, Georgia 30332-0405 U.S.A.
Administration Office 404•894•3200
Finance Office 404•894•7400
Graduate Program 404•894•3204
Undergraduate Office 404•894•3203
Fax 404•894•8336 or
web site: http://www.me.gatech.edu/

NASA Contractor Report _____

OPTIMIZATION IN STRUCTURAL ACOUSTICS USING FEM/BEM

S.P. Engelstad and E. A. Powell
Acoustics
Lockheed Martin Aeronautical Systems
Marietta, Georgia 30063-0685

and

K.A. Cunefare, S. Crane, V. Biesel, and B. Dater
Department of Mechanical Engineering
Georgia Institute of Technology
Atlanta, Georgia 30332-0405

October 1997

Prepared for
NASA Langley Research Center
Contract NAS1-20102 Task 5

PREFACE

This report was prepared by Lockheed Martin Aeronautical Systems (LMAS) and Georgia Institute of Technology (GT) under Task Assignment 5 of Contract NAS1-20102 with NASA Langley Research Center. This report contains the results conducted from February 1994 through November 1995. Dr. S.P. Engelstad is the overall principal investigator at LMAS, and Dr. Ken Cunefare is the principal investigator at GT. The NASA technical monitor was J. H. Robinson.

CONTENTS

LIST OF FIGURES

.....to be continued

OPTIMIZATION IN STRUCTURAL ACOUSTICS USING FEM/BEM

S.P. Engelstad, K.A. Cunefare, S. Crane, V. Biesel, B. Dater, E. A. Powell

SUMMARY

This report documents the results of a research program to develop a computational scheme using Finite Element and Boundary Element Methods (FEM/BEM) to minimize noise transmission into an aircraft fuselage interior by optimizing selected structural parameters. The algorithm is composed of MSC/NASTRAN (FEM) to model the structure, AAC COMET/Acoustics (BEM) to model the acoustic fluid, and CONMIN and COMPLEX as the optimizers. The algorithm can treat single- and multi-frequency excitations with multiple objective and constraint options. The potential and applicability has been validated against idealized unstiffened and stiffened cylinders, as well as against a more complex model of an actual airframe. Shell (skin) thickness and stiffener cross section dimensions were selected as design variables, and significant noise reduction potential by tailoring these details was demonstrated with little or no impact on weight. Various objective functions/constraints were evaluated. The best performing formulation minimizes the sum of pressure squared subject to constraints on weight and bounds on design variables. The computational efficiency and performance of the algorithm has been evaluated.

1. INTRODUCTION

This report presents the research accomplishments of a joint Lockheed/Georgia Tech research program directed toward optimizing the acoustic environment inside aircraft structures. The objective of the research was to develop design tools such that the structure of an aircraft fuselage may be tailored in such a way as to minimize the interior noise levels.

It is desirable that future aircraft be designed to have quieter passenger cabins, eliminating the need for retrofitted active or passive noise control systems. Designing quiet structures is itself a form of passive noise control, and falls under the broad category of Multidisciplinary Design Optimization (MDO). MDO is defined as a formal design methodology based on the integration of disciplinary analyses and sensitivity analyses, optimization and artificial intelligence, applicable at all stages of the multidisciplinary design of aerospace systems [1]. Design of quiet aircraft cabins is multidisciplinary in that it requires satisfaction of not only acoustic goals and constraints, but also structural goals and constraints such as weight, stress and aeroelastic effects. Figure 1.1 shows a typical MDO problem statement [2], where the constraints are equations modeling conditions that must be satisfied and the goals represent conditions that are desired but not required for a successful design. A_r and A_s are functions that model the multiple design objectives of the problem.

The objective, constraint, and goal functions in a MDO problem model the often conflicting goals of a variety of disciplines. This makes the multidisciplinary design process extremely complicated, requiring many iterations of time-consuming analyses coupled with a mathematical programming algorithm as a means of optimizing the system. In addition, due to the complexity

and often high nonlinearity of MDO problems, it is nearly impossible to guarantee that a solution is truly optimal. It is more likely that a set of local optimum solutions will be generated rather than a single global optimum. It remains the task of the designer to choose from among this set of optimal solutions the one which best satisfies not only the goals and constraints defined in the MDO problem, but also meets more intangible standards such as design experience and intuition. While MDO offers many benefits to design engineers, industry has been reluctant to confront the difficult challenges that it also presents. Cohn, in discussing structural optimization, points out that while a vast amount of literature exists on the subject, there are few instances where optimization has been applied to real problems in industry [3]. He states that optimization can aid the design process in three ways: (1) goal-orientation of the design approach; (2) tedium reduction; (3) decision-making help, trend finding, and preliminary design guidance. Although MDO may be difficult to implement, it offers a number of far reaching benefits to the designer, and it is beginning to be embraced by the aerospace industry for optimization of aircraft structures and performance.

FIND

The vector of **design variables** (**x**)

SATISFY

The **constraints**

$$A_u(\mathbf{x}) \left\{ \begin{matrix} \leq \\ = \\ \geq \end{matrix} \right\} G_u \qquad \text{for all u}$$

The **goals**

$$A_t(\mathbf{x}) \left\{ \begin{matrix} \leq \\ = \\ \geq \end{matrix} \right\} G_t \qquad \text{for all t}$$

MAXIMIZE

$A_r(\mathbf{x})$ for all r

MINIMIZE

$A_s(\mathbf{x})$ for all s

Figure 1.1 - General Model of a Multidisciplinary Design Optimization Problem

The research at hand sought to exploit the current state of the art in structural dynamic modeling codes, acoustic radiation modeling codes, and optimization to tailor the structural details of cylindrical aircraft structures for minimum interior noise levels. The research considered two academic cylindrical shell models: one bare isotropic model and one stiffened model, and a model derived from the production analysis model for a commercial aircraft manufacturer.

To conduct the intended optimization on these models, an extensive program development and integration effort was performed. This development effort involved the development and use of a UNIX shell script to integrate optimization codes (CONMIN and COMPLEX), a structural analysis code (NASTRAN, by McNeal-Schwendler (MSC)), and an acoustic analysis code (COMET/Acoustics, by Automated Analysis Corporation (AAC)).

For the development of the basic algorithm and capability, we considered an idealized fuselage modeled as a cylinder segment. We sought to minimize a measure of the interior noise within the

cylinder, while imposing a constraint on the weight of the cylinder. Other variations on this objective include a combined minimum weight and noise objective, and also minimum weight with constraint on noise. Other constraints include structural-integrity, including local stress limits and buckling. We consider both single-frequency and multi-frequency (using a peak-tracking algorithm) acoustic and structural excitations. The design tool has the capability to perform cross-section optimization on stiffener members. Further, it can include pressure-stiffening effects, and the ability to discriminate between which structural modes to include in the peak-tracking based on percentage of strain energy associated with the modes.

A great deal of research has examined optimal design for minimum weight [4-6], minimum fundamental frequency [7], specified displacement [8], etc. However, the research reported here, with its use of a desired acoustic response as a fundamental component of the objective function, appears to be relatively unique. Some recent work that seeks to integrate acoustic considerations into the design optimization process include those of the Naghshineh [9] and Lamancusa [10]. The Naghshineh work [9] presents a means to tailor certain material properties to achieve a desired minimum noise condition, but without constraints on weight. The Lamancusa work [10] presents a number of different formulations for acoustic objective functions. Hambric [11] considered a number of different optimization formulations as applied to the exterior radiation from cylinders. In light of the above, and to the best of our knowledge, the integrated design tool developed under the research project documented in this report represents a unique capability within the aerospace industry. Note that several software modeling companies, including McNeal-Schwendler and SDRC, are moving to incorporate similar capabilities as those developed here into their commerical products.

In the following sections, we review the Finite Element Method/Boundary Element Method (FEM/BEM) solution/modeling procedures, the theoretical basis for our optimization approaches, the computational structure of the integrated optimization algorithm, the results of our model studies, and our conclusions.

2. FEM/BEM MODELING

2.1 Solution Procedures

The structural/acoustics problem discussed in this report involves a solution of the linear harmonic structural dynamics equations coupled with the linear wave equation. The structural problem is solved using the MSC/NASTRAN FEM solution, while the acoustic problem is solved using the COMET/Acoustics BEM solution. A brief review of the governing equations follows here, but since the primary focus of this work is in the area of optimization, the FEM/BEM formulation details are omitted.

The general form of the equilibrium equation for the finite element discretized degrees of freedom of the linear structural system are:

$$[M]\{\ddot{u}\} + [B]\{\dot{u}\} + [K]\{u\} = \{P(t)\} \tag{2.1}$$

where $\{u\}$ is the vector of grid point displacements , $\{\dot{u}\}$ is the vector of grid point velocities, $\{\ddot{u}\}$ is the vector of grid point accelerations, [M] is the mass matrix, [B] is the damping matrix, [K] is the structural stiffness matrix, and $\{P(t)\}$ is the time-dependent applied force vector. A frequency response solution assumes a harmonic loading of the applied force vector at the jth element. Assuming a steady state solution of Eq. (2.1) and constant M, B, and K matrices results in a harmonic displacement solution of the following form:

$$[-M\omega^2 + iB\omega + K]\{\tilde{u}\}e^{i\omega t} = \{\tilde{P}\}e^{i\omega t} \tag{2.2}$$

Note that the factor $e^{i\omega t}$ can be eliminated from Eq. (2.2), and becomes an underlying factor of the solution. The vector $\{\tilde{P}\}$ is a frequency dependent set of dynamic loads on the structure. The displacement solution $\{\tilde{u}\}e^{i\omega t}$ is differentiated to produce the velocity solution required for the acoustic analysis. To account for stiffening effects, the converged nonlinear stiffness matrix, K_{NL}, is used in place of the linear stiffness matrix K.

The acoustic boundary element method (BEM) is used for the required interior and exterior acoustic analyses. The governing differential equation is

$$\nabla^2 p + k^2 p = 0 \tag{2.3}$$

where ∇^2 is the Laplacian operator, k is the acoustic wavenumber, and p is the acoustic pressure. This equation is the Helmholtz equation, the time harmonic case of the linear wave equation. Equation (2.3) and its fundamental solution, the free space Green's function, are used to derive the governing integral equations over the acoustic domain. This volume integral can be expressed as a surface integral by Green's theorem. The surface integral is called the Helmholtz Integral Equation, and may be used to solve for the pressure anywhere in the acoustic domain, including on the surface. The Helmholtz Integral Equation is typically implemented through discrete elements mapped onto the surface of the structure, leading to what is called the Boundary Element Method (BEM). Typically, the BEM requires specified normal velocity boundary conditions. Several alternative implementations exist for the acoustic BEM, including what is termed the indirect BEM. For the indirect BEM, the boundary conditions are the differences in pressures and differences in the gradient of the pressures across the boundary.

Discretization of the surface geometry and numerical integration lead to a system of algebraic equations for unknown surface quantities (pressures or pressure differences) at discrete points on the surface. In matrix form these equations are fully populated. This system of equations can be solved to yield the values of the boundary variables. Once the boundary variables are known, it is then possible to determine the acoustic quantities anywhere within the acoustic domain. Typically, this is done at a number of discrete points within the volume, called "data recovery nodes".

2.2 Model Descriptions

The numerical models are described in this section. This includes the test cylinder models used to evaluate the performance of the algorithm, and the Cessna fuselage model.

2.2.1 Test Models. In this study, unstiffened and stiffened uniform thickness cylinders, clamped at both ends are investigated to represent an idealized fuselage structure. The excitation is a single tone exterior monopole source on one side of the fuselage, chosen to represent a propellor source. The cylinder geometry and excitation were modeled after that of the NASA Composite Test Cylinder [12] and also the numerical model of Grosveld, et al. [13]. Figure 2.1 illustrates the structural finite element model for the unstiffened cylinder. A cylindrical coordinate system (r,θ,x) is used with the origin in the center of the clamped end, and with the x-axis running along the length of the cylinder. The aluminum cylinder has length $L = 3.66$ m, a radius of 0.838 m, and a thickness of 1.7 mm. Selecting to study only symmetric modal response, only one quarter of the cylinder is modeled ($0 \le x \le L/2$, $0 \le \theta \le \pi$). A direct frequency response solution is used to compute the structural velocity response in NASTRAN. Structural damping at 1% of critical is applied to the cylinder.

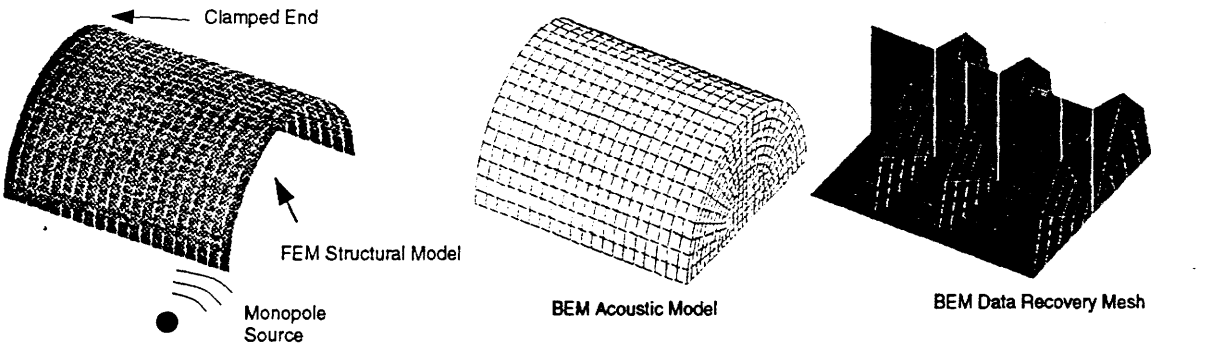

Figure 2.1 - Finite Element and Boundary Element Models

The primary exterior acoustic field is due to a single monopole source located at 0.168 m from the shell and at $x/L = 0.5$ and $\theta = 0$. Since a one-way coupled structural acoustic formulation is utilized here, the exterior and interior acoustic problems are solved separately, using the indirect BEM solution in COMET/Acoustics. Thus, prior to optimization, the exterior acoustic problem is solved to determine the blocked pressure due to the monopole on the outside of the cylinder. This pressure is integrated to produce the external loading of the NASTRAN FEM model, and for a

single frequency analysis. this loading remains constant throughout the optimization. The NASTRAN FEM structural and COMET/Acoustics BEM interior acoustic responses are computed repeatedly in the optimization process. The design variables selected for this model were the shell thicknesses and stiffener cross-section dimensions.

Figure 2.1 also illustrates the BEM boundary mesh and original data recovery interior mesh (refinements to this mesh will be discussed in Section 5.2). The boundary mesh density was set to handle the wavelengths appropriate for an analysis frequency of 250 Hz or less. The initial data recovery mesh was modeled after that in Grosveld, et al. [13], however the mesh density was dramatically reduced. A total of 188 data recovery nodes were used in this mesh.

For the stiffened version of the structural model, frame and stringer stiffeners were added to the same cylinder. For this model, design variables were not only shell thicknesses, but also heights and lengths of stiffener section dimensions. This model has exactly the same number of nodes as in the unstiffened problem since the frame and stringer stiffeners are modeled using offset beam elements. Figure 2.2 shows the FEM model with stiffeners, including the initial cross-section dimensions.

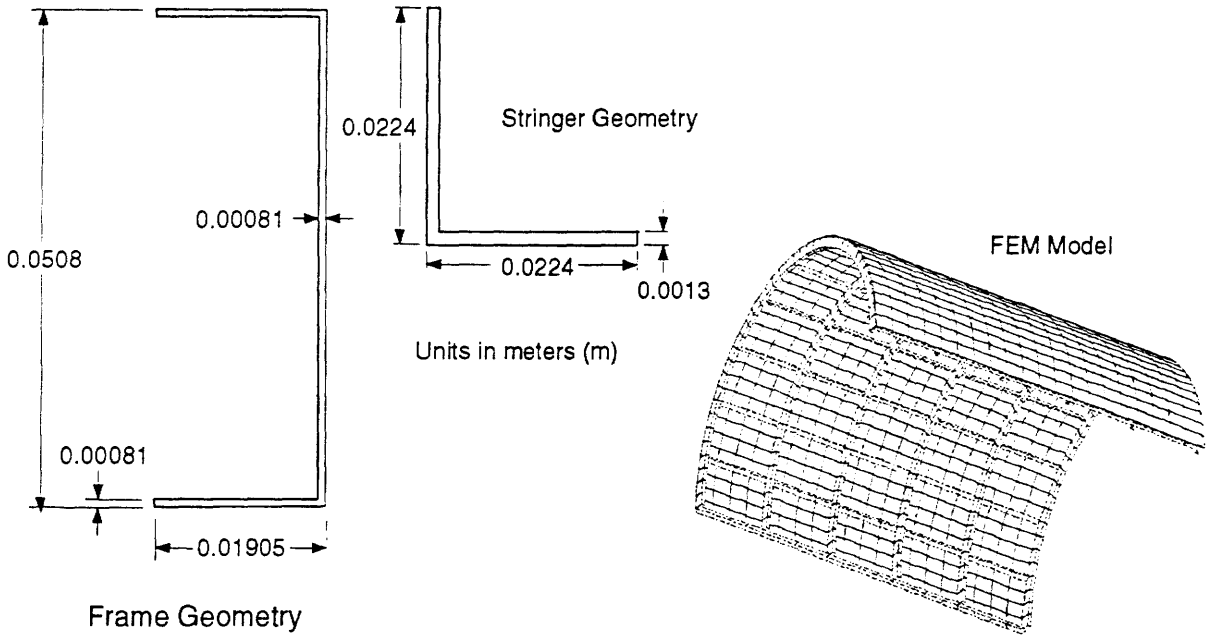

Figure 2.2 - FEM Model with Stiffeners

2.2.2 Cessna Fuselage Model. A model of a Cessna Citation III was constructed to test the performance of the algorithm and potential noise reduction for a real fuselage structure. The description of this model and results are given in Chapter 7. The results discussed in this report prior to chapter 7 refer to the test cylinder models described in the previous subsection.

3. OPTIMIZATION APPROACH

Section 1 described the multidisciplinary design optimization problem in its most general form. The general formulation is intended to show the broad range of application of MDO, and the fact that the design variables, constraints, goals, and objectives can model a system with elements from many different disciplines. In reality, such a general problem statement is extremely difficult to transform into a working model. While a vast number of mathematical programming algorithms exist, few if any are capable of solving the problem of Figure 1.1. This section presents a description of the two optimization algorithms, CONMIN and COMPLEX, used in this research. Subsequently, we present the formulations for the optimization problem.

Many methods of constrained optimization are single-objective, requiring that multi-objective problems be recast in single-objective format. They do not recognize goals, only constraints. These algorithms seek a single, unique optimal solution to the design problem. As mentioned in Section 1, this is rarely possible, and instead several solution attempts may yield several different designs from which the optimum can be chosen.

We implemented two single-objective optimizers in the course of this research: CONMIN [14], a FORTRAN program that uses a modified form of Zoutendijk's method of feasible directions algorithm to solve constrained problems and the conjugate direction method of Fletcher and Reeves to solve unconstrained problems; and COMPLEX, a FORTRAN program that implements M. J. Box's [15] algorithm.

CONMIN can optimize both linear and nonlinear objective functions. CONMIN was chosen for its familiarity, having been used in previous research, its ease of implementation, and because it could solve problems with initially infeasible solutions.

COMPLEX can treat the same objective functions as CONMIN, however, where CONMIN requires gradient information for the objective and constraints, COMPLEX does not. This makes COMPLEX suitable for analyses where the calculation of gradients is too computationally intensive, or where gradients are not available. COMPLEX is a direct-search optimizer.

3.1 CONMIN - Method of Feasible Directions

The general optimization problem of Section 1 can be rewritten for the case of single-objective constrained optimization using the method of feasible directions as:

$$\text{Minimize } f(\mathbf{x}) \tag{3.1}$$

$$\text{Subject to } g_j(\mathbf{x}) \le 0 \quad \text{for } j = 1, 2...J \tag{3.2}$$

$$\mathbf{x}_L \le \mathbf{x} \le \mathbf{x}_U, \tag{3.3}$$

where Eq. (3.1) represents a single-objective function of the vector of design variables x. Equation (3.2) represents a set of inequality constraints implicit or explicit in the design variables, and Eq. (3.3) represents upper and lower bounds on the design variables, or side constraints. This formulation does not consider equality constraints, because such constraints do not have a feasible interior. As mentioned by Vanderplaats [14], equality constraints may be treated as an analysis

sub-problem or may be considered by treating some of the design variables as dependent variables. As long as the conditions represented by equality constraints are remembered, they may be omitted from the formulation. In this research, all constraints were modeled as inequalities.

As is standard for all direct methods of nonlinear optimization, the method of feasible directions proceeds iteratively, choosing a new vector of design variables at each step that hopefully results in an improvement in the objective function over the previous step. The new vector of design variables is chosen by moving a certain distance and direction in the design space from the previous vector of design variables. A linear approximation of the problem is used to determine the search direction. Once the direction is known, the N-dimensional design problem becomes a one-dimensional line search at each step. This process is stated mathematically as

$$x^q = x^{q-1} + \alpha^* S^q \tag{3.4}$$

where q is the number of the current iteration, **S** is a search direction, and α^* is the step distance in that direction that minimizes the objective function. It is necessary to determine a direction **S** such that the step $\alpha^* \mathbf{S}^q$ be both usable and feasible, that is, it must reduce the objective while ensuring that no constraints are violated. The condition that **S** be usable can be stated as

$$\nabla f(x^q) \cdot S^q \leq 0 \tag{3.5}$$

where $\nabla f(x^q)$ is the normalized analytic gradient of the objective function. The condition of feasibility for search direction **S** is

$$\nabla g_j(x^q) \cdot S^q \leq 0 \quad j=1,2,...,NAC \tag{3.6}$$

where $\nabla g_j(x^q)$ is the normalized analytic gradient of the j^{th} active constraint and NAC is the number of active constraints. A constraint is defined as being active if the condition $g_j(x^q)=0$ holds. Figure 3.1 is a diagram of a two-dimensional problem with a single constraint, showing the relationship of the usable-feasible region to the gradients of the objective and constraint.

The search direction **S** can be found by solving

$$\text{Maximize } \beta \tag{3.7}$$

$$\text{Subject to } \nabla f(x^q) \cdot S^q + \beta \leq 0 \tag{3.8}$$

$$\nabla g_j(x^q) \cdot S^q + \theta_j \beta \leq 0 \quad j=1...NAC \tag{3.9}$$

$$\mathbf{S} \text{ Bounded.} \tag{3.10}$$

This problem will attempt to find a search direction that is opposed to the directions of the gradients of the objective and constraints. The θ_j are "push-off" factors that push the design away from the active constraints. The choice of the θ_j is important. If they are zero, the resulting search direction will be tangent to the constraints and the objective will be reduced quickly. However, there is a risk that the constraints will be frequently encountered if they are nonlinear. If the θ_j are large, the search direction will tend to be tangent to the gradient of the objective and will not reduce the objective by very much, but the constraints will not be encountered at every step. The

values of θ_j can be made variable, and by using a penalty function an initially infeasible design (where violated constraints are also considered active) can quickly be brought into the feasible design space. In this case the objective function would be modified to be

$$\text{Maximize} \quad -\nabla f(x^q)\cdot S^q + \phi\beta \tag{3.11}$$

where the constraint of Eq. (3.8) is eliminated but the others remain unchanged, and ϕ is a weighting factor similar to the θ_j.

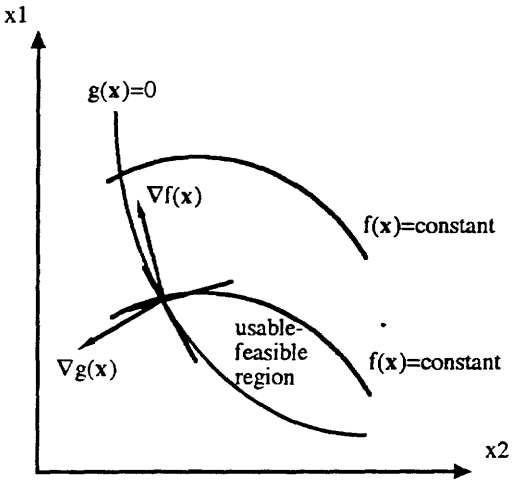

Figure 3.1 Diagram of Usable-Feasible Region in a Two-Dimensional Design Space

The condition that **S** be bounded can be handled by requiring

$$y^q \cdot y^q \le 1 \qquad y^q = \begin{Bmatrix} S_1^q \\ \vdots \\ \dfrac{S_{NDV}^q}{\beta} \end{Bmatrix} \tag{3.12}$$

where NDV is the number of design variables. This transformation makes the problem of Eqs. (3.7) - (3.10) a linear problem with one quadratic constraint. By applying the Kuhn-Tucker conditions, this can be converted to a purely linear problem. The Simplex method can be employed to solve this problem. If the final result is such that β equals zero, then $S^q \cdot S^q = 0$ and the design is a relative optimum, otherwise S^q is a usable-feasible direction and the next step of the optimization can proceed.

Having determined a search direction **S**, it is now necessary to perform a one-dimensional search along **S** to determine a step size α^* that minimizes the objective. This can be done using any of a number of one-dimensional search strategies. CONMIN uses two- and three-point interpolation to approximate the objective in one dimension. The minimum value of this one-dimensional function is then easy to determine. Knowing α^* and **S**, Eq. (3.4) can be used to compute the design variables for the next iteration.

3.2 COMPLEX Method

The nonlinear optimization method chosen for this approach is M.J. Box's Complex Method [15]. As mentioned previously, it is a direct-search algorithm, requiring calculations of only the objective function and constraints. The Complex Method was chosen for its ability to span large portions of the design space, thereby providing a better chance of finding the global optimum, and for its ability to solve constrained minimization problems. The Complex Method assumes that satisfying the explicit (side) constraints of the variable values does not guarantee a feasible point (i.e., satisfying the implicit constraints).

The Complex Method of nonlinear constrained optimization is an extension of the simplex method of unconstrained optimization. Like the simplex method, the Complex Method "is based on the generation and maintenance of a pattern of search points and the use of projections of undesirable points through the centroid of the remaining points as the means of finding new trial points." [16] When inequality constraints are applied to the simplex method, problems arise with the generation of an initial simplex of points. As each point is generated it must be tested for feasibility, and if it is found to be infeasible, it must be adjusted. This adjustment destroys the regularity of the simplex. Also, the points must be sequentially generated, rather than being defined using the formula for a regular simplex. These considerations led Box to propose the Complex Method [15], which uses an irregular complex of points in place of a regular simplex of points.

Figures 3.2 to 3.5 show how this implementation of the Complex Method operates. The *'s in the figures indicate the modifications (additional logic) which were added to the original algorithm for this research.

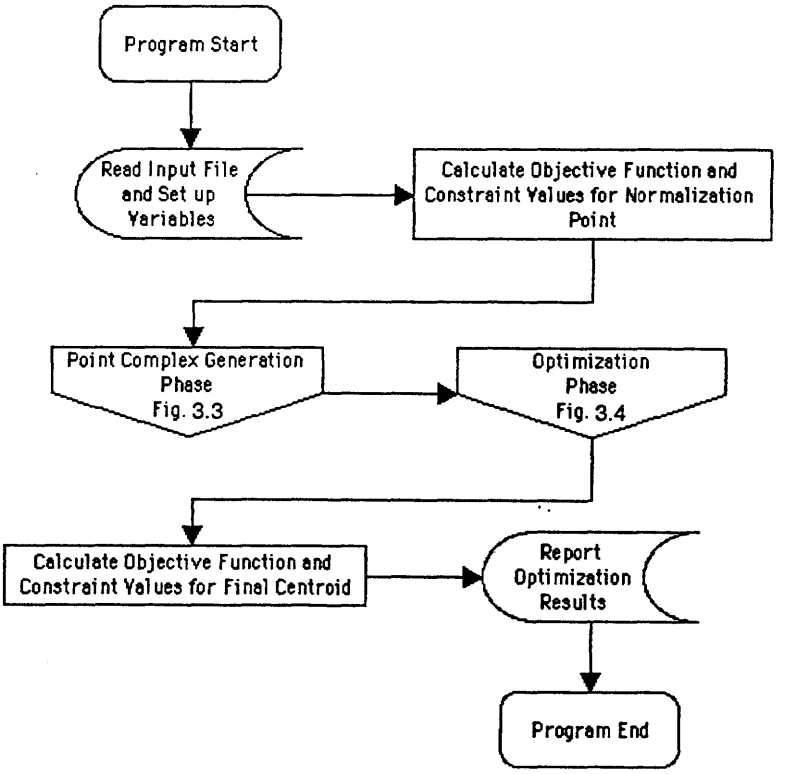

Figure 3.2 - COMPLEX Main Program Schematic

The Complex Method attempts to optimize (minimize in this implementation) the objective function by reflecting bad points through a centroid to find a better point. The initial steps set up the run by randomly generating a complex of points that should contain at least N+1 points, where N is the number of design variables (Figure 3.3).

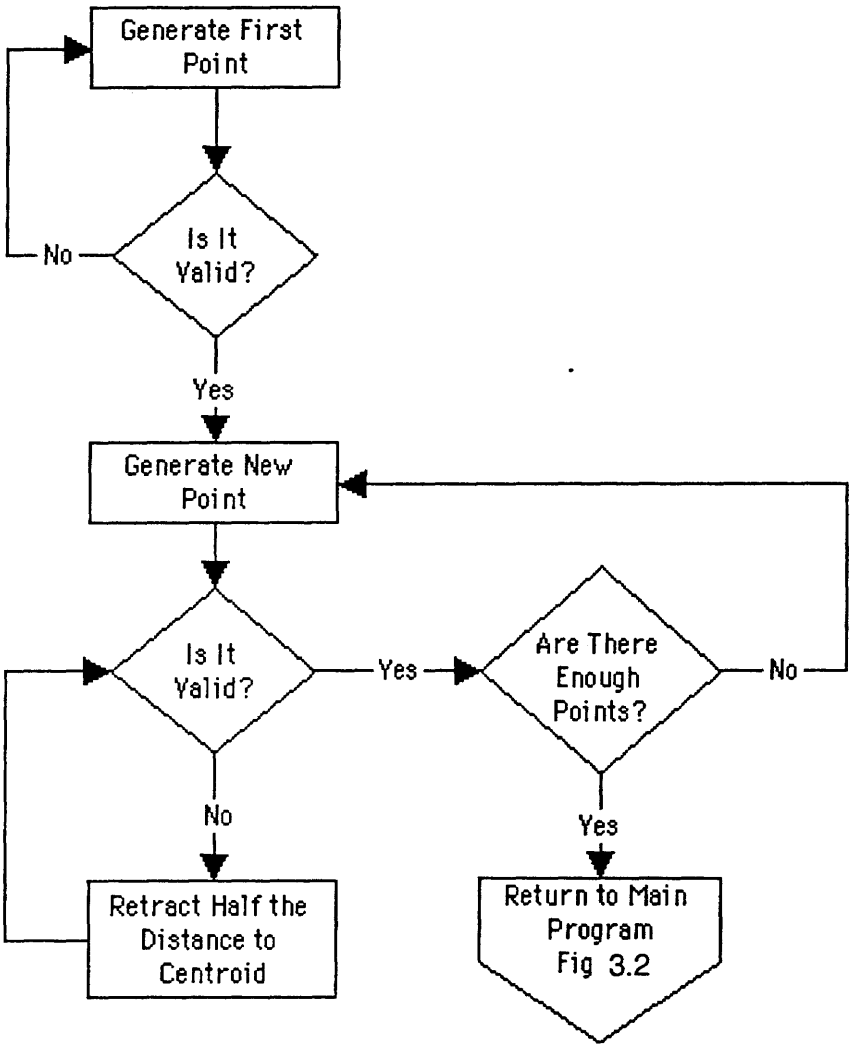

Figure 3.3 - COMPLEX Point Generation Phase Schematic

After a set of valid (satisfying all constraints) points has been generated, the algorithm moves to the optimization phase of the run (Figure 3.4). In this phase, the method calls for the improvement of the worst point in the complex (the point with the highest objective function value). To improve a point, the algorithm reflects it through the centroid of the remaining points. If the new point is worse, or it violates an implicit constraint, it is retracted half the distance to the centroid. The method continues in this manner until two convergence criteria are met (discussed in the next section), or the maximum number of function evaluations is reached (this is set by the user).

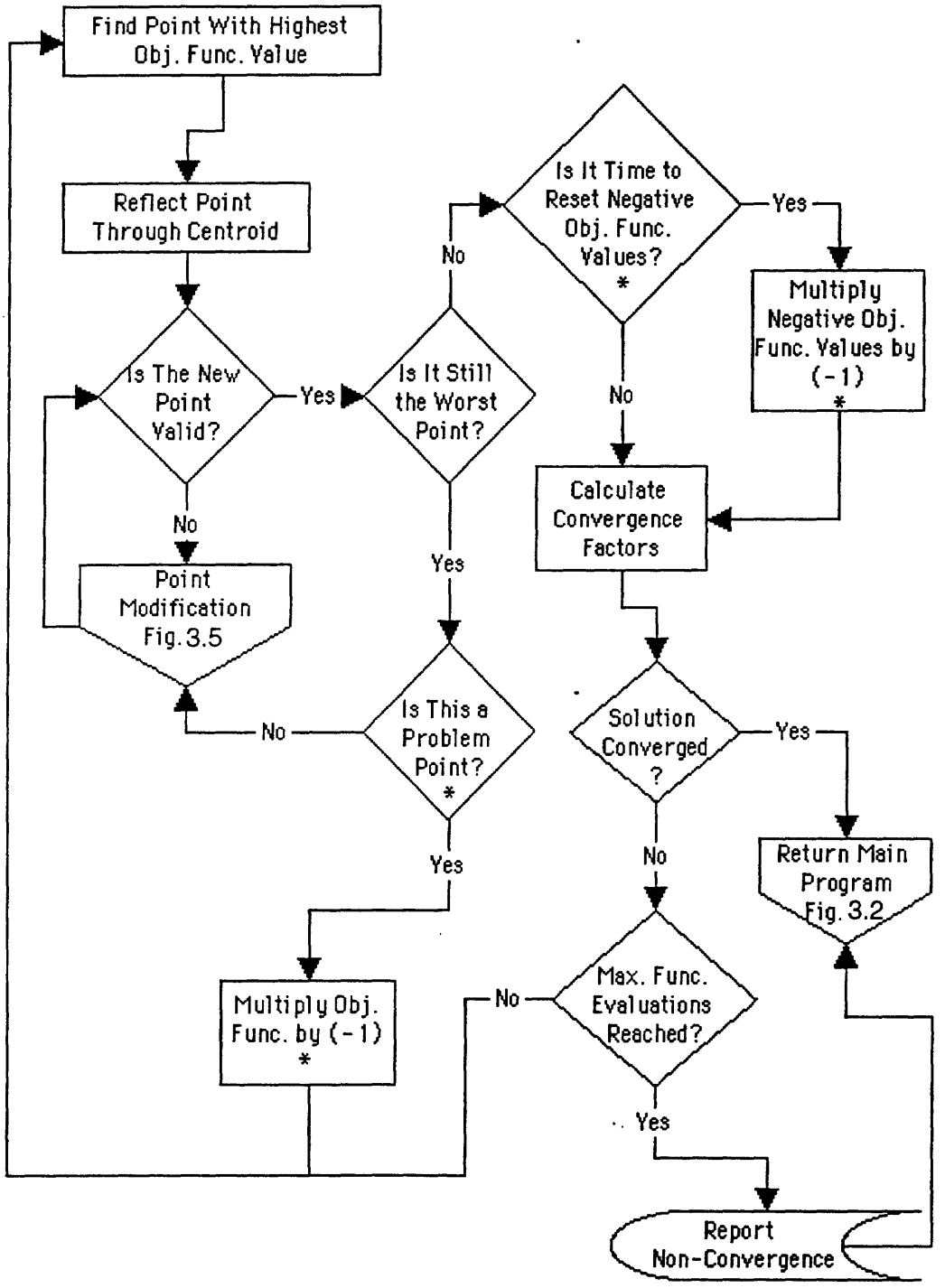

Figure 3.4 - COMPLEX Optimization Phase Schematic

As was briefly described above, the method starts with an initially feasible point (in this implementation, this point is randomly generated), and from there, a set of P trial points is generated (Figure 3.3) by

$$x_{i,j} = x_i^l + r(x_i^u - x_i^l) \tag{3.13}$$

where:

- $i = 1, 2, ..., N$,
- $j = 2, 3, ..., P$,
- $x_{i,j}$ = a design variable value,
- r = a random number between 0 and 1,

and where P is a number not less than N+1. If a new point is infeasible (it violates one or more of the implicit constraints), it is retracted half the distance to the centroid of the valid, previously generated points. An invalid point is retracted until it becomes feasible. Notice that Eq. 3.13 will always produce a valid point with respect to the explicit constraints.

When a set of P feasible points has been generated, the method moves to the optimization phase (Figure 3.4). It takes the point with the highest (for minimization) or lowest (for maximization) objective function value, and reflects it through the centroid of the remaining points,

$$x^n = \bar{x} + \alpha(\bar{x} - x^r) \tag{3.14}$$

where:

- x^a = the new point
- $\bar{x}$ = the centroid of the remaining points,
- x^r = the rejected point,
- α = the reflection parameter.

The centroid of the remaining points is defined by,

$$\bar{x}_i = \frac{1}{P-1}\left[\sum_{j=1}^{P}(x_{i,j}) - x_i^r\right] \tag{3.15}$$

where, i is 1,2,...,N. It is possible that some of the new point's design variable values violate the explicit constraints (variable bounds). If this occurs, these design variable values are reset to the value of the bound that they violate.

When a new point has been calculated, the objective function and constraints are evaluated. There are now three possibilities [16]:

- The new point is feasible and its function value is not the highest of the set of points. In this case, the method continues with the selection of the point with the highest objective function value as the next point to be reflected.
- The new point is feasible and its objective function value is the highest of the current set of P points. This type of point is retracted half the distance to the previously calculated centroid.
- The new point is infeasible. In this case, the point is retracted half the distance to the centroid as well.

The method continues until the two stopping criteria are met, or the maximum number of function evaluations is exceeded. The first stopping criterion is based on the objective function values of all P points in the complex. This convergence criterion,

$$\sum_{j=1}^{P} \left[f(x_j) - \bar{f} \right]^2 \leq \varepsilon \tag{3.16}$$

where

$$\bar{f} = \frac{1}{P} \sum_{j=1}^{P} f(x_j) \tag{3.17}$$

is the sum of the squared differences between each point's objective function value and the average objective function value of the points in the complex. The criterion is met if this value is less than or equal to the value of ε (a user defined variable). The second criterion that must be met for convergence of the solution is a measure of the design space covered by the complex of points

$$\frac{\sum_{i=1}^{N} \sum_{j=1}^{P} \left(x_{i,j} - \bar{x}_i \right)^2}{x^{tot}} \leq \delta \tag{3.18}$$

where

$$x^{tot} = \sum_{i=1}^{N} \left(x_i^u - x_i^l \right)^2 \tag{3.19}$$

where

$$\bar{x}_i = \frac{1}{P} \sum_{j=1}^{P} x_{i,j} \tag{3.20}$$

and where, i is 1,2,...,N. When both of these criteria have been met, the method has converged to an optimum point.

Several additions (indicated with *'s in Figures 3.2 - 3.5) were made to the original method of optimization during this research. Occasionally, situations were encountered where the optimization program would get "stuck." When these situations were found, attempts were made to eliminate their future occurrence by adding additional search logic to the existing method. These additions originated with this research, and were not found in the literature, and as such represent a new contribution.

Often, during the optimization phase of a run (Figure 3.4), a better point could not be found by retracting half the distance to the centroid. When no appreciable change in a point can be detected through a retraction, meaning that the point is very close to the centroid, the point is reflected in the opposite direction,

$$x^n = \bar{x} - \alpha (\bar{x} - x^r) \tag{3.21}$$

This causes the new point to be on the same "side" of the centroid as the original, rejected point, except that it is α times farther away from the centroid. If this point is still not acceptable, it is again retracted half the distance to the centroid. This type of search allows the optimizer to find design improvements that were inaccessible with the original algorithm.

If the negative reflection (Equation 3.21) and subsequent retractions also fail to find a better point, the method begins a search of the vector of points formed by the rejected point and the centroid (Figure 3.5). This is accomplished by modifying a variable that replaces α in Equation 3.14. This new variable is varied from 2.0 to -2.0 by increments of 0.1. Once again, if an explicit constraint is violated for a design variable, that design variable is set to the value of the constraint. This movement along the vector formed between the original worst point and the centroid of points samples some areas that are missed when the point is successively retracted half the distance to the centroid.

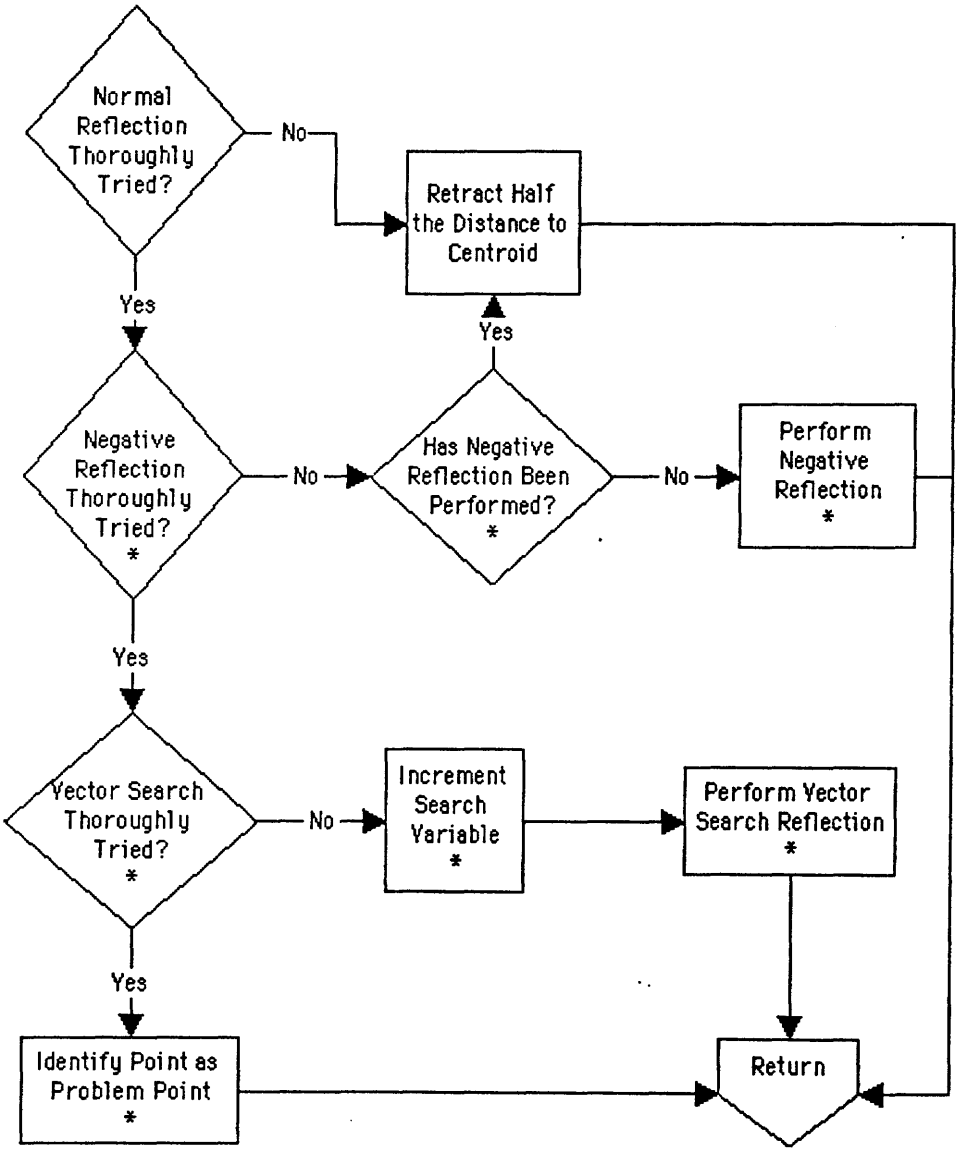

Figure 3.5 - COMPLEX Point Modification Schematic

A point that cannot be improved upon by any of these methods is said to be a problem point. Instead of throwing this point away and generating a new one, the optimizer ignores it. To do this, the program sets the problem point's objective function value to the negative of its current value (Figure 3.5). This makes it the lowest value, and provides a simple method of identification. Any points with negative objective function values are excluded from centroid or convergence criteria calculations. This technique would clearly not work with an objective function that could have negative values. In this implementation though, it is impossible to have a true negative objective function value, so this technique is acceptable.

After a set number of improved, feasible points have been found, the objective function values of points that are negative are reset to positive values. This is done in the hopes that the centroid of the complex of points has moved far enough to allow these problem points to be improved upon.

3.3 Objective Function Formulations

Four objective function formulations were implemented. The four formulations address different means of considering interior noise and weight. A relatively simple problem (low node-count cylinder model) was used in the development and testing of the design tool. The baseline formulation considers only the interior acoustics of the cylinder, with no explicit limit on weight. The remaining three formulations consider both the acoustics and the weight of the cylinder. These remaining formulations are referred to as the acoustic problem, the weight problem, and the compound problem, where the names refer to the property that is being minimized (compound implies that both acoustics and weight are being minimized simultaneously). The following sections detail each of these objective function formulations.

3.3.1 Baseline Formulation. This formulation only considers the interior acoustic behavior of the cylinder model. The objective is to minimize the sum of the squares of the acoustic pressure amplitudes measured at the data recovery nodes of the cylinder model. The only constraints are side constraints that impose upper and lower bounds on the design variables. Stated mathematically, the optimization problem is

$$\text{Minimize} \quad f(x) = \frac{\sum_{i=1}^{NDRN} |\hat{p}_i(\mathbf{x})|^2}{(\sum p^2)_{ref}} = \frac{\sum_{i=1}^{NDRN} \hat{p}_i(\mathbf{x})\hat{p}_i^*(\mathbf{x})}{(\sum p^2)_{ref}} \tag{3.22}$$

$$\mathbf{x}_L \le \mathbf{x} \le \mathbf{x}_U, \tag{3.23}$$

where $\hat{p}_i(x)$ is the complex pressure, implicitly a function of the design variables, at the i^{th} data recovery node, $\hat{p}_i^*(x)$ is its complex conjugate, and NDRN is the number of data recovery nodes in the cylinder. The gradient of the objective function with respect to the j^{th} design variable, x_j, is

$$\frac{\partial f}{\partial x_j} = \sum_{i=1}^{NDRN} \left(\hat{p}_i \frac{\partial \hat{p}_i^*}{\partial x_j} + \hat{p}_i^* \frac{\partial \hat{p}_i}{\partial x_j} \right) = 2 \sum_{i=1}^{NDRN} \mathrm{Re}\left(\hat{p}_i \frac{\partial \hat{p}_i}{\partial x_j} \right) \tag{3.24}$$

where Re represents the real part of the argument and the derivative $\frac{\partial \hat{p}_i}{\partial x_j}$ is the global structural acoustic sensitivity derivative.

3.3.2 Acoustic Formulation. The acoustic formulation seeks the vector of design variables that minimizes the sum of the squared acoustic pressures subject to the side constraints and to a constraint on the total weight of the structure. In a similar manner, Lamancusa [10] looked at optimizing the thickness of an isotropic plate to minimize radiated acoustic power, subject to a constraint on the mass of the plate. The formulation is stated as:

$$\text{Minimize} \qquad f(x) = \frac{\sum_{i=1}^{NDRN} \hat{p}_i(\mathbf{x})\,\hat{p}_i^*(\mathbf{x})}{(\sum p^2)_{ref}} \tag{3.25}$$

$$\text{Subject to} \quad \frac{W}{W_{Max}} - 1 \le 0 \tag{3.26}$$

$$\mathbf{x}_L \le \mathbf{x} \le \mathbf{x}_U. \tag{3.27}$$

W is the total weight of the structure, and W_{Max} is a user-specified maximum weight. Notice that it is entirely possible, and in fact likely, that the initial weight of the cylinder will exceed the specified maximum, indicating an infeasible starting point. This is not a problem for either CONMIN or COMPLEX , which are able to move the design into the feasible space. As in the baseline formulation, the objective function is nonlinear, and the added constraint on the weight is linear in the design variables.

3.3.3 Weight Formulation. The weight formulation seeks the vector of design variables that minimizes the weight of the structure subject to design variable side constraints and a constraint on the maximum value of the sum of the squared pressures. Again, Lamancusa [10] investigated a similar formulation for a plate model, where mass was minimized subject to a constraint on the radiated acoustic power. The weight formulation is stated as:

$$\text{Minimize} \quad f(\mathbf{x}) = W/W_{ref} \tag{3.28}$$

$$\text{Subject to} \quad \frac{\sum_{i=1}^{NDRN} \hat{p}_i(x)\hat{p}_i^*(x)}{\left(\sum p^2\right)_{Max}} - 1 \le 0 \tag{3.29}$$

$$\mathbf{x}_L \le \mathbf{x} \le \mathbf{x}_U, \tag{3.30}$$

where $\left(\sum p^2\right)_{Max}$ is the maximum sum of the squared pressures. The user specifies this maximum average value for the squared pressure at the data recovery nodes, and this number is multi-

plied by the number of nodes to determine the maximum sum. Note that the objective function in this case is linear while the constraint is nonlinear. The weight formulation is in effect the converse of the acoustic formulation, and it will be observed that they produce very similar results.

3.3.4 Compound Formulation. The compound formulation seeks to find the vector of design variables that simultaneously minimizes the sum of the squared acoustic pressures and the structural weight. Because CONMIN can only minimize a single-objective function, it is necessary to find a way to cast this multi-objective problem into a single-objective problem. Bendsøe et al. [17] used a method whereby a multi-criterion problem could be handled by minimizing bounds on the criteria. This concept is applied here. The objectives, the pressure sum and the weight, are normalized by their initial values and required to be less than bounds β_a and β_w, respectively. These bounds are considered to be two additional design variables, and their weighted sum is taken as the new objective function, where μ_a and μ_w are the respective weighting factors. The weighting factors allow one or the other objective to be considered more important. It is necessary to use the "beta" variables since it is physically meaningless to minimize the sum of the normalized pressures and weight. The "beta" variables allow the pressures and weight to be recovered at any step in the optimization. Not using this bounding variable method would require additional post-processing to recover the optimal values of the objectives. The mathematical statement of the formulation is:

$$\text{Minimize} \quad \mu_a \beta_a + \mu_w \beta_w \tag{3.31}$$

$$\text{Subject to} \quad \frac{\sum_{i=1}^{NDRN} \hat{p}_i(x)\, \hat{p}_i^*(x)}{\left(\sum p^2\right)_{Ref}} - \beta_a \le 0 \tag{3.32}$$

$$\frac{W}{W_{Ref}} - \beta_w \le 0 \tag{3.33}$$

$$\mathbf{x}_L \le \mathbf{x} \le \mathbf{x}_U, \tag{3.34}$$

where $\left(\sum p^2\right)_{Ref}$ is the initial value of the sum of the squared pressures (before the optimization process began), and similarly W_{ref} is the initial weight of the structure. The "beta" variables are initially set to be 1.0, to make both constraints active initially. In addition, upper and lower bounds on the "betas" are set to be very large and very small, to allow them to vary freely. In this way, it can be seen that Eq. (3.32) and (3.33) represent rather flexible constraints. Notice that this method allows additional objectives to be modeled, merely by adding additional "beta" variables and constraints. As with the weight formulation, the objective for the compound formulation is linear, but represents a different quantity. The acoustic constraint is nonlinear, and the weight constraint is linear.

3.4 Additional Constraints - Structural Integrity: Stress and Buckling

There are several additional constraints, dealing with buckling and structural integrity, that may be added to any of the above formulations. These constraints use information generated by the Finite Element Analysis program (NASTRAN) to determine if a given design is structurally sound. If it is not, the design is rejected. The additional constraints are represented generically as

$$G_z(x) = \frac{g_z(x)}{g_z^{max}} - 1 \qquad (3.35)$$

where Gz(x) is the value of the normalized constraint, $g_z(x)$ is the calculated value of the constraint, and g_z^{max} is the maximum allowable value for the constraint. Using this representation (Eq. 3.26), a constraint is violated if its normalized value is greater than zero. This makes the task of checking the new design for feasibility simpler for the optimization program. The program only needs to check the returned array of constraints for numbers greater than zero.

For these "integrity" constraints, translator or extraction programs are used to find the appropriate data within the various output datasets. The following describes the explicit integrity constraints.

3.4.1 Stress Constraint Formulation. Static stress loads throughout the structure can be calculated for each model design using a separate NASTRAN or static FEM run. Resultant stresses can be compared to known, allowable limits and reported to the optimizer as constraints so that only structurally feasible designs are considered.

For this work, the maximum and minimum principal stresses at the outer surfaces or at the mid-plane of model elements of interest are compared to upper and lower bounds for each element. Two constraints exist for each element (one for the upper bound, one for the lower bound). The stress constraint formulation for the upper bound on the maximum principal stress is

$$[(\sigma - \sigma_{lower}) / (\sigma_{upper} - \sigma_{lower})] - 1 \leq 0 \qquad (3.36)$$

The stress constraint formulation for the lower bound on the minimum principal stress is

$$[(\sigma_{upper} - \sigma) / (\sigma_{upper} - \sigma_{lower})] - 1 \leq 0 \qquad (3.37)$$

Note that for each formulation, the stress value is normalized to the range of allowable stress. This is consistent with the treatment of weight and acoustic constraints discussed previously.

3.4.2 Buckling Constraint Formulation. Structural buckling can be calculated using a separate NASTRAN or static FEM run which calculates limiting buckling eigenvalues. The buckling constraint is formulated as

$$-(BFACK / BMIN) + 1 \leq 0 \qquad (3.38)$$

where BFACK is the buckling factor (eigenvalue) calculated by NASTRAN and BMIN is the lowest allowable eigenvalue for the design.

4. ALGORITHM IMPLEMENTATION - DESIGN TOOL

This section presents the mechanics of implementing the overall optimization algorithm. The algorithm requires information to compute the objective functions, the constraint functions, and the functions' gradients. The objectives and constraints are based on acoustic pressures, structural weights, and, optionally, static measures of structural integrity. This information is not computed in the optimizer code itself, but rather is supplied by external codes. While each of the functions described in Section 3 are fairly simple, the fact that the data required to compute these functions is provided by codes external to the optimizer leads to a complex integration and coordination task.

The computational structural acoustic design tool is intended to be robust and flexible. It is easily modifiable to fit a variety of computer system architectures. The heart of the design tool is a 1330-line UNIX Korn shell script. The script has been designed to be portable, and it has been running at NASA Langley Research Center and at Georgia Tech on DEC Alpha workstations, and at Lockheed on an SGI Indigo 2. Note that the script can control a heterogeneous computing environment, with different pieces of the overall algorithm executing on different platforms, so long as there is reliable communication between platforms. The shell controls the interaction of three main programs and three supporting codes and also provides error-trapping capabilities to detect problems with any of the integrated programs. The modular structure of the UNIX shell script, based on defined shell functions, simplifies modifications and expansions. A description of the launch and input line options of the shell script is located in Appendix A.

The user provides two input files containing parameters that define the programs to be used for each type of analysis and their locations, parameters that define the optimization (objective and constraint formulation, convergence criteria), and parameters that define the FEM/BEM models to be used. These files are read by the shell script and several supporting FORTRAN codes to configure and structure the analysis. A detailed listing of all input parameters for the two files is located in Appendices B & C.

Figure 4.1 is a flowchart depicting the generalized analysis tasks that must occur each time the optimizer requires information. Depending on whether the optimizer requires objective or gradient information on a given iteration, the shell script will control tasks that operate in such a manner as to provide the correct data. The basic flow is the same for both cases. Once the optimizer has been launched and has written instructions for a set of design parameters, the following tasks must occur: Structural modes are calculated (FEM) to determine resonance frequencies for a given design state. These frequencies become the forcing frequencies in the structural response (or sensitivities) solution (FEM). The structural response in turn is used to generate interior velocity boundary conditions so that the acoustic pressures (or sensitivities) inside the structure may be calculated (BEM). At this point, the objective and constraint functions or gradients are calculated using a FORTRAN routine and this information is returned to the optimizer. The optimizer runs throughout the entire course of the design optimization procedure but is temporarily suspended every time new structural and acoustic analyses are required.

The optimizer is currently configured to be either CONMIN or COMPLEX. Both have been described in Section 3. All FEM analyses of the structural model are performed by MSC/NASTRAN running on a workstation such as a DEC ALPHA and an IBM RISC 6000. It is not necessary for NASTRAN to run on the same machine as the shell script. The user is required to prepare all NASTRAN datasets describing the structural model and any structural loading conditions. If the optimization is for one fixed frequency only, any external acoustic loads must

be determined prior to the run execution, with the pressures applied as harmonically varying loads at the structural element nodes, with the resultant dynamic forces included by the user in the NASTRAN response model. External acoustic loads and interior acoustic analyses are computed using the boundary element code COMET/Acoustics [18]. The acoustic analysis for the cylinder models is uncoupled, meaning that the vibration of the structure is not considered to be affected by the internal acoustic medium. The user is required to provide a COMET dataset, which defines not only the boundary elements on the inner surface of the cylinder, but also the acoustic pressure data recovery nodes.

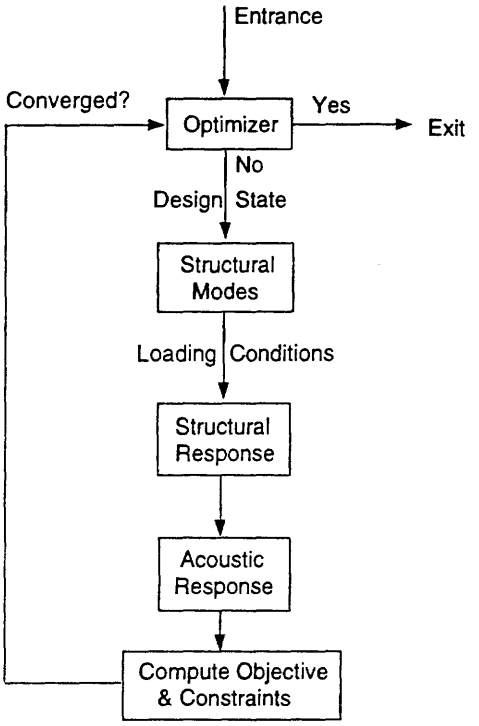

Figure 4.1 - Flow chart of generalized optimization tasks handled by the design tool

Figure 4.2 is a detailed flowchart depicting the interaction of the analysis and all supporting programs within the shell. The design tool handles many variations of analysis: single/multiple frequency, beamshape optimization, structural integrity analysis, unpressurized/pressurized structures, and structural/acoustical excitation. These variations all contribute to the complexity of the logic flow.

Figure 4.3 is the same detailed flowchart of the design tool, highlighting the steps that occur in every optimization run. Once the shell script has initialized its own variables and defined the parameters of the run, a FORTRAN program, OPTSETUP, is executed to read in the input parameters for the optimizer. The optimizer is launched and the shell script cycle of optimization is begun. The optimizer writes a file containing a design state and a request for either objective function or gradient information, then is suspended. A FORTRAN program, UPDNAS, is then executed to update all NASTRAN models with the current design state. The NASTRAN response model is executed once its external loads are updated (for a basic single frequency run these external loads are constant and the response model is launched following UPDNAS). When gradients are required, the NASTRAN response model also calculates the structural sensitivities

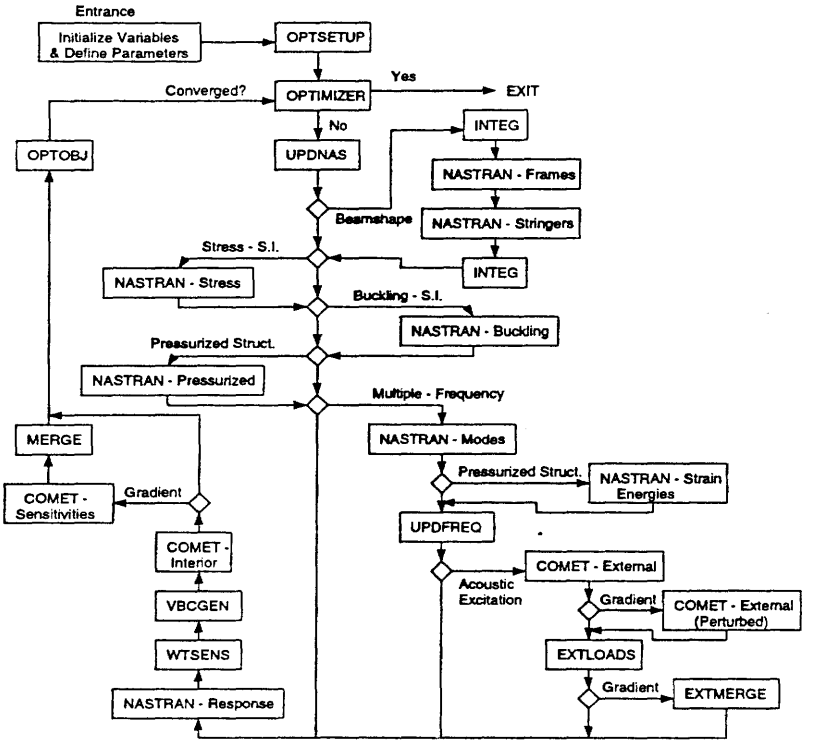

Figure 4.2 - Flow chart of design tool

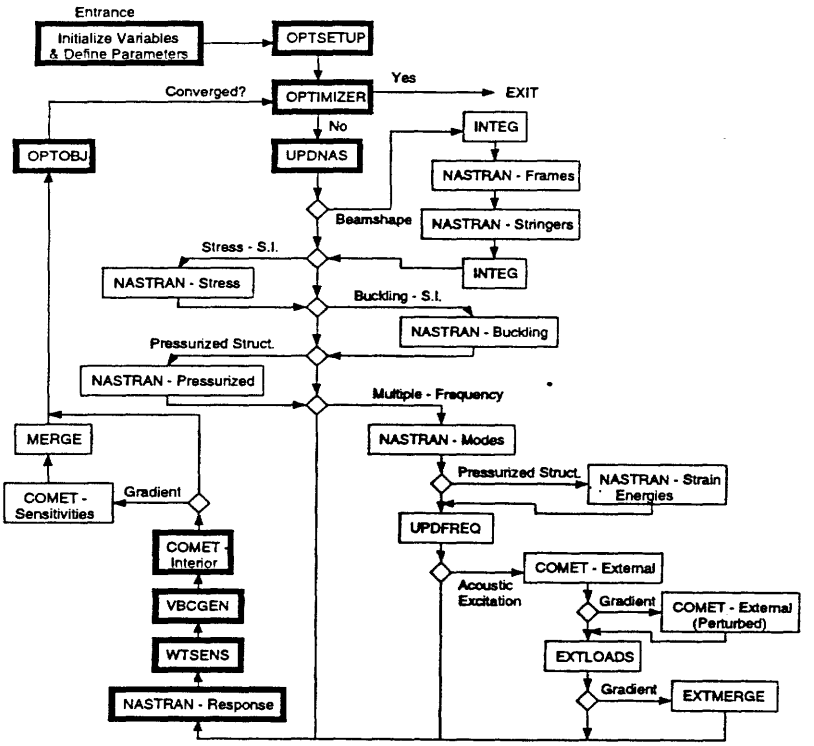

Figure 4.3 - Flow chart of design tool highlighting staple events of run

(of the interior surface velocities to changes in the design state). The program WTSENS is used to read the total cylinder weight from the NASTRAN response results. When gradients are required, WTSENS also reads the sensitivities of the weight to changes in the design variables. The VBCGEN program then translates structural surface velocities from the NASTRAN response results into a format readable by COMET for use as velocity boundary conditions. The interior COMET model is then executed to calculate the acoustic pressures. Finally, the acoustic pressures and model weight are read by a FORTRAN code, OPTOBJ, which calculates the objective and constraint functions required by the optimizer. When gradients are required by the optimizer, OPTOBJ reads the acoustic and weight sensitivities and calculates the gradients.

The flowchart in Figure 4.4 highlights the programs used to handle beamshape optimization and structural integrity constraints. When beamshape optimization is being performed, the INTEG code is used to determine the section properties associated with a mesh defining the section perimeter. These properties are then written into the NASTRAN design data sets. When structural integrity constraints are desired, the NASTRAN stress and/or buckling static models are executed. These branches of the run logic are independent of the other variations of analysis and are not displayed in subsequent figures in order to simplify the flow chart.

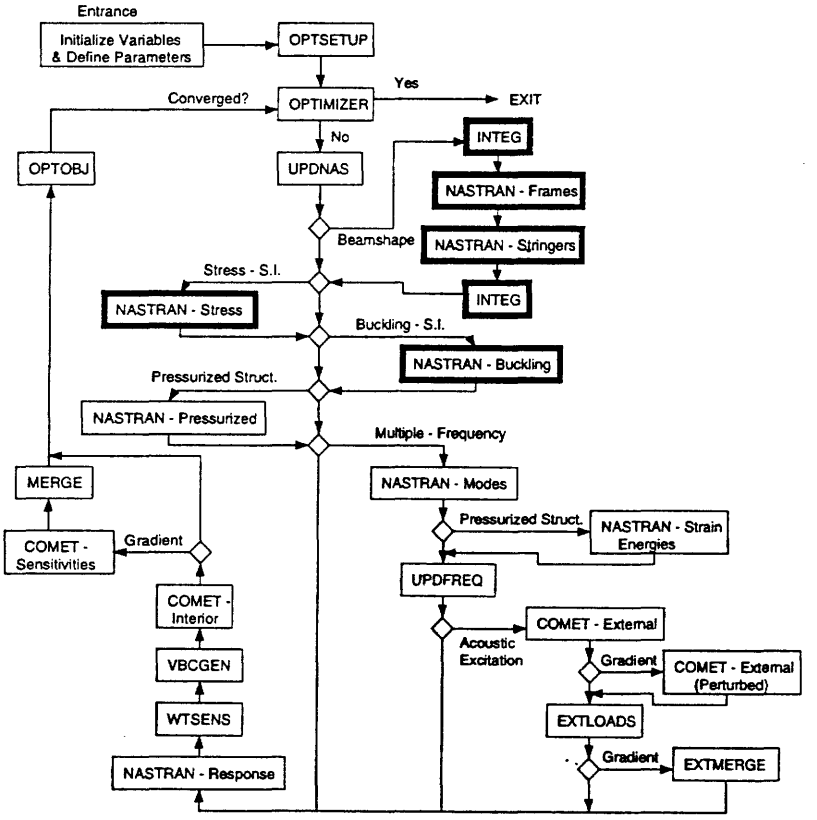

Figure 4.4 - Flow chart of design tool highlighting beamshape and structural integrity events

The flowchart in Figure 4.5 highlights the NASTRAN runs which are executed for the case when pressure-stiffening is to be incorporated. The "Pressured" run produces a stiffness matrix associated with the internal pressure, for subsequent inclusion in the stiffness matrix for modes determination. The "Energies" run calculates the strain energies associated with each mode within

the analysis bandwidth. This is used to discriminate between global-response modes and very localized modes. This reduces the computational effort in the peak-tracking multi-frequency algorithm. UPDNAS and UPDFREQ are signaled by the shell script to perform specific tasks to handle the pressurized case.

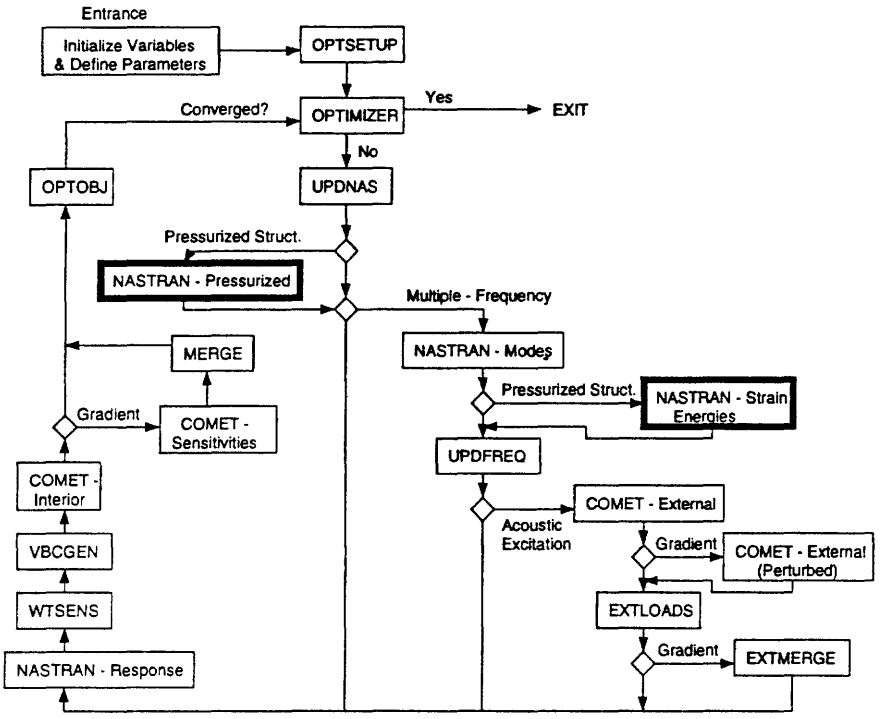

Figure 4.5 - Flow chart of design tool highlighting multiple frequency analysis events

The flowchart in Figure 4.6 highlights the programs which are utilized to handle multiple frequency optimizations. Once updated with the current design state, the NASTRAN modes model is run to calculate structural resonant frequencies. The UPDFREQ program then reads these frequencies and modifies the NASTRAN response model and COMET models so that analysis will include them. When the excitation of the structure is acoustical, an external COMET model is run to calculate the surface pressures on the structure exterior. The EXTLOADS program then translates the COMET surface pressures into a format readable by NASTRAN for use as loading conditions.

The flowchart in Figure 4.7 highlights the programs which are launched to calculate objective and constraint gradients. The acoustic gradient, the sensitivity of interior acoustic pressure to change in design state, is calculated by chain rule differentiation,

$$\frac{\partial p_i}{\partial x_j} = \frac{\partial p_i}{\partial v}\frac{\partial v}{\partial x_j} \tag{4.1}$$

where $\partial p_i/\partial x_j$ represents the sensitivity of the pressure at node *i* due to change in design variable *j*. In Eq. (4.1), v is the surface normal velocity on the interior of the structure, $\partial p_i/\partial v$ is the sensitivity produced by COMET, and $\partial v/\partial x_j$ is the sensitivity produced by NASTRAN. At the most general level, the MERGE program combines the sensitivity results from NASTRAN and the interior

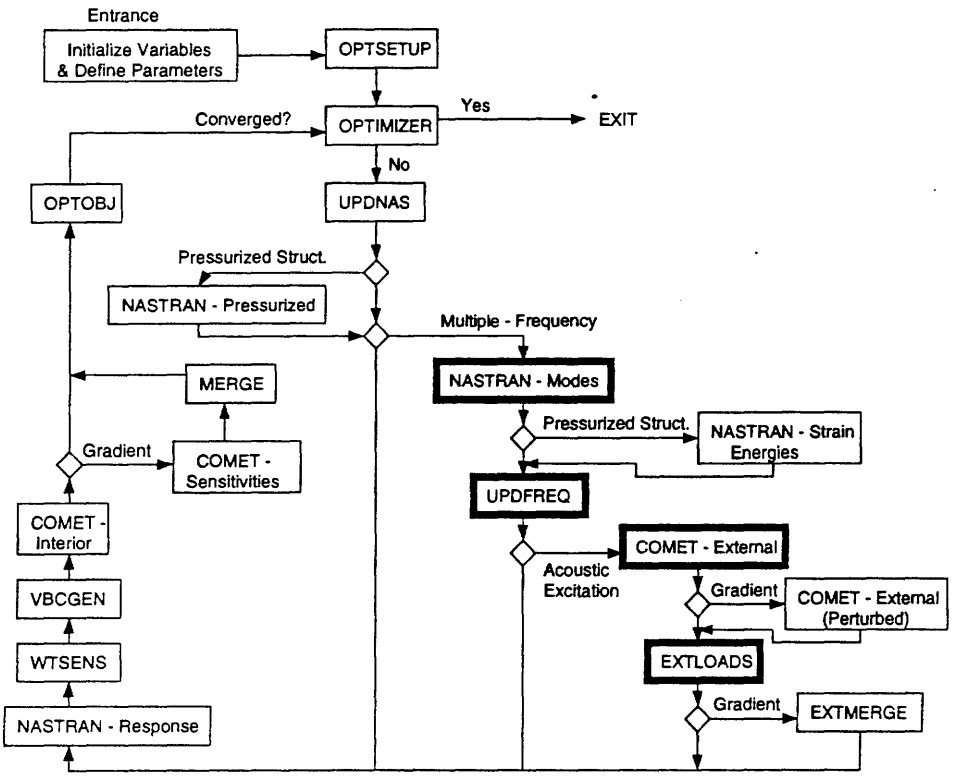

Figure 4.6 - Flow chart of design tool highlighting events for pressurized structures

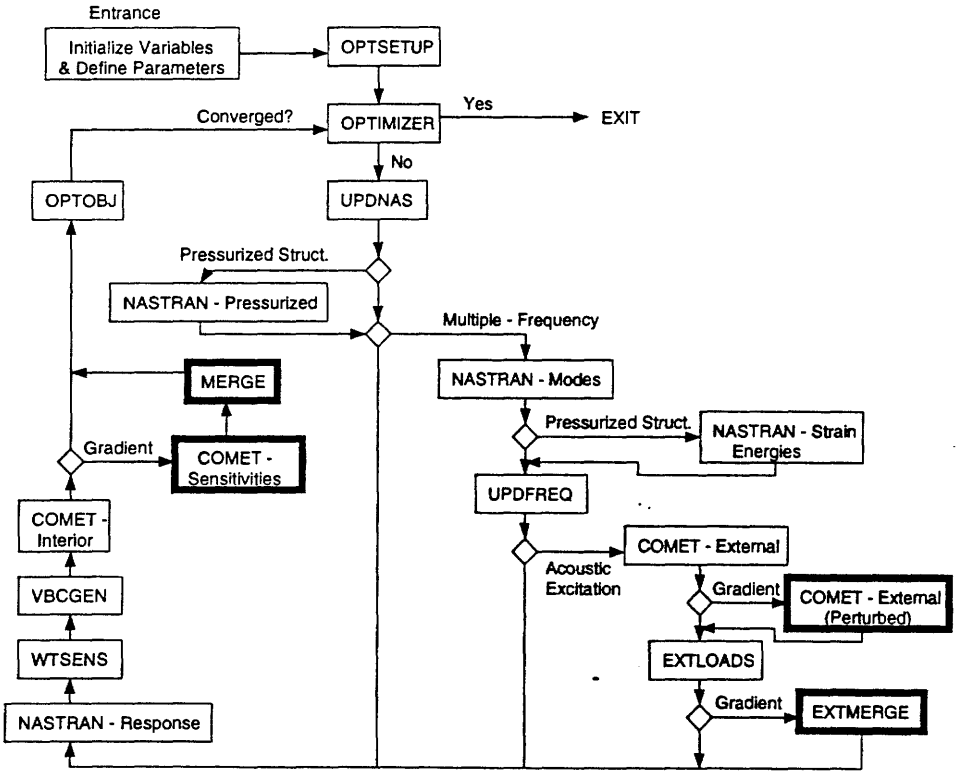

Figure 4.7 - Flow chart of design tool highlighting events for gradient calculation

COMET run to calculate the total sensitivity. OPTOBJ then processes the sensitivity results and submits the gradients to the optimizer. However, there is one subtlety that must be accounted for when considering multi-frequency analyses: the peak frequencies will shift with changing design variable, and this will change the exterior pressure distribution. This causes a non-zero sensitivity of the excitation to changes in design variables. However, NASTRAN assumes this sensitivity to be zero. Therefore, we explicitly compute a force sensitivity as

$$\frac{\partial f}{\partial x_j} = \frac{\partial f}{\partial \omega}\frac{\partial \omega}{\partial x_j} \tag{4.2}$$

Note that this force sensitivity term is identically zero for a single frequency analysis, and zero for all "fixed" frequencies (e.g., interior cavity mode frequencies). During script execution, this force sensitivity component of the acoustic gradient is calculated first. An external COMET model is executed which solves for the exterior pressures at slightly perturbed frequencies from the current set of peaks under consideration. These results, in conjunction with the exterior pressure results from the first external COMET run, are used by EXTLOADS to calculate the sensitivity of exterior pressure to change in frequency (this operation of EXTLOADS is controlled by the shell). The EXTMERGE program then chain-rules this force-to-frequency sensitivity with NASTRAN results of resonance-frequency-to-design-variable sensitivity, and outputs the result in a format readable by NASTRAN. The subsequent NASTRAN response run incorporates the force sensitivity into its calculation of the total surface velocity sensitivity.

In summary, the basic components of the algorithm are:

- OPTSETUP - To define the run parameters for the optimizer.
- Optimizer - (CONMIN or COMPLEX) To perform the actual optimization.
- UPDNAS - To update all NASTRAN models with a given design state.
- INTEG - To integrate beam cross-section properties for beam shape optimization.
- NASTRAN - Finite element code to perform all structural analyses, and compute sensitivities of surface velocity and weight to changes in design variables.
- UPDFREQ - To update NASTRAN response and COMET models with required frequencies for analysis of a given design state.
- COMET/Acoustics - Boundary element code to perform all acoustic analyses, and compute the sensitivity of interior pressures to changes in the surface normal velocity at the boundary.
- EXTLOADS - To translate COMET exterior pressure output into boundary conditions for NASTRAN, and to compute the sensitivity of external loads to changes in frequency.
- EXTMERGE - To translate force sensitivities into NASTRAN format.

- WTSENS - To read structural weight and weight sensitivities from NASTRAN output.

- VBCGEN - To translate NASTRAN velocity output into boundary conditions for COMET/Acoustics.
- MERGE - To combine structural sensitivities from NASTRAN and acoustic sensitivities from COMET/Acoustics.

- OPTOBJ - To compute the completed objective and constraint functions/gradients.

- The UNIX shell script - To coordinate the execution of, and data interchange between, the components.

A complete listing of all files generated by the shell script and the various algorithm components is located in Appendix D.

The shell script also implements an automatic restart capability. The gradient descent algorithm will terminate execution based on either a rate-of-convergence criteria or an absolute convergence criteria. If the algorithm terminates based on rate of convergence, restarting the algorithm from the last design state frequently leads to a period of accelerated improvement as compared to the iterations prior to the restart. If the algorithm terminated based on absolute convergence, there will be no improvement. The control script automates the restart process for the algorithm. The restart function saves all pertinent files from the initial run, then relaunches the control loop. No user intervention is required for the restart capability.

The UNIX shell script and the supporting FORTRAN codes of the design tool have been delivered to NASA Langley and are available for use. NASTRAN and the various AAC codes are commercial and must be leased.

5. ALGORITHM PERFORMANCE AND IMPROVEMENT

This section presents the results of various efforts to understand the relative performance of each of the objective function formulations, and of efforts to improve the overall algorithm performance. Section 5.1 presents detailed information comparing the different formulations as obtained with CONMIN. Section 5.2 presents the results of a study conducted to determine if lower node-count data recovery meshes would perform adequately, and yield equivalent results to the initial mesh. Section 5.3 briefly discusses the implementation of a concept termed dynamic remeshing, leveraging the results of the reduced-density mesh study, for the purpose of improving algorithm performance.

5.1 Objective Function Formulation Assessment - Single-frequency CONMIN Based

Relative performance assessments used a low node-count coarse cylinder model extensively in testing and developing the formulations. This "coarse" mesh cylinder model used all the same geometry and properties as the "fine" mesh models in Figure 2.1, except the mesh density was much lower, providing a less accurate solution. The advantage of this approach was that it provided rapid turn-around on analyses, due to the low node count leading to low iteration times (as compared to the full "fine" mesh production models). Further, the expectation that the qualitative performance of each formulation applied to the coarse model would apply to the full production model was borne out.

In order to compare the effectiveness of the optimization problem formulations and their computational efficiency, each formulation was used to optimize the coarse cylinder model under a variety of constraint conditions and from three different starting points in the design space. CONMIN alone was used for this exercise. Multiple initial design states are needed to assess if a single optimal solution exists for each set of objectives and constraints. The standard starting design for the model is a uniform thickness of 1.7 mm for each of the design variables, corresponding to a weight for the quarter cylinder of 217.9 N. The other two starting designs are chosen to set all the design variables either to their upper or lower bounds. Table 5.1 summarizes these three initial design states.

Table 5.1 - Initial Design States of the Coarse Cylinder Model

Initial Design State	Design Variable Values (mm)	Weight of Quarter Cylinder (Newtons)	Objective (dB)
Upper	2.21	283.2	-5.22
Middle	1.70	217.9	-2.94
Lower	1.19	152.5	0.16

Care must be taken when comparing functions based on the pressures at data recovery nodes, for both coarse and full production models. The excitation used here is arbitrary, and the models themselves have vastly different levels of refinement. Therefore, the initial interior levels between the two models, for the same exterior forcing, can not be expected to be equal. Further, the initial

level and reduction from this initial level is of limited value, as the initial value is a strong function of the initial design state. Indeed, any discussion of dB reduction from the initial level is essentially meaningless. The ending levels are what is significant and comparable between formulations. Therefore, an arbitrary zero dB reference was selected such that all starting and ending points can be expressed with respect to this reference.

The following sections detail the results of the coarse cylinder optimizations. The first section presents the results for the baseline formulation, which was used during the initial development of the design tool. The next three sections present the results of each of the three remaining optimization formulations.

5.1.1 Baseline Formulation. The baseline formulation was run once with each of the initial design states. Recall that the baseline formulation seeks the vector of design variables that minimizes the sum of the squared pressures at the data recovery nodes, and that cylinder weight is not considered. The coarse model has only one data recovery node. Table 5.2 presents the results of these optimization runs, and includes information on the number of iterations required to achieve the optimum.

Table 5.2 - Results of the Baseline Optimization Formulation

	Relative Objective Function (dB)		
Initial Design State	Initial Objective	Final Objective	Algorithm Iterations
Upper	-5.22	-14.84	6
Middle	-2.94	-14.88	7
Lower	0.16	-14.79	9

The observation that the final values of the objective function are essentially the same for each of these cases suggested that they have each individually converged to the same final design state. This was the case, as may be observed from the final vector of design variables for each case, presented in Table 5.3.

Table 5.3 - Final Vector of Design Variables for the Coarse Model, Baseline Formulation

	Design Variables (mm)					Cylinder
Initial Design State	1	2	3	4	5	Weight (N)
Upper	2.21	2.21	2.21	1.19	1.19	230.67
Middle	2.21	2.21	2.21	1.19	1.19	230.67
Lower	2.21	2.21	2.21	1.19	1.19	230.67

Notice that the optimal design lies at the bounds, i.e. the upper side constraints are active for variables 1, 2, and 3, and the lower side constraints are active for variables 4 and 5. Also notice that the optimal design has increased thickness toward the free end of the quarter cylinder (the center of the full cylinder) and reduced thickness at the clamped end. The weight of the cylinder at the optimal design point, because it is not constrained, has increased by 5.9% over the weight of the standard cylinder.

5.1.2 Acoustic Formulation. Each of the three remaining formulations consider the weight of the cylinder as some aspect of the optimization, so that more test cases must be run to explore the behavior of these formulations. The acoustic problem, which seeks to minimize the sum of the squared pressures subject to a weight constraint, was tested with 24 different combinations of initial design and maximum weight constraint. For each constraint case, the cylinder model is started from the same three initial design points as for the baseline formulation. The eight tested constraint conditions on the cylinder weight are summarized in Table 5.4, where constraint case 3 indicates a model where the cylinder weight is not allowed to increase over the weight of the standard cylinder.

Table 5.4 - Constraint Conditions for Coarse Model with the Acoustic Formulation

Constraint Case	Constrained Maximum Weight (N)	Percent of Standard Cylinder Weight
1	240	110%
2	229	105%
3	218	100%
4	207	95%
5	196	90%
6	185	85%
7	174	80%
8	163	75%

It should be noted that the upper initial design point, with a weight of 283.2 N, is infeasible for each design case, as is the middle initial design point for cases 4 through 8. As mentioned earlier, this is not a problem for CONMIN, which quickly drives infeasible designs into the feasible space.

Figure 5.1 is a plot of the results of 24 tests of the acoustic formulation of the coarse cylinder optimization. Two interesting observations may be made from these results. First, there appears to be a nearly linear relationship between the optimal weight and the optimal sound pressure level at the data recovery node in the coarse cylinder. No comparable result has been found in the literature that relates the sound pressure level and weight in this manner for cylindrical structures. Second, the eight groupings of optimal design points in Figure 5.1 closely correspond to the eight constraint cases in Table 5.4.

Figure 5.2 plots the optimization histories for four models with increasingly restrictive weight constraints. The models are all started from the middle initial design point. It is obvious that most of the decrease in the objective function occurs during the first few iterations for each model. The

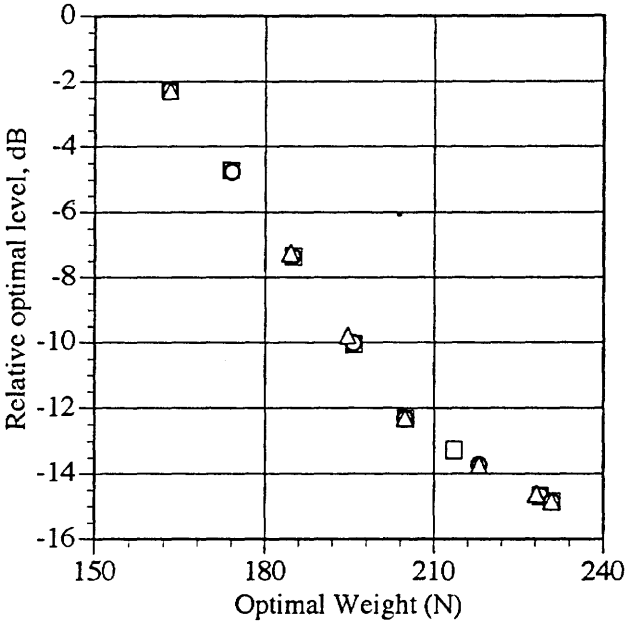

Figure 5.1 - Optimal Sound Pressure Level at the Data Recovery Node vs. Optimal Coarse Cylinder Weight for the Acoustic Formulation, O - Upper Initial State, ❑ - Middle Initial State, Δ -Lower Initial State

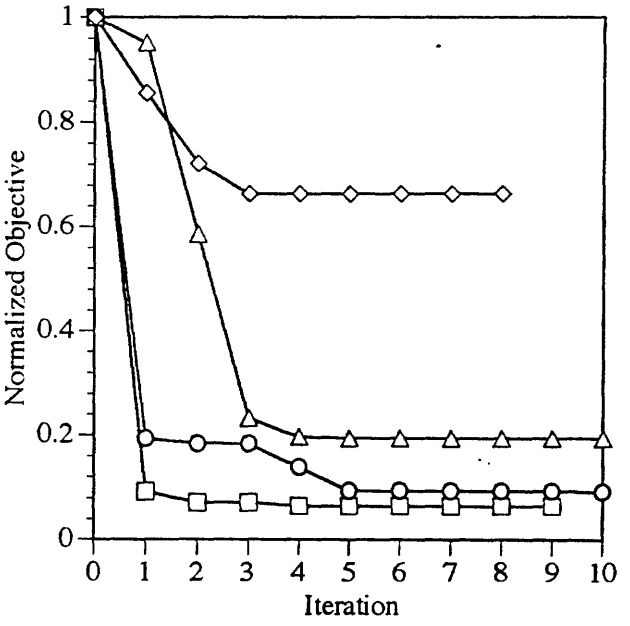

Figure 5.2 - Optimization History for Acoustic Formulation Constraint Cases 1, 3, 5, 7, with Middle Initial Design Point, ❑ - Constraint Case 1, O - Constraint Case 3, Δ - Constraint Case 5, ◊ - Constraint Case 7

decrease in objective function at each of these initial iterations is smaller for the models with more restrictive weight constraints. Because of the generous constraint tolerance within CONMIN, the weight constraints are nearly always active for all of the models, although the weaker constraints on models of cases 1 and 2 are just inside the constraint tolerance most of the time. Finally, notice that each of these optimizations is considered converged when the relative change in the normalized objective function is less than 1% for five consecutive iterations, as specified by the relative convergence criterion in the CONMIN input file.

Similar to the results for the baseline formulation, the optimal vector of design variables for each of the models indicates that the cylinder thickness is at the lower bound at the clamped end, and increases toward the free end. Table 5.5 lists the optimal design variables for the four models of Figure 5.2.

Table 5.5 - Final Vector of Design Variables for Coarse Model with the Acoustic Formulation, Constraint Cases 1,3,5,7, Middle Initial Design

	Design Variables (mm)					Cylinder
Constraint Case	1	2	3	4	5	Weight (N)
1	2.21	2.21	2.21	1.19	1.19	230.93
3	2.21	2.21	1.53	1.19	1.19	213.49
5	1.86	2.21	1.19	1.19	1.19	195.80
7	1.65	1.56	1.19	1.19	1.19	173.82

5.1.3 Weight Formulation. In a similar manner to the acoustic formulation, the weight objective was evaluated using six different constraint cases. For this formulation, the weight is minimized with a constraint on the maximum sum of the squared pressures. A maximum average value is specified for the sound pressure level at the data recovery nodes. This is multiplied by the number of nodes to determine the maximum sum of the squared pressures. Since for the coarse model there is only one node, the user is effectively specifying the maximum sum. Table 5.6 lists the six constraint conditions. Case 2, with a maximum relative SPL of -3 dB, essentially represents the standard (1.7 mm thick) cylinder.

Table 5.6 - Constraint Conditions for Coarse Model with Weight Formulation

Constraint Case	Constrained Relative SPL (dB)
1	0
2	-3
3	-6
4	-9
5	-12
6	-15

The upper initial design point is infeasible with respect to the constraints of cases 3 through 6. The middle initial design point is infeasible for cases 3 through 6, and for case 2 the constraint is active. The lower initial design point is infeasible for constraint cases 2 through 6 and active for case 1. Again, CONMIN is usually able to quickly drive the infeasible designs into the feasible space. Figure 5.3 presents the results of the optimization of the coarse model using this objective and constraint formulation.

This data again shows the almost linear relationship between optimal pressure at the node and optimal weight. As with the acoustic formulation, the optimal solutions for the six constraint cases are distinct from each other. For all the models, the pressure constraint is active for every optimal design, and well within CONMIN's constraint tolerance.

Figure 5.4 shows the optimization histories of four of the models, with increasingly restrictive pressure constraints, all of which started from the middle initial design point. Again it is clear that the greatest decreases in the objective function (the weight), occur early in the optimization process. Notice that the cylinder weight increases for the most restrictive constraint case, number 6, with a relative SPL constraint of -15 dB. This constraint is violated for the duration of the optimization, and the final solution is in fact infeasible. CONMIN is instructed to terminate the process if a feasible design cannot be found for ten consecutive iterations. The other cases do result in feasible designs under the relative convergence criterion.

Although the final designs for constraint case 6 are infeasible, notice from Table 5.7 that these designs are in fact the same optimum found by the baseline model and by acoustic constraint case 1 in Table 5.5. The weight formulation result is only infeasible by a narrow margin, because its constraint of -15 dB is just slightly more restrictive than the relative SPL of -14.84 dB found at the feasible optimum.

Table 5.7 - Final Vector of Design Variables for the Coarse Model using the Weight Optimization Formulation, Constraint Cases 1,2,4,6, Middle Initial Design

	Design Variables (mm)					Cylinder
Constraint Case	1	2	3	4	5	Weight (N)
1	1.21	1.19	1.19	1.19	1.19	153.13
2	1.51	1.40	1.19	1.19	1.19	166.13
4	1.81	2.09	1.19	1.19	1.19	191.49
6	2.21	2.21	2.21	1.19	1.19	230.93

The upper and lower designs of case 2 are different from the middle design shown in the table. The first and second design variables for those designs are about 1.45 and 1.55 mm, resulting in nearly the same overall weight and nearly identical sound pressure levels. This is an instance of a problem having a non unique optimum.

5.1.4 Compound Formulation. For the compound formulation, the objective rather than the constraints is varied to establish seven optimization problem cases. Recall from Eq. (3.31) that the user is free to specify weighting coefficients to the acoustic and weight terms of the objective function, in order to emphasize one objective more than the other. Since the weight of an aircraft tends to be driven by structural and performance requirements rather than acoustic requirements,

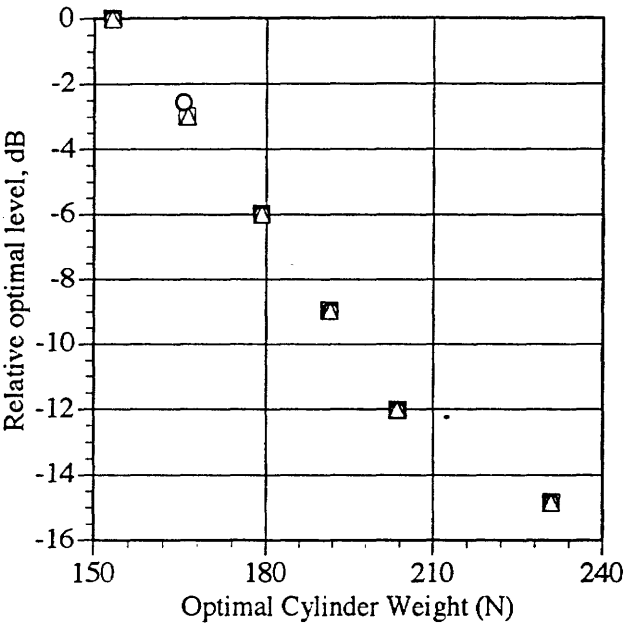

Figure 5.3 - Optimal Sound Pressure Level at the Data Recovery Node Vs. Optimal Coarse Cylinder Weight for the Weight Formulation, O - Upper Initial State, ❑ - Middle Initial State, Δ - Lower Initial State

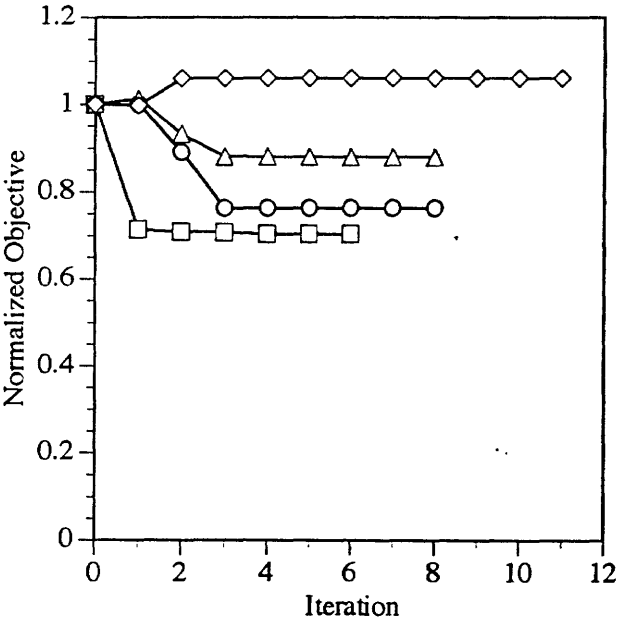

Figure 5.4 - Optimization History for Weight Formulation Constraint Cases 1, 2, 4, 6, with Middle Initial Design Point, ❑ - Constraint Case 1, O - Constraint Case 2, Δ - Constraint Case 4, ◊ - Constraint Case 6

it was decided that for the compound case minimizing the pressures would always be more important than minimizing weight. Table 5.8 lists the acoustic and weight weighting coefficients, μ_a and μ_w, for each of the seven compound objective cases.

Table 5.8 - Objective Cases for the Coarse Model using the Compound Optimization Formulation

Objective Case	μ_a	μ_w
1	1	1
2	2	1
3	3	1
4	4	1
5	10	1
6	100	1
7	1000	1

These particular coefficient pairs are chosen to determine if there is a recognizable behavior in the results of the compound formulation optimizations. Since the initial values of the beta design variables are set to one, the constraints for all of the models are initially active. Figure 5.5 presents the results of the compound formulation optimizations.

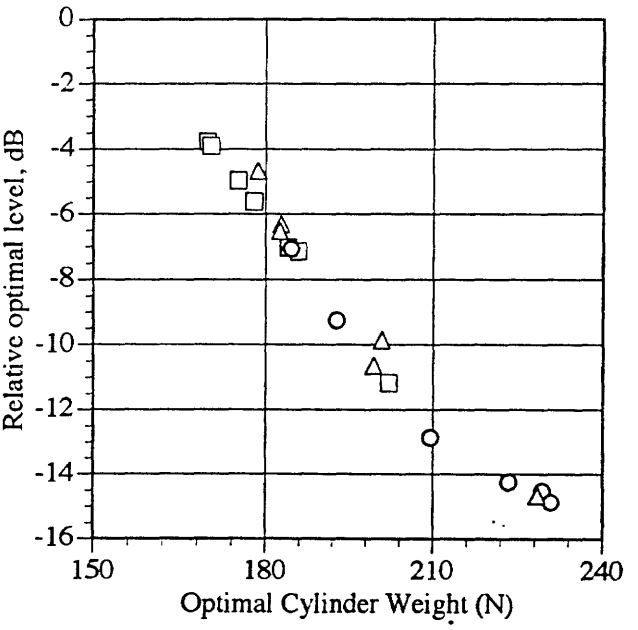

Figure 5.5 - Optimal Sound Pressure Level at the Data Recovery Node Vs. Optimal Coarse Cylinder Weight for the Compound Formulation, O - Upper Initial State, ❑ - Middle Initial State, Δ -Lower Initial State

Once again a linear relationship is observed between the sound pressure level and the weight. For the compound formulation, however, the results of the three initial design states for each objective case do not remain clustered as they do for the acoustic and weight formulations. An example is objective case 1, where the upper initial design converged to a -7.1 dB, 184.6 N optimal design, the middle initial design converged to -3.8 dB, 169.8 N, and the lower initial design converged to -9.9 dB, 200.9 N.

Tracing the optimization history for objective case 2 of the compound formulation gives an excellent example of how CONMIN operates. Figure 5.6 plots the values of the normalized sum of the squared pressures and the acoustic beta variable that bounds it. Figure 5.7 plots the normalized cylinder weight and its bounding variable.

Recall that the objective function for this case is to minimize the weighted sum of the acoustic and weight beta variables. The trace of β_a in Figure 5.6 looks just like that of any of the acoustic or weight formulation objective functions, with large decreases made initially and smaller moves during the later iterations. β_a is not only part of the objective, it is also the constraint on the sum of the squared pressures. The pressure sum tends to run up against the constraint for three iterations at a time, and then jumps deep into the feasible space on the fourth iteration. For this case, objective case 2, the optimization ends while the pressure constraint is inactive, so the optimal sum of the squared pressures is fairly low. For case 3, where the pressure is weighted three times as much as the cylinder weight, the solution converges while the pressure constraint is active, so the sum of the pressures is not as low. This explains the wide variability in the compound results. The optimization ends when the change in the sum of the beta variables is less than the convergence criterion, not necessarily when the sum of the pressures or the weight is at a minimum.

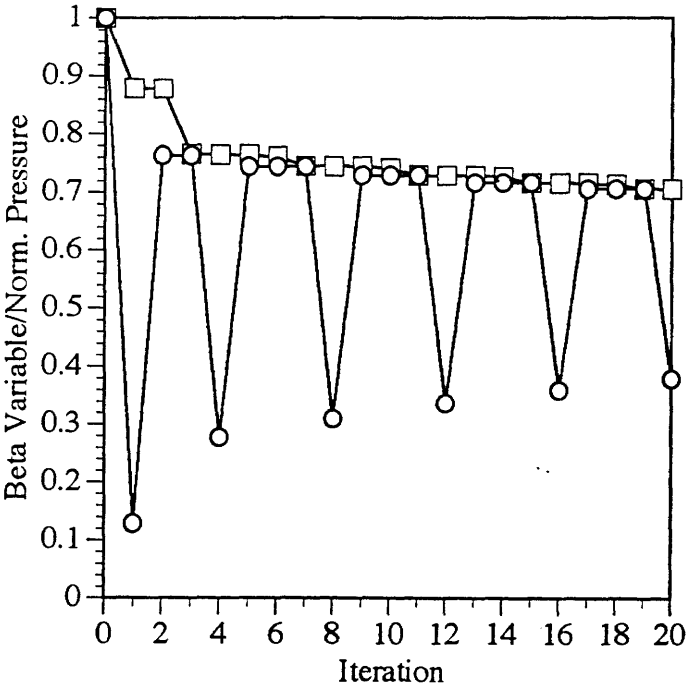

Figure 5.6 - Optimization History of the Acoustic Portion of Compound Objective Case 2, ❑ - β_a, O - Normalized Pressure

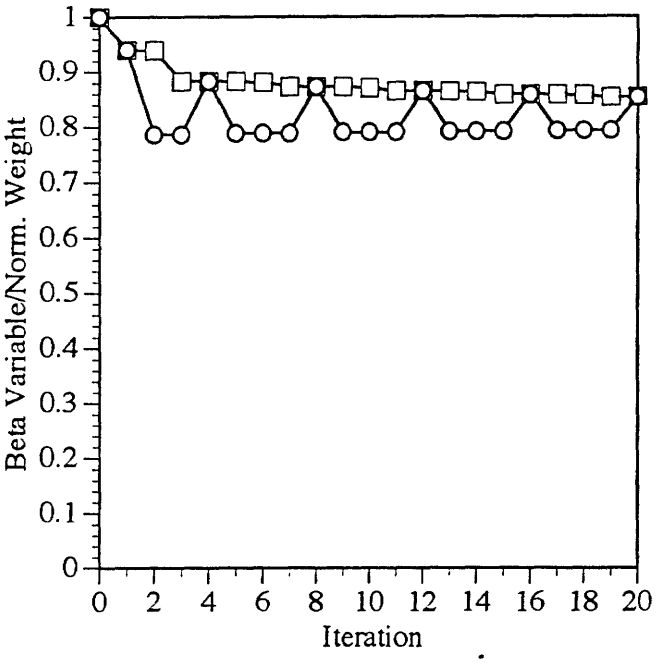

Figure 5.7 - Optimization History of the Weight Portion of Compound Objective Case 2, ❑ - β_w, O - Normalized Weight

The bounding variable on the weight, β_w, is minimized similarly to β_a. Notice that the weight constraint is inactive most of the time. On the iterations where the acoustic constraint is active, the weight constraint is inactive. This indicates that the two objectives, minimum pressure and minimum weight, are conflicting and that it is not possible to completely minimize both at the same time. This behavior can be inferred from the almost linear plot of the optimum designs in Figure 4.5, where a low SPL requires a high weight.

5.1.5 Comparison of Formulations. We have shown that the optimization problem formulations produce very similar results in terms of optimal cylinder design. The plots of the optimal designs produced by each formulation appear to be linear with the same slope. Combining the results of the acoustic, weight and compound formulations into a single graphic yields Figure 5.8. In addition to the optimization results, Figure 5.8 includes data for the case where the design variables are uniform at a given weight (represented by the Δ's). The lines are included to aid the eye. The difference between the upper and lower lines in Figure 5.8 indicates the improvement that can be made in the interior sound field by using the optimal design.

Merely adding weight to the cylinder does not guarantee reduced sound pressure levels in the interior. The shell thickness distribution of the cylinder is an important factor. Recall the optimal design of acoustic case 1 (Table 5.5), which weighs about 230 N even though the weight constraint allows up to 240 N. Because the optimal design variables are at the upper bounds where thickness is increased, any additional weight will have to be added to the thin end of the cylinder and will probably increase the SPL. Therefore, the determining factors in how much the sound pressure can be reduced in the cylinder are the bounds on the design variables first, and then the total constrained weight.

One question that still remains is which, if any, of the formulations is faster and more reliable in finding an optimal solution? To answer this question, statistics on each of the formulations were compiled. Because the time required for the analysis codes to run is the same at each iteration for each formulation, the critical indicator of speed is the number of iterations required to converge to an optimal solution. These statistics compare the number of iterations for all of the coarse model tests run. Table 5.9 presents these statistics.

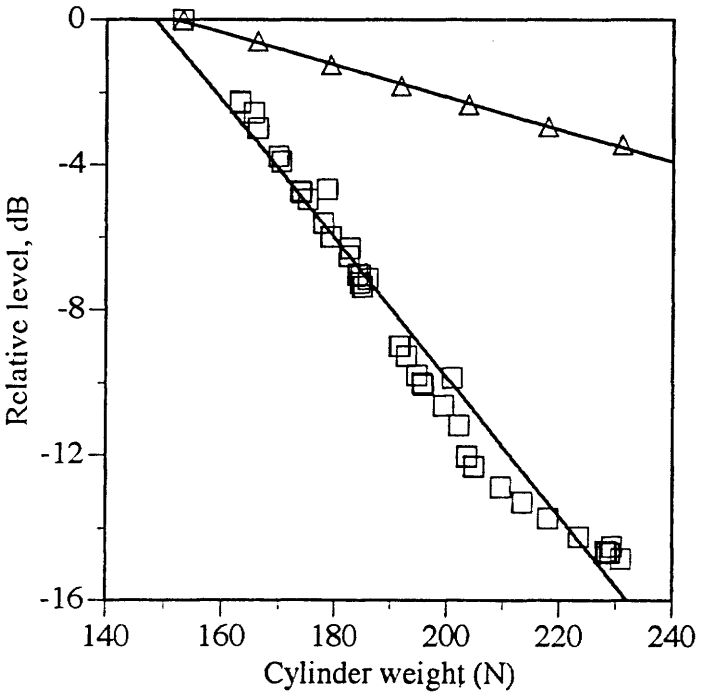

Figure 5.8 - Relative Level vs. Optimal Cylinder Weight for Coarse Models Using the Acoustic, Weight, and Compound Formulations, ❑ - Coarse Model, Δ - Coarse Model Uniform Thickness

Table 5.9 - Iteration Statistics for the Coarse Model Using the Baseline, Acoustic, Weight, and Compound Formulations

			Number of Iterations		
Formulation	# of Models	Average	Minimum	Maximum	Std. Deviation
Baseline	3	7.33	6	9	1.53
Acoustic	24	9.26	6	16	2.47
Weight	18	7.78	5	10	1.63
Compound	21	13.00	6	28	7.11

These results indicate that the baseline formulation tends to be the fastest, although it must be remembered that the baseline formulation does not consider the cylinder weight. Of the three other problem formulations, the weight formulation, on average, converges to an optimal solution faster than the other two. The acoustic formulation is nearly as fast. The compound formulation, however, is very inconsistent in the number of iterations required to converge, and on average takes many more iterations than the acoustic and weight formulations. There is no consistent trend in the number of iterations for the compound formulation.

Based on these findings, it would seem that the weight formulation is the fastest of the three new problems. However, the optimization package CONMIN suffers from numerical instability on some of the cases where the weight formulation is used. For 8 of the 18 tests, CONMIN violated the side constraints on the design variables. NASTRAN then aborts when it is presented with a cylinder design that violates the upper or lower bounds. The source of this problem was not located, although it has been determined that it is a problem internal to CONMIN, and not due in some way to the weight formulation subroutines. By applying additional scaling to the gradients of the objective and constraints, the numerical instability is avoided. This method gives results consistent with the cases where no instability is encountered. In light of this, it seems that the acoustic formulation is the best, being both fast and reliable. The weight formulation tends to be unreliable, and the compound formulation is slow and inconsistent.

5.2 Study of Alternative Data Recovery Meshes

The number of nodes in the data recovery mesh (DRM) is a critical factor in the overall time required to perform pressure and sensitivity analyses. Reduction in the number of nodes in the DRM leads to a direct reduction in the required CPU time. Therefore, an extensive effort was undertaken to characterize the impact of data recovery node location on algorithm performance, with the objective of reducing the overall node count.

The following sections provide a brief review of the data recovery mesh (DRM) study, a summary of the significant results of the study, and conclusions. Section 5.2.1 briefly reviews the concept and basis for evaluation of the alternative data recovery mesh study. Sections 5.2.2 and 5.2.3 deal with the two major areas of investigation for the study, namely the effects of variance of mesh density and sensitivity to design variable starting point. Section 5.3 briefly discusses an algorithm improvement motivated by the results of the DRM study.

5.2.1 Concept for Alternative Data Recovery Meshes. Sound pressure levels and particle velocities are calculated at each node of the DRM. It is at these nodes that acoustic levels are optimized or constraints are imposed. Acoustic sensitivity must be determined for each node as part of the optimization process; sensitivity calculation occurs in the COMET/Acoustics BEM code and can be extremely time consuming. Reduction in node count and location of the DRM both affect the efficiency of the BEM calculations.

The initial DRM used for acoustic optimization is shown in Figure 5.9. It was designed to map the quarter cylinder interior. This initial mesh, DRM-1, has 188 nodes.

Comparisons of DRMs were made using the baseline optimization formulation in which acoustic levels in the cylinder were minimized using a fine-mesh model with 20 design variables. The design variables in this model (the full production "fine" mesh model) were the thickness of groups of elements located in strips along the circumference of the cylinder (See section 6.2 for a

discussion of design variable grouping). Results for each DRM were compared to those for DRM-1. The following parameters were assessed:

- Normalized optimization results (final objective value divided by beginning objective value).
- Optimization results with respect to DRM-1 (calculated by using final design variables from the new DRMs in the optimization algorithm per the DRM-1 model).
- Time analysis (comparison of average and total CPU times for all programs used by the algorithm).
- Sensitivity of optimization results to initial values of design variables.

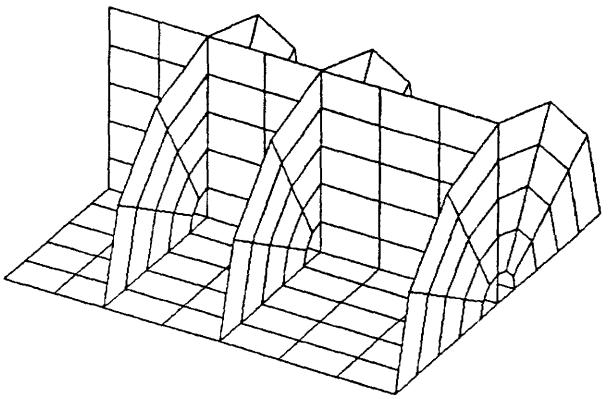

Figure 5.9 - Initial data recovery mesh used for the optimization study.

5.2.2 Comparison of Varying Nodal Density. DRMs were created at a radius of 0.75 meters with varying nodal densities. The six DRM configurations that were evaluated are shown in Figure 5.10. General information for each new DRM and DRM 1 are shown in Table 5.10. The fourth column, L/λ, is the ratio of element length to the acoustic wavelength at 154 Hz and, as a general rule, should be less than or equal to 0.25 (a quarter wavelength). DRMs close to or exceeding this value were investigated in order to study further time benefits and optimization capabilities.

Table 5.10 - Statistics for DRMs with varying nodal densities.

	# of Nodes	# of Elements	Max Distance Between Nodes, L (m)	154 Hz L/λ	Element Aspect Ratio
DRM-1	188	177	0.37	0.17	2.49
0.75m 4x8	45	32	0.36	0.16	1.22
0.75m 3x6	28	18	0.48	0.21	1.23
0.75m 3x5	24	15	0.48	0.21	1.03
0.75m 3x4	20	12	0.57	0.26	1.20
0.75m 2x4	15	8	0.72	0.32	1.25
0.75m 1x2	6	2	1.43	0.64	1.35

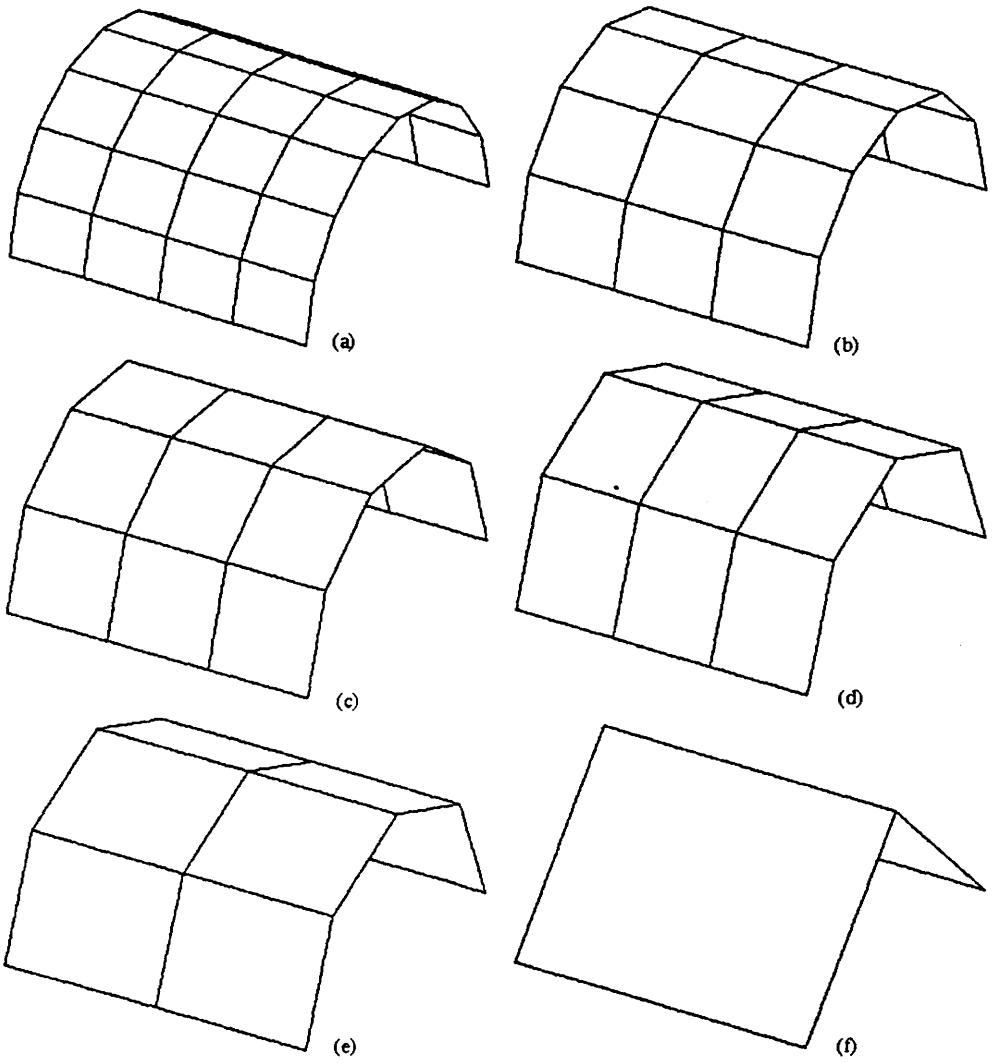

Figure 5.10 - 0.75m radius DRMs: (a) 4x8, (b) 3x6, (c) 3x5, (d) 3x4, (e) 2x4, and (f) 1x2 elements

Optimization results for each DRM are compared with those for DRM 1 in Table 5.11. Normalized final objective values and final objective values with respect to DRM 1 can be seen to converge to approximately the same values. Only with the 1x2 DRM did the objective function converge to a value smaller than that of DRM 1. For each DRM, all 20 design variables also converged to approximately the same values. Resultant maximum sound pressure levels in the model interior varied by at most 2 dB.

Velocities at the nodes located at the bottom edges of the meshes were found to exhibit "hot spots" when the DRM nodes were located very near nodes of the acoustic cylinder mesh. This was due to singularities that occurred in the model solution. These "hot spots" were eliminated by moving the DRM edges away from the floor of the quarter cylinder; this adjustment, however, introduced sensitivity to the initial values of the design variables, as discussed in Section 5.4.

Table 5.11 - Optimization results for DRMs with varying nodal densities.

	Normalized Final Objective Obj.	Final Obj. Val. w.r.t. DRM-1 / Final Obj. Val. DRM-1
DRM-1	0.00123	1.00
4x8	0.00113	1.03
3x6	0.00113	1.00
3x5	0.00116	1.02
3x4	0.00120	1.09
2x4	0.00118	1.00
1x2	0.00068	0.94

The time analysis is displayed in Table 5.12. All DRMs exhibited the same behavior with respect to time analysis: the smaller the node count, the shorter the time required for runs associated with the COMET/Acoustics BEM code. Merge CPU times were also shorter; as discussed earlier, the Merge code combines COMET sensitivity information with NASTRAN structural sensitivity information. Total CPU time was also dependent on the total number of iterations required for convergence of the optimization solution. Only the 1x2 DRM required approximately the same number of iterations as DRM 1. This may have been due to the sparseness of the mesh or to the large element size with respect to a wavelength.

Table 5.12 - Average CPU Time Performance for DRMs. All times in seconds.

	Total CPU	CONMIN	MERGE	NASTRAN	VBCGEN	Comet Sensitivity	Comet Pressure	# of Iters
DRM-1	209619	6.33	386.89	937.59	6.97	116113	36.82	22
4x8	108748	6.58	96.11	905.80	6.95	29111	14.95	19
3x6	112230	6.62	61.54	1203.92	6.97	19247	17.74	19
3x5	84706	6.24	53.31	872.96	7.07	16502	12.59	18
3x4	77969	6.36	45.67	860.66	6.99	14040	12.28	18
2x4	62977	6.37	35.81	884.63	7.06	11358	11.65	14
1x2	83676	6.27	16.74	855.69	6.93	5945	10.66	21

Objective value histories are plotted for the DRMs in Figure 5.11. Every mesh shows significant reduction (more than two magnitudes) after only one iteration of the optimization code. All DRMs converge very close to the objective value minimum within the first ten iterations.

Based on optimization results and time analysis, the 2x4 and 3x5 DRMs were selected to study the effect of varying the DRM radius. Although the 1x2 DRM exhibited exceptional optimization performance it was not selected for two reasons: the distance between DRM nodes was significant with respect to the acoustic wavelength and the number of iterations required for a final solution canceled the time advantage of the sparse mesh.

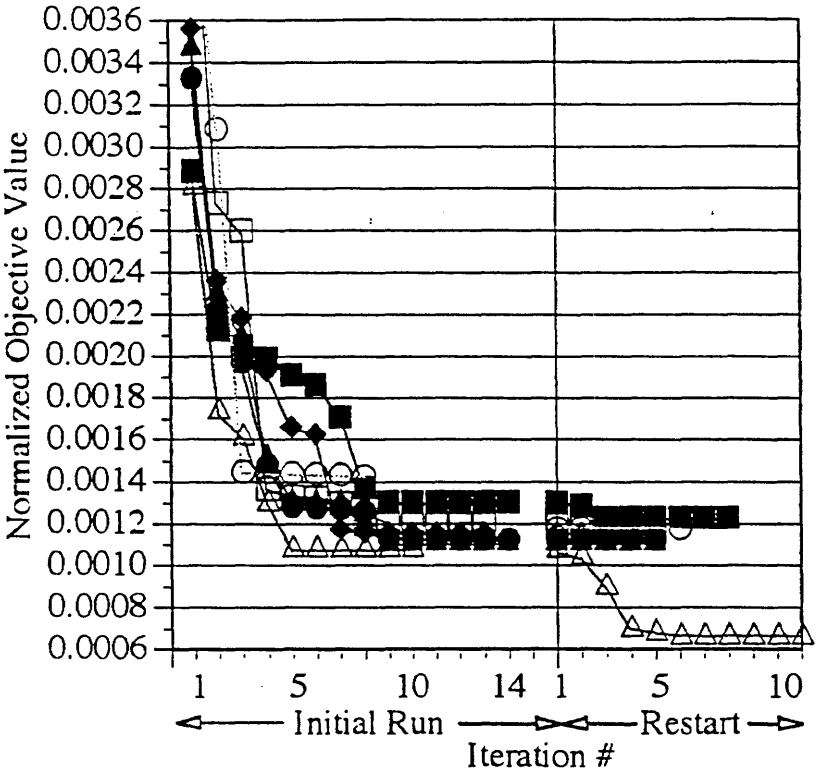

Figure 5.11 - Objective function histories of 0.75m radius DRMs. Initial runs begin at 1.0
■ DRM-1, ● 4 x 8, ▲ 3 x 6, ◆ 3 x 5, □ 3 x 4, ○ 2 x 4, △ 1 x 2

Varying the radius of the meshes within the interior produced no significant differences, in either objective function performance or algorithm time performance.

5.3 Dynamic Remeshing

The results of the alternative DRM study indicated that an extremely coarse DRM, even the 1x2 mesh, may yield extremely rapid progress as compared to the finer meshes, but not be able to fully converge to the same optimum as the finer meshes. These observations led to the genesis of a hybrid approach to the algorithm, where an extremely coarse DRM is used to provide rapid progress in the initial phase of the algorithm execution. For the restart phase, the algorithm transitions to a finer DRM to zero-in on the final optimum. This concept was termed dynamic remeshing, and was implemented in the script. No user intervention is required, once the input data sets are properly configured.

5.4 Sensitivity to Start Point.

Throughout the analyses performed in this research, the final design state and objective function does depend upon the starting design state. For CONMIN, which is a gradient-descent style algorithm, this is readily understood by considering a topography with lots of local valleys: depending upon where the optimization starts, the algorithm will descend into different valleys. This is indicative of a sensitivity to the starting point.

We may illustrate the impact of starting point sensitivity by considering results generated during the alternative mesh study documented above. In the solution found using DRM-1 the final design variables were in a descending pattern (i.e. design variable #1 was greatest and #20 was least). As the bottom edges of the DRM were raised in order to eliminate hot spots, the models were found to converge to a minimum that was an approximate mirror image of the minimum found by DRM-1 from the same starting point. Design variables were oriented in an ascending pattern and the resulting profile of sound pressure levels and particle velocities were reversed with respect to the cylinder plane perpendicular to the acoustic source. This behavior actually illustrates that there are multiple possible local minima, with the possibility of dramatically different design states yielding approximately equal objective function values.

Selected optimization results for the DRMs tested with regard to start point sensitivity are shown with results for DRM-1 in Table 5.13. In the table, the notation 175° refers to the arc of the circumference that the DRM spans (the DRMs in Section 5.2.2 span 180°). All DRMs demonstrated some sensitivity to initial design values. Of the DRMs tested, only the 0.75m, 4x8 DRM with an arc of 175° achieved the same optimum design state as DRM-1 from the mid-value starting point.

Table 5.13. Start Point Sensitivity Optimization Results

	Final Obj. Val. w.r.t. DRM-1 / Final Obj. Val. DRM-1	Design State
DRM-1	1.00	Descending
4x8 175° Lower	1.13	Descending
4x8 175° Middle	0.89	Descending
4x8 175° Upper	1.07	Ascending
2x4 175° Lower	0.85	Descending
2x4 175° Middle	1.03	Ascending
2x4 175° Upper	1.03	Ascending
1x2 175° Lower	0.95	Descending
1x2 175° Middle	1.03	Ascending
1x2 175° Upper	1.03	Ascending

5.5 Optimizer performance: CONMIN vs. COMPLEX

Table 5.14, below, shows the total number of function and gradient evaluations used in a number of fine model runs. These statistics demonstrate the difference between a gradient-search algorithm (CONMIN) and a direct-search algorithm (COMPLEX) when the number of objective function evaluations required to complete a run is considered. The best run of COMPLEX on the Long-20 model (described in Section 6.2) used 655 function evaluations to reach a solution. CONMIN used 173 function and gradient evaluations to reach its optimum point, which has a better objective function value, for this model.

For each run of COMPLEX, CONMIN needs to be run from several different starting points in order to search roughly the same volume of the design space. Each of these CONMIN runs would use relatively the same number of function and gradient evaluations. The number of evaluations required to search a comparable amount of the design space with CONMIN would quickly approach that for COMPLEX's runs.

The number of function evaluations required for COMPLEX to reach convergence will, of course, depend on the criteria set by the user and the model being optimized. The lower the convergence criteria, the more function evaluations needed for the solution to converge. Likewise, a model with a small number of local optima will take less time to solve than a model with a large number of such points.

Table 5.14 - Total Function and Gradient Evaluations for COMPLEX and CONMIN Fine Model Optimization Runs

Optimizer	Model	Run	Total Evaluations
COMPLEX	Long-20	1	655
COMPLEX	Long-20	2	801
COMPLEX	Long-20	3	801
COMPLEX	Long-20	4	836
COMPLEX	Circ-20	1	721
COMPLEX	Circ-20	2	549
CONMIN	Long-20	1	173
CONMIN	Circ-20	1	53

6. OPTIMIZATION TEST STUDIES

In Section 5, extensive discussion was directed toward algorithm performance using a relatively coarse mesh model tool for quick evaluation. In Section 6, optimization for the fine mesh test cylinder models are discussed. These models have the mesh fidelity to accurately capture the solution for the frequency/wavelengths under study. In this section examples of optimal solutions using CONMIN are given for unstiffened and stiffened models, including graphics to illustrate the physics of the solution. In Section 6.1, details of the optimization problems under study are discussed for the unstiffened and stiffened models. Section 6.2 discusses the design variable groupings that were utilized in the problems. Section 6.3 presents and discusses results of the fine mesh studies.

6.1 Unstiffened/Stiffened Models

Optimization was performed with the four above objective/constraint options while tailoring either the thickness distribution of the shell elements, or for the stiffened model also beam section dimensions. The optimization for this work was performed either single frequency or multi-frequency.

Figure 6.1 shows a summary plot of the vibration natural modes of this unstiffened cylinder, the vibration natural modes of the stiffened cylinder, and the acoustic natural modes of the cylindrical cavity. For the cavity only the zero order radial acoustic modes are plotted in Figure 6.1. Due to the symmetry defined in the problem, only odd axial mode numbers of the structure occur, and only even axial modes of the cavity are excited. The frequency selected for the monopole excitation and the optimization corresponds to that of the (2,1) mode of the unstiffened cylinder at 154.2 Hz. A contour of this mode shape is shown in Figure 6.2. This mode was selected as one that responds well to the excitation, and efficiently forces the cavity. In Figure 6.1, it is seen that the (2,1) structural mode at 154.2 Hz forces the off resonance response of the (2,0) and (2,2) acoustic modes at 197.2 and 218.0 Hz, respectively. The peak acoustic interior level is 4.4 dB for this unstiffened cylinder, based on an arbitrary zero dB reference. This reference was selected as a maximum average SPL for both the unstiffened and stiffened models, and all starting and ending points are expressed in terms of this reference (as was done in Section 5.1). For the stiffened cylinder, the same structural resonance (2,1) mode was studied, which for this problem is at a frequency of 137.9 Hz. At this frequency, the coupling with these cavity modes is less efficient than the unstiffened model, with a peak acoustic level of -0.6 dB.

In optimization (using CONMIN), for problems such as this that may have many different local minima, it is important to evaluate many different starting points in the design space. As was done in the coarse cylinder study, three different starting points were evaluated, an upper, middle, and lower point. The middle starting point corresponds to an on-resonance condition with the (2,1) structural mode. This middle starting point is typical of the multi-frequency analysis, which will attempt to reduce peak responses at resonance.

6.2 Design Variable Grouping

Design variable groups are created to limit the total number of design variables, and to study design trends. For the unstiffened model, two different shell thickness design variable groupings

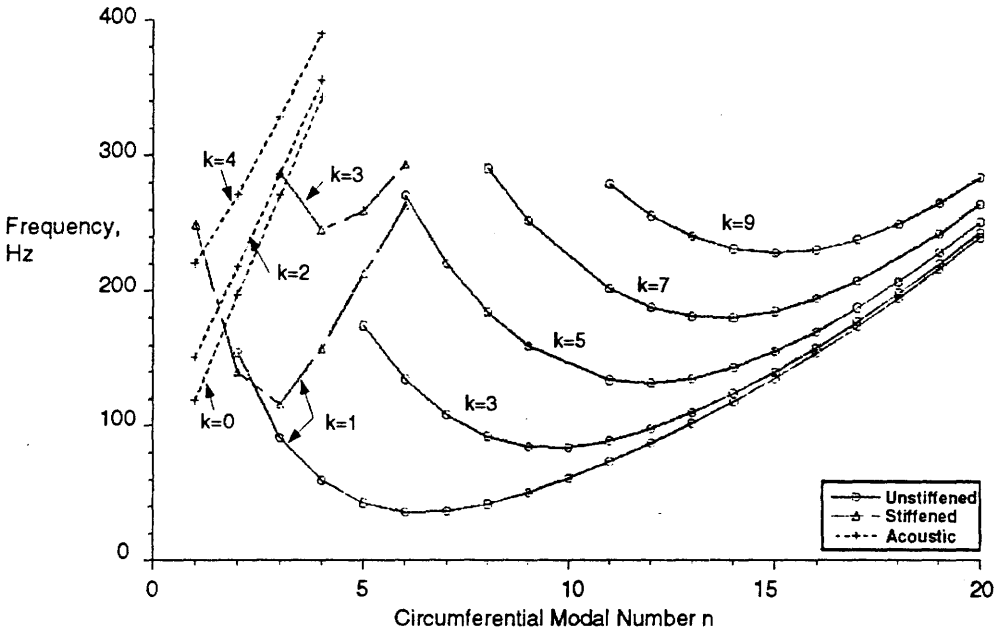

Figure 6.1 - Cylinder and Cavity Natural Modes (k = axial mode no.)

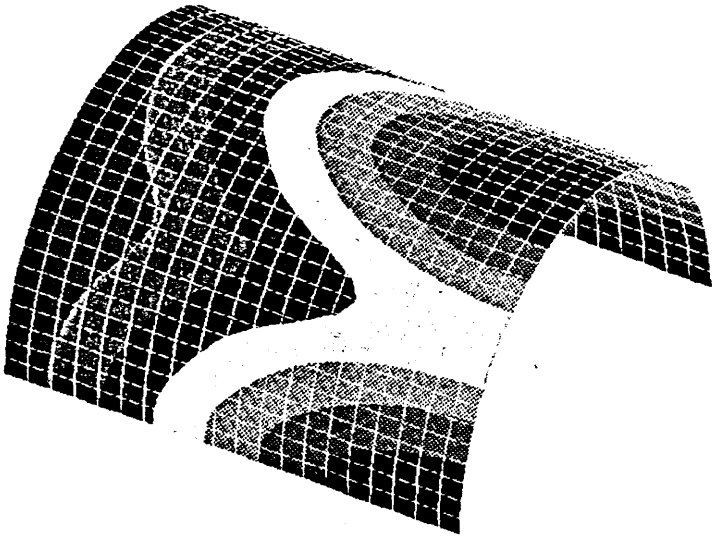

Figure 6.2 - Contour of (2,1) Cylinder Natural Mode (154.2 Hz)

are studied: 20 circumferential arcs allowing design variation in the longitudinal direction (called the "Circ-20" model), and 20 longitudinal strips allowing design variation in the circumferential direction (called the "Long-20" model, see Figure 6.3). For the stiffened model, coarser groupings were utilized which include both shells and beam elements also in longitudinal and circumferential strips. These stiffener groups are also illustrated in Figure 6.3. For the circumferential direction, they consist of 10 shell groups, 10 stringer groups, and 5 frame groups (25 total design variables). These circumferential stiffener groupings are called the "Circ-25" model with shell groups and the

"Circ-15" model without shell groups. For the longitudinal direction, they consist of 10 shell groups, 10 frame groups, and 11 stringer groups (31 total design variables). The longitudinal stiffener groupings are called the "Long-31" model with shell groups and the "Long-21" model without shell groups. The equations relating the area and inertias of these beams to the cross-section dimensions were incorporated in the NASTRAN file using DEQATN and DVPREL2 input cards. These nonlinear relationships allow the element properties to be related to the height and leg dimension of the stiffeners. Referring to Figure 2.2, the height of the frame channel section, and the equal leg length of the stringer angle section were selected as the stiffener design variables in this model.

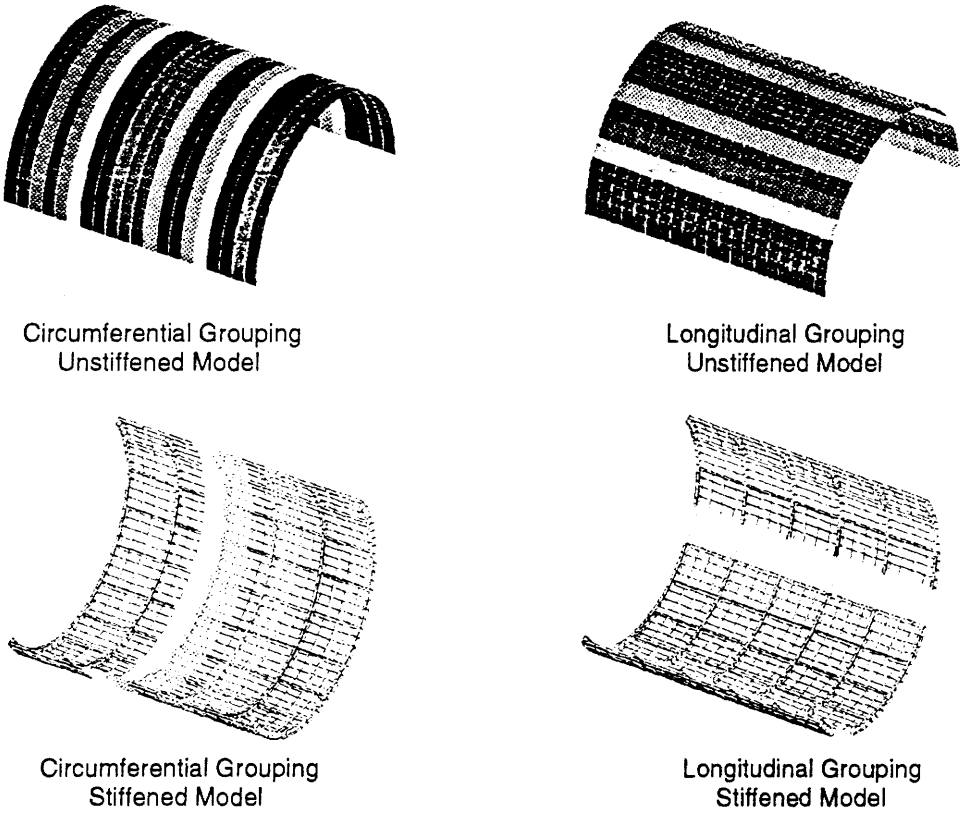

Figure 6.3 - Design Variable Grouping Studies

6.3 Summary of Results

As previously mentioned, four different types of design variables were selected. These were the shell thicknesses for the unstiffened model, both shell thicknesses and beam dimensions for the stiffened model, stiffener inertia properties for the stiffened model, and a separate case in which the design variables were grid point locations of the cross section of the stiffeners, allowing beam cross section shaping. In the following, detailed discussions and illustrations are typically given for a single optimization case in each of the design variable sections, followed by a summary plot or table for all cases at the end of each section. The first four sections are examples of single frequency optimization, with the final section, 6.3.5, describing results from the multi-frequency optimization.

6.3.1 Design Variable - Shell Thickness Only (unstiffened, single frequency). The sample case discussed in detail in this section is the acoustic objective to minimize the global acoustic levels by tailoring the thickness distribution of the shell elements, with a side constraint on the weight such that it does not exceed the initial weight. The starting point is the the middle point, which is the on-resonance starting condition. In Figure 6.4, the unoptimized and optimized velocity distributions are presented. Recall that prior to optimization, the structure is on resonance with a (2,1) natural mode. After optimization, the velocity distribution is very complex with very short wavelength motion, both in the axial and circumferential directions. This distribution does not couple well with the global acoustic response of the cavity. Note also that this mode is actually too complex in the circumferential direction for the grid density of the FEM model to capture accurately. This is a problem that does not typically occur in the stiffened models.

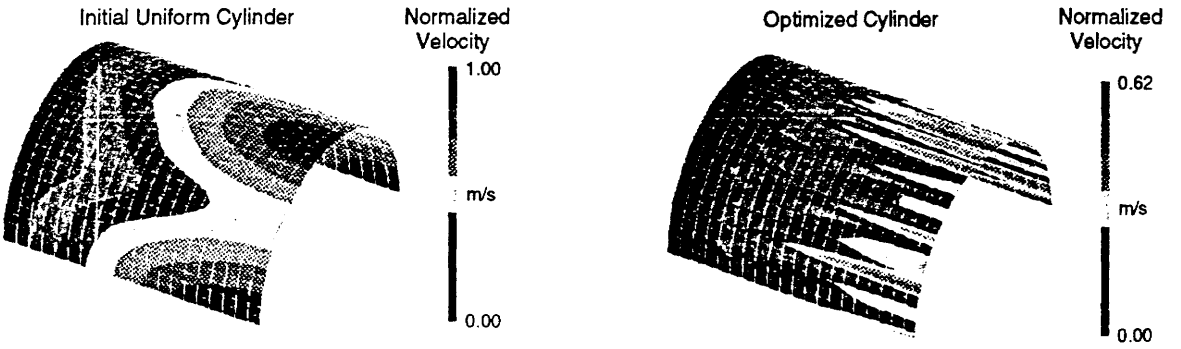

Figure 6.4. - Unoptimized and Optimized Velocity Distributions - Unstiffened Cylinder

Figure 6.5 illustrates the initial and optimal interior noise distributions for this case. Prior to optimization, the acoustic pressure has the characteristics of the (2,1) structural mode shape. Following optimization, the pressure contours maintain a similar distribution, but are globally reduced. Utilizing the same arbitrary zero dB reference as in Section 6.1, the peak acoustic level was initially 4.4 dB and was reduced to -9.6 dB, a reduction of 14 dB from the starting point for this single case. The global average acoustic level was initially -4.6 dB, which has been reduced to -19.6 dB, a reduction of 15 dB. The reductions from initial to ending level are given here simply to quantify this particular example. It is noted again that the ending levels are what is significant when comparing different optimization cases and starting points.

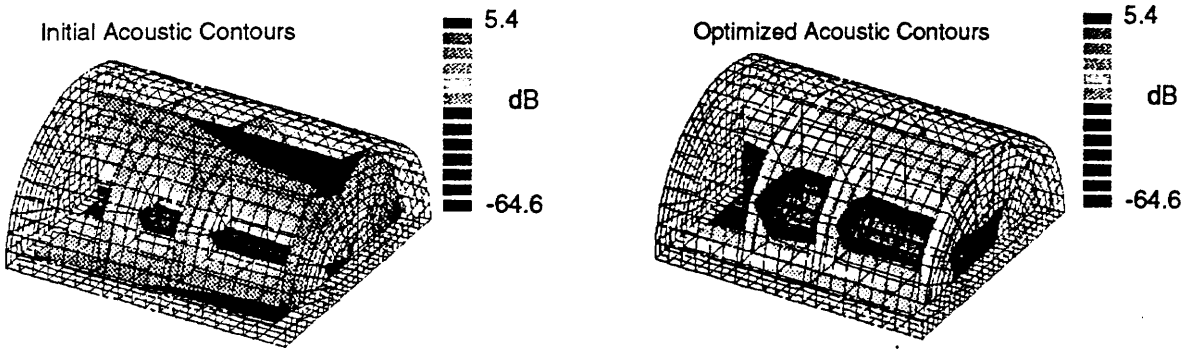

Figure 6.5. - Unoptimized and Optimized Interior Noise Distributions - Unstiffened Cylinder

The thickness distributions before and after optimization are illustrated in Figures 6.6. It is interesting to note that the optimized thickness distribution shows the effect of the nonsymmetric loading on one side of the shell. The optimal thickness contours represent a harmonic distribution about the shell circumference. With this harmonic variation of thickness and mass, the overall weight actually decreased by 8% from the starting point.

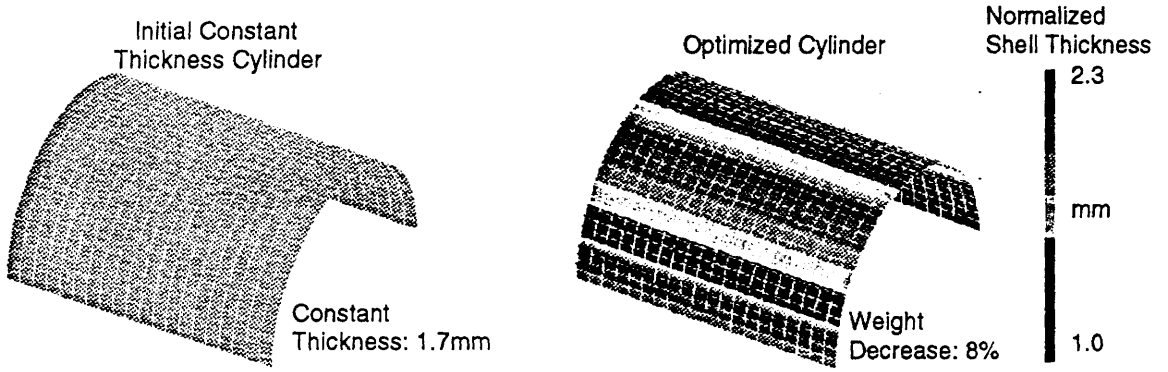

Figure 6.6. - Unoptimized and Optimized Shell Thickness Distributions - Unstiffened Cylinder

Figure 6.7 is a plot summarizing the results of 40 optimizations of the unstiffened model using all four objective/constraint formulations. As seen previously in Section 5 using the coarse cylinder model, a somewhat linear relationship exists between the optimal weight and optimal sound pressure level. Notice that the fine mesh cylinder results here contain considerable scatter in the data as compared to the results in Section 5. This is the result of many more design variables in the problem, giving the optimizer more degrees of freedom. The upper line represents the sound pressure level for the case where the design variables are uniform at a given weight. This curve is included to show the improvement potential available by using the optimal design.

6.3.2 Design Variable - Shell Thickness and Beam Dimensions (stiffened, single frequency). The optimization case discussed in detail in this section is the same as the previous section, the Acoustic objective to minimize the global acoustic levels with a side constraint on the weight such that it does not exceed the initial weight. The starting point is the the middle point, which is the on-resonance starting condition. The design variables are the shell element thicknesses, and also the beam section dimensions as discussed in Section 6.2. In Figure 6.8, the unoptimized and optimized velocity distributions are presented. Note that prior to optimization, the structure is again on resonance with a (2,1) natural mode. After optimization, the velocity distribution has a shorter wavelength modal contribution more like a (4,1) mode. As previously mentioned, this shorter wavelength mode does not couple as well with the global acoustic response of the cavity.

Figure 6.9 illustrates the initial and optimal interior noise distributions for this stiffened cylinder case. The acoustic initial and optimal pressure distributions are very similar in appearance to that shown in the previous section. The peak acoustic level was initially -0.6 dB and was reduced to -25.6 dB, a reduction of 25 dB from the starting point. The global average acoustic level was initially -10.6 dB, which has been reduced to -36.6 dB, a reduction of 26 dB. Again it is noted that these reductions are stated simply to quantify this example, and that ending levels are the significant final result.

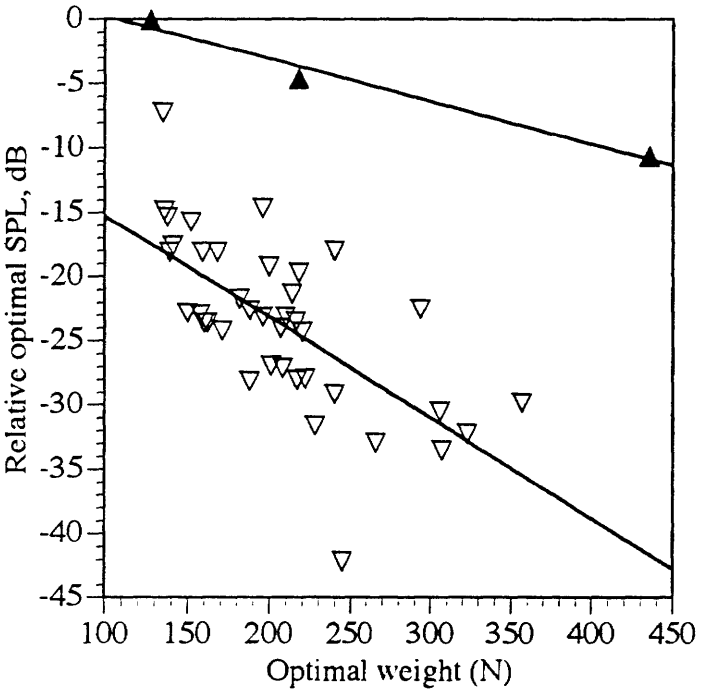

Figure 6.7. - Relative Sound Pressure Level Versus Optimal Cylinder Weight for the Unstiffened Model, ∇ - Fine Model Optimized, ▲ - Fine Model Uniform Thickness

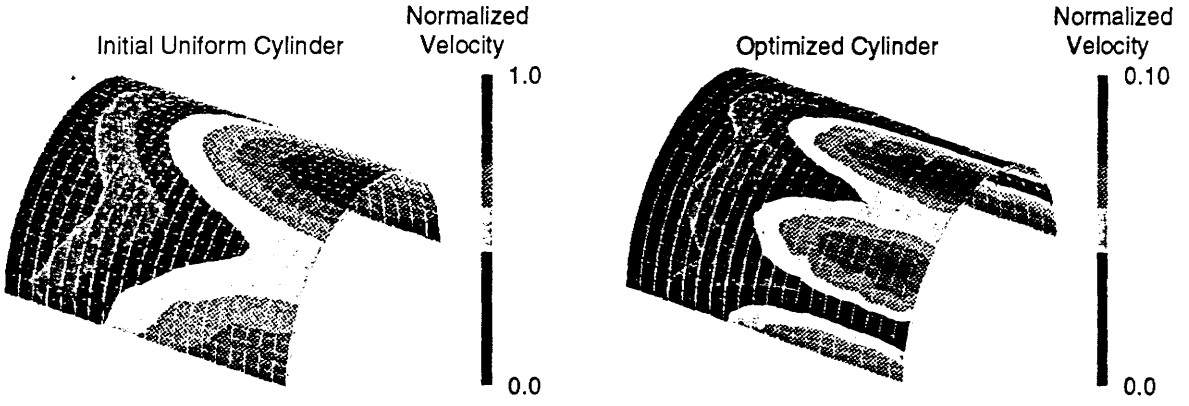

Figure 6.8. - Unoptimized and Optimized Velocity Distributions - Stiffened Cylinder

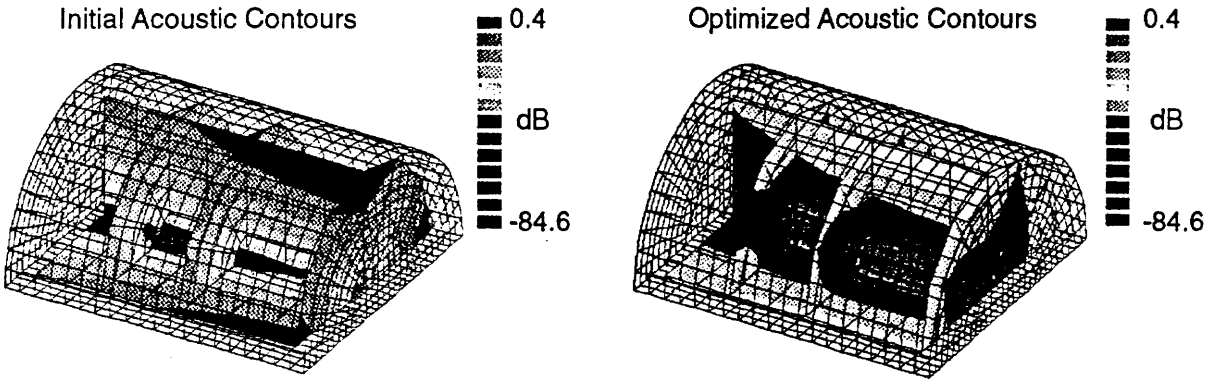

Figure 6.9. - Unoptimized and Optimized Interior Noise Distributions - Stiffened Cylinder

The shell thickness distributions before and after optimization are illustrated in Figure 6.10. Since the shell thickness design variables tended to dominate the design when shell and stiffener design variables were optimized simultaneously, only the shell thicknesses were contoured. For this case, very little change was found in the stiffener design. Once again it is observed that the optimized thickness distribution shows the effect of the nonsymmetric loading on one side of the shell. The optimal thickness contours again represent a somewhat harmonic distribution about the shell circumference, and the weight decreased by 1% from the starting point.

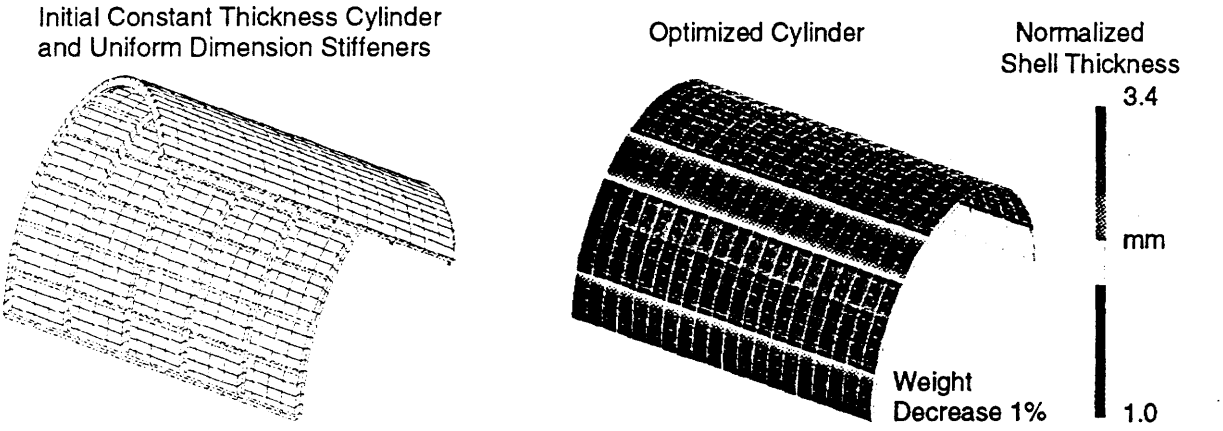

Figure 6.10. - Unoptimized and Optimized Shell Thickness Distributions - Stiffened Cylinder

Figure 6.11 is a plot summarizing the results of 30 optimizations of the stiffened model using the different objective/constraint formulations. In this figure, a relationship is not readily apparent between the optimal weight and optimal sound pressure level (as was seen in Section 6.3.1 for the unstiffened model). This difference between the unstiffened and stiffened model results can be explained by referring to Figure 6.1. Beginning on the y-axis of this figure, at the excitation

frequency of the unstiffened model (154.2 Hz), by traversing to the right it is observed that the modal density of the unstiffened cylinder is quite high. However, for the stiffened cylinder, the modal density is very low at its excitation frequency of 137.9 Hz, and only a few fundamental resonances occur. Thus the unstiffened cylinder, at its various initial and final design states (in this frequency range) tends to remain in a modal rich region, allowing mass control effects to be observed with little effects of shifting from one resonance to another. However, for the stiffened cylinder, the effect of the stiffeners is to decrease the modal density; thus this structure is more stiffness controlled than the unstiffened cylinder, and is highly affected by the amount of overlap with its fundamental resonances. Referring back to Figure 6.11, the filled triangular symbols correspond to the three starting point conditions, and represent a uniform distribution of shell thickness and stiffener dimensions. The middle point of the three is the on-resonance condition with the (2,1) mode, and the other two are considerably off-resonance. In general the optimal design points congregate well below the on-resonant point, and represent a multiple number of improved designs. This figure illustrates the potential for optimizing at the resonant frequencies, as is done in the multi-frequency analysis in which peak responses will be reduced within a frequency band.

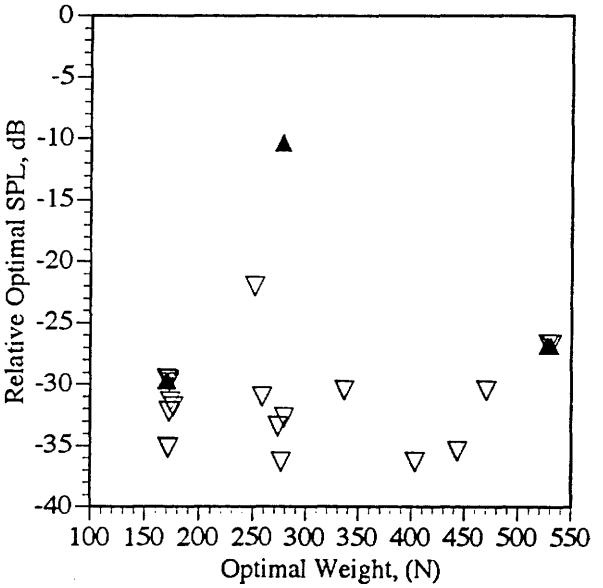

Figure 6.11. - Relative Sound Pressure Level Versus Optimal Cylinder Weight for the Stiffened Model, ∇ - Fine Model Optimized, ▲ - Fine Model Uniform Thickness

6.3.3 Design Variable - Stiffener Inertias Only (stiffened, single frequency). A short study was performed to verify the importance of frame and stringer stiffness to noise reduction. The study was prompted by the discovery of "acoustic" tailoring recently performed on European airplanes including the Dornier 328 turboprop, and the ATR42-500 turboprop. The Dornier 328 utilized optimal spacing of "acoustic stringers", which were high torsion inertia sections of hat shape. The ATR42-500 reinforced seven fuselage frames in the propellor plane. Both airplanes also utilized passive vibration absorbers, and acoustic lining as well.

The optimization cases described in this section utilize stringer and frame cross section inertia properties (I,J) as design variables, with no shell thickness design variables included. The baseline

acoustic objective with no weight side constraint was used. As the previous stiffener studies selected angle sections as the stringer inertia starting point, this analysis began with the stringer inertia of a hat section since the angle section has a very low torsion inertia. The case discussed in detail below utilized the stringer torsion inertia for each of the 10 stringers as the design variable. Figure 6.12 illustrates the stringer model and the stiffener sections.

In Figure 6.13, the unoptimized and optimized velocity distributions are presented. As before, the initial velocity distribution is that of a (2,1) mode shape. For this case, the optimized velocity distribution is a distorted (3,1) mode shape which does not couple as well with the cavity as the (2,1) shape.

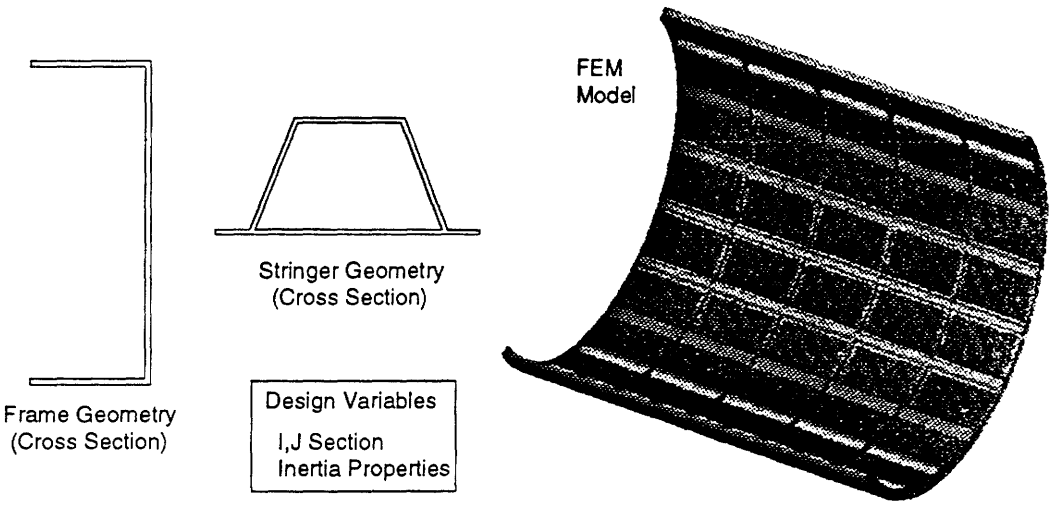

Figure 6.12. - Stiffened Cylinder with New Stringer "Hat" Section

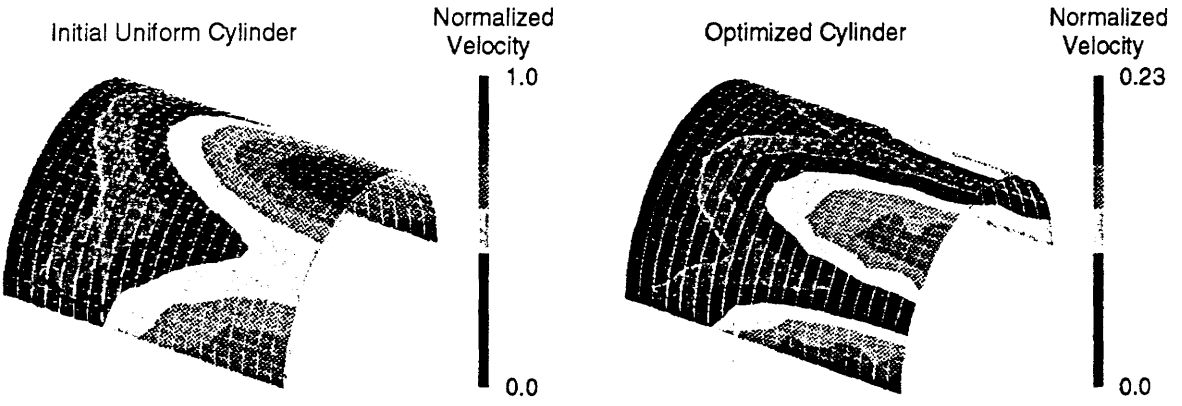

Figure 6.13. - Unoptimized and Optimized Velocity Distributions - Stiffened Cylinder Stiffeners Only

Figure 6.14 illustrates the initial and optimal interior noise distributions for this case. The peak acoustic level has been reduced to -16.6 dB, a reduction of 14 dB. The global average acoustic level was initially -11.6 dB, which has been reduced to -27.6 dB, a reduction of 16 dB.

The torsion inertia distributions before and after optimization are illustrated in Figures 6.15. In this result, the torsion inertia is increased substantially at the top of the cylinder, effectively breaking up the velocity distribution into a (3,1) shape versus the initial (2,1) shape.

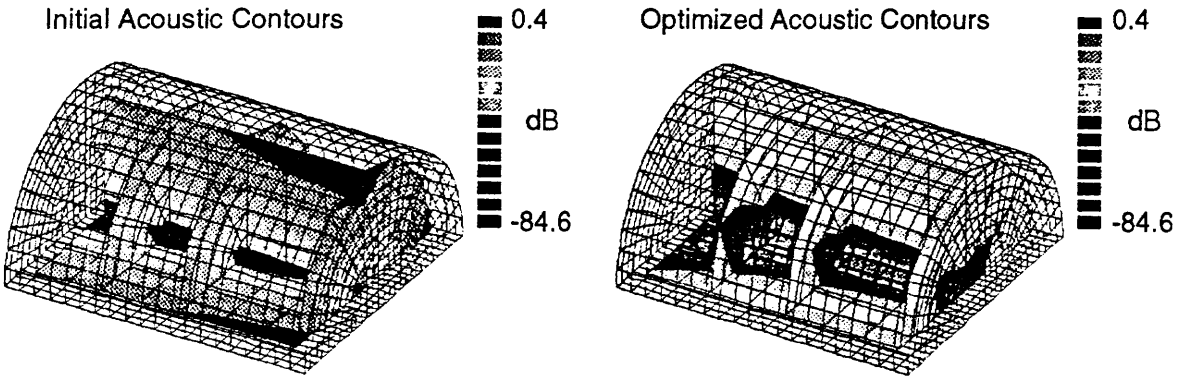

Figure 6.14. - Unoptimized and Optimized Interior Noise Distributions - Stiffened Cylinder Stiffeners Only

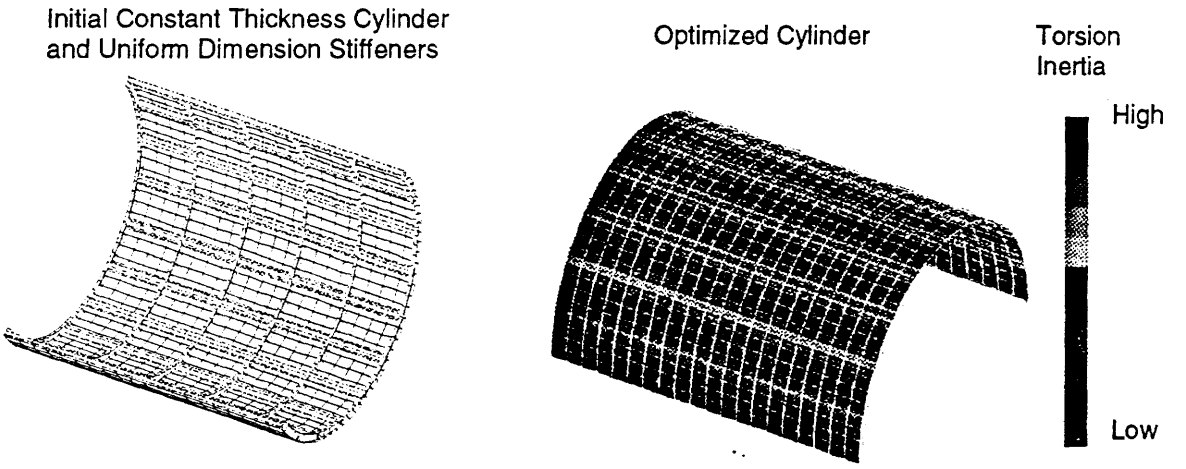

Figure 6.15. - Unoptimized and Optimized Beam Inertia Distributions - Stiffened CylinderStiffeners Only

Table 6.1 summarizes the results of this stiffener study. Five cases were run, with design variables composed of the following stiffness inertia properties: stringer torsion, stringer bending, frame torsion, frame bending, and the final case with all of the above. As the frame bending inertia

and the stringer torsion inertia relate to circumferential stiffness of the cylinder, it is observed that these two cases 1 and 4 showed significant noise reduction (27.8 and 15.7 dB, respectively). On the other hand, the frame torsion and stringer bending inertias relate to longitudinal bending stiffness of the cylinder. The frame torsional stiffness of this channel section is very low initially, and thus a very low noise reduction was achieved of 2.6 dB. In contrast, the stringer bending inertia for the hat section is very similar in magnitude to the stringer torsion and frame bending inertias, and a significant noise reduction was achieved for this Case 2 of 14.9 dB. Case 5 combines all the torsion/bending design variables for both stringers and frames, and comparable reduction to Case 4 with frame bending alone was achieved. The overall results in this section verified the potential for frame and stringer design alone to reduce interior noise.

Table 6.1 Stiffener Study Optimization Results

	Design Variables		Average SPL (dB)		
Case	Stiffeners	Inertias	Initial	Optimized	Reduction
1	Stringers	Torsion	-11.6	-27.3	15.7
2	Stringers	Bending	-11.6	-26.5	14.9
3	Frames	Torsion	-11.6	-14.2	2.6
4	Frames	Bending	-11.6	-39.4	27.8
5	Both	Both	-11.6	-36.6	25.0

6.3.4 Design Variable - Beam Cross Section Shape (stiffened, single frequency). The optimization case in this section utilizes the Acoustic objective to minimize the global acoustic levels by tailoring the beam stiffener cross section shapes, with a side constraint on the weight such that it does not exceed the initial weight. The starting point is the on-resonance starting condition. The shape of the unoptimized structural natural mode is shown in Figure 6.16, which for this structure had a frequency of 140.8 Hz. This frequency was the constant excitation frequency of the optimization.

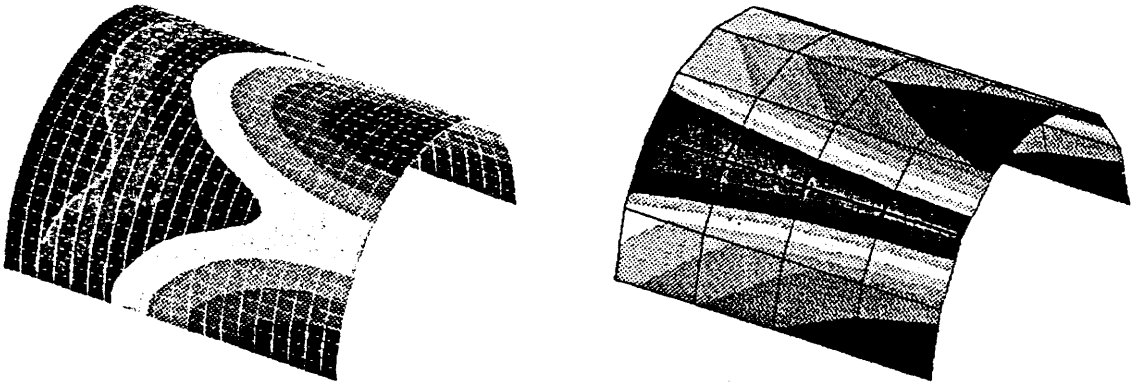

Structure Acoustic Response

Figure 6.16 - Structural Natural Model Shape and Acoustic Response of Data Recovery Mesh to the Structural Natural Mode

In order to perform shape optimization of stiffeners modeled using beam elements, it is necessary to know the area A, inertias I_x, I_y, I_{xy} about the cross-section's X,Y axes, the torsion constant J, and the centroidal and shear center locations. Since in this example we are using the method of feasible directions to do the optimization, we also need the sensitivity derivatives of the responses with respect to the design variables. These properties and derivatives must be evaluated when requested by the optimizer at each iteration. NASTRAN has the capability of accepting properties such as A, I_x, I_y, I_{xy}, J, etc. in equation form as they would be programmed in FORTRAN. In order to compute the equations, a separate finite element code was written to integrate these area properties over the cross sections as they exist at each iteration. This stand alone finite element code was written such that it did not output the values of the properties (A, I_x, I_y, I_{xy}, J, etc.), but the property equations as a function of certain prescribed x,y coordinates of the mesh for that cross section. These X,Y coordinates correspond to the design variables of the cross section. Having coordinates as design variables allows one to alter the shape of the cross section. Figure 6.17 shows the frame and stringer cross section shapes, along with the finite element discretization. Shown here are a channel section for the frame, and the two cases studied for the stringer cross section, i.e. an angle (Case I) and an open box (Case II). The labeled points indicate the design variable locations, with a subscript x corresponding to an X-direction design variable, and subscript y to a Y-direction design variable. Note that some nodes only have an x subscript, some a y subscript, while others an x,y subscript. Each x or y at a node indicates a separate design variable, with the direction indicating the degree of freedom. By specifying only one of the coordinate directions at a node, the shape is thus constrained in the other direction. This is a way of limiting or constraining the design.

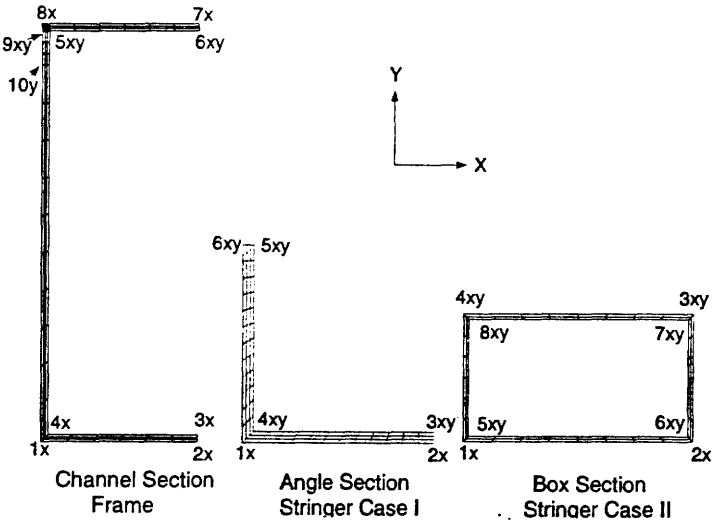

Figure 6.17 - Frame and Stringer Cross Section Shapes and Finite Element Discretization

It should be noted that at each iteration in which the FEM/BEM solution was run, the cross section finite element code had to be run to evaluate the property equations. The cross section code, called BEAMSHPE, requires a prior finite element discretization of the cross section shapes. This was performed using an automated meshing code (MSGMESH, by MSC/NASTRAN). The meshing code was run prior to each BEAMSHPE execution. It should be

noted here that a coarse finite element discretization was found adequate to evaluate the area properties accurately.

At this stage we can vary the coordinates of the two cross sections at every iteration due to changes in x_i, y_i coordinate design variables. In order to independently vary the cross sections of the 5 frames and 11 stringers in the model, we would require 175 coordinate design variables for Case I. This would be excessive, and is really not necessary. Instead we introduced design variables which basically were scale factors of each parent cross section, which are multiplied by each coordinate equally to uniformly scale the section up or down. Equation (6.1) shows the relationship between a property value A (area), the scale factors S, and design variable coordinates x_i and y_i, where g represents the equation for the area in terms of coordinates of x_i and y_i.

$$A(S, x_i, y_i) = g(S*x_i, S*y_i) \tag{6.1}$$

A separate scale factor was applied to each frame and stringer in the model. Since there were 5 frames and 11 stringers, a total of 16 scale factor design variables were required. Adding these to the 23 coordinate design variables for the parent cross sections of Case I, we had a total of 39 design variables. Case II, which utilized the open box section for the stringer, had a total of 43 design variables.

When performing optimization using any gradient search method, the starting point in the design space is very important. It is ususally necessary to evaluate many starting points in order to approximately locate a global minimum. In the case at hand, we have a mixture of coordinate design variables and scale factor design variables. Depending on the initial values of the scale factors relative to the coordinates, the gradients of scale factors or coordinates can be dominant. As it is possible to adjust the coordinate values with the scale factors and still have the same property starting values, the coordinates and scale factors were adjusted so that the initial gradients for scale factors versus coordinates were comparable in magnitude for the same values of the properties. This was done so as not to bias the design towards a cross section shape change versus a spatial scale change. These starting values were varied for several different optimization runs, to test for sensitivity to starting point.

Each design variable, whether it is a scale factor or a coordinate, has upper and lower bounds. These were allowed to be quite generous, except for the case where a coordinate change may cause a line of the outline of the area to pass over another line, thus resulting in a negative area, or inertia property. These bounds were used to control and maintain realistic values. In addition to the design variable bounds, a weight constraint was placed on the total cylinder weight such that the initial weight of the entire stiffened cylinder was not exceeded.

Figure 6.18 shows the changes in the acoustic objective and weight over the history of the iterations for both cases. The objective is given in pressure squared normalized by the initial pressure squared, and the weight is normalized by the initial weight. For Case I the global objective was reduced by 8.6 dB and for Case II by 7.2 dB. Note that in both cases the weight, which was constrained to not exceed the initial weight, was actually reduced by 5%. Also note that each design iteration required approximately 15 minutes CPU on an SGI Power Indigo II workstation, with a total of 19 CPU hours for Case I and 26 CPU hours for Case II.

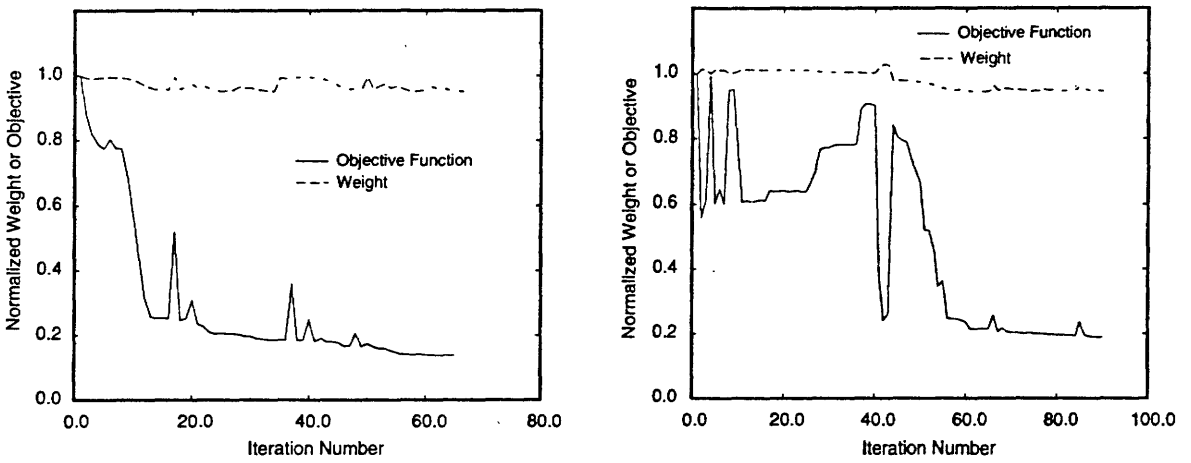

Iteration History - Case I

Iteration History - Case II

Figure 6.18 - Objective Function and Weight

In Figure 6.19, the before-and-after-optimization parent cross section shapes are presented. Note that the sections have been greatly enlarged for clarity. For both cases, dramatic changes inI the shape of the cross-sections were not found. Typically thinning down of the sections, maintaining inertia while reducing weight are the trends for the channel. Attempts were made to allow the channel (frame) section the freedom to develop another leg at the top (away from the attachment to the shell), and only a bump is noticable. It is evident that the angle's stiffness and mass are reduced considerably. Generally the box section simply has thinned down walls. It should also be remembered that the thinner sections are still multiplied by the scaling factors.

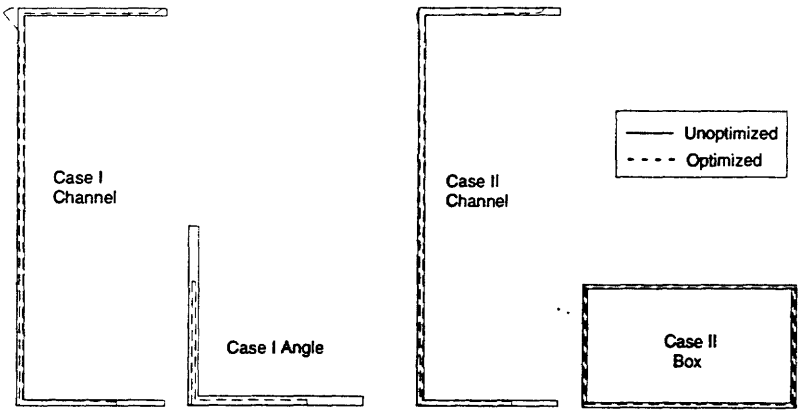

Figure 6.19 - Before and After Optimization Cross Section Shapes

The dominant change in the stiffener design tended to be in the scaling variation from stiffener to stiffener over the cylinder, represented by the scale factor design variables. Figure 6.20 illustrates this trend. The scale factors are magnified and multiplied by the parent sections to show

the relative changes in size over the cylinder. In general, the frame relative size changes can be seen, but not much visible variation is evident in the stringers, either for the angle or the box section. It is noticeable that the relative changes in the frames is larger for Case I than for Case II.

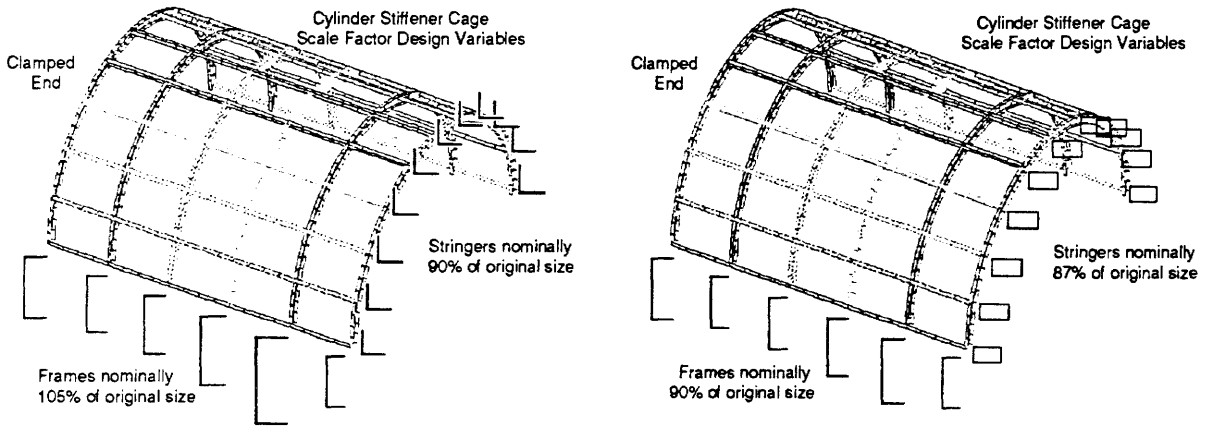

(a) Case I (b) Case II

Figure 6.20 - Relative Changes in Stiffener Size Over the Cylinder

A plot of the scale factors over the surface of the cylinder is not a good indicator of how they will affect the dynamic response of the cylinder, or the acoustic response of the interior. Figure 6.21 contains plots of the cross section properties of the frames and stringers normalized with respect to the initial values prior to the optimization. These properties include the scale factors, areas, and inertias (I_x, I_y, I_{xy}, J). Note that the area changes are proportional to the square of the

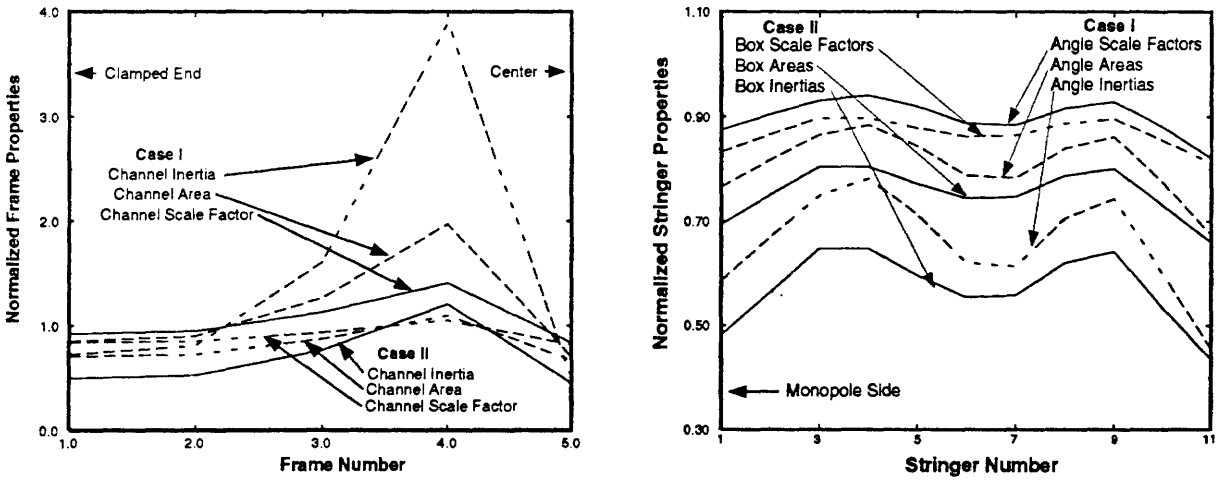

(a) Frame Properties (b) Stringer Properties

Figure 6.21 - Normalized Cross Section Properties Over the Cylinder

scale factors, and the inertias to the fourth power of the scale factors. In these figures, it is evident that small changes in scale factors result in large changes in inertias. It is the inertias that strongly affect the bending behavior of the shell, and thus the acoustic response of the interior. In Figure 6.21a, it is clear that the inertias are much larger for Case I than in Case II. In Figure 6.21b, a sinusoidal variation in stiffness properties around the circumference is evident for both cases (this result has been evident in many of the other cases). For Case I, the stringers were nominally 90% of original size, and for Case II 87% of original size. For the open box cross section, the torsion constant J is two orders of magnitude larger than the angle torsion constant. It is believed that this section is thus more efficient, explaining why the scale factors are generally smaller for both the frames and stringers for Case II than in Case I. This is particulary evident in the frame scales, as much larger variation is required in the frames for Case I to affect the structure than for Case II.

Looking back at Figure 6.16, this starting natural mode of the structure is a (2,1) mode, i.e. two sine waves in the circumferential direction and one half sine wave in the longitudinal direction (recall that only half the longitudinal and circumferential directions are modeled). Figure 6.16 also contains a contour of the magnitude of the acoustic response at the subject frequency to this structural mode. The acoustic variation is the result of the (2,1) structural mode forcing the off resonance response of the (2,0) and (2,2) acoustic modes at 197.2 and 218.0 Hz, respectively. The acoustic mode shapes have a two sine wave variation circumferentially, and a $\cos(k\pi x/L)$ variation in the longitudinal direction, where k=0 or 2 for these modes. In Figures 6.22a and 6.22b, this same acoustic behavior is plotted in a normalized fashion along with the changes in inertias along the longitudinal and circumferential axes, respectively. The acoustic curves are the pressure squared acoustic objective normalized by the maximum level in the contour, and the inertias are normalized by the maximum intertia. The particular case displayed is that of Case I. Case II has very similar trends. Focusing on Figure 6.22a, which corresponds to the longitudinal direction, the acoustic variation is a slowly increasing function, while the inertia variation has a

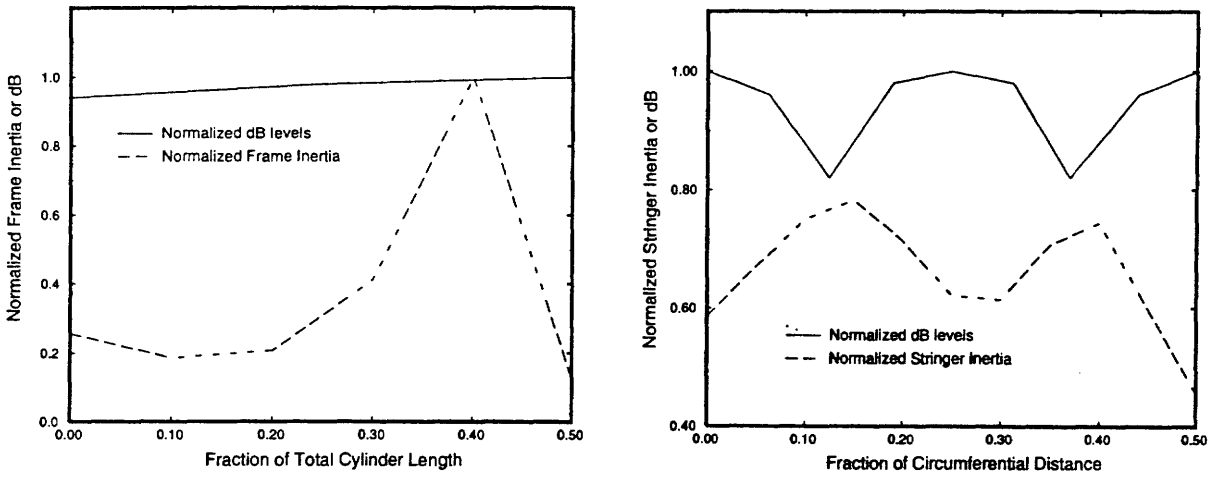

(a) Frame Properties

(b) Stringer Properties

Figure 6.22 - Normalized Acoustic Response and Normalized Frame and Stringer Inertia Properties over the Cylinder

spike near but prior to the center. In Figure 6.22b, the acoustic variation appears to be that of two full sine waves around the half circumference (sin(kπx/L) where n=4), due to the fact that the "pressure squared" objective is plotted and thus the negative part of the wave has become positive (the pressure is actually still an n=2 wave). The stiffener inertia around the circumference is also an n=4 sinusoidal distribution, except it is different in phase by 180 degrees. This design trend brings to mind the phase cancellation techniques of active noise control.

6.3.5 Multiple Frequencies. In this section, multiple frequency optimization was performed on the stiffened cylinder models using CONMIN and the acoustic objective formulation. The Circ-15 (C15) and Long-21 (L21) models were used, in a total of five cases. The five cases were:

1. L21_Mid_BL. Long-21 model, mid-design variable starting point, acoustic formulation, no weight constraint (baseline).
2. L21_Mid_1.0. Long-21 model, mid-design variable starting point, acoustic formulation, weight constrained to be ≤ initial weight of mid starting point.
3. L21_Mid_1.1. Long-21 model, mid-design variable starting point, acoustic formulation, weight constrained to be ≤ 1.1 times weight of mid starting point (10% increase).
4. C15_Mid_BL. Circ-15 model, mid-design variable starting point, acoustic formulation, no weight constraint (baseline).
5. C15_Low_1.0. Circ-15 model, low-design variable starting point, acoustic formulation, weight constrained to be ≤ initial weight of mid starting point.

The common excitation spectrum for these multifrequency cases is depicted in Fig. 6.23. The excitation bandwidth captured several structural modes and one acoustic cavity mode.

The interior response spectra for the beginning and five ending optimal design states corresponding to the five cases are shown in Figure 6.24. The response spectra was obtained for each case by averaging the interior response across all data recovery nodes for each analysis frequency within the bandwidth.

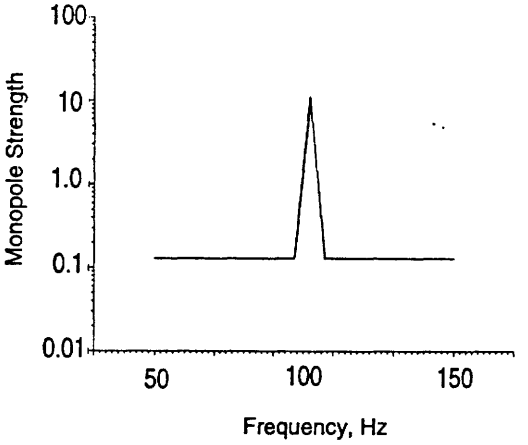

Figure 6.23 - Multi-frequency Excitation Spectrum

With the exception of case 4, all analyses yielded significant improvement as compared to the baseline starting point over the entire bandwidth, not just at the peak frequencies. Examining the structure of the response, it is evident that some modal frequencies were moved about, though only one was moved completely out of the range. The acoustic mode response near 119 Hz was reduced, as well. Note that had the end-points of the frequency range been included in the peak-tracking algorithm, then shifting a resonance to just outside of the band would also be taken into account.

Figure 6.25 presents the ending optimal normalized design states in the same sequence, top to bottom, as the cases defined above. The best response spectra is that in Case 5, which corresponds to a slight perturbation of the design variables about their lower bounds. Table 6.2 summarizes the total average sound pressure level reduction across the bandwidth and the normalized ending weights. Note that the weights are not significantly changed from the reference starting design states, even though the sound pressure level reductions are quite substantial. As we observed in the single frequency studies, it's not just the amount of weight on the structure, it's how you use it that makes the difference.

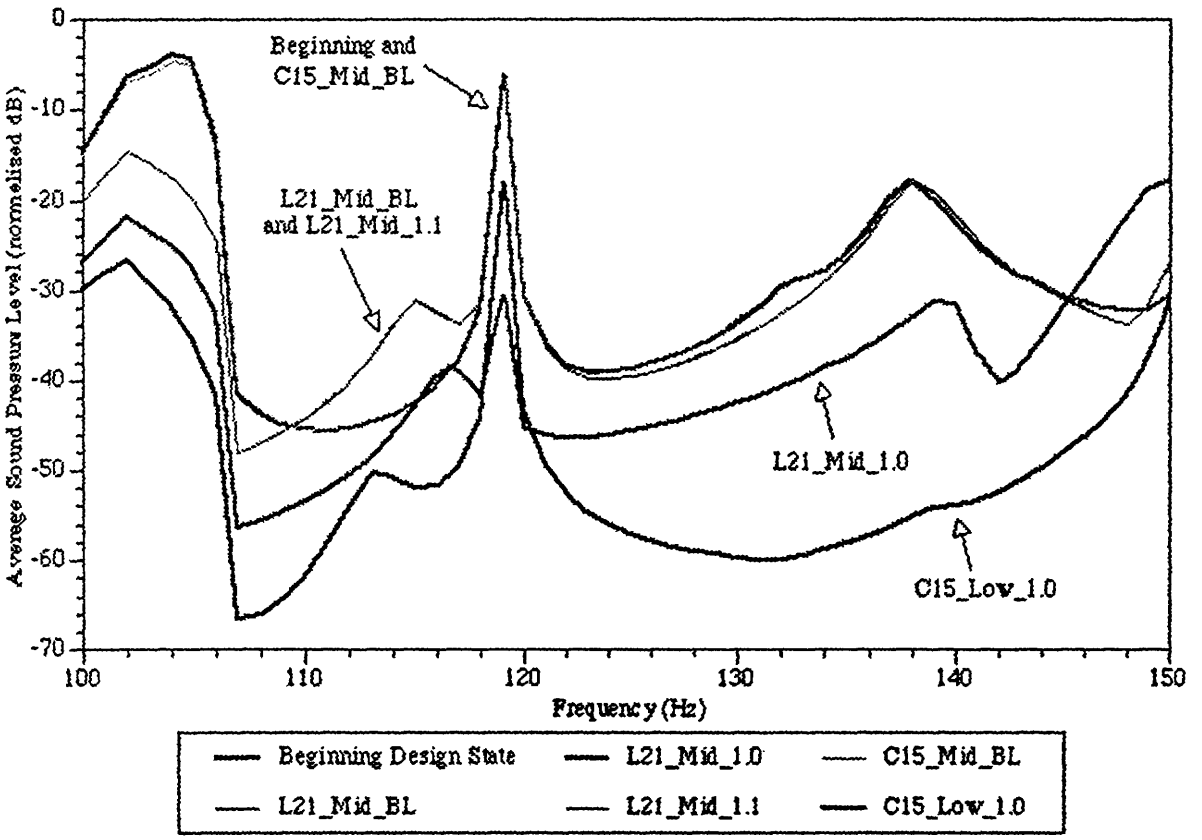

Figure 6.24 - Average SPL vs. Frequency for Different Starting States of Stiffened Models

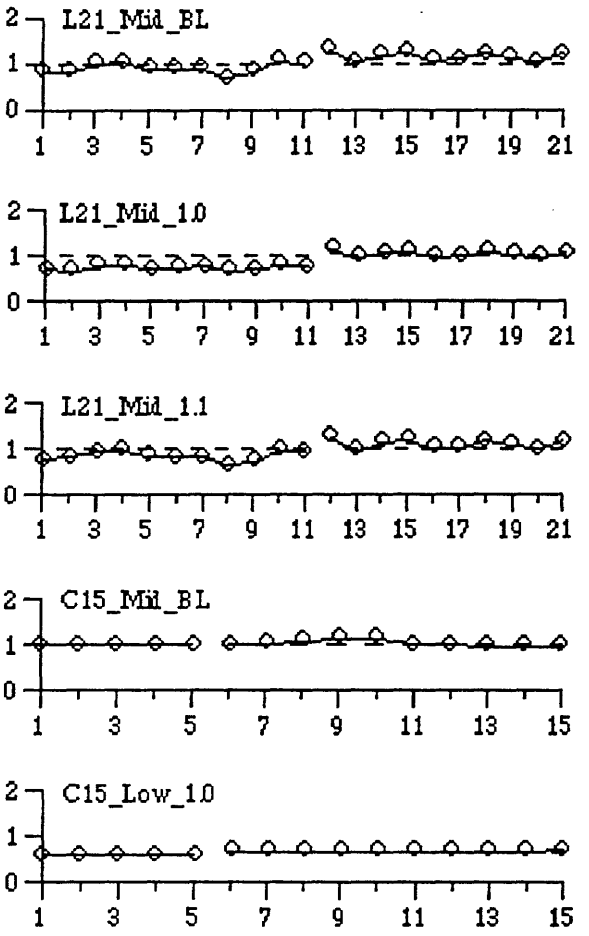

Fig. 6.25 - Normalized Design States for Multi-frequency Optimizations

Table 6.2 - dB Reduction as Compared to Reference Starting Design, Ending Weights Normalized to Reference Starting Design

Case	dB Reduction	Normalized Ending Weight
L21_Mid_BL	5.9	0.996
L21_Mid_1.0	17.0	0.981
L21_Mid_1.1	5.9	1.001
C15_Mid_BL	0.6	1.005
C15_Low_1.0	19.2	0.943

7. CESSNA FULL AIRCRAFT OPTIMIZATION STUDY

In Section 7, an optimization study of a Cessna Citation III business jet fuselage structure is discussed. The actual aircraft modeled is a test specimen that exists in the Virginia Polytechnic Institute Acoustics Lab and is used for noise control testing. This aircraft has the wings and tail control surfaces removed, and the true condition of the aircraft was modeled. Cessna Aircraft Company constructed the structural finite element model of the aircraft, and Lockheed Martin Aeronautical Systems Company constructed the acoustic boundary element model of the cabin interior. Figure 7.1 shows a picture of the aircraft.

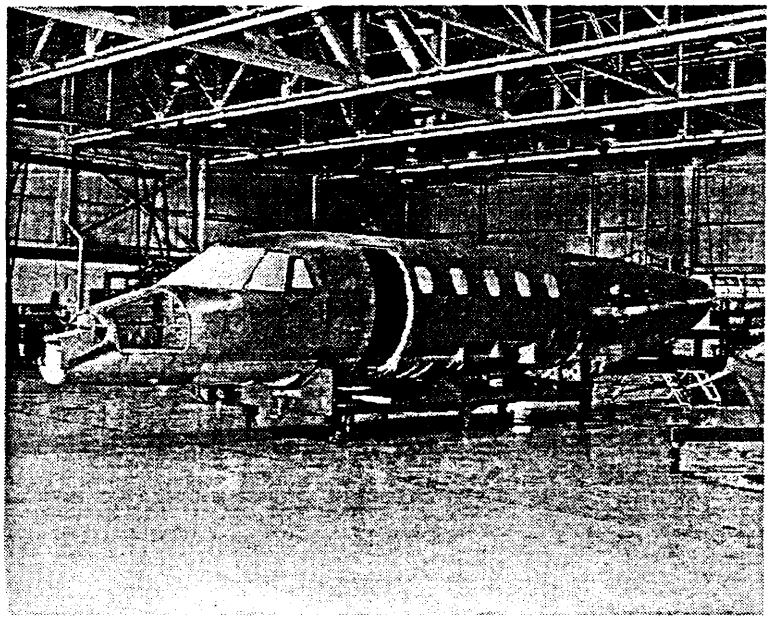

Figure 7.1 - Photograph of Cessna Citation III Fuselage
Located at the VPI Acoustics Lab

In the following sections, the model development, analysis, and optimization of this aircraft is discussed. Section 7.1 presents the results of some preliminary modeling studies, which were prerequisite to constructing the structural finite element model. Section 7.2 discusses the finite element and boundary element models, including boundary conditions, load conditions, and excitation. Section 7.3 summarizes the dynamic modal response of the structure and the acoustic response of the interior cabin. Section 7.4 describes the optimization objective and constraints, including the six optimization cases selected for study. Finally, Section 7.5 presents the results of each of the six optimization cases.

7.1 Preliminary Modeling Studies

In this section, the results of four different modeling studies, conducted to guide the development of the full aircraft Cessna Citation III structural finite element model, is presented. Section 7.1.1 discusses a study on mesh density requirements versus cpu time, Section 7.1.2 presents a study of plate element versus beam elements to model the frame and stringer stiffeners, Section

7.1.3 reviews a study on the effects of shell membrane stiffening due to cabin pressure, and Section 7.1.4 discusses a modeling study of the effect of frame cutouts.

7.1.1 Mesh Density Requirements. A stiffened cylinder finite element structural model was constructed to test the mesh density requirements for the particular cylinder size and stiffening characteristics of the Cessna fuselage. The cylinder was modeled with CQUAD4 plate elements for the skin and CBEAM elements to model the frame and stringer stiffeners. This idealized stiffened cylinder was 6 feet in diameter, and 20 feet long, with the average stiffening characteristics of the Cessna fuselage. A modal analysis was conducted in NASTRAN for each mesh density studied, followed by a post-processing operation to determine if the mesh was fine enough for the modes of interest. The computers designated for the optimization analysis were also benchmarked for the amount of CPU time required to run each problem. Figure 7.2 shows a natural mode of this test cylinder modeled with the final selected mesh density. As the goal of the optimization is to tailor structural modes which are global in nature, with wavelengths much longer than the subpanel dimensions (a subpanel is bounded by two stringers and two frames), then the mesh density was not sized to accurately capture the subpanel modal behavior. The final mesh density recommended from this study utilized 1 node between each stringer, and 3 nodes between each frame. This density allowed a reasonable CPU time expenditure and accurate capture of the frame and stringer global modes.

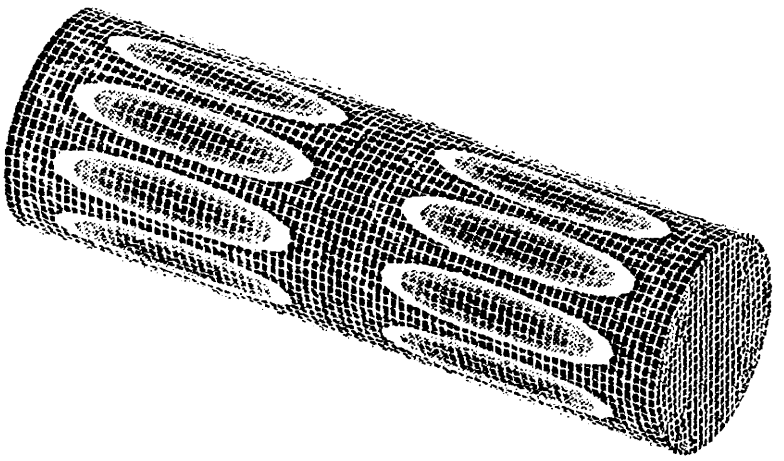

Figure 7.2 - Natural Mode of Ideal Stiffened Cylinder

7.1.2 Stiffener Modeling: Plates vs. Beams. A study was performed to determine if beam elements could be used to accurately model the Cessna fuselage stiffened (shell structure) dynamic behavior. Two stiffened panel models were generated, both composed of 7 frames and 7 stringers, with a resulting 36 bays or subpanels. Each model used the same CQUAD4 (plate) element mesh for the skin. One model utilized plate elements for the frame and stringers, while the other used CBEAM elements. A modal analysis was conducted with each model, and the resulting fundamental modes (frequency and mode shape) were compared to verify the ability of the beam/plate model to predict the modes of the all plate model. Three different modeling techniques were evaluated for the beams: (1) utilized the doubler areas in the inertia, neutral axis and shear center offset calculations of the beams, (2) utilized a portion of the skin thickness/width as well as the

doubler to compute the neutral axis, and (3) was the same as (1) except it neglected the shear center offset (still included the neutral axis offset however). Case (3) was evaluated to determine if shear center offsets could be ignored, as it was known that shear center offsets are not allowed in MSC/NASTRAN when performing a nonlinear analysis, and this nonlinear analysis was required to include the effects of pressure stiffening. Figure 7.3 shows a comparison of the fundamental mode predicted using the all plate model, and the beam/plate model using Case (3). It can be seen that good agreement in both shape and frequency was evident with these two modeling techniques for this "global" mode . It should also be noted, however, that although the global modes of these stiffened panels were accurately predicted with the beam/plate model, that the subpanel modes did not agree at all with the all plate model (these results are not shown). Two reasons for this are evident. First, neither the all plate or the beam/plate models had enough mesh fidelity to accurately predict the subpanel modes, and the beam elements do not produce the correct "stiffness footprint" which bounds the subpanels, leading to larger effective subpanel dimensions for the beam/plate model and lower predicted subpanel frequencies. The results of this study led to recommendations that the fuselage model be constructed using the beam/plate approach, that the shear center offsets be neglected so that the nonlinear solution can be conducted, that the doubler be included in the neutral axis and inertia calculations for each beam (and not included in the plate thickness), and that portions of the skin area not be included in these neutral axis and inertia calculations.

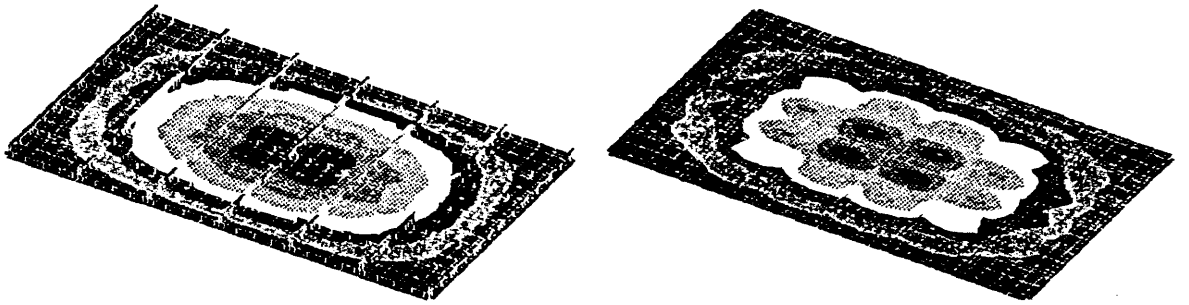

(a) Plate element only model
Fundamental mode at 81.0 Hz

(b) Plate and beam element model
Fundamental mode at 80.6 Hz

Figure 7.3 - Comparison of the First Two Natural Modes

7.1.3 Effects of Shell Membrane Stiffening Due to Cabin Pressure. A brief look at pressure stiffening effects on these stiffened shells was undertaken. The analysis was performed by applying the in-plane tensile loads due to pressurization to the flat stiffened panel of Figure 7.3, and also by applying the internal pressure loads to a quarter model of a stiffened cylinder. Both cases require a static nonlinear analysis to be performed as the first step, in which the nonlinear stiffness matrix is written to the database at the final converged load step. This is followed by a modal analysis in which the nonlinear stiffness is read from the database and used in conjunction with the mass matrix to compute the natural modes. In both cases, the frame and stringer (global) modes increased in frequency from 5-15 Hz, but the appearance of the first subpanel modes was increased in frequency by around 80 Hz. Again, the analysis is not considered accurate for the subpanel modes due to the lack of model fidelity. However, it is obvious that the pressure stiffening effect is very important, and must be included in the analysis when that static loading is present.

7.1.4 The Effect of Frame Cutouts. A quick study was performed to evaluate the effect on the global modes of holes cut in the frames at stringer-frame intersections, which allow the stringers to pass through without any discontinuity in the stringer. The flat stiffened panel model of Section 7.1.2 (Figure 7.3) was modified to include these holes, with the local effect on the model mesh shown in Figure 7.4. These holes (cutouts) were included at every stringer/frame intersection in this model, except at the outer boundary where the boundary conditions were applied. Table 7.1 contains the results of this study. It is evident that the cutouts had only a minor effect on the global modes. As a result of this study, no modifications were made to the Cessna fuselage model to account for frame cutouts.

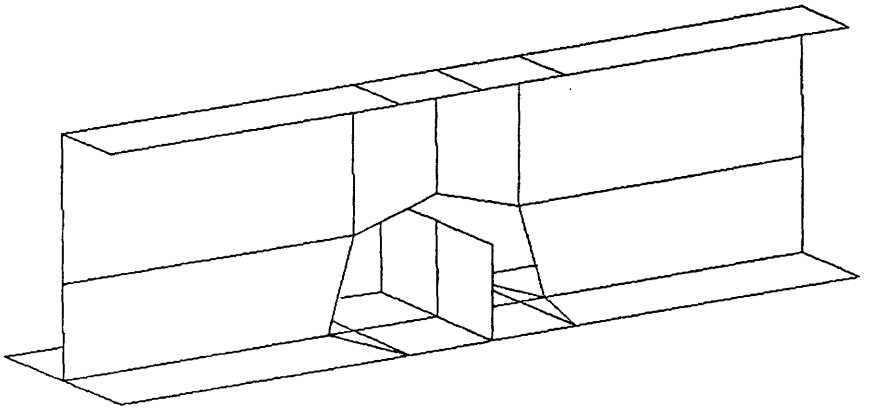

Figure 7.4 - Local Mesh modification to Account for Frame Cutouts

Table 7.1 - Comparison of Frequencies With and Without Frame Cutouts

Mode Number	Without Cutouts (Hz)	With Cutouts (Hz)
1	81.04	80.64
2	87.47	87.09
3	106.96	106.82
4	144.27	144.52

7.2 Model Description

Figure 7.5 illustrates the finite element and boundary element models used to predict the acoustic levels in the Cessna aircraft. This aircraft does not have wings or tail control surfaces, and thus are neglected from the structural model. The engines, which are tail mounted on the left and right sides, are represented in the model as concentrated masses at their respective centers of gravity. Rigid elements are used to connect in a spider-like fashion from the c.g. of each engine to its structural mounting points. As mentioned in the previous section, the structural FEM model is

developed using CQUAD4 and CTRIA3 NASTRAN plate elements, with CBEAMS used to model the frame and stringer stiffeners. In general, the fidelity of the structural model can be best described as having three grid points between each frame grid, and one grid point between each stringer grid. A direct frequency response solution is used to compute the structural velocity response in NASTRAN. Structural damping at 1% of critical is applied to the cylinder.

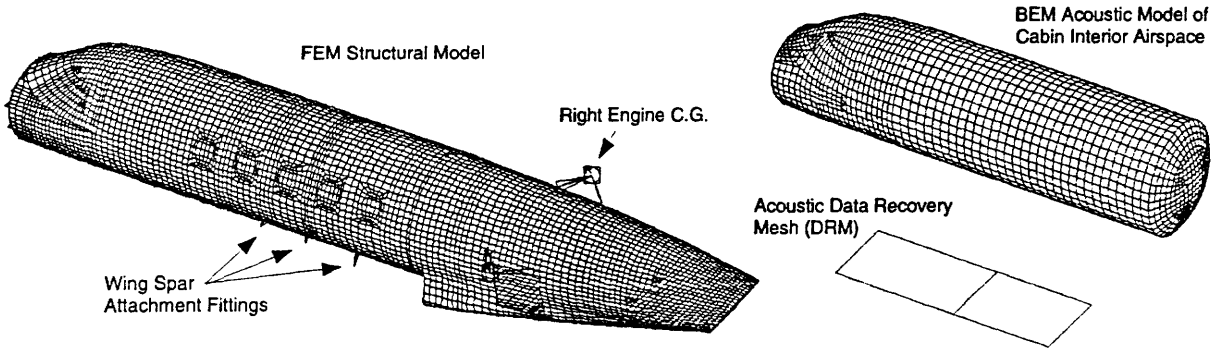

Figure 7.5 - FEM and BEM Models of the Cessna Citation III

The boundary conditions are different for the dynamic and static solutions. For the dynamic frequency response solution, the structure is free to move in the rigid body mode representing vertical (Y-direction) translation. Very large numerical masses, four orders of magnitude larger than the total fuselage mass, are used to "shake" the fuselage with an enforced velocity at the engine mounts of .15 inches/sec (peak). The two engine excitations are in the vertical direction, and are in phase with each other. The intent of this excitation is to simulate the n1 imbalance of the engine. This is a geared engine, and the actual n1 speed corresponds to a frequency of 350 Hz for the n1 rotor, but the fan speed is geared to 195 Hz. Thus the excitation velocity is enforced at 195 Hz. The actual spectrum of the excitation is assumed to be constant in magnitude above and below 195 Hz, so that the optimization is not allowed to simply shift troublesome structural modes away from the 195 Hz frequency. As for the linear static (structural integrity) stress solutions, the structure is grounded at the wing spar attachment fittings, shown in the figure. Thus the structure tends to bend about the wing attachments points.

A MSC/NASTRAN DMAP was written to solve a technical difficulty caused by the enforced motion dynamic solution. The large masses must be subtracted from the true mass of the structure when the weight constraint optimizer option is turned on. The DMAP subtracts this mass, and maintains numerical accuracy of the true weight of the structure. Prior to this DMAP, the total weight was printed from NASTRAN including the large masses, and an accurate true weight of the structure was lost due to the number of significant figures in the print format.

The effects of pressurization of the aircraft fuselage are of interest in this study. Internal pressurization, usually of the order of 10 psi differential between the inside and outside of the fuselage, results in membrane stiffening of the aircraft skins, a nonlinear effect. Thus the subpanel modes, whose wavelength corresponds to the dimensions of the panels bounded by the frames and stringers, are greatly affected by this pressurization stiffening. The effect can be as much as a

doubling of the subpanel frequency. In order to quantify this affect, nonlinear MSC/NASTRAN Solution 106 is used which includes the nonlinear terms in the strain-displacement relations resulting in geometric nonlinearities. The model is loaded with the static internal pressure, and the resultant nonlinear stiffness matrix at the final load step is saved on a database. The dynamic solutions (modes and frequency response) read the nonlinear stiffness matrix from the database and incorporate it with the computed mass matrix to compute solutions. Note that in order to properly ground the fuselage model for the nonlinear static solution, but yet still allow rigid body motion in the dynamic solution (the boundary conditions for the nonlinear static stiffness and dynamic solutions must be the same), weak springs on the order of 10 lb/in are used to connect the two engine c.g. grid points to ground. These springs result in very low "rigid body" natural frequencies which do not couple with the dynamic response at 195 Hz.

Figure 7.5 also illustrates the BEM boundary element mesh and data recovery interior mesh. The boundary element mesh density was set to handle the wavelengths appropriate for an analysis frequency of 200 Hz or less. The data recovery mesh is very coarse, with each node point corresponding to a passenger head location located in the cabin. The pilot head locations were not included in the data recovery mesh. These six locations are the points where the acoustic objective function is evaluated. The acoustic boundary conditions are the normal velocities of the bounding fuselage walls. The fuselage walls are considered untrimmed; no acoustic treatment boundary conditions are included in the model, and no global acoustic damping is used. The structural acoustic formulation utilized here is uncoupled (one-way coupled), and thus the structural velocities which become the boundary conditions for the acoustic model are solved separately from the acoustic solution.

7.3 Modal/Response Survey

As part of a model checkout, a survey of the velocity responses of the fuselage FEM model to the 195 Hz vertical shaking excitation was performed. This was done along with a modal survey of the structure to determine the modal density and wavelength characteristics in the frequency range of 195 Hz. Of concern was the appearance of subpanel modes in this frequency range, which the model did not have the fidelity to handle, and for which the beam elements did not give a correct solution.

Figure 7.6 shows the shell velocity response at 195 Hz, in the unpressurized state. This response is dominated by subpanel modes, and thus its accuracy is in question. This frequency is thus too high for the model, as the subpanel modal responses are dominant in this range. In addition, these kinds of responses are not long enough in wavelength to be affected by design changes to the stiffeners. Longer wavelength modes which are really stringer/frame modes, are the target for the optimization. Thus, it was decided that the unpressurized model was inappropriate for the 195 Hz excitation, and the frequency of excitation needed to be reduced. Figure 7.7 shows the velocity response of the model at 108 Hz. This contains large wavelength behavior, sprinkled with some subpanel responses. It was decided to choose the frequency range of 105-115 Hz for the excitation for the unpressurized study. This reduces the interest in the results of this study, as the actual n1 fan speed is at 195 Hz. However, the model is more accurate in this range. Figure 7.8 is a contour of the natural mode shape at 108.1 Hz, which is very similar to the velocity response contour at 108 Hz.

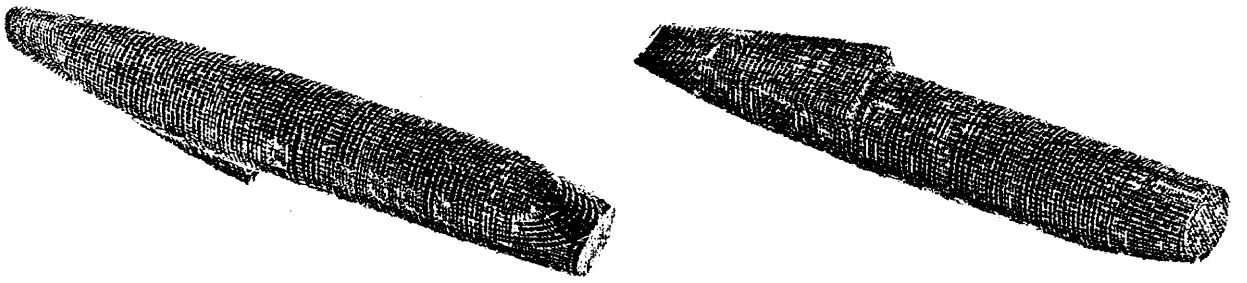

Figure 7.6 - Unpressurized Model, Shell Velocity Response at 195 Hz

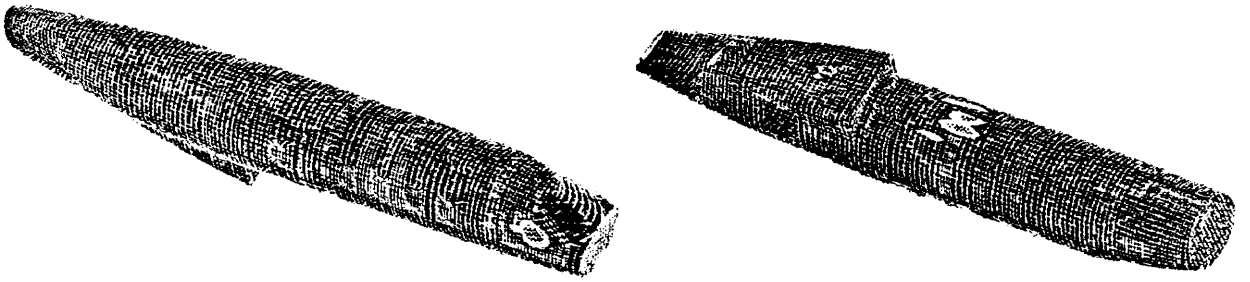

Figure 7.7 - Unpressurized Model, Shell Velocity Response at 108 Hz

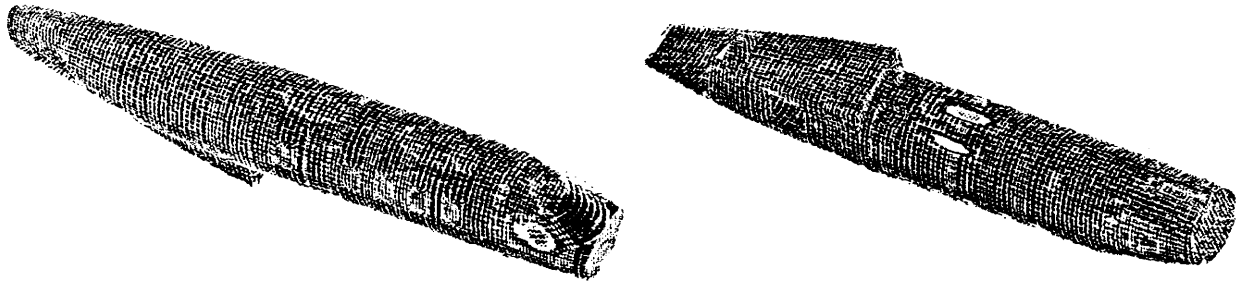

Figure 7.8 - Unpressurized Model, Mode Shape at 108.1 Hz

In Figure 7.9, the velocity response of the fuselage FEM model to the 195 Hz vertical shaking excitation of the pressurized model is presented. Note that only the cabin section is pressurized, not the tail. Figure 7.10 presents the natural mode shape at 196.5 Hz of the pressurized model, which is closest in frequency to the 195 Hz excitation. It is evident that the subpanel behavior is absent from the pressurized cabin walls as expected, but is still present in the unpressurized tail section. This subpanel modal behavior in the tail is a source of possible inacurracy. As the wavelengths of the responses/modes in the pressurized cabin walls are indicative of stringer/frame modes (longer wavelengths), then the model is considered much more accurate (than the unpressurized solution) and also more suitable for stiffener design optimization. As the majority of flight conditions are in the pressurized state, then this pressurized study at 195 Hz, should be of great interest.

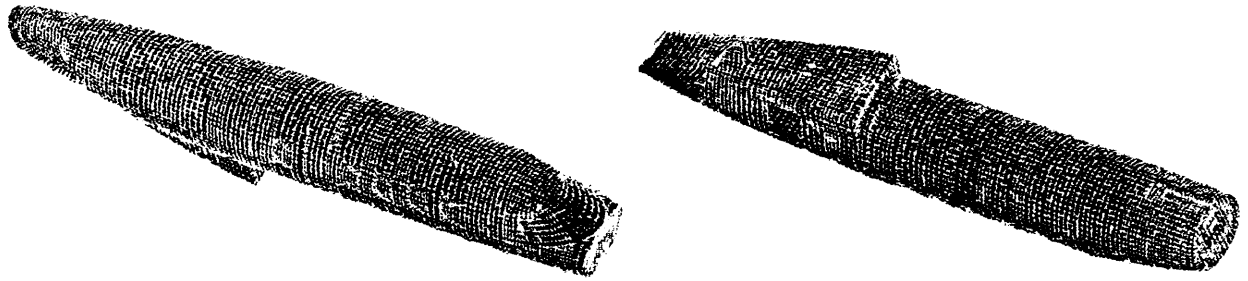

Figure 7.9 - Pressurized Model, Shell Velocity Response at 195 Hz

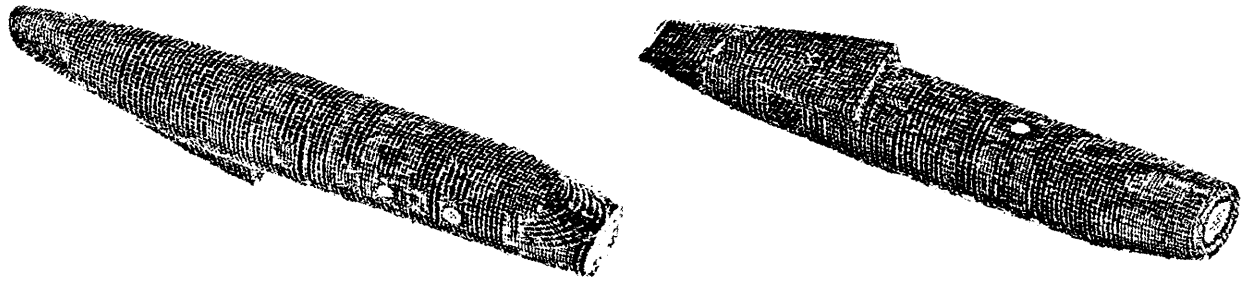

Figure 7.10 - Pressurized Model, Mode Shape at 196.5 Hz

The COMET/Acoustics BEM acoustics model was utilized by itself to determine if any acoustic natural modes exist within the frequency ranges of study. A detailed frequency sweep was performed using an internal monopole source off of the centerline. For the 190-200 Hz range, the sweep did not identify a single strong resonance frequency in the cabin. Between 194 and 195 Hz, different points within the cabin peaked at different frequencies. A fixed frequency for objective function evaluation was selected at 194.5 Hz, based on these results. For the 105-115 Hz range, there was a strong resonance at 111.0 Hz. Thus a fixed frequency corresponding to an acoustic mode was selected for objective function evaluation at 111.0 Hz in the unpressurized case.

A brief acoustic "panel" contribution study was performed to guide in the selection of design variables to be used in the optimization. This analysis capability is available within COMET/Acoustics, and for the fuselage would potentially locate groups of BEM elements in the acoustic model (panels) which strongly affect the data recovery acoustic responses at the passengers head locations. The "effective" panel contribution solution was utilized, which is formulated such that if the surface velocity of a particular panel is zero, the contribution of that panel is zero. This acoustic solution would indicate areas where a reduction of surface velocity coming from the structure would result in significant reduction in acoustic levels at the data recovery points. After post processing several of these panel sensitivity solutions, it was determined that stiffener design variables would be required over the entire cabin walls, as there was not a particular location which consistently had high sensitivity. Thus it was not feasible to isolate the design variables to a specific area of the fuselage, as it was hoped would be learned from the panel study.

In setting up the multi-frequency optimization analyses, it was noted that there were as many as 20 structural modes in the frequency ranges under study (105-115 Hz for the unpressurized

model, and 190-200 Hz for the pressurized model). Since the multi-frequency algorithm chooses the natural frequencies in the selected range as excitation/response frequencies, then each of these 20 eigenfrequencies would require an objective function evaluation. However, after surveying the velocity responses and modal behavior, it was noted that many of these modes did not have significant strain energy in the cabin walls, but involved mainly responses of the tail section. It was decided to screen out these tail section modal frequencies from the frequency list of objective function evaluations. This was done using a modal strain energy approach, in which the modal strain energy of the elements in the cabin walls was computed, and ratioed to the total strain energy of all the elements in the model. For any modes in which this ratio was greater than or equal to 0.20, its eigenfrequency was retained in the objective function evaluation list. The others were deleted from the list. In MSC/NASTRAN, this was handled for the unpressurized runs by simply requesting strain energy output in the solution for natural modes. For the pressurized case, computation of modal strain energy from a nonlinear stiffness matrix is not supported. This was resolved by writing a DMAP (Direct Matrix Abstract Program) alter to the NASTRAN modes solution, which computed the linear stiffness, and read in the nonlinear eigenvectors computed from a previous modes solution. It then computes the approximate strain energy using the linear stiffness (K_L) and the nonlinear eigenvectors (U_{NL}), as shown in Equation 7.1.

$$S.E. = 1/2\ K_L\ U_{NL}^2 \tag{7.1}$$

It has been found that the use of this approximate nonlinear strain energy screening technique, used only to screen out modes with low strain energy in the cabin walls from the objective function evaluation list, is an effective tool. Many mode shapes were plotted and studied along with their approximate nonlinear strain energy, to evaluate the desired screening responses of this tool.

7.4 Optimization Case Description

A MSC/NASTRAN structural design model, consisting of 34 design variables was created. The design variables are linear scale factors of the beam element cross section sizes, and design equations were input to relate these scale factors to the section properties (area, I1, I2, I12, J). A scale factor for a particular beam element cross section, S, is related to the areas and inertias as:

$$Area_{new} = S^2\ Area_{old} \tag{7.2}$$

$$I_{new} = S^4\ I_{old} \tag{7.3}$$

This type of design variable was selected for simplicity, as the beam properties were supplied from Cessna as areas and inertias, and the original cross section shapes were not known. It should be noted that this design variable to property relation ignores changes in the neutral axis offset. It was decided that this was an acceptable approximation. Initially, a design variable was created for each beam cross section property. Linking equations were written in NASTRAN to group the design variables so that a single variable controls the size of either a single stringer or a localized group of stringers, and likewise for the frames. SDRC/IDEAS was used to renumber the elements of the model supplied by Cessna to facilitate this grouping, and a FORTRAN code was written to per-

form various sorting functions and generate the necessary NASTRAN input cards related to design variables, design equations, design linking, and sensitivity response.

The "acoustic" optimization formulation was utilized, whose objective is to minimize the sum of squared acoustic pressures at the data recovery points (passenger head locations) with constraints on weight. Cases were included with constraints on structural integrity, and all had upper and lower bound side constraints on the design variable ranges. Cases with and without static cabin pressure were included as well.

Checkouts were performed of the NASTRAN structural model including the design model, and system scratch disk space limitations were discovered due to the number of design sensitivity responses required. Reducing the number of design variables seemed to be the only solution, as the number of velocity responses is fixed by the number of elements bounding the acoustic interior cavity. A plan was formulated to run the COMPLEX algorithm initially with the 34 design variables, since this optimizer does not require sensitivity computation. Information from this run concerning dominant design variables were to be used to reduce the design variable count and a more focused second run to be made using CONMIN. Note that this second CONMIN run could only be made for unpressurized (linear) solutions, as sensitivities can only be computed in NASTRAN from a linear solution. This second CONMIN run was never made, due to time constraints on the project.

Considerable development was required for the structural integrity (stress constraint) NASTRAN model. Six load cases, consisting of an upbending load, downbending load, and a side bending load, all three with and without internal pressure, were applied. These loads represent an envelope of the worst cases. Buckling of the fuselage due to these load cases was not considered, as Cessna felt that this was not an important design driver for this length of fuselage. Initial linear stress analysis using these load cases revealed very high bending stresses in the skin (quad) elements, mainly due to the pressure loading. In contrast, the nonlinear static solution for the pressure loading results in very little bending through the skin thickness, as the load is carried mainly in membrane stress. The linear stress computation at the midplane of the plate elements, which do not include bending stresses, were very similar to the nonlinear solution. It was decided to utilize only the linear midplane (membrane) stresses in the plate elements, and ignore the linear bending stresses in these elements.

Extensive discussions/analysis occurred with Cessna, concerning how to handle the compression of plate elements (in panels which buckle under low compressive stresses) in linear stress analysis. The normal industry practice is to modify the NASTRAN CQUAD4 elements so that their membrane stiffness is removed, such as replacing them with CSHEAR elements. This is a manual operation, which cannot be performed in an automated optimization loop. Instead of modifying the stiffness of these elements, it was decided to reduce the effective allowables of the neighboring stringer beam elements. As a result, Cessna provided local effective compression allowables for the stringer beam elements, which adjust the ultimate compression/crippling allowable of the beams, due to the presence of the skin elements which buckle at low compressive stress levels. Cessna also provided modifications to the beam elements in the NASTRAN model to include stress computation points on the cross sections. Elements representing the wing spar attachment fittings were also added to the model in order to apply restraints to ground at those locations without locally overstressing the model. This change significantly reduced the number of element stresses that were exceeding allowables, but several problem areas remained where minor stress exceedance still occurred. It was decided that for expedience, the state of the current

baseline (unmodified) model would be considered good from a stress viewpoint, and thus any element stress that was within 90% or greater than its local allowable, that element's allowable was bumped up to 1.15 times the baseline element stress. This allowed the optimizer to accept the baseline design as a feasible point, and gave some design freedom to change the model. It was felt that due to the conservatism discovered in the linear stress analysis, which results in excessive bending in some areas, that this increase in allowable was acceptable. In addition, it should be noted that the structural integrity analysis performed within the optimization will be at a preliminary design level, and thus a detailed stress analysis must be done in the appropriate stress group following any design changes recommended by this acoustic optimization methodology.

Table 7.2 summarizes the six optimization cases studied in this project for the Cessna aircraft model. Note that Cases 1 and 2 are single frequency optimizations. In Cases 1-4, the design variables were allowed to vary +/- 20%, but when structural integrity (stress) constraints were applied, these bounds had to be tightened. For the integrity constraint cases, the design variable bounds used were 0.95 - 1.1. Since the median of this range was no longer centered at the starting point of 1.0, then the weight constraint was relieved a little, and the total fuselage weight was allowed to increase 3%. It should be noted that the elements representing the wing spar attachment fittings were added to the model for Cases 5 and 6 only.

Table 7.2 - Design Optimization Cases for Cessna Model

Case	Frequency (Hz)	Design Variable Bounds	Weight Constraint	Integrity Constraints	Pressurized?
1	110	0.8 - 1.2	0% Increase	None	No
2	195	0.8 - 1.2	0% Increase	None	Yes
3	105 - 115	0.8 - 1.2	0% Increase	None	No
4	190 - 200	0.8 - 1.2	0% Increase	None	Yes
5	105 - 115	0.95 - 1.1	+3% Increase	Yes	No
6	190 - 200	0.95 - 1.1	+3% Increase	Yes	Yes

7.5 Optimization Results

The following sections present the results for each of the optimization cases in Table 7.2. For each case the reduction in acoustic objective function, the change in weight, shell normal velocity contours and acoustic contours of the data recovery points (single frequency cases only), the acoustic spectra (for multi-frequency cases), and the final design contours are discussed.

7.5.1 Case 1 - Single Frequency, Weight Constraint, Unpressurized. The acoustic objective was reduced from the initial level for this case by 5.9 dB. The weight at the best optimal design was 99.6% of the initial weight. Figures 7.11 and 7.12 compare the shell normal velocity magnitudes before and after optimization (plotted on the same normalized scale). In these figures, it is not readily evident that the optimized velocities are better for noise reduction. In fact, the velocity magnitudes are locally larger for the optimized case. What is evident is a slight redistribution of the velocity contours. It is noted also the strong presence of subpanel response in a ring near the cockpit. This is a source of inaccuracy in the model at this unpressurized frequency. Figure 7.13

presents acoustic contours of the acoustic pressures at the six passenger head locations, before and after optimization. It is evident that the acoustic responses have changed in shape as well as overall levels. In Figure 7.14, a pictorial representation of the locations of the stiffeners which were selected as design variables is given. The red color indicates the locations of these stiffeners. Since the design variables are the same for all cases, this figure applies to all cases, and will not be repeated. Figure 7.15 shows contours of the optimum design variable values (stiffener scale factors), which gives an indication of relative changes to the stiffening. In this figure it is evident that the front bulkhead and frames near the nose have been stiffened, and frames from the mid-fuselage to the rear have been softened. The velocity responses in Figures 7.11 and 7.12 reflect these changes through higher responses near the rear floor. Changes to the front bulkhead reponses are not evident in the figures, as they are probably too low to show up in the contours.

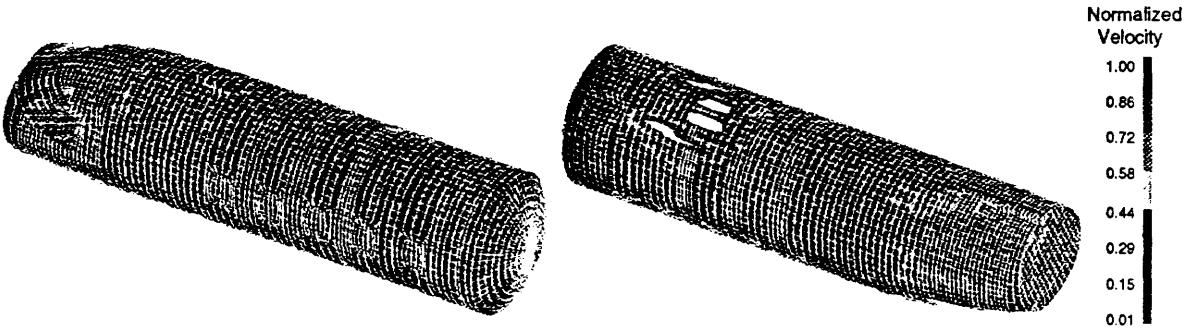

Figure 7.11 - Case 1 - Contours of the Velocities Before Optimization

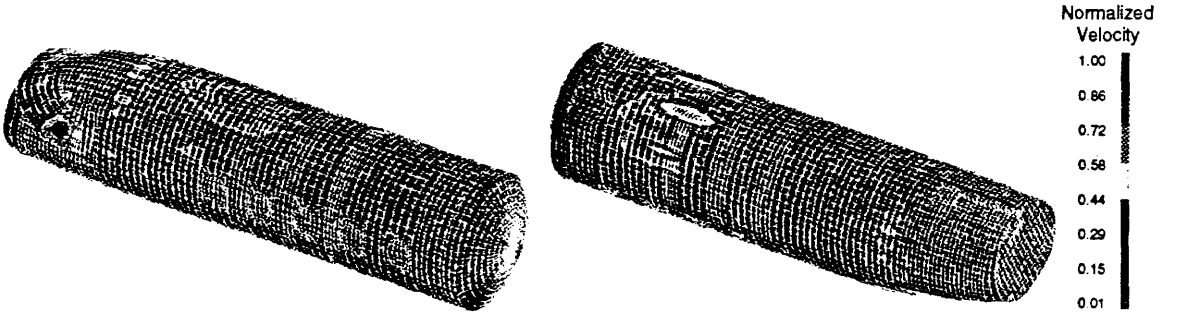

Figure 7.12 - Case 1 - Contours of the Velocities After Optimization

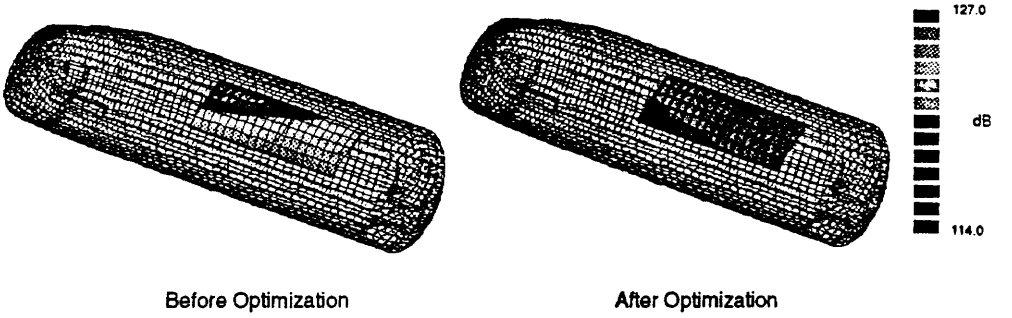

Figure 7.13 - Case 1 - Contours of the Acoustic Pressures at the Passenger Head Locations

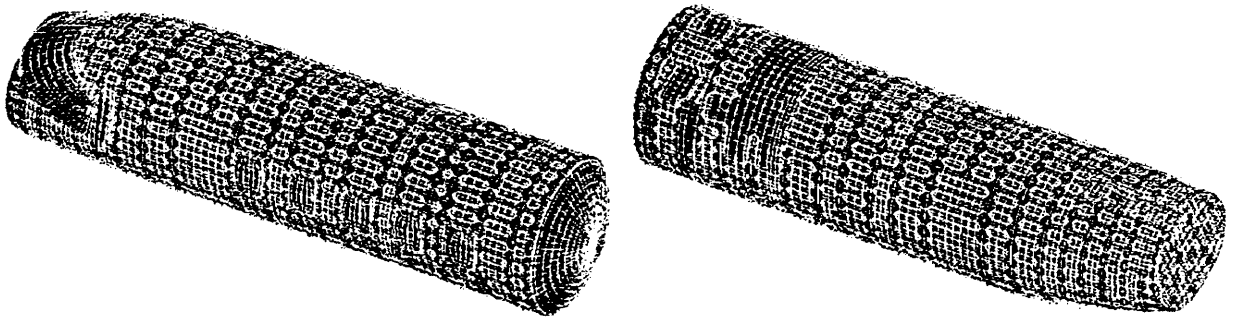

Figure 7.14 - Contours of the Original Design State

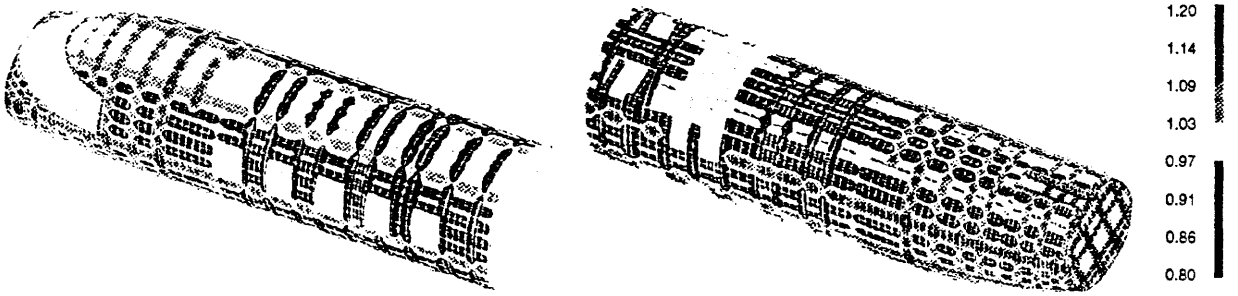

Figure 7.15 - Case 1 - Contours of the Optimum Design Variable Scale Factors

7.5.2 Case 2 - Single Frequency, Weight Constraint, Pressurized. The acoustic objective was reduced from the initial level for this case by 7.5 dB. The weight at the best optimal design was 99.6% of the initial weight. Figures 7.16 and 7.17 compare the shell normal velocity magnitudes before and after optimization (plotted on the same normalized scale). It is evident that the velocities have been reduced at the front bulkhead for the optimal case. Other changes, before and after optimization, other than a minor reshaping of the contours, are not apparent. Note, however, that these velocity contours involve much more global motion than was seen in the previous unpressurized case. This type of global motion, indicative of longer wavelength modal behavior, is the type of response that this low frequency optimization is expected to improve. It is expected that the pressurized cases, therefore, will have higher noise reduction than the unpressurized cases. Figure 7.18 presents acoustic contours of the acoustic pressures at the six passenger head locations, before and after optimization. Once again, it is evident that the acoustic responses have changed in shape as well as overall levels. Figure 7.19 shows contours of the optimum design variable values. In this case, the stiffeners on the bulkhead were reduced slightly, and moving aft from the nose, there is an alternating stiffening and softening of the frames. A similar alternating behavior is evident in the stringers as well.

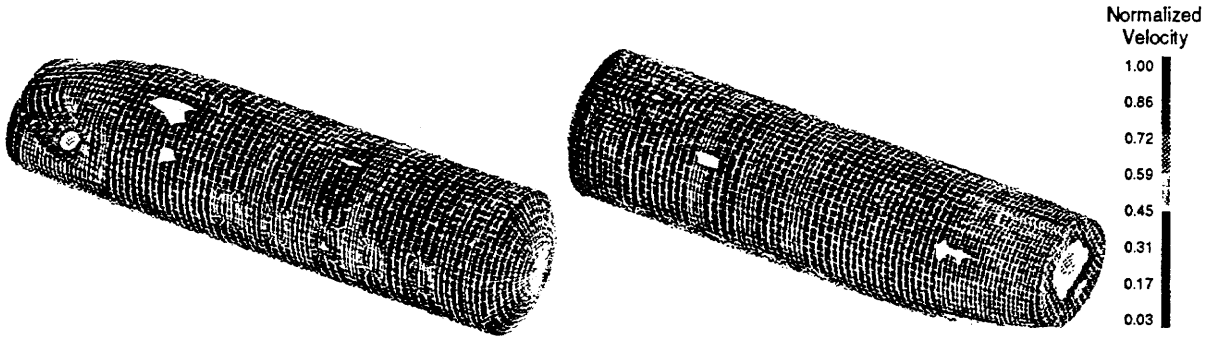

Figure 7.16 - Case 2 - Contours of the Velocities Before Optimization

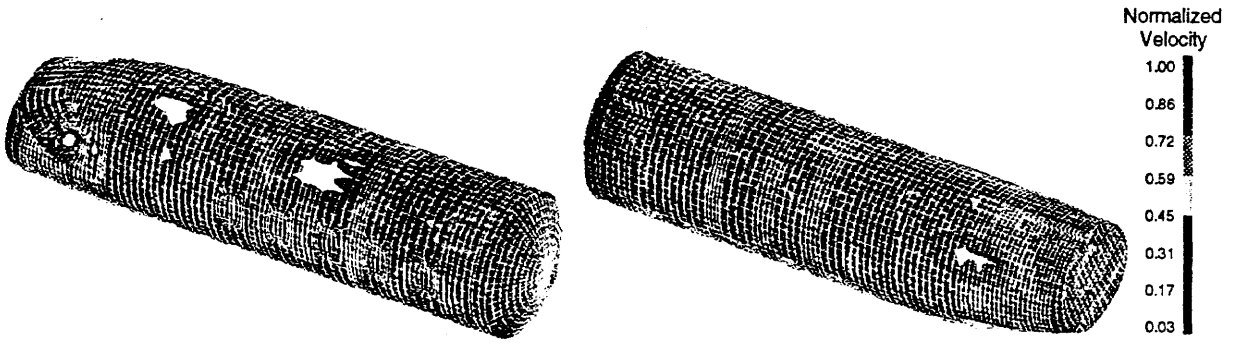

Figure 7.17 - Case 2 - Contours of the Velocities After Optimization

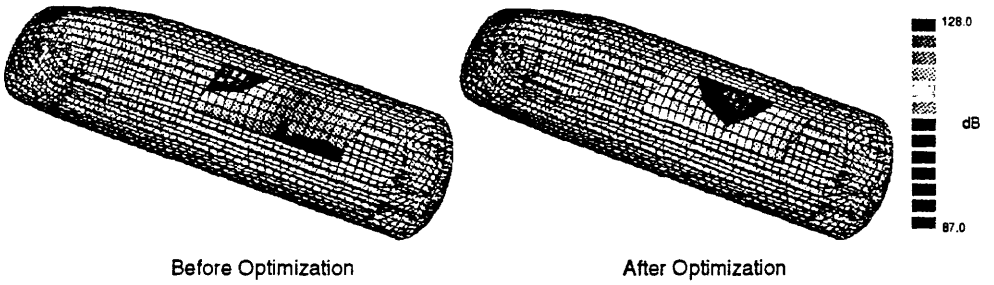

Figure 7.18 - Case 2 - Contours of the Acoustic Pressures at the Passenger Head Locations

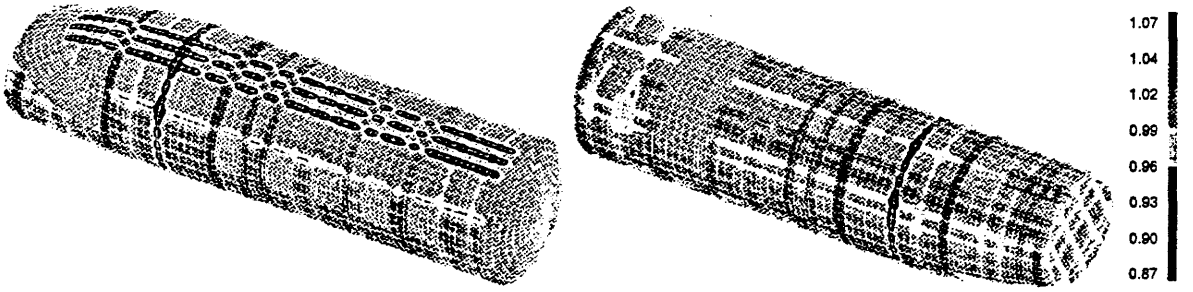

Figure 7.19 - Case 2 - Contours of the Optimum Design Variable Scale Factors

7.5.3 Case 3 - Multi-Frequency, Weight Constraint, Unpressurized. The acoustic objective was reduced from the initial level by a maximum of 4.7 dB, and the design state corresponding to this is labelled the "best design". The weight at this design was 98.6% of the initial weight. Figure 7.20 contains six acoustic spectra plots, one for each data recovery point in the model, which correspond to the six passenger head locations. Within each plot, the initial spectrum is compared to the three best optimal design spectra. From a review of these plots, it is evident that the best design has reduced levels for the first peak in all six locations. However, overall the improvement is not dramatic. Figure 7.21 shows contours of the optimum design variable values (stiffener scale factors) for the best design. In this design, the stiffener scale factors on the nose are increased (stiffened), followed by alternating stiffening and softening of the frames moving aft from the nose. The stringers have an alternating stiffening and softening behavior, but it tends to occur in larger groupings than the frames.

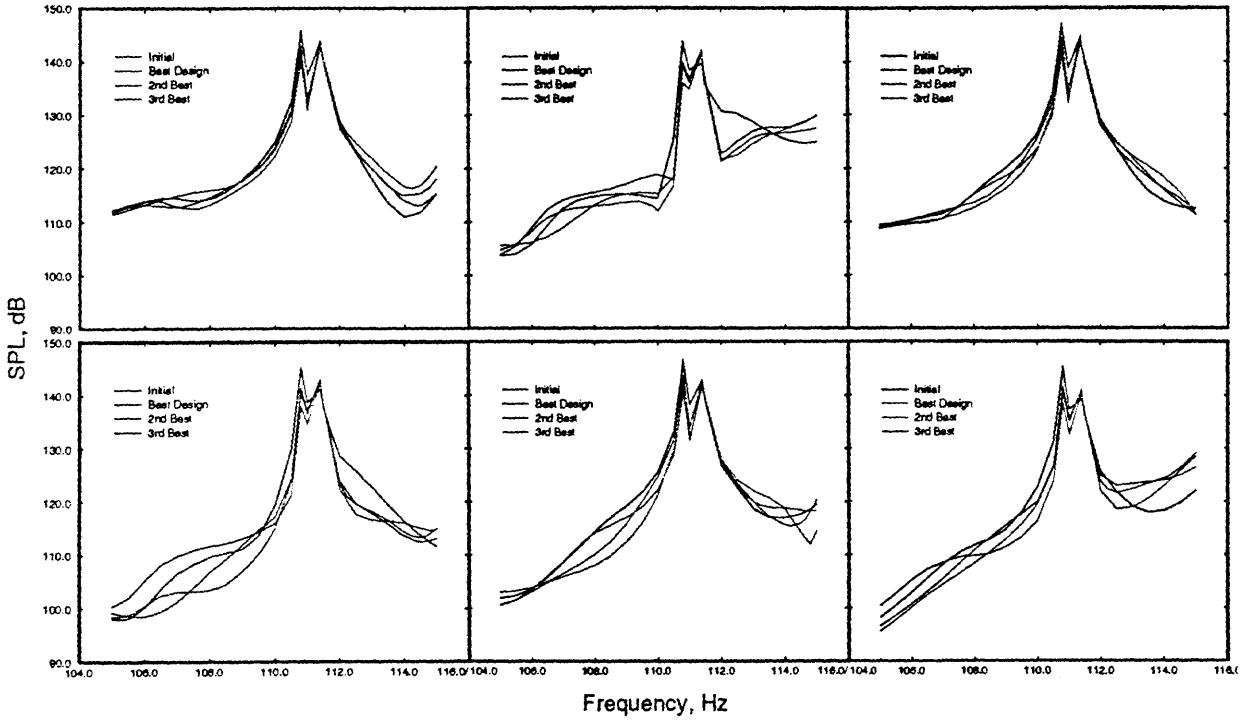

Figure 7.20 - Case 3 - Comparisons of the Acoustic Spectra for the Top Three Designs at the Six Passenger Head Locations

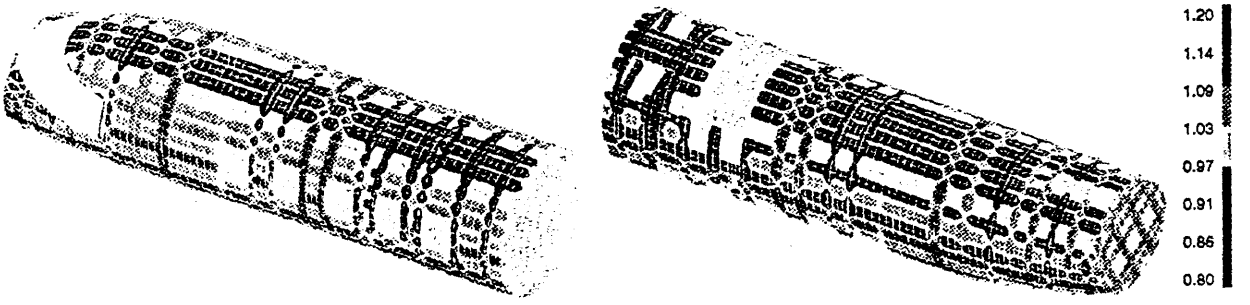

Figure 7.21 - Case 3 - Contours of the Optimum Design Variable Scale Factors

7.5.4 Case 4 - Multi-Frequency, Weight Constraint, Pressurized. The acoustic objective was reduced from the initial level for this case by 6.3 dB for the best optimized design (highest reduction of objective). The weight at the best design was 99.4% of the initial weight. Figure 7.22 contains the acoustic spectra plots for the initial and three best designs, at each of the six passenger head locations. In these plots it is discovered that the best design actually has a slightly higher reponse than the initial at two of the passenger locations. However, the 2nd best design has noticeable reduction in all locations. The overall reduction for the 2nd best design was 6.1 dB, with a final weight of 98.7% of the initial weight. Figure 7.23 shows contours of the optimum design variable values for the best design. In this design, the stiffener scale factors on the nose are decreased (softened), followed by alternating stiffening and softening of the frames moving aft from the nose. The stringers again have an alternating stiffening and softening behavior, but it tends to occur in larger groupings than the frames.

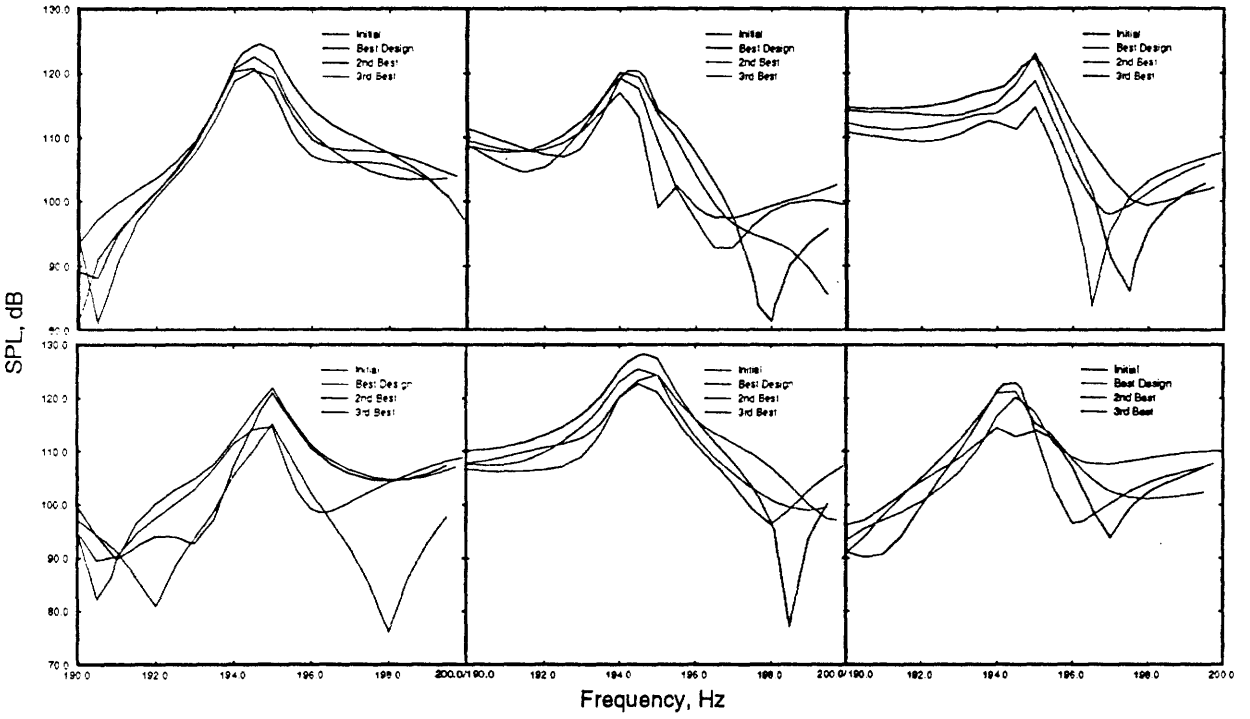

Figure 7.22 - Case 4 - Comparisons of the Acoustic Spectra for the Top Three Designs at the Six Passenger Head Locations

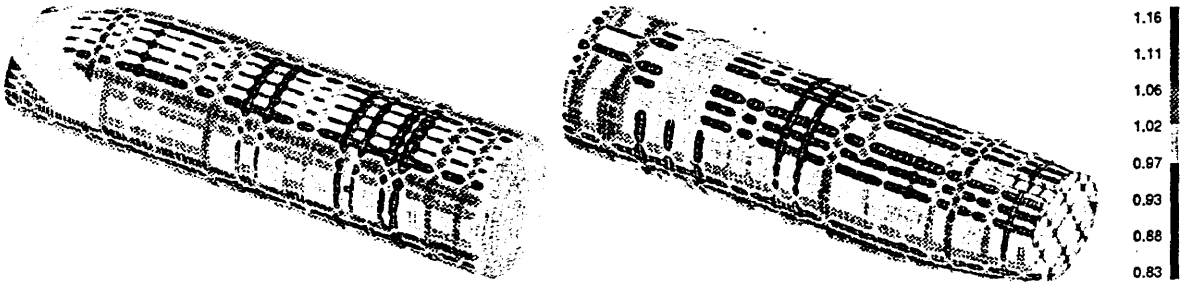

Figure 7.23 - Case 4 - Contours of the Optimum Design Variable Scale Factors

7.5.5 Case 5 - Multi-Frequency, Weight Constraint, Integrity Constraints, Unpressurized. The acoustic objective was reduced from the initial level for this case by 1.5 dB for the best optimized design. The weight at the best design was 101.7% of the initial weight, even though the constraint allowed a possible 3% weight increase. Figure 7.24 contains the acoustic spectra plots for the initial and three best designs, at each of the six passenger head locations. Due to the tightening of the design variable bounds, and the addition of the stress constraints, very little improvement is noticed for this case. Figure 7.25 shows contours of the optimum design variable values for the best design. Similar design trends as in Case 3 are noticed here, except for much smaller design variable scale factors. Once again, stiffening is noticed on the front bulkhead, followed by alternating stiffening and softening.

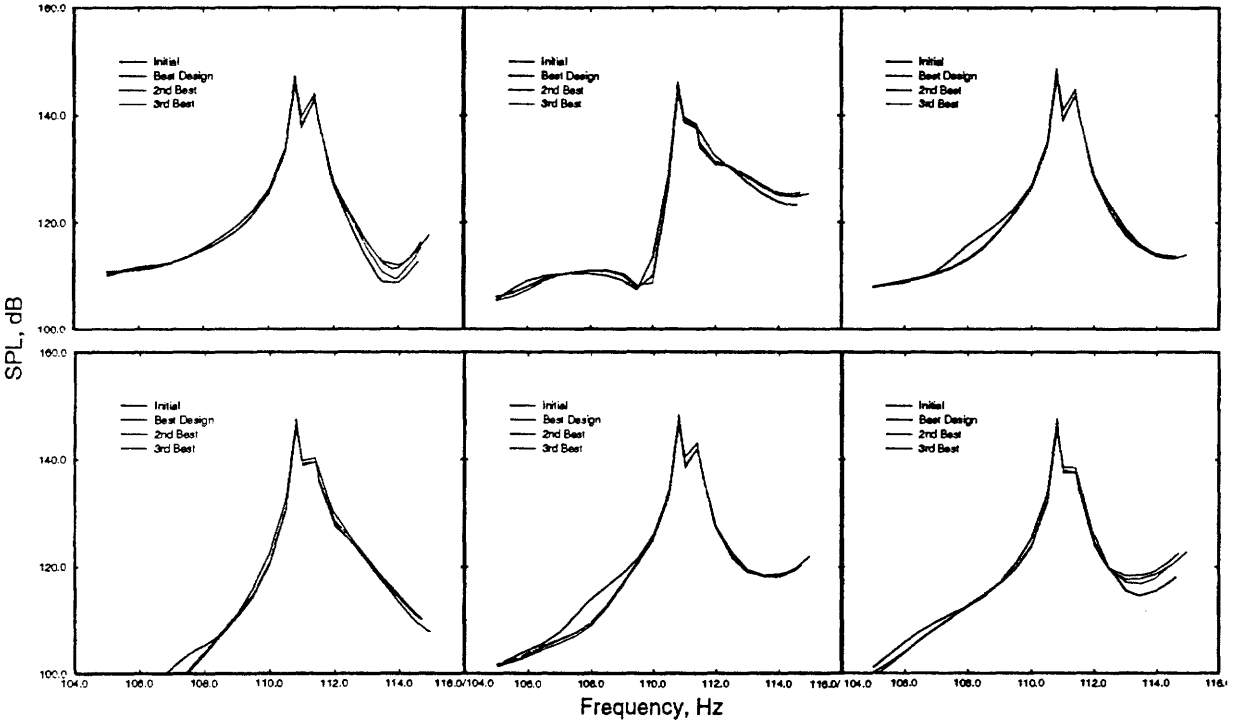

Figure 7.24 - Case 5 - Comparisons of the Acoustic Spectra for the Top Three Designs at the Six Passenger Head Locations

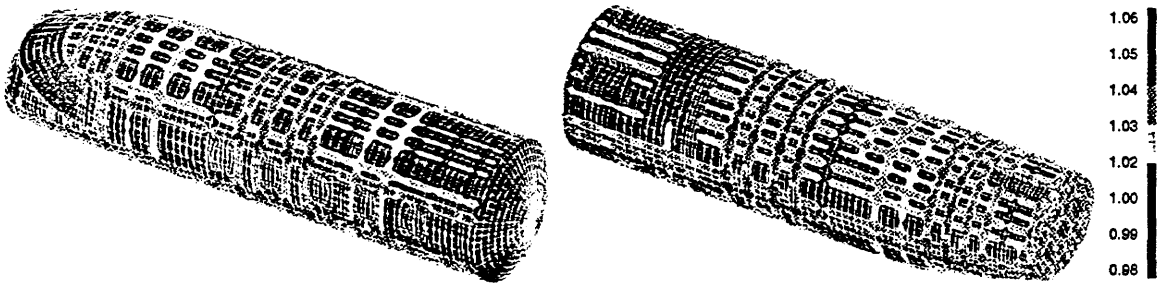

Figure 7.25 - Case 5 - Contours of the Optimum Design Variable Scale Factors

7.5.6 Case 6 - Multi-Frequency, Weight Constraint, Integrity Constraints, Pressurized. The acoustic objective was reduced from the initial level for this case by 5.0 dB for the best optimized design. The weight at the best design was 101.7% of the initial weight, even though the constraint allowed a possible 3% weight increase. Figure 7.26 contains the acoustic spectra plots for the initial and three best designs, at each of the six passenger head locations. In this case, the best design showed noticeable reduction in the peak response for all six locations. Figure 7.27 shows contours of the optimum design variable values for the best design. Similar to Case 4, the stiffener scale factors on the nose are slightly decreased (softened), followed by alternating stiffening and softening of the frames moving aft from the nose. The stringers again have an alternating stiffening and softening behavior.

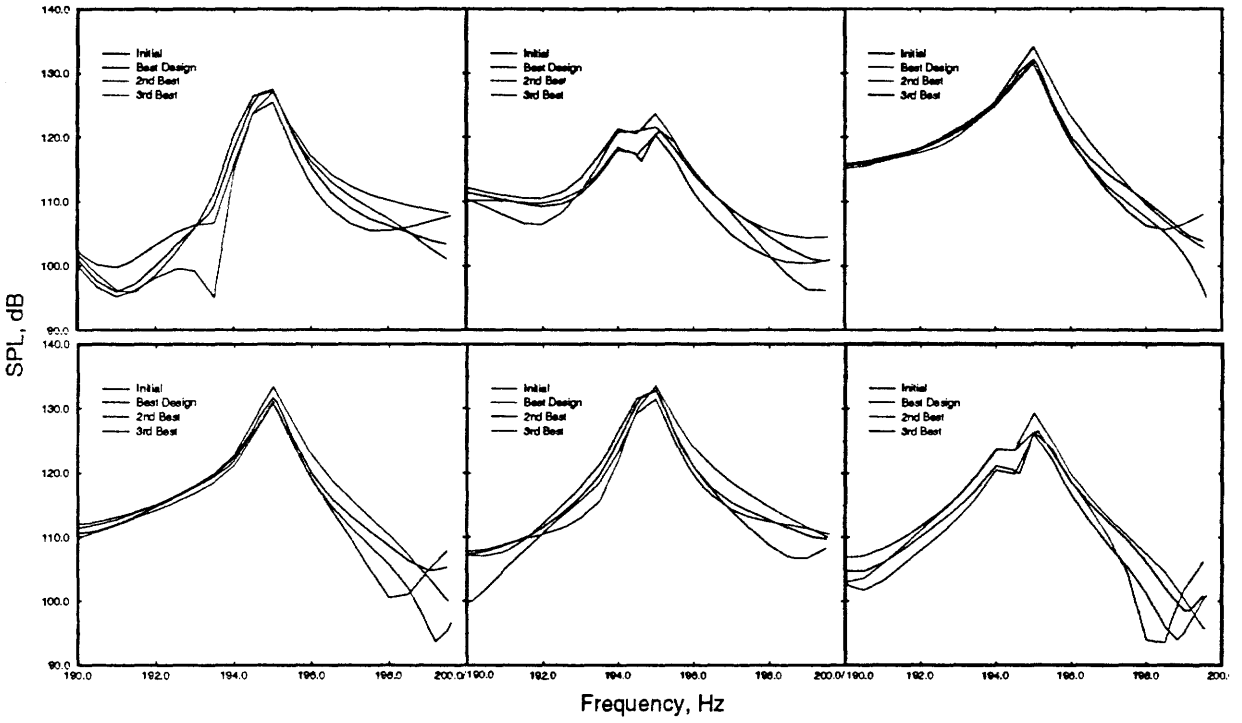

Figure 7.26 - Case 6 - Comparisons of the Acoustic Spectra for the Top Three Designs at the Six Passenger Head Locations

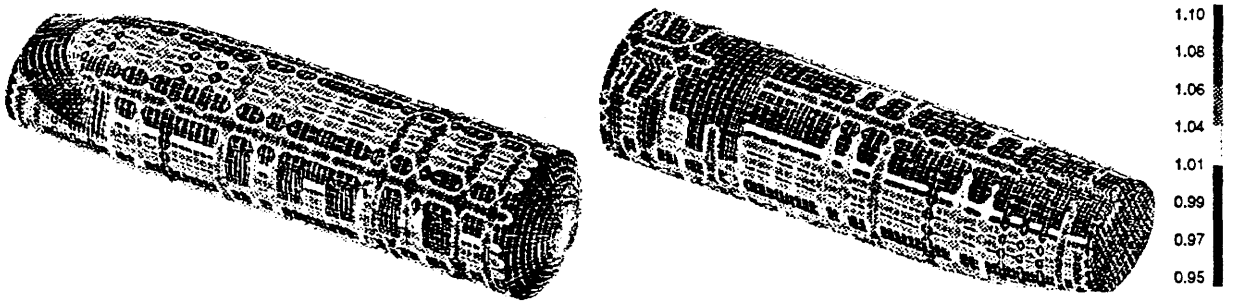

Figure 7.27 - Case 6 - Contours of the Optimum Design Variable Scale Factors

7.5.7 Discussion of Cessna Model Results. In this subsection, the results of the Cessna optimization study are discussed. To facilitate this discussion, Table 7.3 presents a summary of the reductions in objective function from the original design (for each case), and % of initial weight for the three best designs of Cases 3-6. The single frequency results are not included, as they are considered of less interest.

Table 7.3 - Summary of Design Optimization Results for Cessna Model

Case	Design	dB Reduction of Objective Function	% of Initial Weight
3	Best	4.7	98.6
3	2nd Best	3.8	97.3
3	3rd Best	3.6	98.6
4	Best	6.3	99.4
4	2nd Best	6.1	98.7
4	3rd Best	5.6	99.9
5	Best	1.5	101.7
5	2nd Best	1.4	101.8
5	3rd Best	1.3	101.8
6	Best	5.0	101.7
6	2nd Best	4.5	101.3
6	3rd Best	3.5	101.1

It is evident from Table 7.3 that the pressurized cases (4 and 6) achieved much more noise reduction than the unpressurized cases. This is as expected, as the velocity responses of the pressurized fuselage were more global in nature, characterized by stiffened shell modal response. Many of the responses in the unpressurized cases included subpanel (skin) modes, which were too short in wavelength for the fidelity and element selection of the model, and were not easily affected by sizing of the stringer and frames. Even in the 105-115 Hz frequency range, the unpressurized model lacked both fidelity in skin elements between stringers and frames, and required plate elements in the stiffeners as opposed to beams. Recall from Section 7.1.2 that the beam stiffened panels did not predict the subpanel modal behavior accurately.

As for Cases 5 and 6, involving structural integrity (stress) constraints, more development work is needed to apply these constraints accurately. To account for panel buckling (and loss of membrane stiffness), stiffener crippling, and other local effects, the local allowables were adjusted to the point that they were very conservative. In addition, to reduce the multiple real load cases to six required an "enveloping" of the worst loading conditions. This resulted in additional conservatism. Use of the linear static solution to predict the stresses due to pressurization added inaccuracy, as this solution predicted very high bending stresses on the outer and inner surfaces of the plate elements. These are unrealistic, as most of this pressure load actually results in membrane stress. A comparison of the linear and nonlinear solutions using this pressure loading resulted in the use of the mid-surface principal stresses instead of the bending stresses at the outer fibers of the elements. As a result of these layers of conservatism and possible inaccuracies, the stresses computed for the unmodified fuselage initially violated the stress allowables. It became

necessary to increase the allowables such that the original design was considered good from a stress point of view. To give some design freedom, the initially exceeded allowables were adjusted such that they were 15% greater than the initial stresses. In addition, the weight was allowed to increase by 3% if required. As seen in Table 7.3, the weight only increased by 1 to 2%.

Inclusion of the stress constraints resulted in the tightening of the upper and lower bounds of the design variables. This was done in order to achieve more feasible solutions in the analysis time available. From this point of view, the stress constraints performed their intended function, to "screen" the design from unreasonable stress exceedance from a preliminary design point of view. The resulting stiffeners were only allowed to vary in cross section linear dimensions from 95% to 110%.

As for the optimization algorithm performance, it is evident that the single and multi-frequency algorithms performed their intended functions of reducing the noise levels within the design space. Although the intention was to reduce the acoustic tones induced by n1 engine imbalance, the excitation was conservatively considered to be a flat spectrum at +/- 5 Hz from the actual 195 Hz tone. Even with this excitation, the acoustic levels were reduced in this 10 Hz bandwidth. As for run time (real time), this varied by computer system. The NASA platform averaged about 8 hrs per iteration, while the Georgia Tech machine required only half that time. The COMPLEX algorithm typically achieved a new feasible point for the stress constraint runs approximately 1 out of 3 iterations. For the multi-frequency cases, convergence of the algorithm was never achieved, as each case had to be halted so that another could be started. Typically each case was halted after the initial "complex" of 36 feasible designs was achieved and the COMPLEX optimization had been performed long enough so that many points had been improved and thus replaced. For example, 100 points were replaced for Case 3 and 60 for Case 4 before these cases were halted. However, only 19 points were replaced for Case 5 and 10 for Case 6 before these were halted. These last two had to be stopped early so that the results could be post-processed for the report, and it is therefore possible that additional improvement could have been achieved for them.

8. SUMMARY AND CONCLUSIONS

This report documents the results of a four year (1994-1997) joint Lockheed Martin/Georgia Tech research program directed toward optimizing the acoustic environment inside aircraft structures. An optimization design tool has been developed, which allows the structure of an aircraft fuselage to be tailored in such a way as to minimize the interior noise levels at selected discrete frequencies or frequency bandwidths.

A computational optimization algorithm has been created composed of MSC/NASTRAN (FEM) to model the structure, AAC COMET/Acoustics (BEM) to model the acoustic fluid, and either CONMIN or COMPLEX as the optimizer. A portable UNIX shell script has been written to integrate the four major programs, and other necessary translator codes. To the best of our knowledge, this integrated design tool represents a unique capability within the aerospace industry.

The potential and applicability of the algorithm has been validated against idealized unstiffened and stiffened cylinders. Single and multiple frequency optimal design with multiple objective/constraint options has been demonstrated. Shell (skin) thickness and stiffener cross section dimensions were selected as design variables. The various objective function/constraints were evaluated, with the best performing formulation one which minimizes the sum of pressure squared subject to constraints on weight and bounds on design variables. Computational efficiency of the algorithm has been increased significantly through improvements to the COMET/Acoustics BEM code, associated data translators, and studies which selected optimal data recovery points. Weight, static stress, and buckling constraints have been integrated into the algorithm.

An optimization study of a Cessna Citation III business jet fuselage structure was undertaken to study the application of this tool to a real fuselage. The intention was to reduce the noise level of a tone induced by an engine imbalance of the fan rotor (n1), by altering the frame and stringer stiffening distributions. These changes were to be made without violating structural integrity constraints or dramatically increasing fuselage weight. Both single and multiple frequency algorithms performed well, with reductions in noise levels of 5 dB for a pressure stiffened fuselage with weight and stress constraints.

It is recommended that the prediction tools used in this optimization algorithm be thoroughly validated. Whereas the optimization studies in this report have shown the potential of the noise reduction design technique, the application of the prediction tools still requires more study.

9. REFERENCES

1. S. L. Padula, "Progress in Multidisciplinary Design Optimization at NASA Langley," NASA Langley Research Center, Report No. 107754.

2. F. Mistree, B. Patel, and S. Vadde, "On Modeling Multiple Objectives and Multi-Level Decisions in Concurrent Design," in *Proceedings of Advances in Design Automation*, 1994.

3. M. Z. Cohn, "Theory and Practice of Structural Optimization," in *Optimization of Large Structural Systems, Vol. II* (Kluwer Academic Publishers, The Netherlands, 1993).

4. J. E. Taylor, "Minimum-mass bar for axial vibration at specified natural frequency," *AIAA J.*, **5** (1911-1913), pp. 406-412 (1967).

5. M. J. Turner, "Design of minimum mass structures with specified natural frequencies," *AIAA J.*, **5**, pp. 406-412 (1967).

6. C. Y. Sheu, "Elastic minimum-weight design for specified fundamental frequency," *Int. J. Solids Structures*, **4**, pp. 953-958 (1968).

7. N. Olhoff, "Optimal design of vibrating rectangular plates," *Int. J. Solids Structures*, **10**, pp. 93-109 (1974).

8. L. J. Icerman, "Optimal structural design for given dynamic deflections," *Int. J. Solids Structures*, **5**, pp. 473-490 (1969).

9. K. Naghshineh and G. H. Koopmann, "A design method for achieving weak radiator structures using active vibration control," *J. Acoust. Soc. Am.*, **92**(3), pp. 856-870 (1992).

10. J. S. Lamancusa, "Numerical optimization techniques for structural-acoustic design of rectangular panels," *Computers & Structures*, **48**(4), pp. 661-675 (1993).

11. S. A. Hambric, "Formulations and Methods for Robust and Efficient Optimization of Acoustic Radiated Noise Problems," NSWCCD-SSD-95-006, Naval Surface Warfare Center, Carderock Division, March, 1995.

12. A. C. Jackson, F. J. Balena, W. L. LaBarge, G. Pei, W. A. Pitman, and G. Wittlin, "Transport Composite Fuselage Technology - Impact Dynamics and Acoustic Transmission," NASA CR - 4035, 1986.

13. F. W. Grosveld, T. J. Coats, H. C. Lester, and R. J. Silcox, "A Numerical Study of Active Structural Acoustic Control in a Stiffened, Double Wall Cylinder," Proceedings of NOISE-CON 94, National Conference on Noise Control Engineering, Ft. Lauderdale, Fl., May 1-4, 1994, pp. 404-408.

14. G. N. Vanderplaats and F. Moses, "CONMIN - A FORTRAN program for constrained function minimization: user's manual.," NASA Ames Research Center, Report NASA TMX-62282.

15. M. J. Box, "A New Method of Constrained Optimization and a Comparison with other Methods," *Computer J.*, **8**(1), pp. 42-52 (1965)

16. G. V. Reklaitis, A. Ravindran, and K. M. Ragsdell, *Engineering Optimization: Methods and Applications*, 1983, New York: John Wiley and Sons, Inc.

17. M. P. Bendsøe, N. Olhoff, and J. E. Taylor, "A Variational Formulation for Multicriteria Structural Optimization," *J. Struct. Mech.*, **11**(4), pp. 523-544 (1983-84).

18. "COMET/Acoustics User Document", Automated Analysis Corporation, Ann Arbor, MI.

APPENDIX A

Usage Guide to NASA Shell Script

Usage for NASA Shell Script:

$Cmd -c Filename [options]

$Cmd refers to the current name of the shell script. The most current version is ns7.3. The script must either be in a directory specified in your login shell's PATH variable, or you must use the full path to the script to execute it.

Required Input

-c Filename — Filename of the Variable Input file CFILE. The Variable Input file name must be the complete name of the file containing the optimization run parameter definitions. This file is utilized by the shell script and most support codes to configure the run.

Basic Options

-H hostfile — File name of configuration file to use in place of the default host file. Default is **host.cnf**.

-q — Flag to indicate that NASTRAN jobs on remote machine are submitted via NQS rather than in the background. Default is submit in background.

-x — Flag to turn on first level of shell debug output

-X — Flag to turn on full shell debug output

Restart Options

The -B, -E, -EF, -eX, -IF, -I, -M, -N, -O, -pr, -P, -R, -S, -SI, -U and -W options provide the user a restart capability for the script. These options apply to files that are generated for the starting set of velocity boundary conditions, design variables, external loads and frequencies. The default condition for all of these options is no restart available. When used, the restart capability assumes for the current set or subset of input data files, that the appropriate set or subset of output files from the relevant codes already exist.

-B — Multi-frequency runs. Flag to indicate initial NASTRAN Buckling results already exist, with name **BUFILE.f06**

-E — Multi-frequency runs. Flag to indicate initial COMET external pressure results already exist for the current set of frequencies with name **EXFILE.rslt** , and that the initial perturbed external solution also exists, with name **tmpns.updfcompert.rslt**.

-EF pid — Multi-frequency runs. Flag to indicate frequency interpolation files for the COMET external analyses already exist with file names **freq*pid**.

-eX — Multi-frequency runs. Flag to indicate initial EXTLOADS results exist in file **load.dat**

-IF pid	Multi-frequency runs. Flag to indicate frequency interpolation files for the COMET internal analyses already exist with file names **freq*pid**.
-I	Single frequency runs. Flag to indicate that initial INTEG results exist for a BEAMSHAPE analysis
-M	Single and multi-frequency runs. Flag to indicate that initial MERGE results already exist. The specific file name is specified in the host configuration file.
-N	Single and multi-frequency runs. Flag to indicate that Nastran results for the current design variables already exist. The script will explicitly test for NFile.f04, NFile.f06, and the file specified on the ASSIGN OUTPUT4 card in NFILE.
-O	Multi-frequency runs. Flag to indicate initial NASTRAN Modes results already exist, with name **MOFILE.f06.**
-pr	Flag to indicate that NASTRAN pressurized static results already exist, with filenames **NPrFile.f06**, **NM106.DBALL**, and **NM106.MASTER**.
-P	Single and multi-frequency runs. Flag to indicate that COMET internal pressure results already, with name **AFILE.rslt**.
-R	Single and multi-frequency runs. Flag to indicate that COMET restart file already exists, with name **AFILE.RES2** or **AFILE.RES4**.
-S	Single and multi-frequency runs. Flag to indicate that COMET sensitivity file exists, with name **AFILE.sens.**
-SI	Flag to indicate initial NASTRAN static Stress Constraint results exist, with name **SIFILE.pch.**
-U	Multi-frequency runs. Flag to indicate initial UPDFREQ results exist, and that the perturbed external COMET data set exists. The script will check for **updfreq.out** and **tmpns.updcompert.dat**.
-W	Single and multi-frequency runs. Flag to indicate that initial WTSENS results exist. The script will check for file **weights.out**.

-P tells the script that an initial pressure solution has already been generated, and an associated COMET/ACOUSTIC restart file, for the current velocities and design variables. The script assumes the pressures are in the file **AFILE.rslt**, and the restart file is **AFILE.rest**. The script assumes that the **AFILE.dat** file is configured to generate pressure solutions from the restart file.

-R tells the script that a COMET/ACOUSTIC restart file exits, but not pressures. The script assumes restart file name is **AFILE.rest**. The script assumes that the **AFILE.dat** file is configured to generate pressure solutions from the restart file.

-M tells the script that a MERGE output file already exists, for the current velocities and design variables. The script assumes the file's name is **AFILE.sens**.

Dynamic Remeshing Options

The dynamic remesh options permit the user to use a different interior data recovery node mesh for the restart run than is used in the base run.

-dm Filename Flag to indicate dynamic remeshing, plus root filename of comet input file with different mesh than in AFILE

-dS Flag to indicate a sensitivity file exists for the second comet input file, with same root file as file from -dm, name.sens

Miscellaneous Options

-z Flag to suppress the clean up of various scratch and temporary files that are generated in the course of a run. Note that this option is currently the default state, that is, all files are preserved.

Notes

Output from COMET is written to **comet.out**.

Merge writes its standard output and error to **merge.out**.

vbcgen writes its error output to **vbcgen.err**.

The script will extract the sensitivity output file name specified on the "ASSIGN OUTPUT4=filename . . ." line of the NASTRAN input file.

Shell Script Output Files

ns7.3.optimizer.out Multi-frequency runs. Flag to indicate initial NASTRAN Modes results already exist, with name **MOFILE.f06**

ns7.3.log Single and multi-frequency runs. Flag to indicate that COMET internal pressure results already, with name **AFILE.rslt**

APPENDIX B

Guide to the ns7 Configuration File

Version ns7 of the optimizer shell script implements an external configuration file. This configuration file permits certain aspects of the overall optimization algorithm to be defined external to the script itself, such that the script is much less platform specific. We anticipate that all platform specific localizations to be implemented through the configuration file, rather than hard-coded in the shell script. In addition, the configuration file provides enhanced flexibility for future upgrades and script modifications, including implementation of the hybrid algorithm.

The data in the configuration file provides the script with information about the explicit location, name, host, output files and etc. for the various subcomponents of the overall optimization algorithm. The individual lines of the configuration file have the form:

KEYWORD=

where KEYWORD is a specific string used to identify a particular item. The sequence of the lines in the configuration file is not important.

The basic information in a configuration file tells the script the path to a given code, the network name of the host on which to run the code, the user's login name on that host, the relative path from the login directory to the directory containing the code's input files, and a root name for certain execution monitoring files generated by the script for that code. If the code is being run on the same platform as the script, then host and user information may be omitted from the file. Since the script must be invoked from the directory with the data files, the relative paths to the data files for codes running on the same host as the script may also be omitted.

The following are two examples of configuration files. The first file is configured to run at NASA Langley. The second file is configured for the Lockheed Martin (LMAS) environment. Following the files is a description of the keywords and their significance.

The NASA host.cnf file is significantly shorter than the LMAS host.cnf file, as it takes greater advantage of default user, host and relative path information.

NASA host.cnf

```
Optimizer1=/usr2/users/cunefare/bin/tc.exe
Optimizer2=/usr2/users/cunefare/bin/tc.exe
COMET=/scr/software/comet3.0/comet/bin/comet
CHost=sonique
EXTLOADS=/usr2/users/cunefare/bin/ext_loads
EXTMERGE=/usr2/users/cunefare/bin/ext_merge051096
NASTRAN=nastran
NHost=edan
NHostPS=-A
```

MERGE=/usr2/users/cunefare/bin/mrgsens
MName=mrgsens
MHost=sonique
MHostPS=-A
UPDFREQ=/usr2/users/cunefare/bin/upd_freq
VBCGEN=/usr2/users/cunefare/bin/vbcgen.alpha
VName=vbcgen
VHost=sonique
VHostPS=-A
WTSENS=/usr2/users/cunefare/bin/wtsens.alpha
WName=weights
WHost=edan
WHostPS=-A
INTEG=/usr2/users/cunefare/bin/integ052396
ToPrint=$4
Rsh=rsh
CONTINUE=19

Lockheed Martin host.cnf

Optimizer1=/users/ranger/g596063/scripts/conmf3.exe
Optimizer2=/users/ranger/g596063/scripts/conmf3.exe
COMET=/usr/local/comet-3.0/bin/comet
CHost=ranger
CUser=g596063
C_rpath=coarscyl/kentest
EXTLOADS=/users/ranger/g596063/scripts/ext_loads
ExHost=ranger
ExUser=g596063
Ex_rpath=coarscyl/kentest
EXTMERGE=/users/ranger/g596063/scripts/ext_merge_ls.exe
ExMerHost=ranger
ExMerUser=g596063
ExMer_rpath=coarscyl/kentest
NASTRAN=nastran
NHost=str_1
N_rpath=coars_cyl
NHostPS=-A
NUser=engelst
NNFS=TRUE

```
MERGE=/users/engelst/bin/mrgsens.rs6000
MName=mrgsens
MHost=str_1
MHostPS=-A
MUser=engelst
MNFS=TRUE
M_rpath=coars_cyl
UPDFREQ=/users/ranger/g596063/scripts/upd_freq
UHost=ranger
UUser=g596063
U_rpath=coarscyl/kentest
VBCGEN=/users/engelst/bin/vbcgen.rs6000
VName=vbcgen
VHost=str_1
VHostPS=-A
VUser=engelst
VNFS=TRUE
V_rpath=coars_cyl
WTSENS=/users/engelst/bin/wtsens.rs6000
WName=weights
WHost=str_1
WHostPS=-A
WUser=engelst
WNFS=TRUE
W_rpath=coars_cyl
ToPrint=$3
Rsh=/usr/bsd/rsh
CONTINUE=25
```

Keyword Definitions

OPTIMIZER1	Specifies the complete path name to the optimization code used in the first stage of the algorithm.
OPTIMIZER2	Specifies the complete path name to the optimization code used in the second (restart) stage of the algorithm.
COMET	Specifies the complete pathname to the comet command.

CHost	Specifies the host where COMET is to run.
CName	Specifies a file name for redirection of COMET Standard Error and Standard Output.
CUser	Login name of user on CHost.
C_rpath	Relative path on CHost from login directory to input data directory.
EXTLOADS	Specifies the complete pathname to the external loads program.
ExHost	Specifies the host where the external loads program is to run.
ExUser	Login name of user on ExHost.
Ex_rpath	Relative path on ExHost from login directory to input data directory.
EXTMERGE	Specifies the complete pathname to the external loads sensitivity merge program.
ExMerHost	Specifies the host where the external loads sensitivity merge program is to run.
ExMerUser	Login name of user on ExMerHost.
ExMer_rpath	Relative path on ExMerHost from login directory to input data directory.
NASTRAN	Specifies the command name for NASTRAN.
NHost	Specifies the host where NASTRAN is to run.
NHostPS	Specifies the form of the ps command on NHost that will generate a listing of process IDs, including the pid for NASTRAN (the script will issue the command "ps NHostPS" as part of a routine to monitor the status of NASTRAN).
NUser	Login name of user on NHost.
N_rpath	Relative path on NHost from login directory to input data directory.
MERGE	Specifies the complete pathname to the MERGE program.

MName	Specifies the filename generated by MERGE of output sensitivities (this name is hardcoded in MERGE by AAC).
MHost	Specifies the host where MERGE is to run.
MHostPS	Specifies the form of the ps command on MHost that will generate a listing of process IDs, including the pid for MERGE (the script will issue the command "ps MHostPS" as part of a routine to monitor the status of MERGE).
MUser	Login name of user on MHost.
M_rpath	Relative path on MHost from login directory to input data directory.
UPDFREQ	Specifies the complete pathname to the UPDFREQ program.
UHost	Specifies the host where UPDFREQ is to run.
UUser	Login name of user on UHost.
U_rpath	Relative path on UHost from login directory to input data directory.
VBCGEN	Specifies the complete pathname to the VBCGEN program.
VHost	Specifies the host where VBCGEN is to run.
VHostPS	Specifies the form of the ps command on VHost that will generate a listing of process IDs, including the pid for VBCGEN (the script will issue the command "ps VHostPS" as part of a routine to monitor the status of VBCGEN).
VUser	Login name of user on VHost.
V_rpath	Relative path on VHost from login directory to input data directory.
WTSENS	Specifies the complete pathname to the WTSENS program.
WHost	Specifies the host where WTSENS is to run.

WHostPS	Specifies the form of the ps command on WHost that will generate a listing of process IDs, including the pid for WTSENS (the script will issue the command "ps VHostPS" as part of a routine to monitor the status of WTSENS).
WUser	Login name of user on WHost.
W_rpath	Relative path on WHost from login directory to input data directory.
ToPrint	Used to specify which argument of a string of arguments to write to output. This is used as part of the timing routines, and will essentially select which of a sequence of output arguments from the ps command to interpret as time information.
Rsh	Specifies the form of the rsh command to use from the local host where the script is running.
CONTINUE	Specifies the numeric value of the CONTINUE signal on the host where the optimizer runs.

APPENDIX C

Variable definitions in VARIABLE INPUT data file (Usually abbreviated as var.in)

The VARIABLE INPUT file is used to define the NASTRAN and COMET/ACOUSTICS model filenames and to override default parameters in the various optimizers and codes that are available to the user of the ns7 shell script.

Control parameters to the programs COMET, INTEG, NASTRAN, OPTOBJ, OPTSETUP, UPDFREQ, and UPDNAS are input using the VARIABLE INPUT file. The parameters are used by the codes to control some aspect of their execution. COMET/ACOUSTICS computes the interior and exterior acoustic fields. The INTEG code is required during Beamshape Optimization. NASTRAN computes the structural modes and response. OPTOBJ calculates the objective and constraints for each run. OPTSETUP translates all optimizer variables to the optimizers. UPDFREQ is used to update model files with current frequencies in multi-frequency optimization runs and in frequency sweeps. UPDNAS is used to update the NASTRAN model files with decision variables from the optimizer.

All input cards to the VARIABLE INPUT file are optional except those that identify the filenames of the finite and boundary element models to be used for the execution of the run. In particular, the COMET interior model which computes the internal sound pressures and the NASTRAN response model which computes the velocities on the interior surface of the structure must always be identified using the VARIABLE INPUT file.

The default values of the control parameters are overridden by including a keyword and a value in the VARIABLE INPUT file. A keyword corresponds to a variable name defined in the codes or script. If a keyword does not appear, then the default value for the corresponding variable will be used.

Objective function and constraint selection are made through the VARIABLE INPUT file through inclusion of appropriate keywords and values.

Parameters are formatted in the VARIABLE INPUT file using a specific keyword in columns 1-10 and the variable value or string in consecutive fields of 10 columns on the same line. All keywords and values must be left justified within their 10 columns wide fields. The programs and script looks for explicit strings with specific justification. Therefore, any text that is not a keyword, or any keyword that is not left justified, will be ignored.

1. Required Model Filenames and Input Variables for NASTRAN and COMET Execution.

The following is an example of NASTRAN and COMET model and parameter inputs contained in a VARIABLE INPUT file. These parameters are read and processed by the shell script.

```
****BEGIN VAR.IN FILE****

*** NASTRAN ***

STRUCTURE   RESPONSE    cn
STRUCTURE   MODES       cm
STRUCTURE   PRESSURED   cn_stat
STRUCTURE   DESIGN      cn_ds
STRUCTURE   ENERGY      cm_se
STRUCTURE   STRESS      cs
STRUCTURE   BUCKLING    cb

STRUCTURE   MEMORY      20M
STRUCTURE   QUE         q4hr
STRUCTURE   SCRATCH     FALSE
STRUCTURE   SDIR        /usr/temp/

*** COMET ***

FLUID       INTERNAL    ca
FLUID       EXTERNAL    ce
FLUID       RESTART     FALSE
FLUID       MEMORY      20M

****END VAR.IN FILE****
```

In the above example, the lines with asterisks are ignored, since they do not coincide with any of the defined keywords. Also, consider the following:

```
  FLUID     EXTERNAL    ce
FLUID       EXTERNAL    ce
```

Only the second line of the above two lines would actually be processed, as the first line's keyword is not left-justified. This may be exploited by the user to leave various alternative lines in the file for reference, while ensuring that the contents of the reference line is ignored.

All STRUCTURE (NASTRAN) and FLUID (COMET) cards are input with three total fields. The second field is a keyword which identifies the filename or parameter to be set in the third field.

1.A. Required Filename Keywords

The following lists the keywords that are required by the shell script for successful run execution.

Variable/ Keyword 1	Variable/ Keyword 2	Default Value	Significance
STRUCTURE	RESPONSE	none	A string variable identifying the filename (prefix only) of the NASTRAN structural response model. Required.
FLUID	INTERNAL	none	A string variable identifying the filename (prefix only) of the COMET internal acoustic response model. Required.

1.B. Optional Filename Keywords and Input Variables for NASTRAN and COMET.

The following lists the optional keywords that are utilized by the shell script to launch NASTRAN and COMET models correctly.

Variable/ Keyword 1	Variable/ Keyword 2	Default Value	Significance
STRUCTURE	MODES	none	A string variable identifying the filename (prefix only) of the NASTRAN structural modes model. Inclusion of this card and model filename triggers the execution of structural modes analysis for multi-frequency analysis.
STRUCTURE	PRESSURED	none	A string variable identifying the filename (prefix only) of the NASTRAN static pressurized structural response model. Inclusion of this card and model filename triggers the execution of pressurized structural analysis. A STRUCTURE DESIGN card must also be included in the VARIABLE INPUT file for pressurized analysis.
STRUCTURE	DESIGN	none	A string variable identifying the filename (prefix only) of the NASTRAN design file which contains design state equations for the update of pressurized structure models. This card must be included whenever pressurized analysis is being performed.

STRUCTURE	ENERGY	none	A string variable identifying the filename (prefix only) of the NASTRAN strain energy model for use in mode calculation of pressurized structures. Inclusion of this card and model filename is required for the execution of multi-frequency pressurized structural analysis.
STRUCTURE	STRESS	none	A string variable identifying the filename (prefix only) of the NASTRAN static stress model. Inclusion of this card and model filename triggers the execution of structural integrity stress constraint analysis.
STRUCTURE	BUCKLING	none	A string variable identifying the filename (prefix only) of the NASTRAN static buckling model. Inclusion of this card and model filename triggers the execution of structural integrity buckling constraint analysis.
STRUCTURE	MEMORY	none	A string variable identifying the amount of memory required for the successful execution of all NASTRAN models.
STRUCTURE	QUE	none	A string variable specifying the time queue of all NASTRAN models.
STRUCTURE	SCRATCH	TRUE	A string variable (TRUE or FALSE) which controls the utilization by NASTRAN of scratch files.
STRUCTURE	SDIR	none	A string variable specifying the directory to which all NASTRAN scratch files are written.
FLUID	EXTERNAL	none	A string variable identifying the filename (prefix only) of the COMET external acoustic response model. Inclusion of this card and model filename triggers the execution of the external COMET analysis for acoustic loading of the structure.
FLUID	RESTART	TRUE	A string variable (TRUE or FALSE) which controls the creation and utilization of COMET restart files.

FLUID	MEMORY	4M	A string variable identifying the amount of memory required for the successful execution of all COMET models.

2. General Run and OPTOBJ Input Variables.

The following is an example of general run and OPTOBJ inputs contained in a VARIABLE INPUT file. These variables are read and processed by the shell script and OPTOBJ to control general parameters of the run execution and to control the type of optimization to be performed.

```
****BEGIN VAR.IN FILE****

*** GENERAL RUN VARIABLES ***

TOLER          0.100E-8
LOOPS          1000
RESTART        FALSE

OBJECTIVE      ACOUSTIC
CONSTRNT       WEIGHT          278.0
CONSTRNT       STRESS
CONSTRNT       BUCKLING

OBJ0           0.236133081E-03
OFFSET         WEIGHT          1.0D+5
SCALE          WEIGHT          1.0
SCALE          ACOUSTIC        1.0

****END VAR.IN FILE****
```

The following lists the keywords that are used by the shell script and OPTOBJ for general run control.

Variable/ Keyword	Default Value	Significance
TOLER	1.0E-8	A real number set to the minimum acceptable change in the decision variables. Used to minimize search steps with very small increments in the decision variables.

LOOPS	10000	An integer set to the maximum number of script loops (objective function or gradient calculation).
RESTART	TRUE	A string variable (TRUE or FALSE) which controls the launch of a second optimization beginning with the final design state of the initial optimization.
OBJECTIVE	ACOUSTIC	**OBJECTIVE FUNCTION CARD** The objective card entry is a string variable used to select the objective function to be configured. The OBJECTIVE card selector entry can be one of the following literal strings: ACOUSTIC, WEIGHT, or COMPOUND.
CONSTRNT	selector	**CONSTRAINT CARDS** Constraint cards are used to configure the objective with the appropriate constraints. More than one constraint card may be used in the input file. Each constraint card may have multiple entry fields (each having a field width of 10). The constraint selector entry is a string variable used to specify the type of constraint to be configured and can be one of the following literal strings: ACOUSTIC, WEIGHT, BUCKLING, or STRESS. Default: zero constraints. See sections 2.A-F. for CONSTRNT card formats.
OBJ0	none	A real number having a field width of 16 columns (note this exception to the standard entry field of 10 columns) equal to the (un-normalized) objective function value of the initial design state of the run. The OBJ0 card is used to restart an optimization without having to rerun the first design state so that all objectives may be normalized to the initial value.
SCALE	1.0	**GRADIENT SCALE FACTOR CARD** An objective or constraint gradient may be divided by a scale factor. More than one scale factor card may be used in the input file. Each scale factor card must have two entry fields (each having a field width of 10):

The first entry is a string variable used to specify the type of gradient to be scaled and can be one of the following literal strings: ACOUSTIC or WEIGHT.

The second entry is a real number set to the scale factor.

OFFSET 0.0

OFFSET CARD

A specified offset is subtracted from the specified constraint. Offsets are currently available for weight constraints only. Each scale factor card must have two entry fields (each having a field width of 10):

The first entry is a string variable used to specify the type of constraint to be offset and must be the following literal string: WEIGHT.

The second entry is a real number set to the offset.

2.A. The ACOUSTIC Constraint Card Format.

The ACOUSTIC constraint card format is:

CONSTRNT ACOUSTIC PMAXDB

where PMAXDB is a real number setting the dB value of maximum noise constraint. The optimizer converts the PMAXDB value into an equivalent maximum average pressure magnitude squared, re 20 micro Pascals. The ACOUSTIC constraint is used in this format only with the WEIGHT objective formulation. (See section 2.C. for the COMPOUND objective formulation.)

2.B. The WEIGHT Constraint Card Format.

The WEIGHT constraint card format is:

CONSTRNT WEIGHT WMAX

where WMAX is a real number setting the maximum allowable weight. The WEIGHT constraint is used in this format only with the ACOUSTIC objective formulation. (See section 2.C. for the COMPOUND objective formulation.)

2.C. ACOUSTIC and WEIGHT Constraints with the Compound Objective Formulation.

The COMPOUND objective requires both ACOUSTIC and WEIGHT constraint cards using the following format:

CONSTRNT	ACOUSTIC	BINIT	BLB	BUB	XMU
CONSTRNT	WEIGHT	BINIT	BLB	BUB	XMU

where BINIT is a real number setting the initial value of noise beta variable (Suggest BINIT = 1.0), BLB / BUB are real numbers setting the lower / upper bounds on the noise beta variable (Suggest BLB = 0.0), and XMU is a real number setting the weight factor of the noise beta variable.

The beta variables in the compound formulation are used to drive down normalized functions of weight and noise. Since weight and noise can not be negative, the lower bound is naturally zero. Since the compound formulation applies the beta values as constraints on the normalized weight and noise, the upper bounds may be selected as appropriate to permit or restrict growth of the related parameter (weight or noise). For example, a beta value of 0.5 would require that the corresponding parameter must be reduced by at least 0.5 from its starting value. Conversely, a beta value of 2.0 would permit the related parameter to grow by up to a factor of 2. The "weight" factors on the beta variables are at the user's discretion, and should simply reflect the relative importance the user places on minimizing one parameter over the other.

2.D. The STRESS Constraint Card Format.

The STRESS constraint card format is:

CONSTRNT	STRESS

The STRESS constraint requires no additional fields and can be used with any objective formulation.

2.E. The BUCKLING Constraint Card Format.

The BUCKLING constraint card format is:

CONSTRNT	BUCKLING

The BUCKLING constraint requires no additional fields and can be used with any objective formulation.

2.F. The LINK Constraint Card Format.

The LINK constraint card format is:

CONSTRNT LINK I J T

The LINK constraint implements a constraint as $(X_i - X_j - T)/X_{jo} < 0$, where X_i is the i^{th} design variable, X_j is the j^{th} design variable, T is any real number (including zero), and X_{jo} is the initial value of the j^{th} design variable (used as a scale factor). On the selection card, I and J are integers, and T is any real number, including zero. Any number of LINK constraint cards may be included.

3. OPTIMIZER Input Variables.

The following is an example of optimizer inputs contained in a VARIABLE INPUT file. These parameters are read and processed by the OPTSETUP program.

```
****BEGIN VAR.IN FILE****

*** CONMIN INPUTS ***

ILIM        50
ACC         0.01
TOLER       0.100E-8

IPRINT      5
ITRM        5
CT          -0.1000
THETA       1.0000
ALPHAX      0.5000
ABOBJ1      0.5000
PHI11       5.0000
DABFUN      0.00001

*** COMPLEX ***

MAXFUN      800
ALPHA       1.300
EPSILON     1.000E-04
DELTA       1.000E-04
```

```
CTOLER          -1.000E-09
IRAN            100
COMPSIZE        2
DODESSPC        .FALSE.
DOVECTS         .FALSE.
FEASIBLE        0.989670533E+00    0.100202686E+01    0.539606431E+00

****END VAR.IN FILE****
```

3.A. CONMIN Specific Keywords.

The following lists the keywords that are used only by the CONMIN optimizer.

Variable/ Keyword	Default Value	Significance
ILIM	100	An integer set to the maximum permissible number of iterations.
ACC	0.005	A real number set to the desired accuracy, used as a relative convergence parameter.
TOLER	1.0E-8	A real number set to the minimum acceptable change in the decision variables. Used to minimize search steps with very small increments in the decision variables.
IPRINT	1	An integer controlling the amount of output from CONMIN (1-5) 1 - Minimum output 5 - Maximum output (useful for tracking/debugging) NOTE: This is also used by COMPLEX.
ITRM	3	An integer set to the number of consecutive iterations to indicate relative or absolute convergence.
CT	-0.1	A real number set to the tolerance on feasibility. CT should be less than zero.
THETA	1.0	A real number set to the push-off factors.
ALPHAX	0.1	A real number. Maximum value=1.0. Minimum value=0.001

ABOBJ1	0.1	A real number. Maximum value = 0.2. Minimum value = 0.0001
PHI11	5.0	A real number.
DABFUN	0.001	A real number, used as an absolute convergence parameter.

3.B. COMPLEX Specific Keywords

The following lists the keywords that are used only by the optimizer COMPLEX.

Variable/ Keyword	Default Value	Significance
MAXFUN	200	An integer value representing the maximum number of function evaluations that COMPLEX will allow. This number should be somewhat less than the "loops" number in the 'host.cnf' file to ensure that the optimizer will always be the program which stops a run. A function evaluation is a design point calculation.
ALPHA	1.300	A real number representing the reflection factor for the Complex Method. The point with the highest value of the objective function is reflected through the centroid of the other points: $x_i = \bar{x}_i + \alpha (\bar{x}_i - x_i)$ $i = 1, 2, 3, ... N$ x_i = the i^{th} design variable value for the design point x N = number of design variables $\bar{x}_i$ = the i^{th} design variable value of the centroid Box recommends a value of 1.3 for this variable. It is wise to keep the value above 1.0 to avoid the premature contraction of the point complex.
EPSILON	0.0001	A real value representing one of the two convergence criteria which must be met for COMPLEX to have converged on a solution. This criterion refers to the following equation: This criterion is satisfied if: $\varepsilon \geq \sum_{j=1}^{P} [f(x_j) - \bar{f}]^2$ P = the number of points in the complex

$f(x_j)$ = the objective function value of the j^{th} point in the complex

$\bar{f} = \frac{1}{P}\sum_{j=1}^{P} f(x_j)$ = the average objective function value of the points in the complex

This convergence factor is called the Objective Function convergence. It represents the range of objective function values in the complex of points. Epsilon should be quite small because the objective function values for all of the points should be close together.

DELTA 0.0001 A real number representing the point convergence criterion. It deals with how much of the design space the complex of points covers. This number, like the criterion for the objective function values should be small enough to ensure that the complex has closed in towards the optimum design state. First, the total "size" of the design space is calculated at the beginning of a run:

$$S = \sum_{i=1}^{N} (x_i^u - x_i^l)^2$$

N = the number of design variables
x_i^u = the upper bound of the i^{th} design variable
x_i^l = the lower bound of the i^{th} design variable

The point convergence factor is then calculated as the "percentage" of the design space covered:

The convergence factor is satisfied if:

$$\delta \geq \frac{1}{S}\sum_{i=1}^{N}\sum_{j=1}^{P} (x_{i,j} - \bar{x}_i)^2$$

P = the number of points in the complex
N = the number of design variables
x_{ij} = the i^{th} design variable value of the j^{th} design point
$\bar{x}_i$ = the i^{th} design variable of the centroid
S = the design space "size"

CTOLER -1.000 x 10-9 The real value which essentially defines zero for the purpose of checking the validity of a point (whether it meets the constraint(s)). The constraints are all normalized so that if they are greater than zero, they are violated. This value (the constraint tolerance) should be a negative number, but not too far from zero.

IRAN	100	A positive integer value between 1 and 9,999,999,999 (it may never be less than 1) which serves as the pseudo-random number generator seed value. As long as this number is the same, the pseudo-random number generator will produce the same set of numbers (between 0 and 1), allowing for repeatability of a run.
COMPSIZE	2	An integer value used to determine the size (number of points) of the complex of points to be used in the run. The value given by the user is added to the number of design variables in the model to determine the number of points that will be used. This number may be negative (giving fewer points than the number of design variables), but it may not be less than -(NDES-2). In other words, there may not be less than two points in the complex. If the user has requested a DESIGNSPACE run (DODESSPC = TRUE) this variable serves a slightly different purpose. The user must ensure that the number of points in the complex (NDES+COMPSIZE) is greater than the value of the INCREMENT variable defined below.
INCREMENT	10	An integer value used only when a DESIGNSPACE run is conducted (DODESSPC = TRUE). This value represents the number of steps that the user wishes the program to take to get from the lower variable bound to the upper variable bound.
IDESONE	1	An integer value used only when a DESIGNSPACE run is conducted (DODESSPC = TRUE). This value represents the first design variable value that the user wishes to increment across the design space.
IDESTWO	2	An integer value used only when a DESIGNSPACE run is conducted (DODESSPC = TRUE). This value represents the second design variable value that the user wishes to increment across the design space.
FEASIBLE	none	A series of real numbers, each having a field width of 16 columns, which describe a set of design variables and objective function value which correspond to a feasible design point in the "complex" of the optimization. The FEASIBLE card is used to restart an optimization using existing points. As many FEASIBLE cards may appear in the VARIABLE INPUT file as exist in the "complex" for the run. The design variables are entered consecutively on the line in fields of 16 columns (note this exception

to the standard entry field of 10 columns) and the objective function value is entered last on the line (also in a field of 16).

DODESSPC .FALSE. A logical variable which activates the DESIGNSPACE subroutine. This routine will vary two design variable values (essentially doing an exhaustive search with only two variables) to produce a block of data. This data consists of the objective function values all the way across the design space. The data can then be used to construct a 3-D graph depicting the objective function. The program will take INCREMENT steps from the lower to the upper design variable bounds on each design variable value (IDESONE and IDESTWO).

IF THIS SUBROUTINE IS ALLOWED TO RUN (i.e. this variable is set to TRUE), NO OPTIMIZATION WILL TAKE PLACE.

DOVECTS .FALSE. A logical variable that is used to activate the VECTORGRAPH subroutine. This routine does an analysis along the line between a point and the centroid when that point (after many retractions) could not be improved upon. This routine can be very time consuming. It is recommended that it only be used if the user is looking for information about why the points are failing to improve.

.TRUE. → Vectorgraph can be run
.FALSE. → Vectorgraph cannot be run

4. INTEG and UPDNAS Input Variables.

The following is an example of INTEG and UPDNAS inputs contained in a VARIABLE INPUT file.

```
****BEGIN VAR.IN FILE****

*** INTEG INPUTS ***

STRUCTURE    BEAMSHAPE
FRM_File     frm_msh
STR_File     str_msh
```

```
*** UPDNAS INPUTS ***

STRUCTURE    BEAMS2
NTHK         0
NFRME        5
NSTRNG       10
NORD         2

****END VAR.IN FILE****
```

The following lists the keywords that are used by INTEG and UPDNAS.

Variable/ Keyword	Default Value	Significance
STRUCTURE	none	**STRUCTURE CARD** The STRUCTURE card is currently used to specify NASTRAN models utilizing frames and/or stringers. The STRUCTURE card may have one of several formats, each specified by the first entry which is a string variable (BEAMSHAPE, BEAMS1, or BEAMS2). BEAMSHAPE specifies stiffener shape optimization and requires the additional input of FRM_File and STR_File cards which identify the needed NASTRAN mesh files. BEAMS1 specifies the use of a NASTRAN long-31 model. BEAMS2 specifies the use of a NASTRAN long-21 or cir-21 model and requires input cards for the NTHK, NFRME, NSTRNG, and NORD variables.
NTHK	0	An integer used with BEAMS2 structural models
NFRME	5	An integer used with BEAMS2 structural models
NSTRNG	10	An integer used with BEAMS2 structural models

NORD	2	An integer used with BEAMS2 structural models
FRM_File	filename	A string variable identifying the frame mesh input file used with BEAMSHAPE optimization. The file name should be entered without the ".dat" extension.
STR_File	filename	A string variable identifying the stringer mesh input file used with BEAMSHAPE optimization. The file name should be entered without the ".dat" extension.

5. UPDFREQ Input Variables.

The following is an example of UPDFREQ input cards in the VARIABLE INPUT file.

```
****BEGIN VAR.IN FILE****

**** UPDFREQ INPUTS ****

FREQLOW     100.0D0
FREQHIGH    150.0D0

FIXED       102.00
FIXED       119.1

SPECTRUM    50.0     0.13     0.000
SPECTRUM    97.0     0.13     0.000
SPECTRUM    102.0    10.3     0.000
SPECTRUM    107.0    0.13     0.000
SPECTRUM    150.0    0.13     0.000

STRNERG     0.2D0
SWEEP       1.0

****END VAR.IN FILE****
```

The following lists the keywords that are used by UPDFREQ:

Variable/ Keyword	Default Value	Significance
FREQLOW	none	A real number set to the lower frequency bound (Hz) for a multi-frequency run.
FREQHIGH	none	A real number set to the upper frequency bound (Hz) for a multi-frequency run.
FIXED	none	A real number set to a fixed frequency value (Hz). Any number of FIXED cards may be used, but all values must be within the frequency range set in the FREQLOW and FREQHIGH cards.
SPECTRUM	none	The SPECTRUM cards define the model excitation as a function of frequency. There are three entry fields for the SPECTRUM card: SPECTRUM F REAL IMAGINARY where at each frequency, F, the source strength is defined by its REAL and IMAGINARY parts. Any number of SPECTRUM cards may be used. It is not necessary for the frequency values to be within the frequency range set in the FREQLOW and FREQHIGH cards.
STRNERG	none	A real number set to the minimum allowable modal strain energy. This variable is used to select modes of a pressurized structure which are likely to contribute to the interior sound field.
SWEEP	none	A real number set to the desired frequency increment (Hz) for a frequency sweep run. The existence of a SWEEP card in the file will cause a frequency sweep run to occur.

6. Miscellaneous: The Basis Function.

Basis Function Optimization is no longer available with the ns7 script. The following usage notes have been included as a reference for future work.

The basis function representation requires no special cards in the VARIABLE input file. Rather, the NASTRAN file will have a line as follows:

Line XX
Columns

1-8	$THKLM67	A literal string designating the basis function method
9-24	PMIN	A real number setting the lower bound on the physical variables generated by the basis function
25-40	PMAX	A real number setting the upper bound on the physical variables generated by the basis function

Appendix D

Table of Design Optimization Files

Compiled 3-18-97

Note:
- ~ denotes a filename that is user dependent.
- ^ denotes a filename dependent on an existing filename.
- ≈ denotes a file used for multi-frequency runs only.
- • denotes a file used for beamshape optimization only.
- † denotes a file used for constraint analysis only.
- # denotes a file used for pressurized structure analysis only.

Filename	File Description	Created by	Modified by	Required by
General User-Generated Input Files:				
var.in ~	general input variables	user		script OPTOBJ OPTSETUP UPDFREQ UPDNAS
host.cnf ~	general input	user		script
User-Generated Model Files:				
ca.dat ~	COMET internal model	user	script UPDFREQ VBCGEN	script COMET UPDFREQ VBCGEN
ca.elids ~	COMET	user		MERGE
ce.dat ~ ≈	COMET external model	user	UPDFREQ	script COMET UPDFREQ

Filename	File Description	Created by	Modified by	Required by
User-Generated Model Files (cont.):				
cn.dat ~	NASTRAN response model	user	script	script
			EXTLOADS	EXTLOADS
			UPDFREQ	INTEG
				NASTRAN
				OPTOBJ
				OPTSETUP
				UPDFREQ
				UPDNAS
				WTSENS
lds200.subdmap ~ ≈	NASTRAN response input card	user		NASTRAN
cm.dat ~ ≈	NASTRAN modes model	user	script	script ≈
				NASTRAN
				UPDNAS
cs.dat ~ †	NASTRAN static (stress) model	user	script	script
				NASTRAN
				UPDNAS
cb.dat ~ †	NASTRAN static (buckling) model	user	script	script
				NASTRAN
				UPDNAS
frm_msh.dat ~ •	NASTRAN frame model	user	INTEG	INTEG
				NASTRAN
str_msh.dat ~ •	NASTRAN stringer model	user	INTEG	INTEG
				NASTRAN
cm_se.dat ~ ≈ #	NASTRAN modes strain energy model	user		NASTRAN
				UPDFREQ
cn_ds.dat ~ #	NASTRAN design equation model	user		UPDNAS
cn_stat.dat ~ #	NASTRAN static pressurized loads response model	user	script	NASTRAN
integ.in ~ •	INTEG input	user		INTEG

Filename	File Description	Created by	Modified by	Required by
Archive Files:				
tmpns.var.in.START ^	variable input archive	script		
tmpns.*.dat.START ^	NASTRAN/COMET model archive	script		
tmpns.*.dat.last ^	NASTRAN model archive	script		
tmpns.*.rslt.last ^	COMET output archive	script		
General Script/Optimizer Output and Communication Files:				
shell.out ~	general script output	script	script	
ns7*.optimizer_name.out ^	detailed optimizer output	optimizer	optimizer	
ns7*.log ^	detailed script output of optimization	script	script	
tmpns.optimizer.log	optimizer output	optimizer	optimizer	
tmpns.time.cpu	detailed time output	script	script	
tmpns.time.out	general time output	script	script	
tmpns.optimizer.cmd	communication	script	optimizer	optimizer
		script	script	
tmpns.sedfile9	communication	script	script	
tmpns.signals.out	communication	script	script	script
			optimizer	
tmpns.updnas.dat	design state output	optimizer	optimizer	script
			OPTOBJ	
			UPDNAS	
General Script Files Used to Launch and Track Programs:				
tmpns.job.cmd	launch	script	script	script
tmpns.sniffer.cmd	launch	script	script	script
tmpns.submit.cmd	launch	script	script	script
tmpns.*.rsh	PID tracking	script	script	script
tmpns.*.time	time output	script	script	script

Filename	File Description	Created by	Modified by	Required by
Files Associated with OPTSETUP Execution:				
tmpns.optimizer.dat	OPTSETUP output	OPTSETUP		optimizer script OBTOBJ
tmpns.optsetup.rsh	PID tracking	script	script	script
tmpns.optsetup.time	time output	script	script	script
Files Associated with UPDNAS Execution:				
tmpns.updnas.*.dat ^ (i.e. tmpns.updnas.cb.dat)	modified NASTRAN model	UPDNAS	UPDNAS	script
tmpns.*.dat.last ^ (i.e. tmpns.cm.dat.last)	archived NASTRAN model	script	script	
tmpns.updnas.log	output	UPDNAS	UPDNAS	
tmpns.updnas.rsh	PID tracking	script	script	script
tmpns.updnas.time	time output	script	script	script
Files Associated with Beamshape Optimization:				
deqat.out •	NASTRAN input card	INTEG	INTEG	NASTRAN
integ.out •	output	INTEG	INTEG	
tmpns.int.rsh •	PID tracking	script	script	script
tmpns.int.time •	time output	script	script	script
tmpns.integ.error •	output	script?		
frm_msh_new.dat ^ •	modified NASTRAN input	INTEG	INTEG	script
frm_msh.f04 ^ •	output	NASTRAN	NASTRAN	
frm_msh.f06 ^ •	NASTRAN results	NASTRAN	NASTRAN	INTEG
frm_msh.log ^ •	output	NASTRAN		
str_msh_new.dat ^ •	modified NASTRAN input	INTEG	INTEG	script
str_msh.f04 ^ •	output	NASTRAN	NASTRAN	
str_msh.f06 ^ •	NASTRAN results	NASTRAN	NASTRAN	INTEG
str_msh.log ^ •	output	NASTRAN		
tmpns.frm_msh.dat.START ^ •	archive	script		

Filename	File Description	Created by	Modified by	Required by
Files Associated with Beamshape Optimization (continued):				
tmpns.frm_msh.error ^ •	output	script	script	script
tmpns.frm_msh.f06.START ^ •	archive	script		
tmpns.frm_msh.rsh ^ •	PID tracking	script	script	script
tmpns.str_msh.dat.START ^ •	archive	script		
tmpns.str_msh.error ^ •	output	script	script	script
tmpns.str_msh.f06.START ^ •	archive	script		
tmpns.str_msh.rsh ^ •	PID tracking	script	script	script
Files Associated with NASTRAN Static Pressurized Run				
cn_stat.f04 ^ #	output	NASTRAN	NASTRAN	
cn_stat.f06 ^ #	output	NASTRAN	NASTRAN	
cn_stat.log ^ #	output	NASTRAN	NASTRAN	
cn_stat.pch ^ #	output	NASTRAN	NASTRAN	
nm106.DBALL ^ #	output	NASTRAN	NASTRAN	NASTRAN
nm106.MASTER ^ #	output	NASTRAN	NASTRAN	NASTRAN
tmpns.cn_stat.dat.START ^ #	archive	script		
tmpns.cn_stat.dat.last ^ #	archive	script		
tmpns.cn_stat.error ^ #	output	script	script	script
tmpns.cn_stat.rsh ^ #	PID tracking	script	script	script
Files Associated with NASTRAN Static Run (Stress Constraints):				
SENSI_STAT.OUTPUT4 †	static sensitivities	NASTRAN	NASTRAN	
cs.f04 ^ †	output	NASTRAN	NASTRAN	
cs.f06 ^ †	output	NASTRAN	NASTRAN	OPTOBJ
cs.log ^ †	output	NASTRAN	NASTRAN	
cs.pch ^ †	output	NASTRAN	NASTRAN	OPTOBJ
nm101.DBALL ^ † #	output	NASTRAN	NASTRAN	
nm101.MASTER ^ † #	output	NASTRAN	NASTRAN	

Filename	File Description	Created by	Modified by	Required by
Files Associated with NASTRAN Static Run (Stress Constraints):				
tmpns.cs.dat.START ^ †	archive	script		
tmpns.cs.error ^ †	output	script	script	script
tmpns.cs.rsh ^ †	PID tracking	script	script	script
Files Associated with NASTRAN Static Run (Buckling Constraints):				
cb.f04 ^ †	output	NASTRAN	NASTRAN	
cb.f06 ^ †	output	NASTRAN	NASTRAN	OPTOBJ
cb.log ^ †	output	NASTRAN	NASTRAN	
tmpns.cb.dat.START ^ †	archive	script		
tmpns.cb.error ^ †	output	script	script	script
tmpns.cb.rsh ^ †	PID tracking	script	script	script
Files Associated with NASTRAN Modes Run:				
cm.f04 ^ ≈	output	NASTRAN	NASTRAN	
cm.f06 ^ ≈	output	NASTRAN	NASTRAN	UPDFREQ
cm.log ^ ≈	output	NASTRAN	NASTRAN	
fort.12	output	NASTRAN	NASTRAN	
tmpns.cm.dat.START ^ ≈	archive	script		
tmpns.cm.error ^ ≈	output	script	script	script
tmpns.cm.rsh ^ ≈	PID tracking	script	script	script
Files Associated with NASTRAN Modes Strain Energy Run:				
cm_se.f04 ^ ≈ #	output	NASTRAN	NASTRAN	
cm_se.f06 ^ ≈ #	output	NASTRAN	NASTRAN	UPDFREQ
cm_se.log ^ ≈ #	output	NASTRAN	NASTRAN	
tmpns.cm_se.dat.START ^ ≈ #	archive	script		
tmpns.cm_se.dat.last ^ ≈ #	archive	script		
tmpns.cm_se.error ^ ≈ #	output	script	script	script
tmpns.cm_se.rsh ^ ≈ #	PID tracking	script	script	script